The role of H19, a long non-coding RNA in the immune system

Junjie Yang

Thèse de doctoratde

l'Université Sorbonne Paris Cité

Préparée à l'Université Paris Diderot

Ecole Doctorale BioSPC, ED 562

The role of *H19*, a long non-coding RNA in the immune system

Par **Junjie Yang**

Thèse de doctorat d'Immunologie

Dirigée par **Ana Cumano**

Présentée et soutenue publiquement à Paris le 17/10/2018

Jury

Président du jury : **Antonino Nicoletti**/ **Professor** / **INSERM/ Denis Diderot University (P7)**

Rapporteurs : **Dinis Calado** / **Professor** / **Francis Crick Institute**

Rapporteurs : **Joan Yuan** / **Associate Professor** / **Lund University**

Examinateurs : **Thierry Defrance** / **Professor** / **École normale supérieure de Lyon**

Examinateurs : **Bruno Canque**/ **Professor** / **École Pratique des Hautes Etudes**

Directeur de thèse : **Ana Cumano** / **Professor** / **Institut Pasteur**

Le rôle de *H19*, un long ARN non codant dans le système immunitaire

Résumé :

L'empreinte génomique, une régulation épigénétique unique entraînant une expression génique spécifique aux parents d'origine, est essentielle au développement et à la croissance des mammifères. *H19* est un ARN long non codant exprimé en milieu maternel qui est un régulateur central du réseau de gènes à empreinte contrôlant le développement. *H19* est exprimé pendant le développement embryonnaire dans de nombreux tissus, y compris toutes les cellules hématopoïétiques. Le rôle de *H19* au cours du développement embryonnaire n'a été documenté que pour le placenta où il contrôle la croissance. Le rôle de *H19* dans la lymphopoïèse n'a pas été étudié. Notre laboratoire a précédemment trouvé *H19* comme principal transcrit exprimé sélectivement par les proB du foie fœtal (FF), et exprimé de façon différentielle par des immigrants thymiques précoces et tardives. Cependant, le rôle du gène *H19* dans celui du développement des cellules B, ou même dans le système immunitaire, reste méconnu. Ici, nous avons réalisé une caractérisation complète des perturbations du développement et de la fonction du système immunitaire des souris pour lesquelles un grand segment du locus *H19* a été supprimé.

Dans cette étude, nous avons constaté que le mutant *H19* avait un impact spécifique sur le développement des cellules du FF induisant une augmentation sélective du nombre des cellules proB $BP1^{+}$ présentant des perturbations importantes du réarrangement du locus IgH. On observe également chez les animaux $H19^{-/-}$ adultes une expansion anormale du compartiment B mature. Bien que H19 ne soit plus exprimé après la naissance, les lymphocytes B des souris adultes mutantes présentent un phénotype altéré. On observe en effet des perturbations importantes du profil d'expression du marqueur B220. Les souris $H19^{-/-}$ présentent un défaut d'expansion des lymphocytes B du centre germinatif, ainsi qu'une chute de la production des IgM spécifiques dans le sérum après immunisation. Indiquant une réponse défectueuse des cellules B. De manière cohérente, nous avons trouvé une réactivité réduite au BCR des cellules B naïves $H19^{-/-}$, associée les expériences de reconstitution compétitive ont mis en évidence un altération cellule-intrinsèque de la réponse humorale chez les animaux mutants. Un défaut d'induction de l'expression des molécules du CMHII, CD40, et CD86, qui pourrait être à l'origine des perturbations de la réponse humorale observée chez les souris $H19^{-/-}$. Les analyse de transcriptome réalisées sur les lymphocytes B du centre germinal des animaux mutants ont mis en évidence une expression différentielle des gènes impliqués dans la régulation de l'intensité du signal émanant du récepteur B à l'antigène.

Au total ce travail nous a permis de démontrer l'activité régulatrice exercée par l'ARN non codant H19 sur le développement et la fonction du système immunitaire.

Mots clefs : *LncRNA H19*, développement des lymphocytes B, réponse des lymphocytes B, réactivité BCR, réaction du centre germinal.

The role of *H19*, a long non-coding RNA in the immune system

Abstract:
Genomic imprinting, a unique epigenetic regulation resulting in a parent-of-origin specific gene expression, is essential for normal mammalian development and growth. *H19* is a maternally expressed long non-coding RNA that is a central regulator of the imprinting gene network controlling development and growth. *H19* is expressed throughout embryonic development in multiple tissues including all hematopoietic cells. The role of *H19* during embryonic development has only been documented for the placenta where it controls growth and the role of *H19* in lymphopoiesis has not been investigated. The laboratory has previously found *H19* as the major differentially expressed transcript in two microarrays comparing fetal liver (FL) and bone marrow (BM) derived pro-B cells, as well as between early and late thymic settling progenitors. However, a role for imprinting gene *H19* in B cell development, or even in immune system remains elusive. Here we sought to analyze mice where a large segment of the *H19* locus has been deleted.

In our work, we found that loss of *H19* have specific impact on the FL B cell development by producing increased numbers of $BP1^+$ proB cell. Although $BP1^+$ proB cells from $H19^{-/-}$ FL showed impaired Ig heavy chain V-D-J rearrangement, that increase resulted in a net enlarged B cell compartment in the adult periphery of *H19* mutant. In adult mice, although *H19* is not expressed in B lymphocytes after birth, B cells from $H19^{-/-}$ mice exhibited altered B cell surface phenotype, represented by an upregulated B220 expression on all B cell subsets. After immunization with different T cell dependent antigens, $H19^{-/-}$ exhibits reduced GC B cells, and impaired specific IgM titer in the serum, indicating a defected B cell response in $H19^{-/-}$ mice. Competitive reconstitution analysis showed a B cell autonomous impairment in the B cell response. Consistently we found a reduced BCR responsiveness of $H19^{-/-}$ naïve B cells that together with less efficient upregulation of MHCII and CD40 expression after immunization might be responsible for the impaired immune response in $H19^{-/-}$ mice. Genome-wide transcription analysis revealed differential expression of genes involved in regulating the intensity of B cell receptor signaling.

This work brings new insights on the regulation role of long non-coding RNA *H19* in the early B cell development and immune system

Keywords: *LncRNA H19*, B cell development, B cell response, BCR responsiveness, GC reaction.

Acknowledgement

I moved to Paris three years ago to start a PhD, for me it was a brand-new stage in my life after five years' work in the vaccine industry. I have met wonderful people in the past three years, who have helped me to know myself better, personally and scientifically. I have learnt many things to help me go through my PhD. Here I would like to thank all those who helped and supported me in this course.

First of all, to **Ana Cumano**, my PhD supervisor for giving me the opportunity to join the lab, it is of great courage for you to take me in the lab, because I didn't have a strong CV and I had no experience in the field of hematopoiesis, or even not a solid background in immunology. But you decided to offer me this golden opportunity, I will forever be grateful that our paths have ever crossed. During these years, you have kept challenging and guiding me to become the best of myself, you always gave me the freedom to decide, and encouraged me to try out my ideas even if some were naïve. You thought that it doesn't matter how many mistakes are made as long as one can learn from them. Thanks for teaching me the techniques used in this work, for training me to obtain the critical thinking in doing scientific research. Most importantly, you always saw the positive side when I was pessimistic, always found solutions when I encountered problems. You are a great scientist and manager always encouraging us to follow our interests, to be the best of ourselves. I have been lucky enough to find you and your group in this stage of my life.

To **Monica Sala**, my tutor and also a member of my TAC (thesis advisory committee). You brought me to Paris by initiating this collaboration program between Institut Pasteur and CNBG (China National Biotec Group). I remember clearly how difficult it was the administrative arrangements between the two parties. I really appreciate your effort for bridging the two institutions, the two countries and the two different cultures. You are a very open-minded person who introduced me to the French and Italian culture and helped me to adapt to life in Paris in the very first months. You also carefully followed my thesis, the progression of the project, and regularly gave me some very useful suggestions. I sincerely value the support you provided throughout this process. I hope that in a not far future we will have a deeper collaboration and a fruitful outcome of this IP-CNBG program.

To **Bruno Canque**, **Michel Cohen-Tannoudji**, **Caroline Demangel**, members of my TAC committee. Thanks for kindly following my thesis and giving me precious advice for shaping the direction of this thesis in the past three years. You were always on my side to guide me in various aspects. Your suggestions and guidance were always valuable.

To **Ramy El Said**, my best friend in the Pasteur campus. Thank you for your friendship, for your excellent language skills, without you I cannot imagine how I could have dealt with the

complicated administrative problems. You were always with me and I will always remember in those frustrated days when the experiments didn't work, you introduced me to the ChiCha cafe, the best place to release the pressure.

To the members of the lab: **Delphine Guy-Grand, Paulo Vieira, Antonio Bandeira Ferreira, Rachel Golub, Pablo Pereira, Odile Burlen-Defranoux, Marie-Christine Vougny, Claire Berthault, Thibaut Perchet, Maxime PETIT, Francisca Soares da Silva, Ana C Silva, Florian Specque, Francoise Guinet, Sylvain Meunier**. Thank you for giving me great advice in both the scientific research and life. You were willing to help and your honest comments and advice in the weekly lab meetings were of great help to my thesis. Your friendship and help made my life easier in the past years, I will never forget the happy time with you: the Christmas lunch, the world cup matches, drinking time in 15, etc.

Thanks to those who helped in the course of the project. **Zhi Li, Chloé LESCALE, Armelle BOHINEUST, Nicolas SERAFINI, Bianca BALBINO, Marine OBERKAMPF DE DABRUN, Gilles DADAGLIO** generously shared the reagents or protocols, or helped in doing some of the experiments.

To the **Chinese community in Pasteur**, the weekly Chinese seminar, as well as the after-work activities maintain a tight connection of the community, it is nice to have you guys there to share my scientific ideas, to receive the feedback from different perspectives, to share my happiness and sadness.

Thanks to the **PPU program** and **CNBG** for the financial support. Specially, the activities organized by PPU program: trainings, courses, retreats, etc. It was of great help to interact with different people from different fields. The ideas and culture exchange broadened the eyesight and mind.

Finally, I would like to thank **my family**. What can I say? As the dedication to this dissertation country, without you this would not have been possible. Thank you for encouraging me to pursue my dreams and sharing the happiness and sadness. **To my wife**, for the long cross-country flights and the late-night phone calls. Your support uplifted me every step along this path. **To my son**, you are my best publication, dad loves you. Thank you.

To **France** for being the country that gives me the peace and freedom that my soul needed, and for giving me a place I can call a second hometown

All the Best to all of you, looking forward seeing you back in China, or back in France.

Contents

List of figures and tables

Abbreviations

PAMPs, pathogen associated molecular patterns

BCR, B cell receptor

TCR, T cell receptor

Ig, immunoglobulin

MHC, major histocompatibility complex molecules

AID, B cell–specific activation-induced cytidine deaminase

TdT, terminal deoxynucleotidyl transferase

MZB, marginal zone B cell

FOB, follicular B cell

TD, T cell dependent

TI, T cell-independent

GC, germinal center

HSC, hematopoietic stem cells

FL, fetal liver

BM, bone marrow

CLPs, common lymphoid progenitors

IL7Ra, interleukin 7 receptor alpha chain

LMPPs, lymphoid-primed multipotent progenitors

preBCR, pre-B cell receptor

Rag, recombination activating gene

RSS, recombination signal sequences

CSR, Ig class switch recombination

HLH, helix-loop-helix

Ebf1, Early B cell factor 1

NHEJ, non-homologous end joining

DBS, DNA double strand break

SLCs, surrogate light chains

PI3K, phosphoinositide 3 kinase

PKB, protein kinase B

SYK, Spleen tyrosine kinase

TFH, T follicular helper cells

SHM, somatic hypermutation

CCR7, chemokine receptor 7

DZ, dark zone

LZ, light zone

FDC, follicular dendritic cells

PD-1, programmed cell death protein 1

MBC, memory B cell

LLPC, long lived plasma cell

NFAT, nuclear factor of activated T cells

PirB, immunoglobulin-like receptor B

ITIM, Immunoreceptor tyrosine-based inhibitory motif

ITAM, Immunoreceptor tyrosine-based activation motif

SHIP, SH2-domain-containing inositol polyphosphate 5' phosphatase

PTPRC, protein tyrosine phosphatase receptor type C

SFK, Src family kinase

MAP, mitogen-activated protein

HEL, hen-egg lysozyme

PTM, posttranslational modification

PRCs, polycomb repressive complexes

KMTs, lysine methyltransferases

KDMs, lysine demethylases

EZH2, Enhancer of zeste homolog 2

MOZ, monocytic leukemia zinc finger protein

Lnc RNA, long noncoding RNAs

ICR, imprinted control region

DMR, differential methylation region

BWS, Beckwith-Wiedemann syndrome

SRS, Silver–Russel syndrome

IGN, imprinting gene network

SRBC, Sheep red blood cell

OVA, ovalbumin

RNAseq, RNA sequencing

PCR, Polymerase chain reaction

IL, interleukin

TNFα, tumor necrosis factor alpha

IFRγ, Interferon gamma

WT, wild type

KO, knockout

CD, cluster of differentiation

ELISA, enzyme-linked immunosorbent assay

ELISPOT, enzyme-linked immunospot

MFI, mean fluorescence intensity

EdU, 5-ethynyl-2'-deoxyuridine

LPS, Lipopolysaccharide

S1P, Sphingosine 1-phosphate

FAK, focal adhesion kinase

α4β1, integrin alpha 4 and integrin beta 1

VCAM-1, Vascular cell adhesion protein 1

Abstract

Le rôle de *H19*, un long ARN non codant dans le système immunitaire

Résumé :

L'empreinte génomique, une régulation épigénétique unique entraînant une expression génique spécifique aux parents d'origine, est essentielle au développement et à la croissance des mammifères. *H19* est un ARN long non codant exprimé en milieu maternel qui est un régulateur central du réseau de gènes à empreinte contrôlant le développement. *H19* est exprimé pendant le développement embryonnaire dans de nombreux tissus, y compris toutes les cellules hématopoïétiques. Le rôle de *H19* au cours du développement embryonnaire n'a été documenté que pour le placenta où il contrôle la croissance. Le rôle de *H19* dans la lymphopoïèse n'a pas été étudié. Notre laboratoire a précédemment trouvé *H19* comme principal transcrit exprimé sélectivement par les proB du foie fœtal (FF), et exprimé de façon différentielle par des immigrants thymiques précoces et tardives. Cependant, le rôle du gène *H19* dans celui du développement des cellules B, ou même dans le système immunitaire, reste méconnu. Ici, nous avons réalisé une caractérisation complète des perturbations du développement et de la fonction du système immunitaire des souris pour lesquelles un grand segment du locus *H19* a été supprimé.

Dans cette étude, nous avons constaté que le mutant *H19* avait un impact spécifique sur le développement des cellules du FF induisant une augmentation sélective du nombre des cellules proB $BP1^{+}$ présentant des perturbations importantes du réarrangement du locus IgH. On observe également chez les animaux $H19^{-/-}$ adultes une expansion anormale du compartiment B mature. Bien que H19 ne soit plus exprimé après la naissance, les lymphocytes B des souris adultes mutantes présentent un phénotype altéré. On observe en effet des perturbations importantes du profil d'expression du marqueur B220. Les souris $H19^{-/-}$ présentent un défaut d'expansion des lymphocytes B du centre germinatif, ainsi qu'une chute de la production des IgM spécifiques dans le sérum après immunisation. Indiquant une réponse défectueuse des cellules B. De manière cohérente, nous avons trouvé une réactivité réduite au BCR des cellules B naïves $H19^{-/-}$, associée les expériences de reconstitution compétitive ont mis en évidence un altération cellule-intrinsèque de la réponse humorale chez les animaux mutants. Un défaut d'induction de l'expression des molécules du CMHII, CD40, et CD86, qui pourrait être à l'origine des perturbations de la réponse humorale observée chez les souris $H19^{-/-}$. Les analyse de transcriptome réalisées sur les lymphocytes B du centre germinal des animaux mutants ont mis en évidence une expression différentielle des gènes impliqués dans la régulation de l'intensité du signal émanant du récepteur B à l'antigène.

Au total ce travail nous a permis de démontrer l'activité régulatrice exercée par l'ARN non codant H19 sur le développement et la fonction du système immunitaire.

Mots clefs : *LncRNA H19*, développement des lymphocytes B, réponse des lymphocytes B, réactivité BCR, réaction du centre germinal.

The role of *H19*, a long non-coding RNA in the immune system

Abstract:
Genomic imprinting, a unique epigenetic regulation resulting in a parent-of-origin specific gene expression, is essential for normal mammalian development and growth. *H19* is a maternally expressed long non-coding RNA that is a central regulator of the imprinting gene network controlling development and growth. *H19* is expressed throughout embryonic development in multiple tissues including all hematopoietic cells. The role of *H19* during embryonic development has only been documented for the placenta where it controls growth and the role of *H19* in lymphopoiesis has not been investigated. The laboratory has previously found *H19* as the major differentially expressed transcript in two microarrays comparing fetal liver (FL) and bone marrow (BM) derived pro-B cells, as well as between early and late thymic settling progenitors. However, a role for imprinting gene *H19* in B cell development, or even in immune system remains elusive. Here we sought to analyze mice where a large segment of the *H19* locus has been deleted.

In our work, we found that loss of *H19* have specific impact on the FL B cell development by producing increased numbers of $BP1^+$ proB cell. Although $BP1^+$ proB cells from $H19^{-/-}$ FL showed impaired Ig heavy chain V-D-J rearrangement, that increase resulted in a net enlarged B cell compartment in the adult periphery of *H19* mutant. In adult mice, although *H19* is not expressed in B lymphocytes after birth, B cells from $H19^{-/-}$ mice exhibited altered B cell surface phenotype, represented by an upregulated B220 expression on all B cell subsets. After immunization with different T cell dependent antigens, $H19^{-/-}$ exhibits reduced GC B cells, and impaired specific IgM titer in the serum, indicating a defected B cell response in $H19^{-/-}$ mice. Competitive reconstitution analysis showed a B cell autonomous impairment in the B cell response. Consistently we found a reduced BCR responsiveness of $H19^{-/-}$ naïve B cells that together with less efficient upregulation of MHCII and CD40 expression after immunization might be responsible for the impaired immune response in $H19^{-/-}$ mice. Genome-wide transcription analysis revealed differential expression of genes involved in regulating the intensity of B cell receptor signaling.

This work brings new insights on the regulation role of long non-coding RNA *H19* in the early B cell development and immune system

Keywords: *LncRNA H19*, B cell development, B cell response, BCR responsiveness, GC reaction.

Introduction

1 The immune system

The immune system protects the organism against invasive pathogens or foreign environmental antigens. It is a highly organized and effective system to prevent morbidity through the coordination of various components of this system, such as immune cells and effector molecules. To combat a great variety of pathogens and non-self-antigens, the immune system comprises different layers of defense the most distinguishable of which are innate and adaptive immune systems. The former serves as a first line of defense which plays a crucial role in protecting the organism from pathogens, this process is taking place at the very beginning of the infection through the recognition of some common features of the pathogens, such as the relatively conserved structural moieties in microorganisms, called pathogen associated molecular patterns (PAMPs). However, the function of the innate immune system is limited because the recognition of pathogens is a rather unspecific process through invariant receptors, being therefore inefficient in eliminating infectious organisms. If the innate immune reaction does not eliminate a pathogen, another more effective mechanism called adaptive immune reaction is adopted to better protect the organism. The immune cells and molecules in this system are more specific against pathogens in comparison to the innate immune system. The adaptive immune system, consisting of B and T lymphocytes and a variety of effector molecules, is responsible for the specific humoral and cellular protection against foreign antigens or microorganisms. Furthermore, the immunological specificity of B and T lymphocytes is due to the diversity of antigen receptors on their surface (Tonegawa, 1983). For example, the B cell receptor (BCR) is a membrane bound immunoglobulin (Ig), which can also be secreted after B cell activation to exert their immunological function through binding to foreign antigens or microorganisms. By contrast the T cell receptor (TCR), which is not secreted, can bind to the peptide fragments from foreign antigens presented by major histocompatibility complex molecules (MHC). Moreover, B lymphocytes can adjust their effector functions and adjust the affinity of its immunoglobulin by undergoing somatic hyper-mutation (higher mutation rate in the variable regions of the immunoglobulin genes) to enhance the antibody affinity. During B cell activation immunoglobulins can switch their initial immunoglobulin constant region from M (IgM) and/or IgD to IgA, IgG or IgE antibodies through a process called Ig class switch recombination. Both processes are mediated by AID (B cell–specific activation-induced cytidine deaminase). In addition, the adaptive immune system can also induce a memory response, which mediates a faster and stronger response against re-infection of the same pathogen (Bevan, 2011), and this memory

response provides a long term or even lifelong protection. The synergistic action of both the innate and the adaptive immune system is the basis for a rapid, highly specific and protective immune response against potentially pathogenic microorganisms. This allows survival in a principally hostile microbial environment.

1.1 B cells in the immune system

1.1.1 B1 cells

B lymphocytes, the core cellular mediators of adaptive immunity, are divided into B1 and B2 cells. In contrast to B1 cells, Extensive studies showed that B1 cells mainly localized in peritoneal cavity and pleural cavity, as well as spleen, exhibiting an innate-like immune function for a rapid response characterized by secreting essentially poly-reactive, IgM dominated, low-affinity antibodies. Thus, they are grouped into innate rather than in the adaptive immune branch.

B1 cells are mainly derived from the FL B lymphocyte development (Hayakawa et al., 1985a). One hypothesis to explain the origin of B1 cells is that B1 cells derive from distinct precursors from that of B2 cells (Herzenberg, 2000). However, later studies indicated that B1 cells originate also from adult HSC (Lam and Rajewsky, 1999; Düber et al., 2009), and they share the same progenitors as B2 cells. Recent evidence shows that Lin28b expression in FL HSC correlates with the B1 cells production versus that of B2 cells (Kristiansen et al., 2016).

Phenotypically, B1 cells are characterized as $CD19^{hi}B220^{lo}CD43^{+}CD23^{-}IgM^{hi}IgD^{lo}$, they have self-renewal capacity and can be further divided into B1a and B1b cells by the expression of CD5 on the cell surface of the B1a cells (Baumgarth, 2011). Other major features of B1 cells include less diverse BCR repertoire compared to B2 cells caused by limited usage of Ig heavy chain V segments and lower N sequences insertion in the V-D-J joining mediated by TdT (terminal deoxynucleotidyl transferase) during its development (Schatz and Swanson, 2011).

Because of their anatomical location (various cavities), these cells are more prone to access and respond to pathogens. In this process, Toll-like receptors (TLRs) appear to play an important role in early host defence recognizing conserved structural moieties in microorganisms, called pathogen associated molecular patterns (PAMPs), including LPS, peptidoglycan, sugar mannose, unmethylated CpG DNA, bacterial flagellin, glucans from

fungal cell walls. In addition, activation of innate-like B1 cells can also produce a wide variety of effectors, such as chemokines, cytokines, anti-microbial factors, etc.(Janeway, 2002). However, B1 cells show a limited diversity of BCR and initially produce membrane or secreted form of IgM, and B1 cell response is not antigen specific and lack of memory response which provide a recall response and long-term immunity against pathogens, a feature of the adaptive immune branch.

1.1.2 B2 cells

Another B cell subset called B2 cell, also known as conventional B cell, which comprise two major subsets: marginal zone B cell (MZB) and follicular B cell (FOB). MZB cells, defined as $CD19^{+}B220^{+}IgM^{hi}CD23^{-}CD21^{+}$, are characterized by their ability to effect early and rapid responses against pathogens. MZB cells mainly reside in the unique location called marginal zone in the white pulp of the spleen. They are non-recirculating B cells. Similar to B1 cells, MZB cells produce low-affinity pathogen-specific IgM or IgG3 antibodies after being activated by T cell independent antigens. FOB cells, characterized as $CD19^{+}B220^{+}IgM^{+}CD23^{+}CD21^{lo}$, represent the majority of B lymphocytes in peripheral lymphoid organs such as the spleen and lymph nodes, comprising up to 80–90% of B cells in these organs. FOB cells play a crucial role in the adaptive immunity because of their capability in producing high-affinity, class-switched, and less cross-reactive antibodies against pathogens. Because they are located close to the T cell zone they are well suited to respond to T cell dependent (TD) antigens and eventually effect the GC reactions (Victora and Nussenzweig, 2012b). Under stimulation with pathogens or foreign antigens, FOB cells can be programed with the aid of T helper cells to produce high affinity antigen specific antibodies. This B cell population has the capability to undergo extensive proliferation, somatic hyper-mutation, and Ig class-switching, to give rise high affinity IgG, IgA, and IgE antibodies. In addition, activated B2 cells may undergo further differentiation into antibody secreting plasma B cells, as well as memory B cells. However, in contrast to the rapid response of B1 cells, FO B2 cells requires days to weeks of activation and undergo Ig class-switch.

1.2 The ontogeny of B cell subsets

B lymphocytes derive from multipotent HSC first appear in the FL at about embryonic day (E) 12.5 in mice. These B cell progenitors reside, expand and undergo differentiation in the FL. Shortly before birth they gradually migrate to the BM, and sustain B cell production in BM throughout the life, although the rate of production declines with age (Min et al., 2006). The mechanisms underlying the generation of B1 versus B2 cells as well as those regulating the formation of the different B cell subsets are still incompletely understood.

Two models have been proposed to explain the co-existence of the B1 and B2 (FO and MZ) subsets. The first one is the lineage model that postulates that B1 and B2 cells are derived from distinct progenitors (Hayakawa et al., 1985a). The other theory is called selection model which holds the opinion that the polarization and fate of B1 and B2 cells are driven by the strength of BCR signaling (Berland and Wortis, 2002; Dorshkind and Montecino-Rodriguez, 2007). The evidence of a FL B1 specific progenitor, characterized as lin^- $AA4.1^+CD19^+B220^{lo/-}$, added weight to the lineage hypothesis (Montecino-Rodriguez and Dorshkind, 2006). These B1 progenitors are abundant in the FL and rare in adult BM, which is consistent with the observation of in vivo reconstitution, which demonstrates that FL cell transfer can reconstitute B1 cell compartment but BM transfer is less efficient in that reconstitution (Hayakawa et al., 1985b). Thus, in the lineage model, B1 cells are viewed as mainly produced from fetal B1 specific progenitors, whereas B-2 cells are derived from the B2 progenitors that predominate in the adult BM.

However, This model has been challenged in several experimental systems by other studies, which indicated that B1 cells can also originate from adult HSC (Düber et al., 2009; Lam and Rajewsky, 1999), and share the same progenitors as B2 cells. These observations provide direct support for the selection model, where BCR signaling plays a role in the fate decision of different B cell subsets.

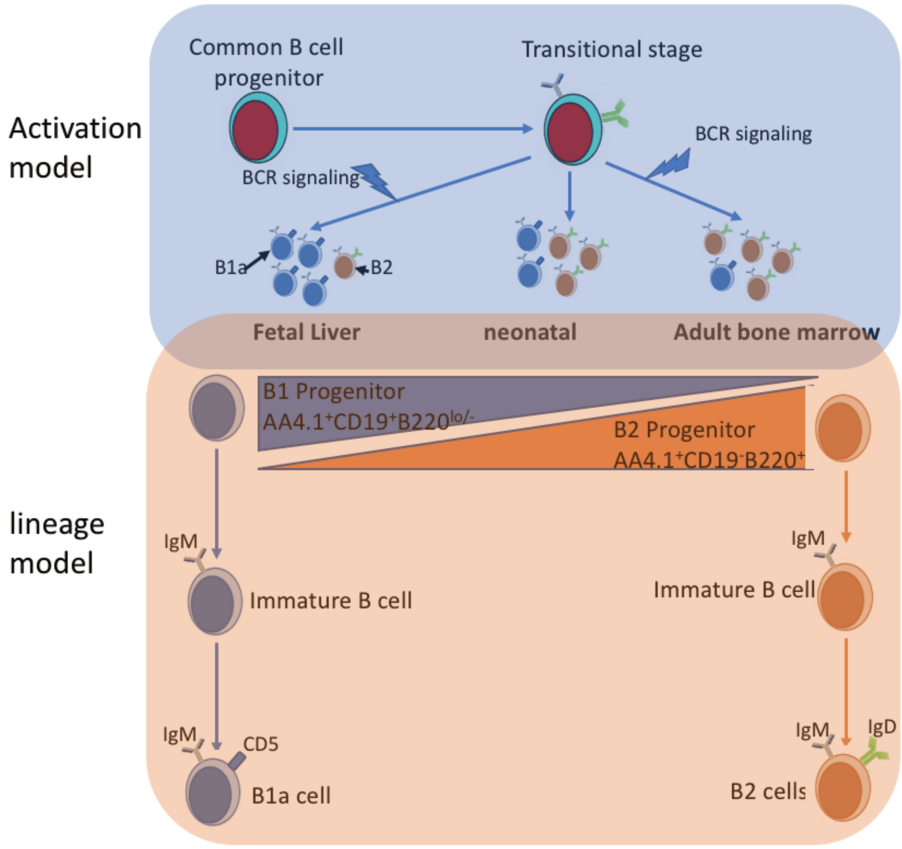

Figure1 Two models for the origin of B cell subsets

The "selection model", also called "activation model" (blue box) proposes that the strength of BCR signaling determines the fate of B cells into either the B-2 or the B-1 cell subsets. The "lineage model" proposes the co-existence of two distinct B progenitors that give rise to B-1 and B-2 cells, respectively. B1 specific progenitors are dominant in the FL, and declines in the adult BM, where B2 specific progenitors account for the majority of progenitors.

2 B lymphopoiesis

2.1 Early B cell differentiation and commitment

Lineage priming and commitment during hematopoiesis is a stepwise process starting with hematopoietic stem cells (HSC, defined as $Lin^-Kit^+Sca\text{-}1^+CD150^+CD48^-$). The HSCs lose the self-renewal capacity and differentiate to multi-potent progenitors (MPP), and then further differentiate to downstream progenitors until the terminal committed lineage cells by gradually restricting their differentiation potential. During lymphoid specification, the common lymphoid progenitors (CLPs, defined as Lin^-IL7Ra^+ $c\text{-}Kit^{lo}Sca\text{-}1^{lo}$), derived from

HSC express the IL7Ra which is a hallmark of lymphoid commitment, are restricted to lymphoid lineage by losing other lineage potential in the BM (Kondo et al., 1997), although CLPs still retained the dendritic cell differentiation potential (Liu and Nussenzweig, 2010) (Douagi et al., 2002). This fate decision process is mainly achieved by differentially expression of lineage specific transcription factors that are the key regulators of the lineage priming and commitment. In this process, transcription factors, such as Ikaros, E2A, PU.1, Ebf1 and Pax5. Hereafter, we will review the role of these key transcription factors in the B cells priming and their identity maintenance.

2.1.1 PU.1

PU.1 is an Ets-domain transcription factor encoded by the *Spi-1* gene and is expressed exclusively in cells of the hematopoietic lineage, the expression of PU.1 is upregulated during myeloid and B-lymphoid cell development (Reya and Grosschedl, 1998)(McKercher et al., 1996). PU.1 can regulate its target genes by binding to a PU-box, which is a purine-rich sequence near the promoter region of target genes.

PU.1 deficient mice die around embryonic day 18 and lack of both B cells and myelomonocytic cells in the FL (McKercher et al., 1996; Scott et al., 1994). The progenitors in the FL are also affected in PU.1 deficient mice and multiple studies showed that HSC (Kim et al., 2004), lympho-myeloid progenitors ($AA4.1^+$, Lin^-)(Scott et al., 1997), as well as CLPs and early B cell precursors ($IL7R^+Kit^+$) are dramatically impaired in PU.1 deficient embryos and in vitro culture showed these progenitors fail to differentiate into B lymphoid or myeloid cells. However, the B cell development deficiency can be partially rescued by enforced expression of the downstream target genes of PU.1, such as transcriptional factor *Ebf1*, over expression of which can give rise to B cells, while over expression of *IL7R* can also lead to B cell growth but at lower frequencies. These observations indicate that PU.1 affecting B cell commitment or development partially through regulating the *IL-7R* (DeKoter et al., 2002) and *Ebf1* genes (Betancur et al., 2010).

Min Y et al described that mice with conditional deletion of *Pu.1* in CD19-expressing B cells produced an increased compartment of cells resembling B1 cells, while B2 cells were compromised. This imbalanced of B1/B2 cell development became more pronounced with

age, indicating that Pu.1 deletion in B cells resulted in a shift from B2 cells to B1-like cells which might associated with B1/B2 cell reprograming (Ye et al., 2005).

2.1.2 *Ikaros*

Ikaros genes belong to a zinc finger transcription factor family, widely expressed in hematopoietic cells that are key regulators of hematopoiesis. *Ikaros* was first identified to regulate Dntt (encoding TdT) (Lo et al., 1991) and CD3d (Georgopoulos et al., 1992) expression, two lymphoid specific genes by binding its regulatory region. In lymphoid lineage development, *Ikaros* deficient mice showed impaired B cell, T cell and NK cell production, while the myeloid lineage and erythroid lineage showed no major differences (Georgopoulos et al., 1994). Similar deficiency phenotype of B, T, and NK cells was also observed in another *Ikaros* null mouse model in which DNA binding site of *Ikaros* transcriptional factor was deleted (Allman et al., 2003). In addition, in the latter mouse model, the hematopoietic progenitors are impaired, with decreased HSC compartment as well as reduced self-renewal capacity and severely decreased CLP numbers (Wang et al., 1996; Nichogiannopoulou et al., 1999).

Ikaros regulates B cell specification, B cell development, maturation and B cell responses in different aspects. *Ikaros* null LMPPs (lymphoid-primed multipotent progenitors) failed to express lymphoid genes *IL7R* and *Flt3*, signals that are critical for early B lineage specification form lymphoid progenitors (Sitnicka et al., 2003). However, B cell development was not rescue by overexpression of *IL7R* and *Flt3* in *Ikaros*$^{-/-}$ LSK cells. Further studies showed that *Ikaros* also induced *Ebf1* expression, which in turn promoted B cell differentiation by activating the B cell transcriptional program, and over expression of *Ebf1* in *Ikaros*$^{-/-}$ LSK cells rescued B cell potential (Sitnicka et al., 2003; Reynaud et al., 2008). In addition, *Ikaros* contributes to B cell development by regulating signaling from preBCR (pre-B cell signaling complex). Conditional deletion of *Ikaros* in proB cells arrested B cell development in proB cell stage by downregulating preBCR signaling associated genes and upregulating integrin signaling related genes (Thompson et al., 2007; Schwickert et al., 2014). *Ikaros* also plays regulatory roles in Igh locus recombination via activating *Rag* gene expression as well as by controlling VH gene accessibility and constricting the Igh locus to allow for antigen receptor recombination (Reynaud et al., 2008). Thus, *Ikaros* promotes and

maintains B cell identity by repressing alternate lineage genes and by concomitantly inducing B lineage specific VH segment rearrangement at the Igh locus.

During B cell response in the periphery, *Ikaros* regulate B cell activation thresholds (Kirstetter et al., 2002), as well as antibody isotype selection via Ig class switch recombination (CSR). *Ikaros* deficient B cells showed higher sensitivity to anti-IgM stimulation and *Ikaros* regulates CSR by activating epigenetic marks and transcription at constant region gene promoters.

Kirstetter et al demonstrated that *Ikaros* mutant mice exhibit an abnormal serum antibody profile, characterized by reduction in IgG3 and IgG1, and increased in IgG2b and IgG2a production (Kirstetter et al., 2002). Mechanistically, *Ikaros* binds the 3' enhancer and S region promoters of Igh locus to increase AID accessibility to Sγ2b and Sγ2a to induce AID dependent CSR to IgG2b and IgG2a. Thus, *Ikaros* is a crucial regulator of CSR through modulating transcriptional competition between S regions.

2.1.3 E2A

The transcription factor E2A is one of the E proteins belong to the helix-loop-helix (HLH) protein family, which regulates genes expression through binding to E box domain of DNA (Massari and Murre, 2000). E2A is required for lymphopoiesis in regulating both B and T cell development, especially controls the initiation of B lymphopoiesis.

During hematopoiesis, HSC differentiate in a stepwise manner into CLPs, which have a B, T and NK cell potential (Nutt and Kee, 2007b). The further differentiation from CLP to B lineage is dependent on several transcription factors, such as E2A, EBF1, and Pax5(Nutt and Kee, 2007a).

B cell development in *E2A*-deficient mice is arrested at the very early stage, at which the initiation of immunoglobulin DJ rearrangements is not yet occurred(Bain et al., 1994; Zhuang et al., 1994; Borghesi et al., 2005). In the absence of E2A lymphoid progenitors failed to express B lineage associated genes, such as *Rag1*, *Pax5*, CD19, CD79a (mb1) and λ5, and *Ebf1* expression is also suppressed. Induced expression of E2A in *E2A*-deficient progenitors can restore *Ebf1* expression by binding and activating the promoter of *Ebf1* gene (Ikawa et al., 2004; Smith et al., 2002; Roessler et al., 2007). Forced retroviral expression of *Ebf1* in *E2A*-deficient progenitors gives rise to proB cells *in vitro* cultures, as well as normal V(D)J recombination at the IgH locus and show normal expression of B-lymphoid genes (Seet et al.,

2004). All the evidence indicates that E2A acts upstream of *Ebf1* and *Pax5* in the initiation of the B lineage differentiation program (Bain et al., 1994; Bain et al., 1997).

2.1.4 Ebf1

Ebf1 (Early B cell factor 1) belong to EBF transcriptional factor family. *Ebf1* is exclusively expressed in B lineage cells and has a regulatory role in the earliest B cell specification and development (Lin and Grosschedl, 1995). Mice deficient in *Ebf1* fail to express B lineage specific genes, such as *Pax5*, *mb-1*, surrogate light chain λ5 and *VpreB*, etc.(Busslinger, 2004; Sigvardsson et al., 2002; Lin and Grosschedl, 1995). B cell development in *Ebf1*$^{-/-}$ mice is blocked and fail to rearrange heavy chain loci. This arrested B cell development phenotype is similar to E2A deficiency mice, suggesting these two factors act in concert to control B cell development. However, compared to *Pu.1*, *Ikaros* and *E2A* deficient mice, which arrest multi-lineage cell development, *Ebf1* inactivation specifically affects B lineage development, indicating that the transcription factors PU.1, Ikaros, and E2A, are expressed prior Ebf1, and the onset of B cell differentiation is initiated by *Ebf1*, which drives B cell specification and commitment.

Ebf1 has abilities to restart B cell program in progenitors deficient in upstream transcription factors, including PU.1 and E2A. Ectopic *Ebf1* expression in *E2A*$^{-/-}$ (Seet et al., 2004), *Pu.1*$^{-/-}$ (Medina et al., 2004), *IL7*$^{-/-}$ (Dias et al., 2005; Kikuchi et al., 2005) mice can to some extend restore B cell development by inducing B lineage gene expression. This suggests that *Ebf1* plays a crucial role in B cell programing.

Ebf1 starts to be expressed in CLPs, and expression correlates with B lineage restriction in Ly6d^{+}Il7R^{+} CLPs (Inlay et al., 2009), at which stage most B cell specific genes are not yet expressed. Expression of Ebf1 in Ly6d^{+}Il7R^{+} CLPs is sufficient to activate a B lineage specific transcription network, comprising genes such as Pax5 (Mansson et al., 2010), accompanied by the silencing of genes of T and NK cells. The importance of *Ebf1* in the proliferation of B lineage cells is highlighted in a mouse model of *Ebf1* conditional deletion (Györy et al., 2012). Nechanitzky et al. showed conditional deletion of *Ebf1* in committed pro-B cells restored innate lymphoid cells (ILCs) and T cells potential after transfer into alymphoid mice. However, the T cells derived from *Ebf1*-deficient proB cells had VDJ rearrangements of loci encoding both B cell and T cell antigen receptors (Nechanitzky et al., 2013), as well as expression of NK, ILC, and T cell specific transcription factors, including

Id2, Gata3 and Tcf7, which are normally suppressed by Ebf1. Thus, Ebf1 is required for B lineage commitment by repressing alternative cell fates.

Interestingly, although Ebf1 is required for starting the B lineage programing by activating the B cell transcriptional network, it seems dispensable for the maintenance of their expression as development progresses. In addition, Ebf1 regulates different sets of genes at different stages of B cell development. Conditional deletion of Ebf1 at later B cell developmental stages did not result in major differences in the expression of a number of *Ebf1* target genes, such as Pax5, mb-1 and CD79b that remained expressed after the deletion of EBF1 (Hagman et al., 1993; Hagman et al., 1991)

2.1.5 Pax5

Pax5 also called B cell lineage specific activator protein (BSAP) is a member of a paired box family 5. *Pax5* is exclusively expressed within the B cell lineage, starting from pro-B stage of B cell development (Fuxa and Busslinger, 2007). One of the important roles of *Pax5* is the regulation of CD19 expression. Deficiency of *Pax5* arrests B cell development in a stage before proB stage in both fetal and adult (Nutt et al., 1997). However, the $Pax5^{-/-}$ progenitors did express *E2A* and *Ebf1*, as well as several other B cell-specific target genes. the B cell development of $Ebf1^{-/-}$ deficient progenitors cannot be rescued by Pax5 over-expression (Medina et al., 2004), suggesting Pax5 functions downstream of E2A and EBF1 in the transcription network of early B cell development (Nutt et al., 1998; Nutt et al., 1997). In addition, in vitro culture in the presence of IL7 shows that $Pax5^{-/-}$ progenitors can generate proB-like cells, while in the presence of other cytokines, $Pax5^{-/-}$ progenitors can differentiate into other lineages, such as macrophages, granulocytes, dendritic cells or natural killer cells. $Pax5^{-/-}$ proB cells also retain T cell potential in reconstitution assays of $Rag2^{-/-}$ mice (Rolink et al., 1999) and in vitro co-culture with OP9-DL1 stromal cells which express the Notch ligand Delta-like 1, suggesting $Pax5^{-/-}$ proB progenitor cells are not fully committed to the B cell lineage (Rolink et al., 1999; Nutt et al., 1999). These studies show that Pax5 is a critical B lineage-specific factor to restrict the differentiation to B lineage pathway and inhibit alternative pathways.

2.2 B cell development

B cell development is a highly organized process, which begins in the FL and later shifts to the BM where it is maintained throughout life. Early B lymphocyte differentiation starts in common lymphoid progenitor cells (CLPs) in the FL during embryogenesis and later in the BM and progresses in a stepwise manner (Inlay et al., 2009). Over the past decades, our understanding of B cell development has greatly progressed. The first comprehensive scheme of B cell development was proposed by Randy Hardy identified 7 different developmental fractions (fraction A to F) of B cell precursors in the BM (Hardy and Hayakawa, 1991). In this scheme, different developmental stages of B lymphocytes were characterized by B cell surface markers, comprising B220, CD43, IgM, HSA (CD24), and BP1. In addition, this study also identified the fractions where the Ig heavy and light chain rearrangements occurred. In the FL, similar subsets can also be found, but the majority of B lymphocytes do not develop beyond the fraction B stage. Fraction A was identified as the first B lineage stage characterized by co-expression of B220, CD43 and low level CD24. Additional studies showed that this subset also include a population of CLP (Martin et al., 2003; Allman et al., 1999).

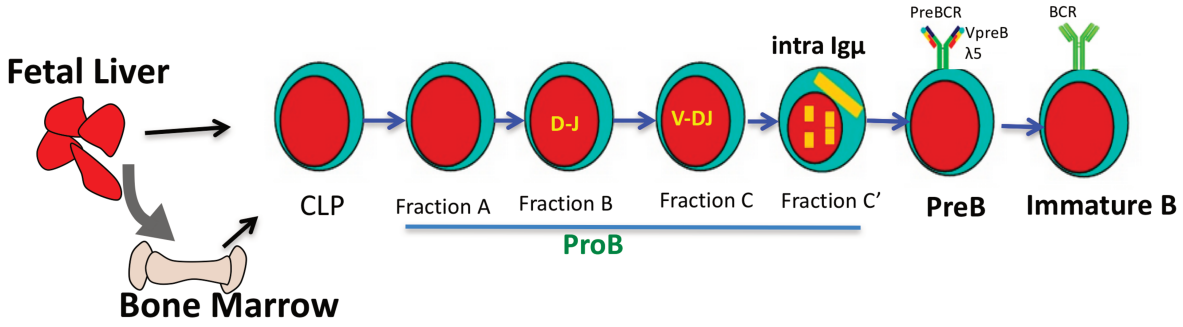

	CLP	Fraction A	Fraction B	Fraction C	Fraction C'	PreB	Immature B
IL7Ra	+	+	+	+	+	+	-
CD19	-	+/-	+	+	+	+	+
B220	-	+	+	+	+	+	+
sIgM	-	-	-	-	-	-	+
intraIgM	-	-	-	-	+	+	+
CD43	-	+	+	+	+	-	-
BP1	-	-	-	+	+	+	-
CD24	-	-	+	lo	hi	hi	-
CD25	-	-	-	-	+	+	-
c-kit	+	+	+	+	-	-	-

Figure 2 Scheme of B cell development and their surface markers

Each developmental stage is indicated by their VDJ rearrangement and Ig heavy or light chain expression status. The hematopoietic stem cells from FL or BM develops into naïve B cells through a number of differentiation steps, including proB, preB and immature B cell stages. proB cells can be further subdivided into four different subpopulations, fraction A, B, C, and C' (Hardy et al., 1991) where different Ig heavy chain locus rearrangement events take place. In fraction B, B lymphocytes are undergoing D to J segment recombination in both loci of Ig heavy chain; In fraction C, B lymphocytes start to rearrange V segment to previously rearranged DJ segment, and after a productive VDJ recombination, intracellular Ig heavy chain is expressed immediately in fraction C'. B lymphocytes at this stage start to express surrogate light chain λ5 and VpreB to form a preBCR together with Ig heavy chain, which mediates the B lymphocyte to go through "positive selection" to reach preB stage, where they initiate Ig light chain rearrangement and expression. After the Ig light chain coupled with heave chain to form a functional BCR on the B cell surface, they will go through "negative selection" to eliminate self-reactive B cell clones or undergo BCR editing to down regulate self-reactivity, followed by egression to the periphery.

2.2.1 Ig heavy chain VDJ rearrangement

The B lineage marker CD19 was introduced to define B cell development and was integrated in the Hardy's scheme. The most immature B lineage cells co-express CD19, B220 and CD43 and can be further subdivided with BP1 and HSA (CD24) cell surface markers into three subsets (fraction B, C and C'). Expression of CD19 first appears in the fraction B cells (defined as $CD19^{+}B220^{+}IgM^{-}CD43^{+}CD24^{+}BP1^{-}$) in the proB stage, marks B lineage commitment and maintenance of B lineage identity, despite that B cell priming is initiated before CD19 expression (Nutt et al., 1999; Rumfelt et al., 2006). In $CD19^{+}$ fraction B stage, B lymphocytes start to rearrange Ig heavy chain (IgH) which are composed of variable (V), diversity (D) and joining (J) antigen receptor gene segments. The Ig heavy chain recombination begins with D_H to J_H at both IgH alleles. This assembly process is mediated by the recombination activating gene 1 and 2 (*Rag1* and *Rag2*), which can bind to the recombination signal sequences (RSSs) that flank the V(D)J gene segments to form the recombination centers (Schatz et al., 1989; Schatz and Swanson, 2011). This process is finely regulated during lymphocyte development (Ji et al., 2010a). During the V(D)J rearrangement, the expression of Rag1/2 is exclusively upregulated in lymphocytes. They form a complex to induce cleavage of DNA double strands at the RSSs, and then the Rag protein cooperates with DNA repair factors to paste the selected DNA double strand ends. This process is called non-homologous end joining (NHEJ). Briefly, the NHEJ is mediated by several core factors comprising Ku70, Ku80, DNA-PKcs (DNA-dependent protein kinase catalytic subunit), Artemis endo/exonuclease, XRCC4, DNA-Ligase IV and Xlf. In the NHEJ of VDJ rearrangement process, first Rag1/2 induced broken DNA ends are recognized and protected by the Ku70/Ku80/DNA-PKcs complex. Then Artemis participates in processing the DNA ends and finally the XRCC4/ DNA-Ligase IV/Xlf complex together with later discovered DNA repair factor PAXX (Paralog of XRCC4 and Xlf) (Xing et al., 2015; Ochi et al., 2015; Craxton et al., 2015) ultimately ligate the ends and reseals the DNA breaks. NHEJ has a critical function preventing genetic instability and controls propensity to develop various types of cancers, notably leukemia and lymphomas (Alt et al., 2013). Through this process the B and T cell receptors generate a large antibody repertoire. Further repertoire diversity is induced by a random insertion of nucleotide without template at the end of DNA double strand break (DBS) by TdT (Schatz and Swanson, 2011).

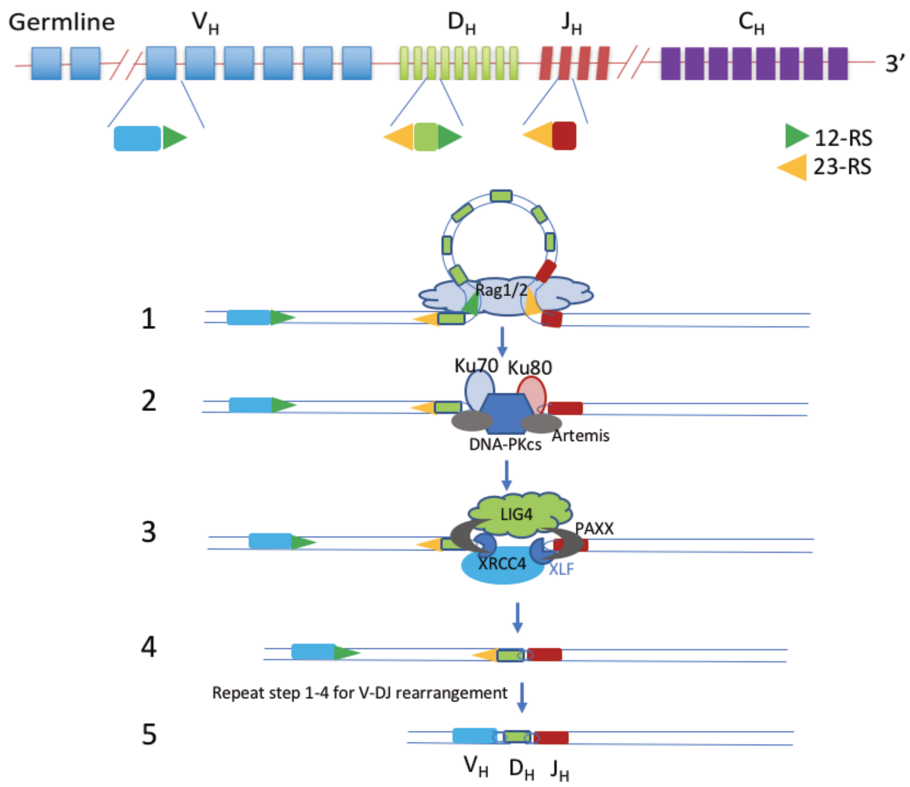

Figure 3 Schematic overview of NHEJ in the V(D)J recombination

DNA double strand breaks are introduced by the RAG proteins, subsequently the DNA is processed and ligated by DNA repair proteins from the NHEJ pathway. Rag1/2 induced broken DNA ends are recognized and protected by the Ku70/Ku80/DNA-PKcs complex. Artemis participates in processing the DNA ends and finally the XRCC4/ DNA-Ligase IV/Xlf/PAXX complex reseals the DNA breaks.

Subsequently, in fraction C defined as $CD19^+B220^+IgM^-CD43^+CD24^{lo}BP1^+$, a variable (V) gene segment can be recombined to a pre-rearranged D_HJ_H-joint to form a $V_HD_HJ_H$ exon, which can code for a variable region of antibody heavy chain when the $V_HD_HJ_H$ rearrangement is productive (in frame) (Jung et al., 2006).

The V(D)J rearrangement allows the generation of highly diverse antibodies by different combination of V, D and J antigen receptor gene segments from the Ig heavy chain (IgH), and V and J segments from the light chain (Igκ or Igλ).

Productive VDJ rearrangement in the fraction C' leads to the expression of the Pre-BCR, which transmits survival signals to the B lymphocyte and triggers several round cell divisions, accompanied by down regulation of Rag1 and Rag2 expression. This developmental stage is also termed larger preB (Mårtensson et al., 2002). Signals from preBCR and the interrupted IL-7R signaling lead the large preB cells to differentiate into resting, small preB stage or

fraction D (defined as $CD19^{+}B220^{+}IgM^{-}CD43^{-}$) where *Rag1* and *Rag2* genes are activated again to mediate Ig light chain locus rearrangement. B lymphocytes that failed to form a productive rearrangement of the Ig chains enter apoptosis.

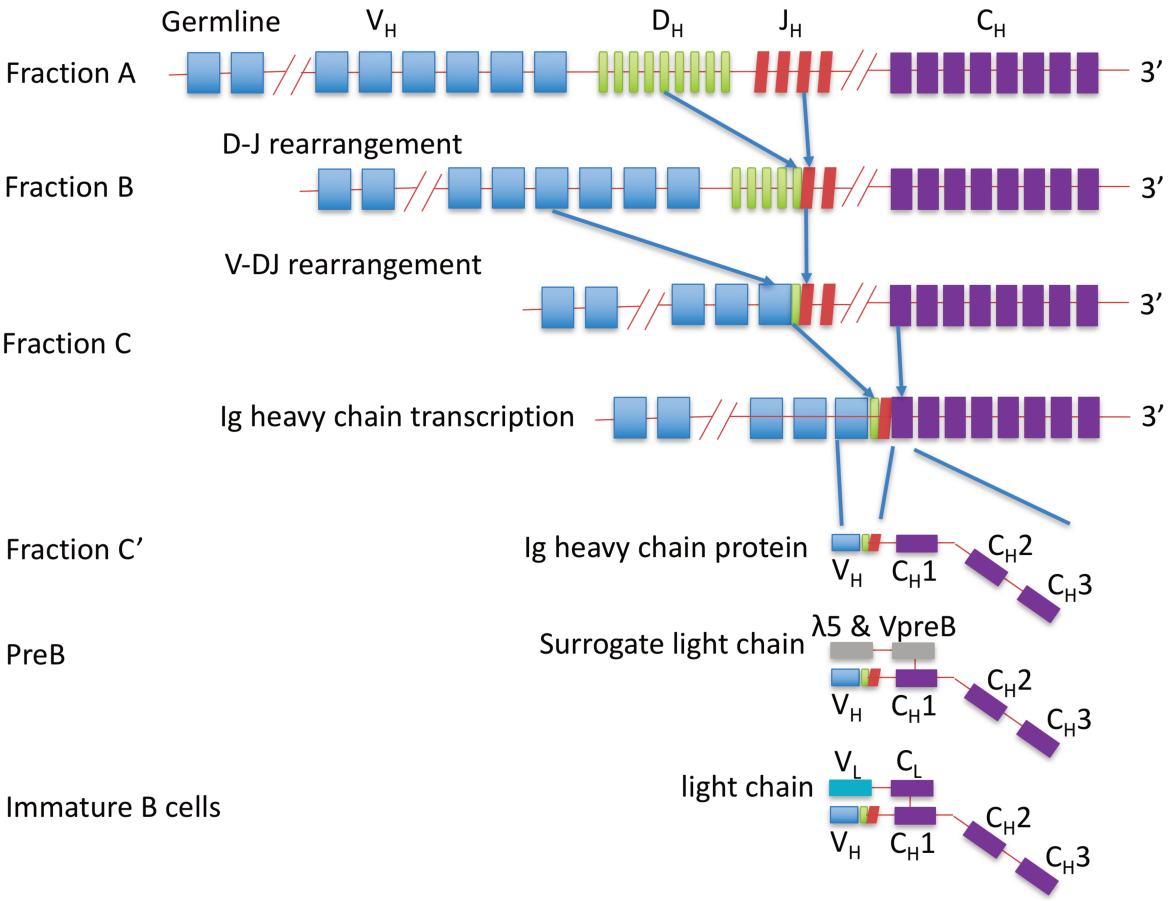

Figure 4 Schematic representation of VDJ rearrangement of Ig heavy chain locus

The recombination events that take place in the immunoglobulin loci are mediated by two enzymes Rag1 and Rag2, expressed mainly during lymphocyte development. In fraction B, Rag proteins first bind the RSS motifs at the 3'end of the D segment and the 5' of the J target segments to mediate recombination. Fraction C Rag proteins target the 3' of the V segment and the 5′of the already rearranged DJ segments, resulting in a VDJ segment. In fraction C', after the formation of a productive VDJ rearrangement, splicing events at RNA level mediate the assembly of the already rearranged VDJ segment with a gene segment of the constant domain to encode the heavy chain, and immediately expression of intracellular Ig heavy chain occurs. B lymphocytes at this stage (preB) start to express surrogate light chains λ5 and VpreB to assemble a preBCR on the cell surface. After light chain rearrangement, they pair with the heavy chain to form a functional BCR on the cell surface of immature B cells.

2.2.2 Pre-BCR selection

Once a productive $V_HD_HJ_H$ recombination has been successful, intracellular Igμ chain is produced in fraction C', defined as $CD19^+B220^+IgM^-CD43^+CD24^{hi}BP1^+$, at which stage B lymphocytes start to assembly Pre-BCR and go through the Pre-PCR check point, also termed positive selection. Pre-BCR complex, similar to the structure of BCR, contains two Igμ chains, two surrogate light chains (SLCs) and signal transduction subunits Igα and Igβ. The difference between the SLCs and the conventional light chain IgL is that, in contrast to a rearranged IgL, the SLC is composed of two germline-encoded invariant proteins, VpreB and λ5. Although Pre-BCR is only transiently expressed, it is an important check point of B cell development. Once the Pre-BCR is expressed on the cell surface, signals from the Pre-BCR provide a rapid feedback and cells undergo further differentiation and maturation. Lack of the components of this Pre-BCR lead to arrested B cell development in proB cell stage. In $\mu mt^{-/-}$ mice, which lack transmembrane region of Igμ, results in a block of B cell development in proB cell stage (Kitamura et al., 1991). In mice deficiency in either SLC component λ5 (Kitamura et al., 1992) or Igα/Igβ (Gong and Nussenzweig, 1996; Pelanda et al., 2002) B cell development is also arrested at the proB cell stage. Similar B cell arrest phenotype has also been observed in mice deficient in VpreB1 and VpreB2, which are two major isoforms of VpreB SLC (Mundt et al., 2001). However, in contrast to Rag1 or Rag2 deficient mice, B cell development in mice lack SLC components (λ5 or VpreB) is not completely blocked, rare light chain rearrangement prior to heavy chain in proB cells can coupled with Igμ form a functional BCR to bypass preBCR check point (Shimizu et al., 2002). The initiation of Pre-BCR signaling is still not clear whether or not is a ligand dependent process. Some studies showed that Galectin-1 and heparin sulfates, produced by the BM stromal cells, can bind the preBCR (Gauthier et al., 2002; Bradl et al., 2003). However, no apparent B-cell phenotype is observed in galectin-1 deficient mice, indicating that it remains possible that the pre-BCR interacts with other ligands. More evidence added by showing the positive charged protein λ5 is crucial for interacting with some matrix structures in the FL and BM microenvironment, such as insulin, lipopolysaccharide, galectin and heparin sulfates (Köhler et al., 2008). The poly-reactive λ5 might mediate the crosstalk between preB cell and the microenvironment and facilitate the preBCR signaling initiation.

PreBCR signaling triggers proliferation (several rounds of division in fraction C') before IgL chain rearrangement in the fraction D stage. This process is thought to be mediated by the PrePCR signaling through phosphoinositide 3 kinase (PI3K)-protein kinase B (PKB, also

called AKT) pathway (Manning and Toker, 2017; Herzog et al., 2009). Pre-BCR signaling also provides a feedback of the productive VDJ rearrangement of IgH locus that feeds back thus inhibiting V_H to DJ_H recombination at the second IgH allele to establish allelic exclusion via downregulating *Rag1/2* expression (Grawunder et al., 1995; Mårtensson et al., 2002). Allelic exclusion is of great importance to guarantee a single BCR specificity on the B cell surface. Mono-specificity of BCR allows efficient generation of self-tolerant B cells and contributes to establishing efficient antigen-specific antibody responses. The decision of which allele is going to rearrange is mainly accomplished by pre-established epigenetic marks, such as DNA methylation and histone modification (Cedar and Bergman, 2008). Thus, antigen receptor genes rearrangement and allelic exclusion ensure the immune system to generate millions of different antibodies to respond against millions of different antigens in a mono-specificity manner.

2.2.3 Ig light chain VJ rearrangement

In fraction D, successful Ig light chain rearrangement leads to the expression of a complete BCR on the cell surface and cells become immature B lymphocytes defined as fraction E ($CD19^+B220^+IgM^+IgD^-$). In this process, B lymphocytes close their IgH chain loci and open the light chain loci including κ and λ chain and the rearrangement machinery is reactivated, i.e. RAG1 and RAG2. Light chain rearrangement first takes place in κ chain locus by bringing together *Vκ* gene segments and *Jκ* gene segments (Woof and Burton, 2004). A functional, in frame-rearranged κ light chain can associate to the pre-expressed IgH to form a BCR expressed on the B cell surface. Failed κ light chain rearrangement from both alleles leads to λ light chain gene rearrangement by bringing together a Vλ and Jλ. Functional λ light chain also can pair with the pre-expressed IgH to form a BCR in immature B cell or fraction E, which can egress from the BM to the peripheral secondary lymphoid organs to complete their maturation (Allman et al., 2001).

This hierarchical light-chain rearrangement process is supported by the evidence that impaired V-J rearrangement was observed by deletion of either Igκ enhancers or deletion of genes encoding histone-modifying enzymes or transcription factors (Inlay et al., 2002; Ribeiro de Almeida et al., 2015). Thus, Igκ locus accessibility is regulated by the recruitment of epigenetic markers as well as transcriptional machinery.

2.2.4 BCR receptor editing

Before the immature B cells leave BM, B lymphocytes undergo another check point resulting in BCR self-tolerance and elimination of B cells bearing a BCR with strong affinity against self-antigens (Norvell et al., 1995). This is accomplished by apoptosis termed clonal deletion or via modifying its receptor to form a low self-reactive BCR through receptor editing (Halverson et al., 2004). The model of receptor editing proposed by Sebastian et al. postulates that B cells that produced an autoreactive BCR, leading to the cross linking of self-antigens, trigger internalization of BCR. This induces a secondary *IgL* gene rearrangements (receptor editing) by downregulating PI3K-AKT signaling and upregulating FOXO transcription factor expression. In this process, PI3K signaling plays an important role in regulating RAG1 and *Rag2* expression. Inhibition of PI3K induces *Rag1* and *Rag2* expression and promotes *IgL* gene recombination. In agreement with this notion is the observation that immature B cells in PI3K subunit p85α deficient mice, in which *Rag1* and *Rag2* expression is poorly suppressed, undergo excessive receptor editing (Verkoczy et al., 2007b). Likewise, mice deficient in spleen tyrosine kinase (SYK) or CD19, both of which molecules are required for PI3K signaling exhibit excessive receptor editing. Receptor editing even in non-autoreactive B cells is promoted by loss of SYK, which suggests that SYK reinforced PI3K signaling suppress receptor editing (Meade et al., 2004). Downregulation of PI3K-AKT signaling results in re-expression of the RAG1-RAG2 recombination machinery (Tze et al., 2005; Verkoczy et al., 2007a). If the editing process result in a non-autoreactive BCR, this is then stably expressed on the cell surface, leading to constant BCR signaling activity, then the PI3K-AKT activity can be restored, which in turn terminate *IgL* gene recombination through downregulation of FOXO transcriptional factor. Consequently, non-autoreactive BCR expression on the B cell surface allows transit through the check point or negative selection and migration out of the BM to the periphery where B cells acquire IgD expression and become mature B cells, which are defined as fraction F stage ($CD19^+B220^+IgM^+IgD^+$) according to Hardy's scheme. These mature B cells (fraction F) can also circulate to other peripheral organs.

3 B cell activation

The activation of B cells can occur with or without T cell help, correspondingly termed as T cell-dependent (TD) responses and T cell-independent (TI) responses.

TI responses can be further divided into TI type 1 (TI-I) and TI type II (TI-II) responses according to the engagement of BCR in the B cell activation. TI-I B cell activation results from the cross linking of TLR and BCR but cannot be accomplished by TLR activation alone. TI-II response is dependent on BCR engagement, or cross-linking of numerous BCRs, i.e. polysaccharides can cross-link the BCR on B cell surface because of their repeated antigenic sites. In a TD response, B cells not only need a signal for BCR, the second signal provided by the T helper cell is also required, this second signal for B cell activation can also come from other cells, such as DCs (Cerutti et al., 2012). The innate-like B cell subsets MZBs and B1 cells are more prone to respond to TI antigens. Their BCR repertoire is limited but showed specificities to TI antigens, such as microbial carbohydrates, glycolipids or the apoptotic cells (Kearney, 2005). Upon activation by antigen, innate-like MZBs and B1 cells can differentiate into antibody producing cells. However, some studies supported that in TI-II immune responses, B cells can generate memory B cells (de Vinuesa et al., 2000; Obukhanych and Nussenzweig, 2006). TD antigens are mainly protein antigens, they have complex structure of antigen epitopes. FOBs are mainly responsible for the response to the TD antigens. Briefly, the naïve B cells in the secondary lymphoid organs, spleen and lymph nodes, get activated after encountering TD antigens and undergo proliferation. Proliferating B cells differentiate into short-lived plasma cells or form a GC, composed of dark zone (DZ) and light zone (LZ). In the DZ, activated B cells undergo clonal expansion. The cells that exit the cell cycle migrate to the LZ, where affinity maturation takes place by receiving signals from antigen presenting follicular dendritic cells (FDCs) and antigen-specific T follicular helper (TFH) cells. The affinity-selected GC B cells can re-enter the GC to regain a cycling phenotype. Alternatively, GC B cells further differentiate to memory B cells (MBC) or to long-lived plasma cells (LLPC) for the serological memory or antibody secreting.

3.1 The germinal center

After B cells activated by antigens the GC appear in the follicles of secondary lymphoid organs in TD response. The chemokine CC receptor 7 (CCR7), which binds the chemokine CC ligand 21 (CCL21), guides the activated B cell towards the T-B zone where GCs are formed. B cells expand extensively and form the DZ, upregulate AID expression, which mediates somatic hypermutation (SHM) and class switch recombination (CSR). AID transfers deoxycytidine into deoxyuridine at the immunoglobulin genes thereby triggering mutagenic

DNA repair (Muramatsu et al., 1999). SHM is a process that introduces random point mutations in the variable-region gene segments of the BCR resulting in altered BCR affinity to antigens. Because mutations are random, this process can lead to unchanged, increased or decreased BCR affinity and to self-reactive BCR. BCR diversification facilitates B cells to form a more efficient BCR to neutralize antigens or pathogens. This process is mainly taking place in the DZ of GC.

In order to select B cells with sufficiently affinity against the antigen encountered, some of the B cells exit cell cycle and migrate to the LZ, where they get signals from FDCs and TFH cells through TCR-MHC complex, as well as cytokine signaling pathway (e.g. IL 21 and IL 4). The FDCs present antigens to B cells by using complement and FcRs rather than antigen-MHC complex (Aguzzi et al., 2014). This allows for antigen-driven selection of high affinity BCR. B cells that do not get selected undergo apoptosis and phagocytosis by macrophages (Smith et al., 1998). B cells that enter LZ also get the help from TFH in a TD response, which is essential for affinity maturation as well as memory B cell production. The TFH cell is a specialized T helper cell subset, which expresses CXCR5, PD-1 (programmed cell death protein 1), ICOS and CD40L and secretes the cytokine IL-21. TFH cells interact with LZ B cells to facilitate B cells selection and also play a role in B cells differentiation into memory B cell or an antibody secreting plasma cell. B cells in the LZ also have a third option, to re-enter the DZ and go through more rounds of proliferation, SHM and selection.

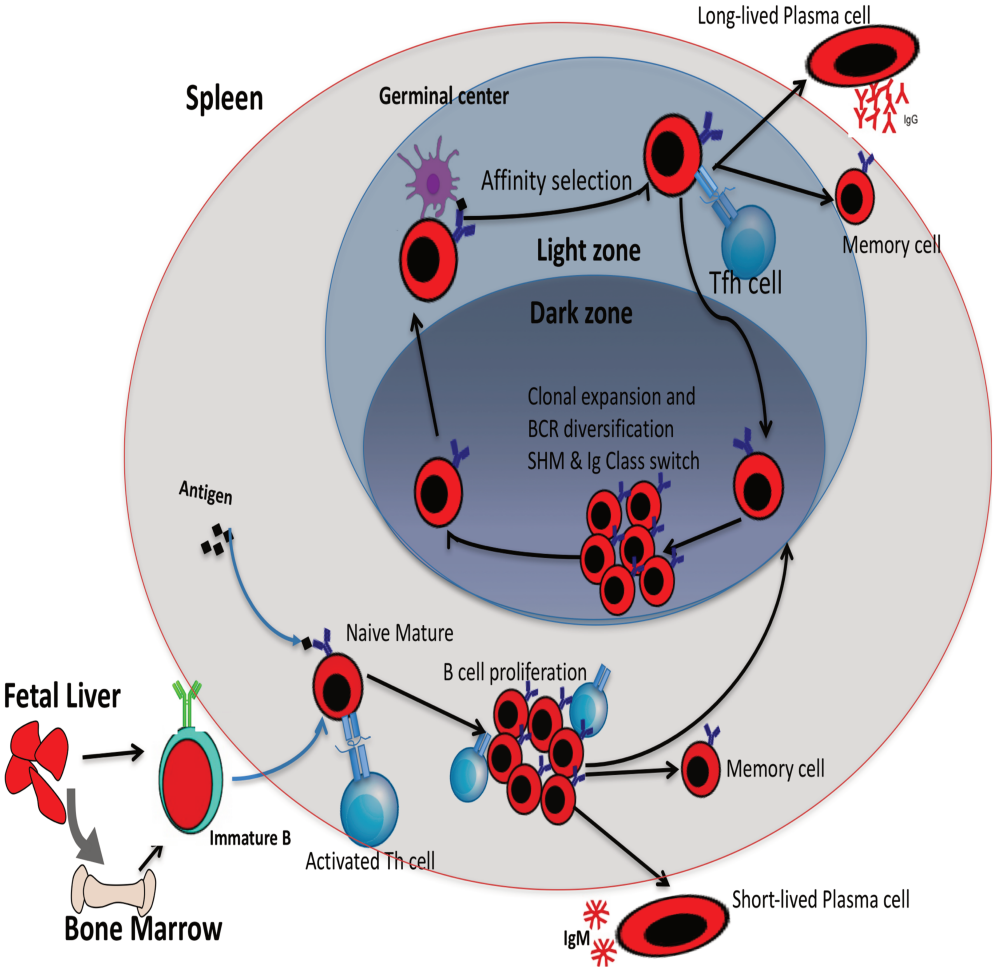

Figure 5 Germinal center reaction

Antigen-activated B and T cells migrate towards the borders of the B cell follicles and the T cell zones of secondary lymphoid organs, respectively, which leads to the establishment of stable B cell–T cell interactions and allows B cells to receive helper signals from cognate $CD4^+$ T cells. Activated B cells and T cells then migrate to the outer follicles, where B cells undergo proliferation. Some of the proliferating B cells differentiate into short-lived plasma cells, and some integrate the GCs. In the DZ of the GC, the clonal expansion of antigen-specific B cells is accompanied by B cell receptor (BCR) diversification through somatic hypermutation and Ig class switch. The B cells that exit the cell cycle relocate to the LZ, where affinity selection takes place through interaction with immune complex-coated FDCs and antigen-specific TFH cells. The selected GC B cells can re-enter the GC cycle. Alternatively, these GC B cells exit the GC, either as memory B cells (GC dependent memory B cells) or as long-lived plasma cells that contribute to serological memory.

CSR is another AID-induced process taking place in GC and the main function of this process is to switch the isotype class of the BCR. Naïve B cells that are antigen-inexperienced express membrane IgM and IgD BCR. After activation by antigen stimulation, these B cells proliferate and receive signals via CD40 and cytokine receptors, which triggers Ig class switch and produce other Ig isotypes, IgG, IgA or IgE. During class switch, the BCR only changes the constant region of the immunoglobulin heavy chain and therefore antigen specificity remains unchanged. This allows different daughter cells from the same activated B cell to produce antibodies of different isotypes that confer different effector functions (e.g. IgG1, IgG2 etc.) (Kaminski and Stavnezer, 2004). Different pathogens can induce distinct cytokine response pattern, which in turn influence Ig class switch profile to better combat the infection (Castigli et al., 2005).

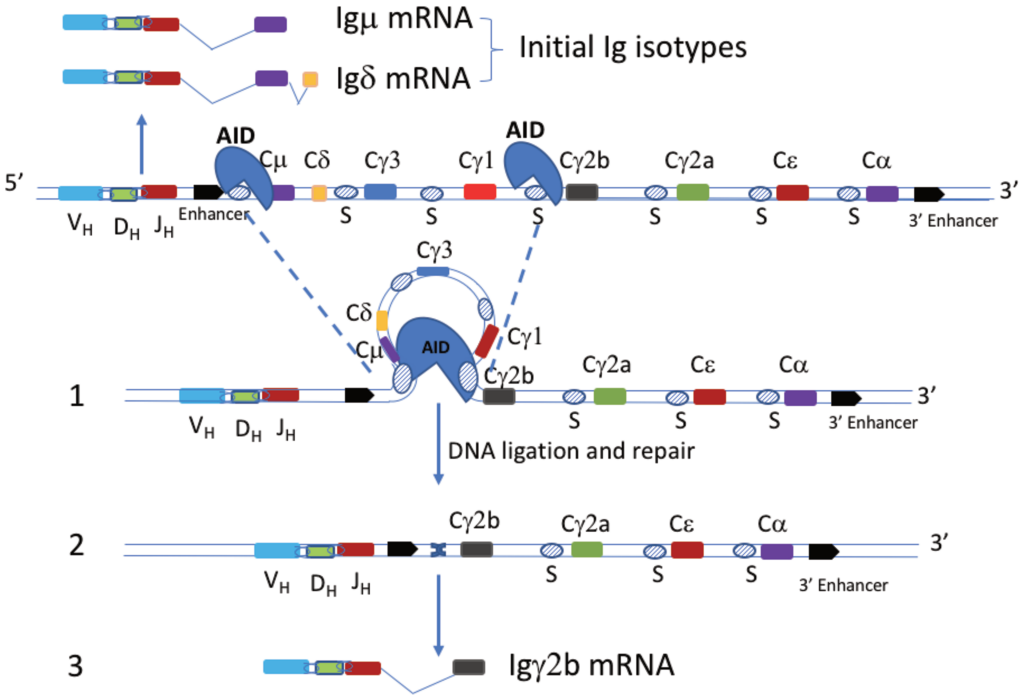

Figure 6 Diagram of Ig class switch

The initial BCRs expressed on the surface of naive B cells are IgM and IgD. During the class switch reaction (e.g. switch to Igγ2b) AID deaminates the Sm and Sγ2b regions, inducing DNA double strands breaks formation. The Sμ and Sγ2b regions recombine through an intrachromosomal deletional recombination, which links the prior rearranged VDJ segment to the *Cγ2b* gene. After RNA splicing, Ig heavy chain γ2b mRNA is expressed. 5' and 3' enhancers are the two major regulators in the expression of Ig heavy chain genes and CSR.

3.2 Plasma cells

Secreted neutralizing antibodies are of great importance to humoral response to protect the host against the infections caused by pathogens. The antibody secreting function is mainly accomplished by plasma cells. Upon activation, B cells can differentiate to centroblasts and antibody producing plasma cells. Plasma cells are larger in size than other B cells because they exhibit a larger cytoplasm containing extended endoplasmic reticulum to maintain the production, storage and secretion of large quantities of antibodies (Pelletier et al., 2006). They are characterized by downregulated pan B cell marker B220, upregulated cell surface marker CD138 and of transcription factor Blimp-1 (Shaffer et al., 2002).

Plasma cells can be divided into two different pools, short-lived and long-lived plasma cells, according their life-span. The life span of short-lived PCs is 3-5 days (Ho F, 1986). They are thought to be generated from extra-follicular foci in the secondary lymphoid organs through a GC independent pathway, majority of the short-lived PCs secrete low affinity IgM antibodies. In contrast, the long-lived PCs can persist for months or years in mice and perhaps decades in human (Manz et al., 1997), they are mainly generated through a GC dependent pathway and secrete high affinity, isotype switched antibodies (Manz et al., 1997). Sustained pathogen specific antibodies secreted by short- and long-lived PCs are essential for protective immunity against infection.

In a TI response, plasma cells can also be generated through a GC independent pathway in the extrofollicular foci in the spleen (Ho et al., 1986), but most are short lived IgM secreting plasma B cells. In a TD response the majority of the plasma cells are produced in a GC dependent pathway (Kräutler et al., 2017), and differentiation into PCs is induced among a discrete subset of high-affinity B cells residing within the LZ of the GC. Majority of long-lived plasma cells home to the BM and reside there for a long-term secretion of antigen-specific antibodies. A small population of long-lived plasma cells can also be found in the spleen (Sze et al., 2000).

3.3 Memory B cells

The success of humoral response also depends on the memory B cell reaction in case of the host encounters the same pathogens again. Antibodies secreted by the plasma cells provide the first layer of humoral defense against reinfection if the antibody concentration is sufficiently high to protect the host. A second line of humoral defense that is pathogen-

experienced memory B cells are rapidly reactivated to produce antibodies. This memory response is typically activated faster, and of greater magnitude and produce antibodies with switched isotypes and higher affinity. As the majority of the antibodies generated following secondary antigen challenge are of switched isotypes and have higher affinity compared to the antibodies generated in the primary response, it is thought that memory B cells derive from the B cells bearing a class-switched and high-affinity B cell receptors (BCRs) on their surface. However, some groups also provided evidence to show the presence of GC independent memory B cells (Taylor et al., 2012; Kaji et al., 2012), as well as unswitched IgM^+ memory B cells (Pape et al., 2011), in addition to the classic GC dependent B memory cells pathway. It's still not clear whether these distinct memory B cell subsets have different roles in the humoral response.

What governs the fate of activated B cells to differentiate into a memory B cell or to a plasma cell through a GC dependent pathway is a question that was addressed in several laboratories (De Silva and Klein, 2015; Nutt et al., 2015; Shlomchik and Weisel, 2012; Victora and Nussenzweig, 2012a). It was shown that the cell fate in the GC can be regulated by signals transduced by CD40, as well as the cytokines IL4 and IL21. In vivo antibody inhibition and genetic deletion studies added more pieces to the puzzle. Blocking GC with anti-CD40 or ICOSL antibodies, lead to a decreased long lived plasma cell (LLPC) response (Takahashi et al., 1998; Taylor et al., 2012). Deletion of CR1 and CR2 (Gatto et al., 2005), interleukin 21 receptor (IL-21R) (Linterman et al., 2010; Zotos et al., 2010), PD-1, PD-L1 and PD-L2 (Good-Jacobson et al., 2010), CD80 (Good-Jacobson et al., 2012) affect proper GC maturation or progression but not GC initiation. All the studies above showed a decreased LLPC numbers, which correlated with improper GC progression while early memory B cell (MBC) populations are mainly unaffected (Good-Jacobson and Shlomchik, 2010). Recently, a study showed that MBC and LLPC could be generated at different time points during the course of the GC maturation or progression (Weisel et al., 2016).

In summary, the quality and quantity of a memory response will be different depending on the GC reaction, T-B contact, the type of B cell activation and the type of antigen, as well as the strength of various signaling involved in this process (Alugupalli et al., 2004).

4 B cell signaling

B cell activation can be achieved thought a complex network of signaling pathways depending on different receptors on the B cell surface. The BCR signaling is one of the most important activators of B cells. Numerous studies have showed the importance of BCR signaling for B cell development, fate and activation. In the B cell development in both FL and BM, signaling through preBCR and BCR are responsible for the preBCR selection, as well as negative selection for eliminating self-reactive B cell or triggering BCR editing, respectively. BCR also plays crucial role during the transition from immature to mature B cell, GC formation and progression, SHM and B cell differentiation into MBCs and LLPCs (Niiro and Clark, 2002). The binding of antigen to the BCR triggers a series of catalytic cascade by activating the protein tyrosine kinase Lyn of the Src family kinases. This process is accomplished by two components of BCR complex, Igα and Igβ, which contain immune-receptor tyrosine activation motifs (ITAMs) in their cytoplasmic tails that can get phosphorylated by Lyn. This can in turn phosphorylate another tyrosine kinase, Syk, that triggers the formation and activation of a multi-component complex, comprising Bruton tyrosine kinase (BTK), AKT, phosphoinositide 3-kinase (PI3K), and B cell-linker protein (BLNK). Signals transduced by BCR co-receptor CD19 is also important for PI3K, BTK and AKT activation, which triggers the downstream signaling cascade, leading to different effects, such as the calcium influx and activation of nuclear factor-κB (NF-κB). This process eventually regulates B cell survival, proliferation, cell fate and response (Srinivasan et al., 2009).

Inhibitory signaling events play an important role in attenuating immune responses through different inhibitory receptors on the B cell surface. Such as CD22, PD-1, CD72 and paired immunoglobulin-like receptor B (PirB), as well as FcR. Signaling downstream of these inhibitory receptors can activate Lyn which in turn phosphorylates their cytoplasmic ITIM. Then activates the SH2-domain-containing inositol polyphosphate 5' phosphatase (SHIP), which dephosphorylates PIP3, leading to Btk and PLCγ2 to dissociate from the cell membrane. The outcome of this process is inhibition of calcium flux and suppression of proliferation by decreasing the proliferative signals transduced by survival factor Akt and/or the mitogen-activated protein (MAP) kinase (Pritchard and Smith, 2003). Thus, the Akt pathway could play a dual role in both inhibitory and activating consequences in B cell response (Limon and Fruman, 2012).

Both positive and negative signals are adopted for the affinity maturation and selection in the GC, to avoid the selection of B cells with low affinity or self-reactive BCRs through apoptosis. In plasma cells, these pathways regulate the antibody production when the presence of antigen-antibody complexes reach potentially harmful levels. It has been shown that mice lacking negative regulatory signals can develop autoimmune diseases (Bolland and Ravetch, 2000; Pritchard and Smith, 2003).

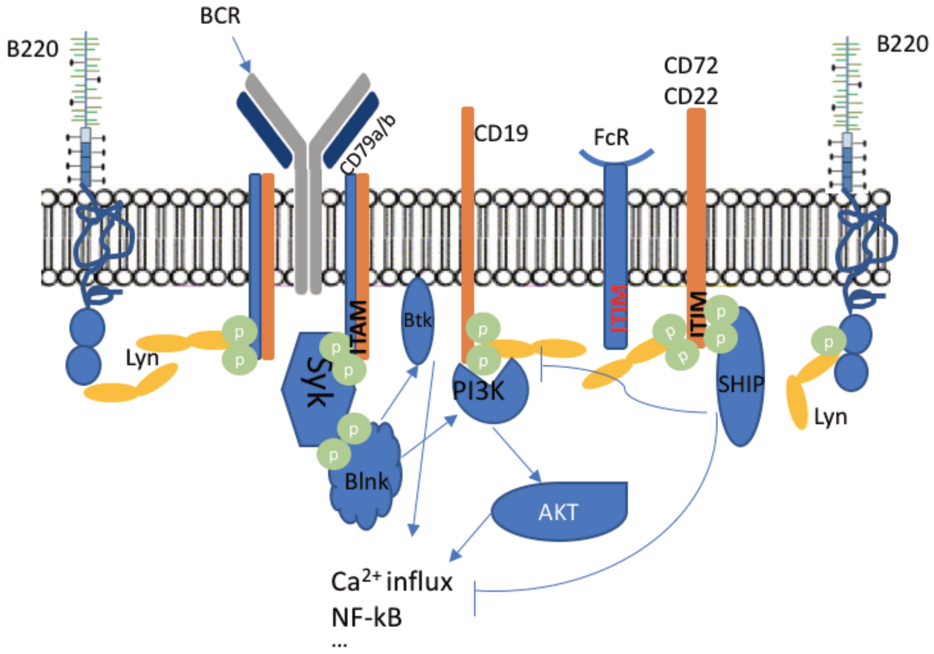

Figure 7 Regulation of BCR signaling.

The BCR complex is composed of a membrane Ig and two non-covalently components CD79a and b. After antigen engagement, CD79a/b recruits the Src family kinase Lyn, which phosphorylates immune-receptor tyrosine activation motifs (ITAMs) on the CD79a/b chains of the BCR complex. Then Syk is activated by binding to the phosphorylated ITAMs. Syk serves as a docking site for Blnk, Btk, PLCg, etc. Together these molecules trigger a series of downstream biochemical events leading to coordinated gene expression, cell activation, and proliferation, or death by apoptosis. BCR signaling is downregulated by a group of phosphatases including SHIP, PTEN, SHP1, etc. CD45 phosphatase activated Lyn can either up- or down-regulate BCR signaling through activating Syk or various phosphatases such as SHIP, through phosphorylates ITIMs of the negative regulator (e.g. CD72, CD22).

4.1 Positive and negative regulation of B cell response by CD45

CD45 is known as protein tyrosine phosphatase receptor type C (PTPRC), which is a member of PTP family. CD45 is exclusively expressed in hematopoietic cells. It plays an important role in regulating a variety of cellular processes, such as cell growth and differentiation. CD45

is composed of one extracellular domain, one transmembrane domain and two tandem intracytoplasmic catalytic segments. It has been shown to have an essential role in T- and B-cell antigen receptor signaling (Kishihara et al., 1993; Byth et al., 1996). CD45 family consists of multiple isoforms, which have different distribution in hematopoietic cells. One of the isoforms dominantly expressed on B cells is CD45R with large amount of glycosylation, which increases the molecular weight to 220kDa, hence named B220. B220 expressed on B cells is of great importance for BCR signaling. Extensive studies demonstrated that CD45 could play a dual role in regulating BCR signaling by either direct interaction with components of BCR complexes or through regulating various Src family kinases (Trowbridge and Thomas, 1994), which could also play dual role in BCR signaling.

In *Cd45* deficient mice, B cell development is arrested, in particular Src family kinase (SFK) activity in *Cd45*$^{-/-}$ B cells is dysregulated (Thomas, 1994; Huntington and Tarlinton, 2004a), and phosphorylation of CD19, a co-stimulator of BCR is also impaired. In addition, *Cd45*$^{-/-}$ B cells show a severely impaired BCR-mediated proliferation, as well as blocked B cell maturation at a transitional stage in the spleen. Furthermore, deletion of autoreactive *Cd45*$^{-/-}$ B cells are also impaired (Zikherman et al., 2012); both phenomena are considered to reflect an increased threshold of BCR signaling.

The molecular and cellular mechanism underlying the defected response of *Cd45*$^{-/-}$ B cells to BCR ligation are a reduced activation of extracellular signal–regulated kinases (Erk1/Erk2) and MAP kinases, phosphatidylinositol-3-OH kinase (PI(3)K) and the transcription factor NF-κB. CD45 expression in B cells is not required for GC initiation but was essential for GC persistence due to failed upregulation of anti-apoptotic Bcl-2 family members and to impaired CD40 signaling-induced proliferation thus triggering B cell apoptosis. The defected GC persistence could be partially rescued by enforced expression of anti-apoptotic factor Bcl-xL (Huntington et al., 2006; Huntington and Tarlinton, 2004b).

CD45 deficient BCR transgenic B cells failed to be negatively selected in the presence of the cognate antigen (Cyster et al., 1996). This study reinforced the notion that in the absence of CD45, BCR signaling is dramatically weakened, leading to the conclusion that CD45 is a crucial positive regulator of the BCR.

CD45 associated BCR signaling transduction through SFKs, such as Lyn and Fyn, can also have negative effects. After BCR stimulation, Lyn rapidly initiates a negative regulatory feedback loop by phosphorylating ITIMs in the cytoplasmic domains of inhibitory receptors such as CD22 and Fcγ RIIB. This allows recruitment of SHP1 and SHIP, facilitating downregulation of the B cell response (DeFranco et al., 1998). CD45 also exerts its negative

regulatory role incorporated with BCR complex following antigen binding. BCR engagement results in the aggregation of multi-signaling-component to form a lipid raft structure, but the CD45 molecule is excluded from the central raft (Weintraub et al., 2000; Shrivastava et al., 2004; Cheng et al., 1999). Because CD45 constitutively inhibits SKFs by dephosphorylating their regulatory sites, the movement of CD45 away from the BCR complex facilitates the phosphorylation and activation of SFKs. The activated SFKs within the lipid raft will then phosphorylate the ITAMs within the BCR complex raft and initiate signal transduction. After a period of activation, CD45 move back to the rafts and re-associate to the BCR complex, leading to reduced Lyn activity through dephosphorylation, which in turn attenuates BCR signaling (Gupta and DeFranco, 2003; Shrivastava et al., 2004). In this process, the dynamic behavior of CD45 serves as a regulator to fine-tune BCR signaling through the regulation of SFKs activity.

4.2 Calcium Signaling in B Cell Activation and Biology

Calcium signals in immune cells may regulate a variety of cellular processes, such as differentiation and activation. For B cells, an increased calcium influx can be induced by the engagement of BCR, as well as chemokine and co-stimulatory signaling. When encountering their specific antigen, intracellular signaling is activated through BCR, which is a fundamentally important event for the development of adaptive immunity. One of the key signals for B cell physiological outputs is the increase of intracellular free calcium ion (Ca^{2+}). The first observation that BCR stimulation induces Ca^{2+} mobilization inside B cells came from a study using labeled $^{45}Ca^{2+}$ ions (Braun et al., 1979). Intensive studies established the important role of Ca^{2+} signaling in B cell responses, and the molecules regulation of Ca^{2+} flux. The binding of an antigen to the BCR triggers the recruitment of multiple signaling components including PTK and their substrates, eventually leading to the activation of phospholipase C-γ2 (PLC-γ2) signaling pathway (Kurosaki and Baba, 2010; Scharenberg et al., 2007). Activated PLC-γ2 hydrolyzes the membrane lipid phosphatidylinositol-4,5-bisphosphate to generate two second messenger products: the membrane lipid diacylglycerol (DAG) and the diffusible soluble inositol-1,4,5,-triphosphate (IP3). IP3 spreads into the cytosol and binds to the IP3 receptors (IP3R) on the membrane of endoplasmic reticulum (ER), leading to the rapid release of Ca^{2+} from the ER store into the cytosol and the extracellular Ca^{2+} influx into the cytosol (Baba and Kurosaki, 2009; Parekh and Putney, 2005). Ca^{2+} influx therefore is linked to the strength of BCR signaling.

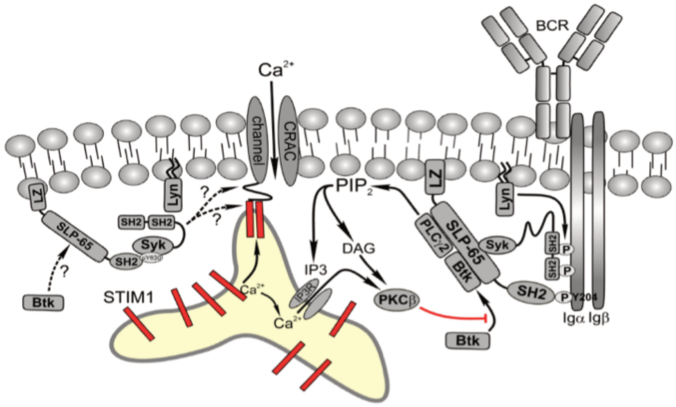

Figure 8 Mechanism of BCR mediated calcium mobilization in B cells (King and Freedman, 2009)

BCR stimulation by antigen activates the Src kinase Lyn, which phosphorylates ITAMs on the Igα and Igβ(CD79a/b) chains to activate Syk that phosphorylates the adaptor protein SLP-65(BLNK). Phosphorylated SLP-65 serves as a docking site for PLCγ-2 and Btk that initiates calcium signaling. Activated PLCγ-2 hydrolyzes membrane PIP2 into diacylglycerol (DAG) and IP3, binding of IP3 to its receptors triggers calcium release from the ER. The decreased calcium levels in ER leads to in turn triggers calcium influx.

5 Epigenetic regulation of B cell development

Epigenetic alterations regulate gene expression to control different cellular functions (Zan and Casali, 2015), through histone modification, such as histone methylation, acetylation, phosphorylation, or ubiquitination, which can lead to altered expression of different target genes, and in turn affecting cell development, or even modulating cell functions in both physiological or pathological conditions (Obata et al., 2015). Epigenetic regulation could be accomplished by various chromatin-modifying epigenetic factors, such as polycomb repressive complexes (PRCs), which can bind to specific targets of chromatin region and catalyze the methylation of Lys27 residues on histone H3 to generate H3K27me2/3 (Van Bortle and Corces, 2012). Lysine methylation in histones is one modification associate with genomic organization, which is accomplished by both lysine methyltransferases (KMTs) and lysine demethylases (KDMs). These two enzymes can introduce or diminish different degrees of methylation at specific lysine residues within the histone tails, leading to specific gene repression or transcriptional activation.

In the context of B cell development and GC response, histone modifications play important roles to fine tune this process, in particularly, B cell differentiation, maturation and activation are all under the control of epigenetic regulation (Good-Jacobson, 2014). Activation of the

transcription factors Ikaros, E47, Ebf1 and Pax5 coupled with epigenetic regulation of lymphoid and B cell-associated genes is responsible for promoting B cell specification and commitment (Santos and Borghesi, 2011). The major epigenetic marker responsible for B lymphocyte commitment is methylation of H3K4 (H3K4me) at the enhancer regions of B cell lineage specific genes (Mercer et al., 2011). Methylation at H3K4 of transcription factors E2A associated genes orchestrates B cell commitment during the CLP to proB transition, and subsequently, B cell specific genes. This process is regulated by the transcription factors EBF and FOXO1 (Lin et al., 2010). In both proB and preB cells, E2A regulates different B cell associated genes expression by introducing H3 acetylation activating marks or repressive methylation markers H3K27me3 to their regulatory regions (Treiber et al., 2010).
Other epigenetic marks, such as ubiquitination, have also proved to play a role in regulating early B cell development. Histone H2A deubiquitinase coding gene *Mysm1* deficient mice show a drastic decrease of B cells in the bone marrow, peripheral blood, and lymph nodes. The mechanisms underlying this phenotype comprise the antagonistic function of MYSM1 PRC1 in the *Ebf1* promoter, increasing the chances to recruit some of B cell lineage specific transcription factors, such as E2A to upregulate *Ebf1* transcription (Jiang et al., 2011).

In proB cells, the most important event taking place is Ig heavy chain locus V(D)J recombination. At the start of the V(D)J recombination, histone H3 acetylation is abundant within a 120 Kb region that contains the DH gene segments, and after DJ rearrangement, the hyperacetylated domain extends to the distal VH segments. The histone modification (acetylation) pattern synchronizes with the V(D)J rearrangement (Su and Tarakhovsky, 2005). Methylation of histone H3 on lysine residues like H3K9 is sufficient to repress RAG protein complex accessibility which in turn decreases the efficiency of V(D)J recombination (Su and Tarakhovsky, 2005). *Pax5* (Johnson et al., 2004) removes this repressive methylation thus enhancing the accessibility of RAG complex. Trimethylation of lysine 4 in histone H3 (H3K4me3) is also shown to correlate well with V(D)J recombination (Ji et al., 2010b). The plant homeodomain (PHD) finger of RAG2 protein can specifically bind to H3K4me3 (Matthews et al., 2007), guiding RAG2 to regions of active chromatin and enhancing the catalytic activity of the RAG complex (Schatz and Ji, 2011).

Epigenetic modifications tightly regulate microRNAs expression thus controlling of B cell development. In particular, S. Kuchen et al showed that the repressive mark H3K27me3 is associated with gene silencing of lineage-inappropriate miRNA during lymphopoiesis (Kuchen et al., 2010). Mice deficient in Ago2, which encodes a protein essential for

microRNA biogenesis and function, showed a block in B cell development at the pro-B cell stage (O'Carroll et al., 2007). Likewise, totally abolishing miRNA by deletion of Dicer in proB cells, results in a complete block in B cell development at the proB cell stage (Koralov et al., 2008). In addition, miR-181, miR-150, miR-17-92, have a regulatory role in proB cells, while miR-34a acts in preB cells, and miR-185 in immature B cells (Kuchen et al., 2010).

6 Epigenetic regulation of B cell response

Following productive Ig recombination and expression of the BCR on the cell surface, B cells undergo terminal differentiation dependent on signals from the BCR (Rajewsky, 1996). The majority of naïve B cells in the periphery are in a resting state. Once activated, they either initiate GC reaction or differentiate into antibody secreting plasma cells or memory B cells. In this process, proliferation and differentiation, including somatic hypermutation and Ig class switch, are associated with genome wide DNA methylation and an overall increase of histone acetylation (Shaknovich et al., 2011). Initiation of GC reaction is regulated by Bcl6. The induction of Bcl6 expression is concomitant with enrichment of activating histone marks H3K9ac and H3K4me3 in the Bcl6 promoter (Ramachandrareddy et al., 2010). Bcl6 inhibits B cell differentiation into plasma cells through transcription repressor functions that likely modify chromatin accessibility to Blimp-1 (Shapiro-Shelef and Calame, 2005). The generation of plasma cells is regulated by Blimp-1. Bcl6 and Blimp-1 act as a pair of transcriptional repressors and work in a mutually exclusive manner (Calame et al., 2003).One of the possible mechanisms is Bcl6 interaction with the chromatin remodeling complex Mi-2/NuRD in GC B cells, leading to the repression of specific genes that are characteristic of plasma cells. This Mi-2/NURD-mediated repression can be achieved through recruitment of histone deacetylases HDAC1 and HDAC2 (Fujita et al., 2003; Fujita et al., 2004). While *Blimp-1* has also been shown to interact with the histone lysine demethylase LSD1 leading to a more accessible chromatin structure to its target genes (Su et al., 2009).

A number of histone modifiers could exert their regulatory role in the B cell response, such as Enhancer of zeste homolog 2 (EZH2) and the histone acetyltransferase monocytic leukemia zinc finger protein (MOZ), the former could modulate Ig heavy chain rearrangement and also essential for GC reaction. The conditional deletion of EZH2, with either *Cγ1*-Cre or *CR2*-Cre, dramatically reduced GC frequency (Béguelin et al., 2013; Caganova et al., 2013a). Both studies demonstrated the regulation of cell cycle genes by EZH2 and inhibition of apoptosis. MOZ deficient mice in all B-cells or in specifically in GC B-cells also resulted in decreased in

GC B-cells (Good-Jacobson et al., 2014) due to defective proliferation correlating to a decrease specifically in DZ B cells.

In the absence of EZH2, there was a reduced $IgG1^+$ memory B cells as well as reduced secondary recall response (Caganova et al., 2013b)(Béguelin et al., 2013; Caganova et al., 2013a). High affinity $IgG1^+$ memory B-cells were also reduced in the absence of MOZ (Good-Jacobson et al., 2014) but IgM^+ memory B cell numbers were increased. Thus, MOZ regulated the composition and functional outcome of the memory compartment. More work is now needed to investigate in detail the role of epigenetic regulation in memory B cell formation and function.

Epigenetic regulation of microRNAs also play very important roles in B cell responses. Distinct miRNA expression profiles regulate naïve B cell activation, GC formation, and terminal differentiation into plasma cell and memory cell (Malumbres et al., 2009a; Zhang et al., 2009). Multiple miRNAs, including miR-155 and miR-125b, have been shown to have a regulatory role in the expression of genes that fine tune B cell GC differentiation (Thai et al., 2007a; Gururajan et al., 2011). MiR-155 can target multiple genes, including *Aicda*, which encodes AID, and Pu.1, thereby regulating sequential B cell differentiation stages (Thai et al., 2007b). By contrast, multiple miRNA molecules, such as miR-15a and miR-16, can cooperatively target one gene, such as *Bcl2* in GC B cells (Malumbres et al., 2009b) .
Taken together, multiple B cell-intrinsic epigenetic regulations may guarantee B cell development and immune response, such as GC formation, SHM, and Ab affinity maturation in the GC reaction, as well as differentiation to memory B cells and long-lived plasma cells.

7 Role of long non-coding RNA in the immune system

Recently, the discovery of long noncoding (*Lnc*) RNAs as essential mediators of cellular biology and potentially important regulators of cell differentiation, development and malignant transformation has shown that they are more than just a “black matter of the genome”. Moreover, *LncRNA*s have a broad range of possible functions at the transcriptional, posttranscriptional and protein level and their aberrant expression significantly contributes to the hallmarks of cancer cell biology. Furthermore, their high tissue- and cell-type specificity makes *LncRNA*s especially interesting as biomarkers, prognostic factors or specific therapeutic targets.

The emergence of *LncRNA*s controlling innate and adaptive immunity raised the possibility that they may be important regulators of immune cells. For example, *Lnc*-DC is required for normal dendritic cell differentiation and function (Wang et al., 2014), IL1b-eRNA and IL1b-RBT46 are required for lipopolysaccharide-induced pro-inflammatory responses in monocyte (IIott et al., 2014) and NRAV modulates cellular responses to viral infections (Ouyang et al., 2014). In T cells, an intronic *LncRNA* NRON abrogates the nuclear transport of nuclear factor of activated T cells (NFAT) and hence modulates expression of interleukin-2 (Willingham et al., 2005) and in B-cell lymphomas, the *LncRNA* Fas-AS1 modulates expression of soluble Fas receptor messenger RNA that functions as an important regulator of apoptosis (Sehgal et al., 2014). Altogether, *LncRNA*s have proven to influence both normal and pathological immune cell development and function.

7.1 *LncRNA H19* in hematopoiesis

7.1.1 *H19*, a Prototype of a Multitask *LncRNA*

Long non-coding RNAs (*LncRNAs*) are transcripts that do not encoding proteins but have a crucial role in various biological functions. *LncRNA*s can exert its regulatory functions through different mechanisms, such act as regulators of its target genes expression. This can be accomplished at different level of regulation, including chromatin organization, transcriptional regulation, and post-transcriptional control. Abnormal or misregulated *LncRNA*s expression has been shown to be associated with cancer and other disorders (Wapinski and Chang, 2011; Tano and Akimitsu, 2012).

H19 is one of the first discovered *LncRNA*s originally isolated in four different laboratories (Davis et al., 1987; Pachnis et al., 1988; Wiles, 1988; Poirier et al., 1991). The 2.3-kb gene is composed of five exons and four small introns and the *H19* RNA is fully capped, spliced and poly-adenylated. The *H19* gene was found to be monoallelically expressed from the chromosome of maternal origin in mouse and in human and, with (Bartolomei et al., 1991; Zhang and Tycko, 1992).

H19 is mainly expressed throughout embryonic development in multiple tissues including hematopoietic cells (Poirier et al., 1991; Pachnis et al., 1988). After birth *H19* has only been detected in muscle satellite cells (Xu et al., 2017; Martinet et al., 2016; Dey et al., 2014a), in cardiomyocytes (Zhang et al., 2017; Liu et al., 2016) and in DN3a thymocytes (unpublished data, IMMGEN database). It is maternally expressed from mouse chromosome 7 and human

chromosome 11p15, together with the neighboring paternally expressed *Igf2* gene (Su et al., 2016). The core regulatory elements of the *H19*/*Igf2* locus include imprinted control region (ICR), which is also called differential methylation region (DMR) and the enhancer, promoters sequences. The ICR or DMR region, located 2kbp upstream of the *H19* promoter, controls the maternal expression of *H19* and paternal expression of *Igf2* by insulating communication between the promoter and enhancers, located downstream of the *H19* gene. Both genes share a common set of enhancers located downstream of the locus (Figure 4). The insulation function of the ICR sequencing is regulated by CTCF (CCTC-binding factor), which can bind to the unmethylated ICR region in the maternal allele. CTCF binding to the maternal ICR acts as an insulator to block the communication between the enhancer and *Igf2* promotor, which may contribute to its silencing (Murrell et al., 2004)(Weber et al., 2003; Kurukuti et al., 2006). In the paternal allele CTCF cannot access this region because of hypermethylation leading to *Igf2* expression (Lewis and Murrell, 2004). Several other *LncRNA*s at the *H19*/*IGF2* locus, such as *IGF2*-AS (Rivkin et al., 1993; Moore et al., 1997), *LncRNA 91H* (Berteaux et al., 2008) and *PIHit* (Court et al., 2011) are transcribed in opposite orientation adding more complexity to the locus regulation.

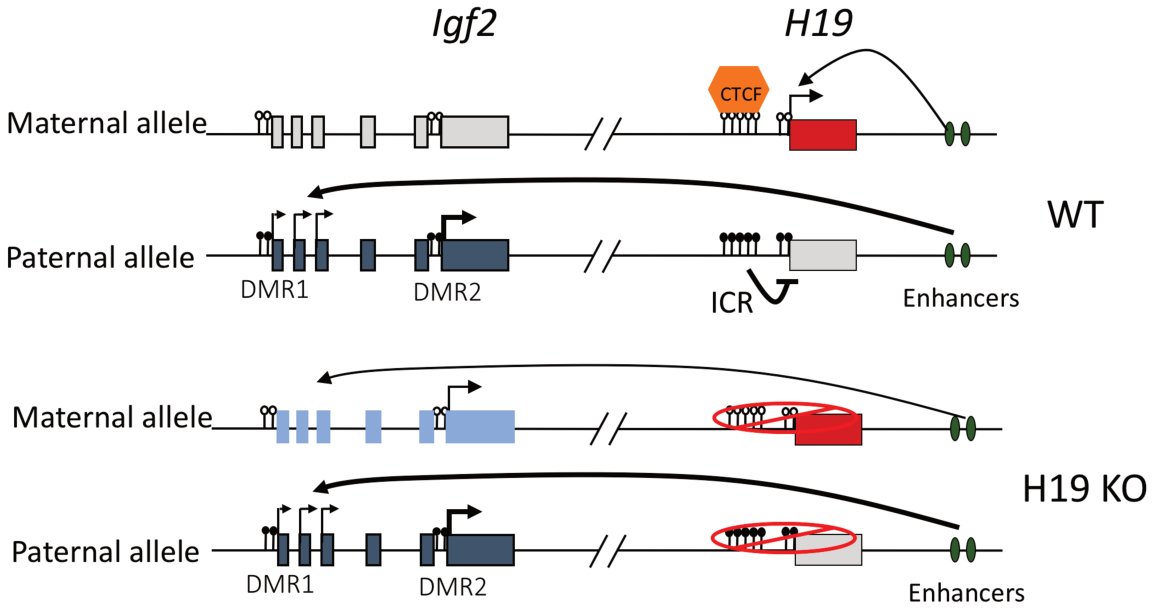

Figure 9 Schematic of *H19* and *Igf2* expression

On the paternal allele (Pat), *Igf2* is activated by the different mesodermal and endodermal enhancers but the enhancers downstream of *H19* are blocked by the CTCF insulation on the maternal allele (Mat). *H19* is activated by the downstream enhancer on the maternal allele but repressed by the silencer on the paternal allele. When the H19 gene and its regulatory region (ICR) are deleted, the CTCF can not bind to ICR region and the insulation function is released, leading to the expression of Igf2 in the maternal allele.

H19 regulates *Igf2* expression through a cis regulatory process that influences growth and development. *H19*$^{-/-}$ mice are viable, but showed an overgrowth phenotype in both embryogenesis and adult life. It has been described that the *H19* locus is linked to the Beckwith-Wiedemann syndrome (BWS) and Wilms' tumors, both are imprinting disorder characterized by postnatal overgrowth, macroglossia, anterior abdominal wall defects and an increased risk of embryonic or childhood tumors (Zhang et al., 1993; Cohen, 1994; Reik et al., 1994). The higher incidence of tumors rises the possibility that *H19* may function as a tumor suppressor (Maher and Reik, 2000). Meanwhile several other extensive studies consider *H19* as being the tumor suppressor gene (Hao et al., 1993; Juan et al., 2000). It has been proposed that a biallelic expression of *Igf2* in Wilms' tumor where *H19* is fully repressed through hypermethylation in *H19* DMR region on both alleles is the cause of the tumor (Dao et al., 1999)(Frevel et al., 1999). In BWS cases, patients also showed deficiency in *H19* DMR region, which lead to *Igf2* expression from both allele, while silencing *H19* expression (Sparago et al., 2004; Prawitt et al., 2005a; Prawitt et al., 2005b). While Loss of *IGF2* expression with a biallelic *H19* expression is responsible for 20 to 60% of cases of Silver–Russel syndrome (SRS) (Peñaherrera et al., 2010). SRS is characterized by embryonic and postnatal overgrowth with facial dysmorphia and corporal asymmetry. All these studies above showed altered gene expression at the *H19*/*IGF2* locus are associated to malignancies and developmental disorders.

On the other hand, various cancers in different tissues, such as breast (Adriaenssens et al., 1998; Lottin et al., 2002), bladder (Cooper et al., 1996), lung (Kondo et al., 1995). showed *H19* overexpression that could contribute to tumor progression and aggressiveness.

7.1.2 The *LncRNA H19* controls genome expression at multiple levels

As described above, *LncRNA*s can exert its roles through different molecular mechanisms by regulating genome expression. The complexity of mechanisms adopted by *LncRNA H19* on gene expression have been illustrated to be extremely diverse at various levels. One mechanism elucidated by Luo and colleagues showed that *H19* can exert its function through chromatin modification, by guiding chromatin modifying enzymes to distinct loci (Luo et al., 2013). In some cases of bladder cancer, *H19* binds to and recruit the histone methyltransferase EZH2 at the E-cadherin promoter, leading to an increase in H3K27me3 repressive marks and to silence the expression of E-cadherin gene (Luo et al., 2013). *H19* has been shown to interact with and physically bind to the methyl-CpG-binding domain protein 1 (MBD1)

(Monnier et al., 2013) to form *H19*-MBD1 complex, which can be recruited to regulate the imprinting gene network, such as *Igf2*, slc38a4, and peg1 (Monnier et al., 2013). This recruitment can lead MBD1 to localize to the *H19* targeted genes and induces methylation at lysine 9 of histone H3 (H3K9me3), probably via the additional interaction with an H3K9 histone methyltransferase.

Another pathway of *H19* regulation is also illustrated by its dual interaction with miR. On one hand, the *LncRNA H19* acts as sponge to sequester miR-106a as well as the miR-let7 family members (Kallen et al., 2013; Imig et al., 2015). On the other end, *H19* serves as a precursor of miR-675 that will in turn post-translationally regulate a number of targets involved in cell tumorigenicity, including RB, IGFR1, SMAD1, SMAD5, CDC6, NOMO1, or RUNX1 (Gao et al., 2012a; Cai and Cullen, 2007; Tsang et al., 2010; Gao et al., 2012b)(Keniry et al., 2012; Dey et al., 2014b; Zhuang et al., 2014). The role of *H19* in tumor progression could also be mediated through its interaction with the tumor-suppressor p53 protein. This association results in partial p53 inactivation (Yang et al., 2012).

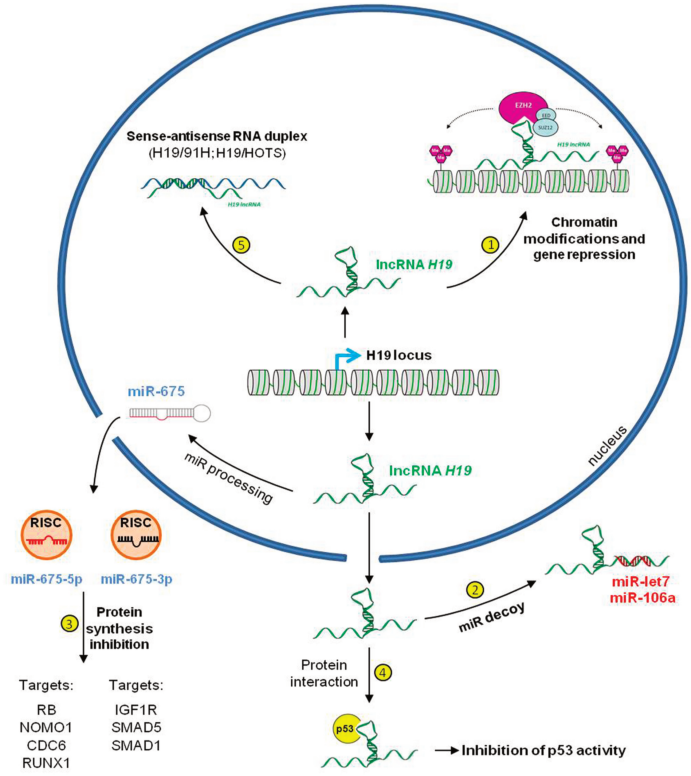

Figure 10 The *LncRNA H19* controls genome expression at multiple levels (Angrand et al., 2015)**.**

H19 acts on chromatin organization through the recruitment of chromatin modifying complex PRC2 and on posttranscriptional control as a miR decoys sequestering miR-106a and miR-let7 or as a precursor for miR-675-5p and miR-675-3p. *H19* also interact with p53 (TP53) and inactivate the tumor suppressor protein action. Possible base pairing between *H19* and the antisense transcripts 91H and HOTS may have biological outcomes.

7.1.3 Regulatory role of *LncRNA H19* in hematopoiesis

The role of *H19* in hematopoiesis showed by Venkatraman et al. (Venkatraman et al., 2013), is to maintain hematopoietic stem cell quiescence. By deleting the DMR region of *H19*/*Igf2* locus from the maternal allele, hematopoietic stem cells lose quiescence and showed an increased differentiation ability through an increased-Igf1r/Igf2 signaling circuit. This increase leads to loss of downstream FOXO-mediated inhibition of HSC cell cycle activity.
This work also supports the idea that imprinted gene networks play an important role in stem cells. Previous work by other groups showed that most imprinted genes were preferentially expressed in the HSC compared to their differentiated progeny (Berg et al., 2011; Varrault et al., 2006; Rossi et al., 2012). This work highlighted the importance of the imprinted genes in development.

Previous studies from our laboratory found that *H19* is the major differentially expressed transcript in microarray data (P. Vieira, personal communication) comparing FL and adult BM derived pro-B cells and between the early (embryonic date 13-16) and late (embryonic date 16-19) thymic settling progenitors (TSPs) (Ramond et al., 2014). Intriguingly, *H19* is also expressed in the adult double-negative 3a (DN3a), a stage at which T lymphocytes undergo TCR beta chains recombination. These observations raised the possibility that *H19* might play a role in developing lymphocytes.

This thesis focuses on the impacts of this *LncRNA H19* on the B cell development in the FL and BM, and B cell response in the adult periphery.

Objective

The global aim of this work is to understand what the is impact of the expression of the *LncRNA H19* in the immune system more specifically in B lymphopoiesis and B cell response. Venkatraman et al. have shown that H19 had a role in hematopoiesis in maintaining hematopoietic stem cell quiescence (Venkatraman et al., 2013). Other studies showed that imprinting gene network regulated developmental events at the embryonic stage and in adult stem cells through epigenetic modifications (Berg et al., 2011; Varrault et al., 2006; Rossi et al., 2012). *H19* is the major differentially expressed transcript in microarray data (P. Vieira, personal communication) comparing FL and adult BM derived pro-B cells and comparing ETP different developmental stages. These data suggested that H19 had a role in the development of the immune system.

This thesis focuses on the impacts of *LncRNA H19* on B cell development in the FL and BM, and on molecular mechanisms affecting the B cell response in the adult periphery.

Our strategy in this work is as the following:

B cell development:

- Characterize the distinct B cell developmental stages in the FL from the embryonic date 13 to 19 and in the BM of the new born and adult mice of wt, $H19^{-/-}$, $H19^{mat-/+}$ and $H19^{+/pat-}$.
- Dissect the differentially affected developmental stage and understand the molecular events affected by the deletion of *H19*

B cell function

- Characterize the B cell phenotype in the peripheral organs
- Investigate B cell response to different T cell dependent and independent antigens at both cellular and antibody response level.
- Explore the molecular mechanisms underlying the differentially response profile of $H19^{-/-}$ mice.

Results

Early B cell development is altered in *H19*$^{-/-}$ FL

Previous data from our laboratory found that *H19* is the major differentially expressed transcript in microarray data (P. Vieira, personal communication) comparing FL and adult BM derived pro-B cells and between early thymic progenitors from the first and second waves (Ramond et al., 2014). Thus, we wondered what was the role *H19* plays in the lymphopoiesis in the FL. Based on the B cell development scheme in the BM described by Hardy (Hardy et al., 1991), B cell surface markers B220, CD43, BP1 and CD24 (HSA) are used to define different stages of B cell development. Briefly, B220^{+}CD43^{+} B lymphocytes are subdivided into four subsets, fractions A (BP1^{-}CD24^{-}), B (BP1^{-}CD24^{+}), C (BP1^{+}CD24$^{+/lo}$), and C' (BP1^{+}CD24^{hi}). A correlation between these surface marker expression and Ig gene rearrangement status was established. The Ig heavy chain genes in cells from fraction A are in germline configuration, whereas the majority of fraction B cells show D-J rearrangement, but rarely V-DJ recombination. Furthermore, complete heavy chain rearrangement mainly takes place in fraction C stage where Igμ is expressed and paired with surrogate light chain VpreB and λ5 to form a preBCR on the surface of majority fraction C' cells, in order to trigger a rapid proliferation and further differentiation. The B cell specific marker CD19 used to characterize committed B cell progenitors (Nutt et al., 1997) is not expressed in cells from fraction A and therefore they are not committed to B cell lineage and also comprise CLP (CLP-2) (Martin et al., 2003) and NK cell progenitors (Rolink et al., 1996). On the other hand, B220^{+}CD19^{+}IgM^{+}CD43^{+}proB cells consist of the three fractions, B, C, and C' subpopulations (Hardy and Hayakawa, 2001). Therefore, we focused on the analysis of these three fractions in the FL of different embryonic stages from both wild type Sv129 and *H19* mutant (on Sv129 background) mice.

We analyzed the expression level of *H19* in proB cells from FL of different embryonic dates (from E15 to E18) and adult BM, we found *H19* is highly expressed in the proB cells from FL, decreased with fetal age, and not expressed in the proB cells from adult BM (Fig 11A). We also observed an overgrowth phenotype in the embryo and in the FL of *H19*$^{-/-}$ (Fig 11B), this was in line with previously reported data (Gabory et al., 2009; Wojdacz et al., 2008). However, unlike *H19* deficient human embryo (Moulton et al., 1994), we have not observed embryonic tumors in *H19*$^{-/-}$ embryos. Further analysis of B cell development in the FL showed the first B lineage cells (B220^{+}CD19^{+}) appear around embryonic day (E) 13.5 in the FL, and during gestation, the majority of B lineage cells remain in the proB progenitor stage.

From E13.5 to around E17.5, pro-B cells are mainly in fraction B, then after E17.5, pro-B cells upregulate the expression of BP1, a molecule predominantly found on early B lineage cells (Wang et al., 1998). BP1 is expressed in the late proB cells, fraction C, C', and maintained its expression in the preB cell stage. We identified these three fractions in E18 FL from both WT and *H19*$^{-/-}$ embryos. Of note, at this developmental stage proB cells accounted for more than 90% of total CD19^{+} lymphocytes in FL of both wt and *H19*$^{-/-}$. However, proB cells of *H19*$^{-/-}$ showed upregulated BP1 on the cell surface (Fig 11C), as well as altered B220 and CD43 expression (Fig 11D). The mean fluorescence intensity (MFI) of B220 showed a higher than 2-fold increase while CD43 MFI exhibited a 2-fold decrease.

Furthermore, BP1 and HSA expression showed that *H19*$^{-/-}$ FL proB cells exhibited an increased fraction C and C' in both frequency (Fig 11C) and absolute cell numbers (Fig 11F), with a 10 and 5-fold increase in fraction C and C', respectively. Myeloid lineage cells as well as the more immature progenitors, such as LSK, HSC and CLP were not affected (Fig 11E). Similar enlarged fraction C and C' was also observed in the adult BM B cell compartment (data not shown), indicating that *H19* impacts the B cell development by generating more proB cells with enlarged late proB cells defined as fraction C and C'.

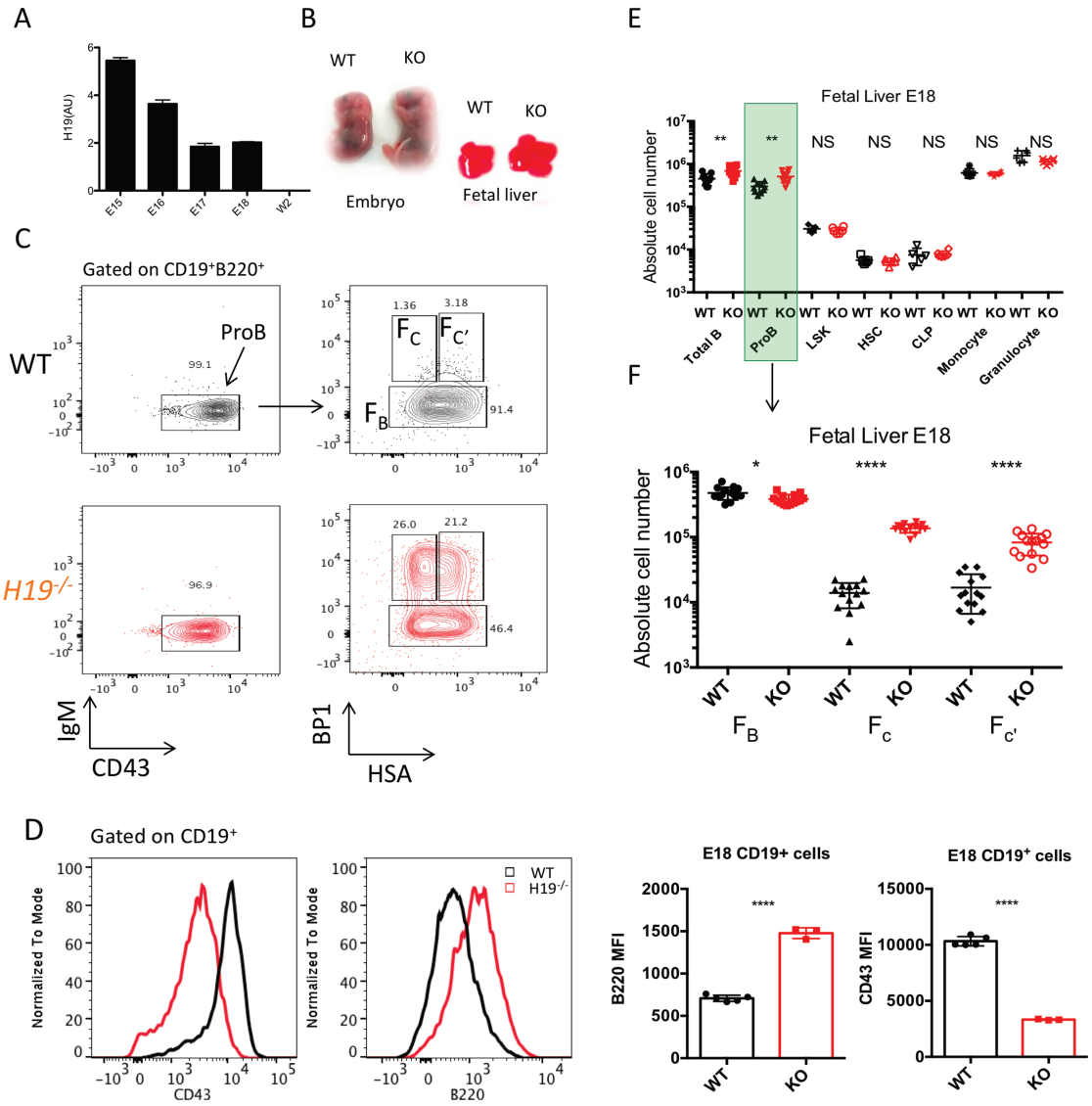

Figure 11 Altered B lineage development in the FL of *H19*$^{-/-}$

(A) The expression of *H19* in the proB cells of E15-E18 FL and adult BM; (B) Size of embryonic day (E) 18 embryo and FL; (C) Immunostaining of B lineage cells in the E18 FL of WT and *H19*$^{-/-}$, proB cells were analyzed and subdivided into fraction B, C and C'; (D) Expression of B220 and CD43 on the surface of E18 CD19^{+} cells from wt and *H19*$^{-/-}$ FL, analyzed by FACS, MFI: mean fluorescence intensity ; (E) The absolute number of B lineage, myeloid lineage and hematopoietic progenitors in E18 FL; (F) The absolute number of fraction B, C, and C' in E18 FL. Data is representative of at least 3 independent experiments with 1-3 pregnant mice(E18) from both WT and *H19*$^{-/-}$ per experiment. *p<0.05; **p<0.01; ***p< 0.001, ****p< 0.0001 unpaired *t test.*

In order to homogenize the genetic background and to confirm that maternally but not paternally expressed *H19* is responsible for the altered B cell development, we generated *H19* heterozygous, including *H19* maternal mutant $H19^{mat-/+}$ and *H19* paternal mutant $H19^{+/pat-}$. The FL of different embryonic dates from these heterozygous embryos, together with that of $H19^{-/-}$ and wt, were analyzed by flow cytometry. We observed the $H19^{mat-/+}$ mice showed a similar B cell development profile as the $H19^{-/-}$ mice with increased proB cells and particularly enlarged fraction C and C' (Fig 12A and 12B), as well as upregulated B220 expression and downregulated CD43 on the B cell progenitor surface (Fig 12C). The phenotype of $H19^{+/pat-}$ mice resembled that of wt mice, indicating that only deletion of *H19* maternal allele leads to the altered B cell development.

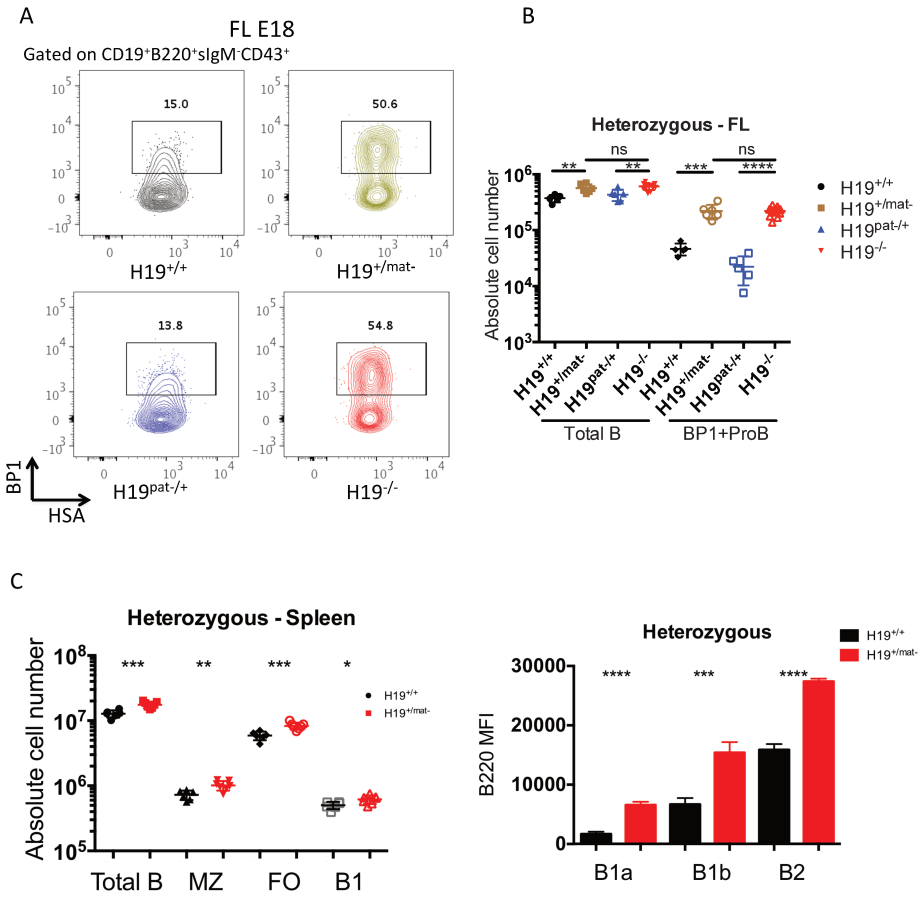

Figure 12 Deletion of *H19* maternal, but not paternal allele lead to the altered B cell development

(A) Immunostaining plot of proB cells in E18 FL of wt, $H19^{mat-/+}$, $H19^{pat-/+}$ and $H19^{-/-}$ embryos, proB cells (gated on $CD19^{+}B220^{+}IgM^{-}CD43^{+}$)were divided into $BP1^{-}$ and $BP1^{+}$ subpopulations and the number of total B cells and $BP1^{+}$ proB cells in the FL of the four genotyped mice were shown in (B); in adult spleen the number of total B cells, MZ, FO, and B1 cells of wt and $H19^{mat-/+}$ was calculated and plotted in (C); histogram represents the expression of B220 on the surface of different B cell subsets from wt and $H19^{mat-/+}$. Data is representative of 2

independent experiments with 3 replicates each experiment. *p<0.05; **p<0.01; ***p< 0.001, ****p< 0.0001 unpaired *t test.*

Altered B cell development *in vitro* culture in absence of *H19*

We next investigated the *in vitro* proliferation and differentiation capacity of the proB cells from E15 FL of both wt and *H19*$^{-/-}$. CD19^{+}B220^{+}IgM^{-}CD43^{+} FL cells were sorted and cultured with OP9 stromal cells, complemented with saturating amounts of IL7, Flt3L and KitL. After 7 days in culture, positive wells with growing colonies were analyzed by flow cytometry and the number of B lymphocytes at different developmental stages was calculated, including proB, preB and IgM^{+} cells. The *in vitro* culture showed that although *H19*$^{-/-}$ proB cells generate comparable number of total CD19^{+} B lymphocytes compared to wt proB cells, they differentiate faster to the preB stage and give rise to more preB cells, as a result, an elevation in IgM^{+} B cells generated by *H19*$^{-/-}$ proB cells occured (Fig 13A), indicating that *H19* could affect B cell differentiation.

Furthermore, LSKs (Lin^{-}c-kit^{+}Scal^{+}) and CLPs from E15 FL of wt and *H19*$^{-/-}$ were sorted and cultured under the same condition as described in the proB culture. Consistent with the previous results from proB cell culture, LSKs and CLPs from *H19*$^{-/-}$ FL generated higher frequency and numbers of BP1^{+}proB cells (Fig 13B and 13C), reinforcing the link between *H19* and B cell proliferation and differentiation.

Altogether, the results above indicate that in absence of *H19*, B cell development is altered resulting in an increased production of B lymphocytes in fraction C and C' in the FL.

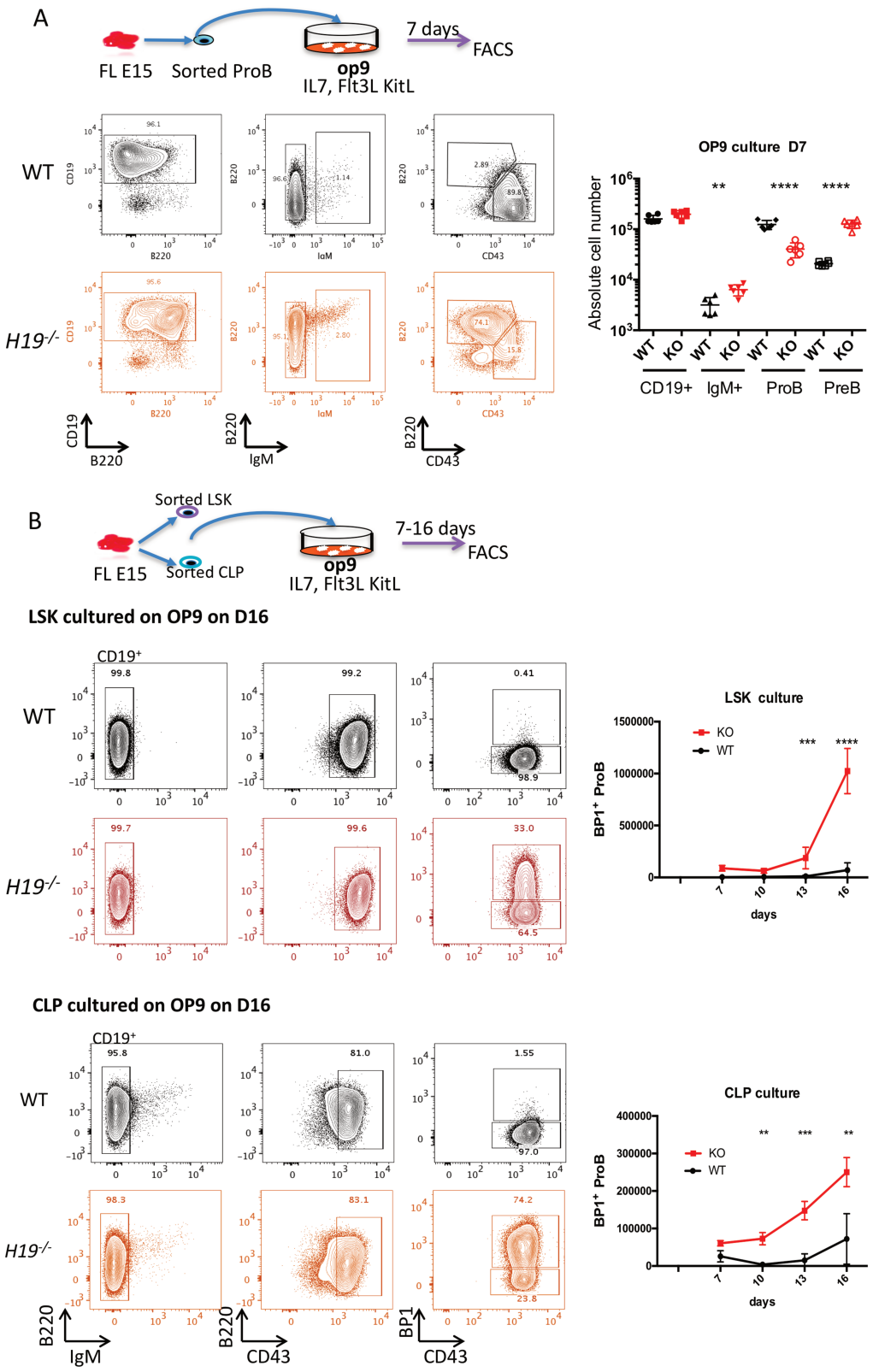

Figure 13 Altered B cell development in vitro culture in absence of *H19*

Sorted E15 proB cells ($CD19^+B220^+CD93^+IgM^-CD43^+$), LSK ($Lin^-c\text{-}kit^+Scal^+$) and CLPs($Lin^-c\text{-}kit^{lo}Scal^{lo}IL7R^+$) from E15 FL of both wt and *H19*$^{-/-}$ (100 cells per well) were cultured on OP9 stromal cells, complemented with saturating amount of IL7, Flt3L and KitL. (A) 7 days after proB culture, B cell proliferation and differentiation was analyzed by flow cytometry, and the number of B lymphocytes in different developmental stages was

calculated, statistical analysis was plotted. (B) LSK ($Lin^-c\text{-}kit^+Scal^+$) and CLPs ($Lin^-c\text{-}kit^{lo}Scal^{lo}IL7R^+$) (100 cells per well) were cultured on OP9 stromal cells for 7, 10, 13 and 16 days. B cell proliferation and differentiation was analyzed by flow cytometry, and kinetic of the number of $BP1^+$proB cells was calculated and plotted. Data represent at least 2 independent experiments.6-10 replicates per experiment. *p<0.05; **p<0.01; ***p< 0.001, ****p< 0.0001 unpaired *t test.*

H19$^{-/-}$ B lymphocytes in fraction C display aberrant Ig heavy chain VDJ rearrangement

As mentioned above, the most marked event taking place in proB cells is the Ig heavy chain VDJ rearrangement. In order to investigate the VDJ recombination status of different sub-populations of E18 FL proB cells from both WT and *H19*$^{-/-}$ embryos, fraction C and C' were sorted and genomic PCR was performed to detect Ig heavy chain D-J and V-DJ rearrangements. PCR amplification was done using primers recognizing the 5' sequence of V_H-J558, D_H-Q52 segments and 3' sequence of J_H4e segment. The D-J rearrangements were identified by paired primers of D_H-Q52 and J_H4e and primers that amplify an IL2 intron sequence was used as a loading control. After separation of the PCR products on agarose electrophoresis and normalization for loaded DNA we found a 1.5-fold increase of Ig germline in fraction C cells from *H19*$^{-/-}$ FL compared to that of WT, indicating that a higher frequency of fraction C cells from *H19*$^{-/-}$ FL did not undergo D-J rearrangement (Fig 14B).

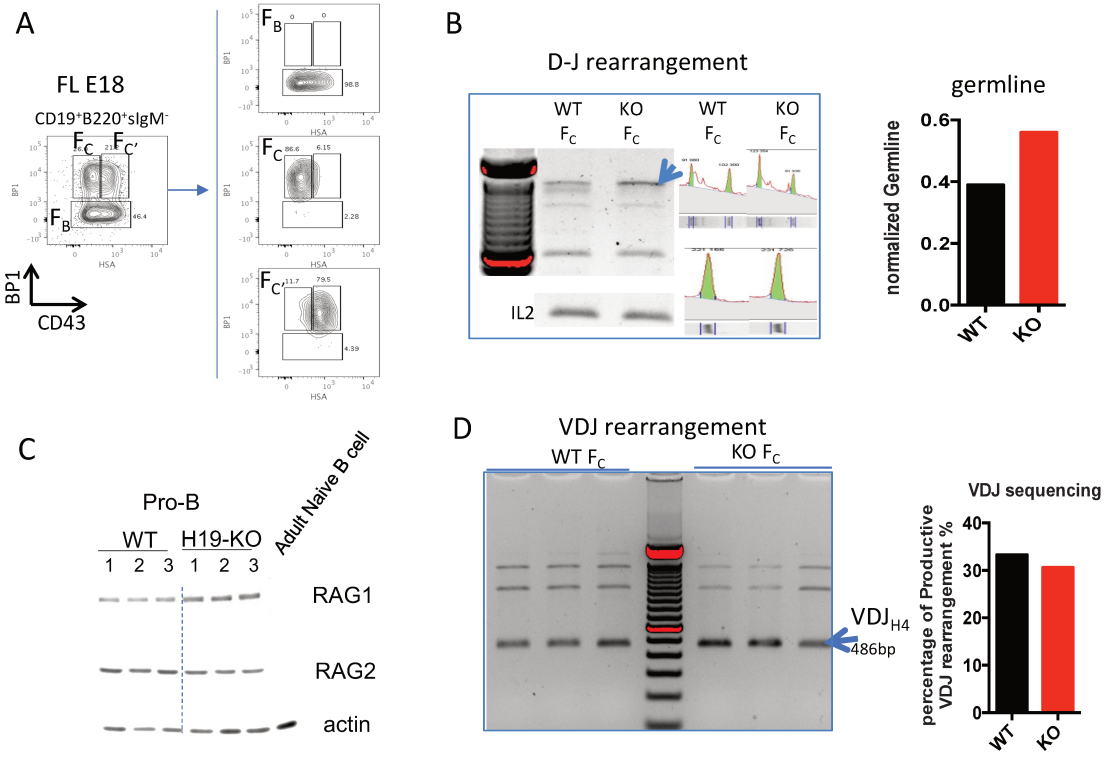

Figure 14 B lymphocytes in fraction C displayed abnormal Ig heavy chain VDJ

rearrangement in absence of *H19*

Genomic DNA was extracted from sorted fraction B, C and C' (labeled as F_B, F_C, Fc', respectively) (A), and Ig heavy chain D-J and V-DJ rearrangement was analyzed by PCR using primers which recognize the 5' sequence of VH-J558, DH-Q52 segments and 3' sequence of JH4e segment. (B) D-J rearrangement PCR product was analyzed by agarose electrophoresis; the intensity of the bands was scanned and the germline band was calculated through normalizing to the loading control. (C) the Rag1/2 expression in the proB cells was measured by western-blot analysis; (D) V-DJ PCR product was analyzed by agarose electrophoresis, and VDJ_{H4} fragment have been purified and cloned into TOPO vector for sequencing, and the rate of productive V-DJ rearrangement was calculated and plotted in the histogram. *p<0.05; **p<0.01; ***p< 0.001, ****p< 0.0001 unpaired *t test.*

To confirm this observation, DNA double strands breaks (DSB) in these subpopulations were analyzed by intracellular staining with anti- γH2AX fluorescence labeled antibody. γH2AX accumulates in the DSBs created by the V(D)J recombination and can be detected by flow cytometry (Sharma et al., 2012; Hopp et al., 2017). Cells in fraction B from both WT and *H19*$^{-/-}$ showed similar γH2AX staining profile. However, in fraction C and C', cells from *H19*$^{-/-}$ FL showed lower frequency of γH2AX positive cells compared to that of wt. In fraction C the frequency of γH2AX^{+} cells accounts for 30±0,8% in wt and 12.6±2.2% in *H19*$^{-/-}$, while in fraction C', 57.2±4.9% in wt and 38.9±1.8% in *H19*$^{-/-}$, respectively. In proB cells, γH2AX not only recognizes cells undergoing DSBs caused by the VDJ recombination but also stains cells undergoing mitosis (Tu et al., 2013). A majority of cells in fraction C' accomplished a productive VDJ rearrangement in Ig heavy chain locus and express preBCR on the cell surface. For that reason, they become highly proliferative and stain positive for γH2AX (Fig 15A). The decreased frequency of γH2AX^{+} cells in fraction C of *H19*$^{-/-}$ FL indicates a lower frequency cells undergoing VDJ recombination.

We performed intracellular IgM staining to analyze the frequency of productive VDJ rearrangements in dividing fraction C' cells. Cells in fraction B and C' from both WT and *H19*$^{-/-}$ showed similar intracellular IgM staining profile. However, in fraction C, cells from *H19*$^{-/-}$ FL showed lower frequency of intra-IgM positive cells compared to that of wt, that is around 22.8±1.9% in *H19*$^{-/-}$ versus 41.8±8,4% in wt (Fig 15B). Although reduced productive Ig heavy chain VDJ rearrangements observed in fraction C of *H19*$^{-/-}$, fraction C and C' in H19 mutant FL still showed an increased absolute numbers of intracellular IgM positive cells compared to the wt resulting in a net increase of B cell production (Fig 15B).

The decreased frequency of γH2AX and intracellular IgM positive cells in the fraction C of *H19*$^{-/-}$ FL also indicates an aberrant VDJ rearrangement profile. Extensive studies showed that B cell progenitors require cell cycle arrest to fulfil the VDJ rearrangement (Lin and Desiderio,

1994). We wondered whether the aberrant VDJ recombination in fraction C in absence of *H19* was caused by the failed cell cycle arrest. To this end cell cycle analysis was performed and the results showed a majority of cells in the fraction C from both genotyped FL are in G1 phase, whereas cells in fraction C' that bear a productive Igμ chain are highly proliferative. Fraction C cells from *H19-/-* FL showed an even lower frequency cells in S/G2/M phase compare to that of wt (Fig 15C), indicating that loss of H19 did interfere with cell cycle arrest in this population. Both fraction C and C' from $H19^{-/-}$ FL showed increased absolute cell numbers in S/G2/M phase, also consistent with the increased B lineage production in the *H19* mutant FL.

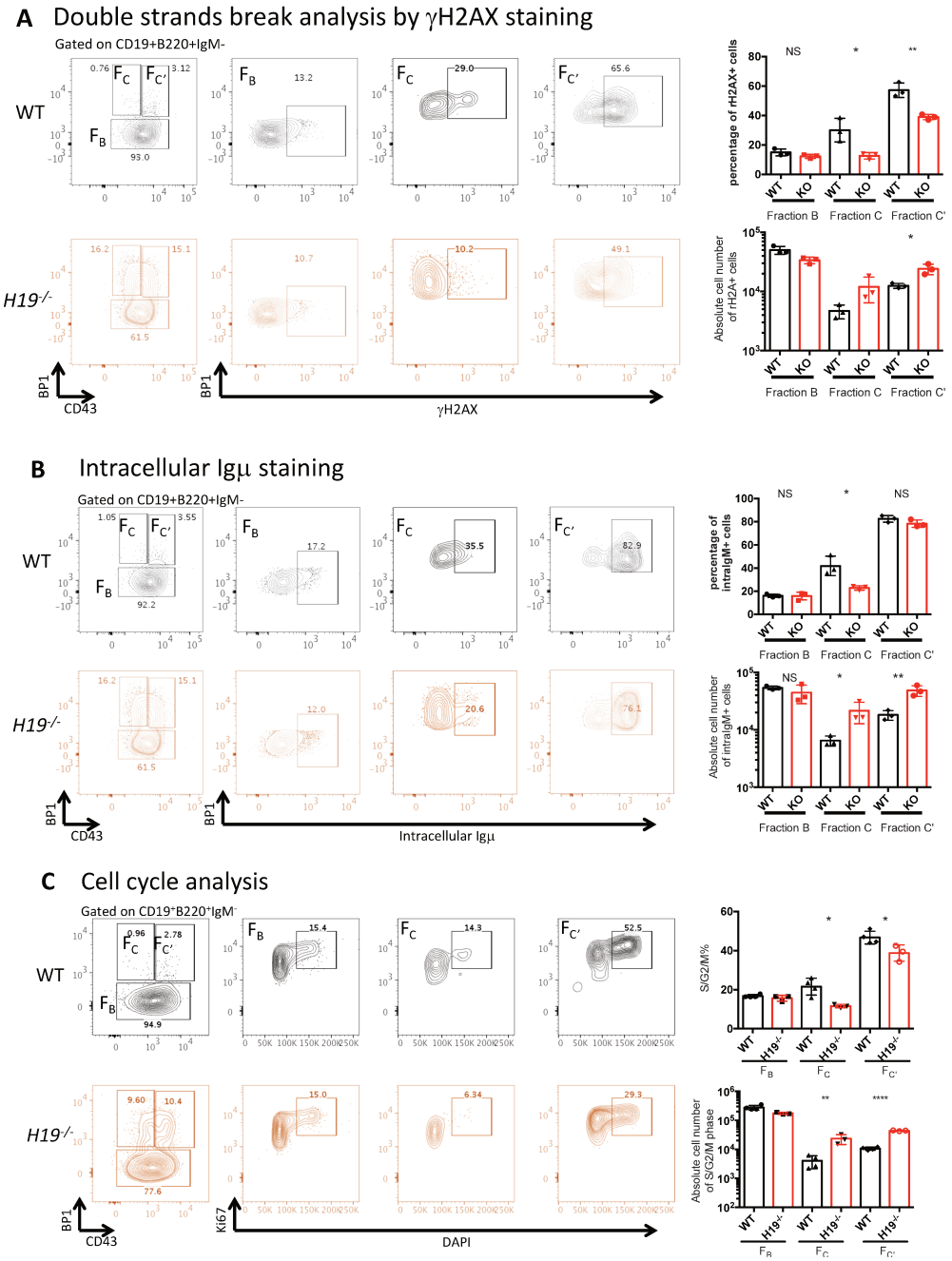

Figure 15 Altered DSBs, intracellular IgM, and cell cycle profile in fraction C subpopulation of E18 FL in absence of *H19*

Fraction B, C and C' cells from E18 FL of wt and *H19*$^{-/-}$ were analyzed by intracellular staining with anti-γH2AX for DNA double strands breaks (DSBs) detection (A), anti-Igμ staining for intracellular Igμ expression(B), and Ki67/DAPI staining for cell cycle analysis(C), respectively. Dot plots shows the staining profile, and the statistical analysis of the frequency and absolute number of γH2AX^{+}, intracellular Igμ+, and S/G2/M phase cells are displayed in the bar charts. Data represent 2 independent experiments. Each has at least 3 biological replicates. *p<0.05; **p<0.01; ***p< 0.001, ****p< 0.0001 unpaired *t test.*

To assess the efficiency of the productive V-DJ rearrangement, we amplified VDJ fragments in DNA from fraction C cells by using V_H-J558 and J_H4e primer pair. The recombination of the V, D and J gene segments can produce non-productive or productive rearrangements. If there are no stop codons in the rearranged VDJ sequence and the constant region is in frame, a heavy chain protein can be produced. Alternatively, if there is either a stop codon or the constant region falls out of frame, no heavy chain protein can be produced corresponding to a non-productive rearrangement. The VDJ amplification showed comparable usage of J_{H1}, J_{H2}, J_{H3} and J_{H4} (Fig 14D). The frequency of productive VDJ rearrangement in WT and *H19*$^{-/-}$ population were 33% and 31% (Fig 14D and Table 1), respectively, indicating once the cells initiate the VDJ rearrangement process similar frequency of productive rearrangements were obtained.

Altogether, the data above indicates that although there is aberrant Ig heavy chain VDJ rearrangement mainly caused by failure in the initiation of D-J, and/or V-DJ rearrangement, fraction C and C' cells in *H19* mutant FL are highly increased, leading to a higher B cell production.

Table 1 The list of VDJ sequencing

	J	D	V
	CAT AGC ATA GTA		TCT TGC ACA GTA ATA
WT1	CAT AGC	AT ACC GTC GTA ATC ATA GTA GAT	TCT TGC ACA GTA ATA
WT2	CAT AGC ATA	GT AGT TAC CAT ACT	TCT TGC ACA GTA ATA
WT3	CAT AGC ATA GTA	A TCG TAA CCA	TGC ACA GAA ATA
WT4	CAT AGC ATA GTA	ATA GTA ACC ATC ATA GTG	TCT TGC ACA GTA ATA
WT5	CAT AGC ATA GTA	ATC ATA GTA	TGC ACA GTA ATA
WT6	CAT AGC ATA	GTA GCT ACT ACC GTA GTA AAA	TCT TGC ACA GTA ATA
WT7	CAT AGC ATA	GT CGT AAC CAT	ACA GTA ATA
WT8	CAT AGC ATA	GT GTA GTA	TCT TGC ACA GTA ATA
WT9	CAT AGC	AT ACC GTC GTA ATC ATA GTA GAT	TCT TGC ACA GTA ATA
WT10	CAT AGC ATA	GT GTA GCT ACT ACC GTA GTA	TCT TGC ACA GTA ATA
WT11	CAT AGC ATA	GT GTA GCT ACT ACC GTA GTA	TCT TGC ACA GTA ATA
WT12	AT AGC ATA GTA	ATC ATA	TCT TGC ACA GTA ATA
WT13	CAT AGC ATA CGT	A ATC ATA GTA	TGC ACA GTA ATA
WT14	CAT AGC ATA GTA	ATA GTA ACC ATC ATA GTG	TCT TGC ACA GTA ATA
WT15	CAT AGC ATA	GTA GTC GTA ACC ATA GTA	TCT TGC ACA GTA ATA
WT16	CAT AGC	G TCG TAA CCA	TCT TGC ACA GTA ATA
WT17	CAT AGC	G TCG TAA CCA	TCT TGC ACA GTA ATA
WT18	CAT AGC ATA GTA	ATA GTA ACC ATC ATA GTG	TCT TGC ACA GTA ATA
WT19	CAG	C TAC TAC CGT AGT AAT	TCC ACA ATA ATA
WT20	CAT AGC	AT ACC GTC GTA ATC ATA GTA GAT	TCT TGC ACA GTA ATA
WT21	CAT AGC	A TAC GTA ATC ATA GTA	TGC ACA GTA ATA
WT22	CAT AGC	A TAC GTA ATC ATA GTA	TGC ACA GTA ATA
WT23	CAT AGC ATA GTA	ATA GTA ACC ATC ATA GTG	TCT TGC ACA GTA ATA
WT24	CAT AGC ATA GTA	ATA GTA ACC ATC ATA GTG	TCT TGC ACA GTA ATA
WT25	CAT AGC ATA	GT GTA GTA	TCT TGC ACA GTA ATA
WT26	CAT AGC	G TCG TAA CCA	TCT TGC ACA GTA ATA
WT27	CAT AGC ATA	CGT AATC ATA GTA	TGC ACA GTA ATA
WT28	CAG	C TAC TAC CGT AGT AAT	TCC ACA ATA ATA
WT29	CAT AGC ATA GTA	GTC GTA ACC ATA GTA	TCT TGC ACA GTA ATA
WT30	CAT AGC ATA GTA	GCT ACT ACC GTA GTA AAA	TCT TGC ACA GTA ATA
WT31	CAT AGC ATA GTA	ATA GTA ACC ATC ATA GTG	TCT TGC ACA GTA ATA
WT32	CAT AGC ATA	GT CGT AAC CAT	ACA GTA ATA
WT33	CAT AGC	G TCG TAA CCA	TCT TGC ACA GTA ATA
WT34	CATAGC ATA	GT GTA GTA	TCT TGC ACA GTA ATA

WT35	CAT AGC ATA	GT GTA GTA	TCT TGC ACA GTA ATA
WT36	CAT AGC ATA GTA	ATA GTA ACC ATC ATA GTG	TCT TGC ACA GTA ATA
WT37	CAT AGC ATA	CC GTC GTA ATC ATA GTA GAT	TCT TGC ACA GTA ATA
WT38	CAT AGC	G TCG TAA CCA	TCT TGC ACA GTA ATA
WT39	CAT AGC ATA	GT GTA GTA	TCT TGC ACA GTA ATA
WT40	CAT AGC ATA	CC GTC GTA ATC ATA GTA GAT	TCT TGC ACA GTA ATA
WT41	CAT AGC ATA	GT GTA GCT ACT ACC GTA GTA	TCT TGC ACA GTA ATA
WT42	CAG	C TAC TAC CGT AGT AAT	TCC ACA ATA ATA
KO1	CAT AGC ATA	G CTA CTA CCG TAG TAA	TCT TGC ACA GTA ATA
KO2	CAG	TCG TAA TCA	TCT TGC ACA GTA ATA
KO3	CAT AGC	G TCG TAA TCA	TCT CTC ACA ATA ATA
KO4	CAT AGC	G TAG CTA CTA CCG TAG TAA	TCT TGC ACA GTA ATA
KO5	CAT AGC ATA GTA	ACG TAG TCA CCA TAG	TCT TGC ACA GTA ATA
KO6	CAT AGC ATA	G CTA CTA CCG TAG TAA	TCT TGC ACA GTA ATA
KO7	CAT AGC ATA GTA	ACG TAG TCA CCA TAG	TCT TGC ACA GTA ATA
KO8	CAT AGC ATA	G CTA CTA CCG TAG TAA	TCT TGC ACA GTA ATA
KO9	CAT AGC ATA GTA	ACG TAG TCA CCA TAG	TCT TGC ACA GTA ATA
KO10	CAT AGC ATA	CG TCG TAA TCA	TCT TGC ACA GTA ATA
KO11	CAG	TCG TAA TCA	TCT TGC ACA GTA ATA
KO12	CAT AGC ATA GTA	ACG TAG TCA CCA TAG	TCT TGC ACA GTA ATA
KO13	CAT AGC ATA	GT CGT ACC TAT AGA	TCT TGC ACA GTA ATA
KO14	CAT AGC ATA GTA	ACG TAG TCA CCA TAG	TCT TGC ACA GTA ATA
KO15	CAT AGC	G TAG CTA CTA CCG TAG TAA	TCT TGC ACA GTA ATA
KO16	CAT	A TCG TAC CTA TAG TGA	TCT TGC ACA GTA ATA
KO17	CAG	TCG TAA TCA	TCT TGC ACA GTA ATA
KO18	CAT	A GCG TCG TAA TCA	TCT TGC ACA GTA ATA
KO19	CAT AGC ATA	G CTA CTA CCG TAG TAA	TCT TGC ACA GTA ATA
KO20	CAT AGC	G TAG CTA CTA CCG TAG TAA	TCT TGC ACA GTA ATA
KO21	CAG	TCG TAA TCA	TCT TGC ACA GTA ATA
KO22	CAT	A TCG TAC CTA TAG TGA	TCT TGC ACA GTA ATA
KO23	CAT	A TCG TAC CTA TAG TGA	TCT TGC ACA GTA ATA
KO24	CAT	A TCG TCC CAA TCG TGT TCC	TGC ATA ATA ATC
KO25	CAG	TCG TAA TCA	TCT TGC ACA GTA ATA
KO26	CAT AGC GTA	G TAA CCA TCA	TCT TGC ACA GTA ATA
KO27	CAT AGC ATA GTA	AG TAG TTA CCA	TCT TGC ACA GTA ATA
KO28	CAT AGC ATA	CG TCG TAA TCA	TCT TGC ACA GTA ATA
KO29	CCAT AGC	G TAG CTA CTA CCG TAG TAA	TCT TGC ACA GTA ATA
KO30	CAT AGC ATA GTA	AC GTA GTC ACC ATA	TCT TGC ACA GTA ATA
KO31	CAG	TCG TAA TCA	TCT TGC ACA GTA ATA
KO32	CAT AGC ATA	GTC GTAC CTA	TCT TGC ACA GTA ATA
KO33	CAT	A TCG TAC CTA TAG TGA	TCT TGC ACA GTA ATA
KO34	CAT AGC ATA	G CTA CTA CCG TAG TAA	TCT TGC ACA GTA ATA
KO35	CAT AGC	G TCG TAA TCA	TCT TGC ACA GTA ATA
KO36	CAT AGC ATA GTA	ATA GTC ACC ATA GTA GCT	TGC ACA GTA ATA
KO37	CAT AGC ATA GTA	AC GTA GTC ACC ATA	TCT TGC ACA GTA ATA
KO38	CAT AGC	G TCG TAA TCA	TCT TGC ACA GTA ATA
KO39	CAT AGC ATA GTA	A TCG TAC CTA TAG	TCT TGC ACA GTA ATA
KO40	CAT AGC	G TAG TAA CCA TCA	TCT TGC ACA GTA ATA
KO41	CAT AGC ATA GTA	AC GTA GTC ACC ATA	TCT TGC ACA GTA ATA
KO42	CAT	A TCG TAC CTA TAG TGA	TCT TGC ACA GTA ATA
KO43	CAT AGC ATA GTA	ACG TAG TCA CCA TAG	TCT TGC ACA GTA ATA
KO44	CAT	A TCG TAC CTA TAG TGA	TCT TGC ACA GTA ATA
KO45	CAT AGC ATA GTA	AC GTA GTC ACCA TAG	TCT TGC ACA GTA ATA
KO46	CAT AGC ATA	G CTA CTA CCG TAG TAA	TCT TGC ACA GTA ATA
KO47	CAT	A TCG TAC CTA TAG TGA	TCT TGC ACA GTA ATA
KO48	CAG	TCG TAA TCA	TCT TGC ACA GTA ATA
KO49	CAT	A GCG TAG CTA CTA CCG TAG TAA	TCT TGC ACA GTA ATA

productive VDJ rearrangement are labeled in red

Igf2 is upregulated in fraction C cells in absence of *H19*

To understand the molecular events affecting initiation of D-J and/or V-DJ rearrangement we performed qPCR for the genes involved in the VDJ recombination machinery, such as *Rag1* and *Rag2*, as well as some other genes in the imprinting network. *Rag1/2* expression showed no difference at both transcriptional (Fig 16) and protein level (Fig 14C) while *H19* mutant fraction C cells upregulated some genes in the imprinting network, such as *Igf2*, *CD81* and *Snurf*, among which *Igf2* stands out for its regulatory role in growth (Leighton et al., 1995). *Igf2* is a maternally imprinted gene, favorably expressed from the paternally inherited allele. Moreover, loss of *H19* leads to *Igf2* upregulation in both skeleton satellite cells and BM HSCs (Gabory et al., 2009; Venkatraman et al., 2013) and caused an accelerated muscle regeneration and HSC differentiation by breaking the quiescence state. This process is at least partially attributed to a gain of function of *Igf2*. In our hands, the upregulation of *Igf2*, as well as its cognate receptor Igf1r was observed in fraction C cells of *H19*$^{-/-}$, suggesting a possible enhanced *Igf2* signaling. Importantly, the upregulation of the transcription factor FOXO1, which is downstream of *Igf2* signaling pathway, was also observed in fraction C cells from *H19*$^{-/-}$ FL, making a possible link between *H19*, *Igf2* signaling and altered B cell development.

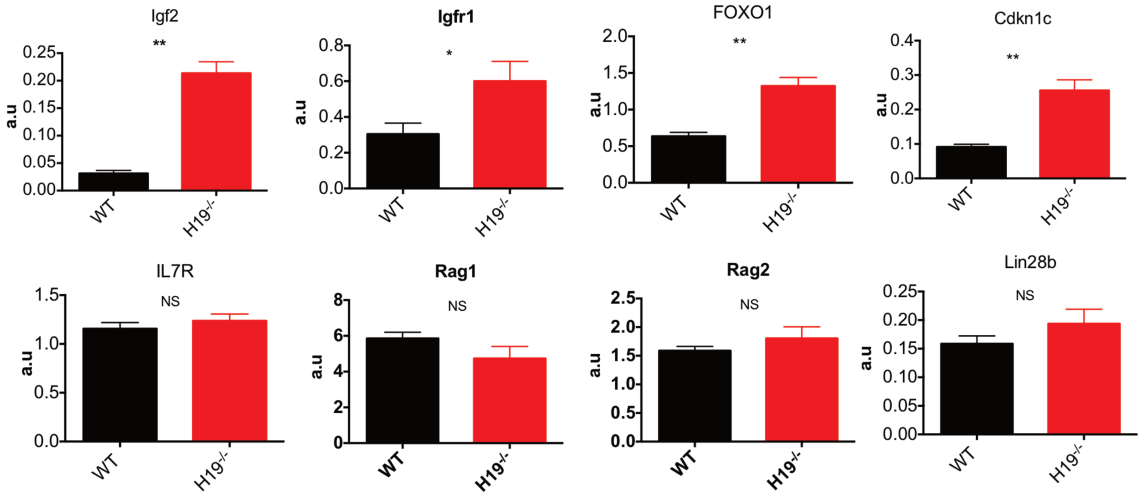

Figure 16 Genes associated to the *Igf2* signaling were upregulated in absence of *H19*

Quantitative RT-PCR gene expression analysis of transcript levels of genes involved in the Igf2 signaling (*Igfr1, FOXO1*) and VDJ rearrangement (*Rag1/2*) in fraction C cells from wt and *H19*$^{-/-}$ E18 FL. Results are presented in arbitrary units (a.u) relative to expression of the control gene *Hprt*. Data of (A) is representative of 2 independent experiments, while 3 independent experiments for (B). *p<0.05; **p<0.01; ***p< 0.001, ****p< 0.0001 unpaired *t test.*

Increased peripheral B cell compartment and altered B cell surface phenotype in the adult of *H19*$^{-/-}$

H19 is expressed during embryonic development but no longer in adult tissues except for the satellite cell compartment in the skeletal muscle and cardiomyocytes (Liu et al., 2016). Although *H19* is the highest differentially expressed gene between embryonic and adult pro-B cells, the effects on B cell development although detectable appeared relatively mild. Moreover, *H19* has been reported to impact the epigenetic landscape of target loci in addition to the regulation of other genes within the imprinting network (Gabory et al., 2009). Therefore, we decided to investigate whether adult *H19* non-expressing adult lymphocytes differ between wild type and mutant mice. Interestingly, we had observed (see below) that adult B cells expressed high levels of the phosphatase CD45 isoform B220 compared to wild type B cells indicating that the absence of *H19* during embryonic development could also impact cells that no longer express this transcript (Fig 17A and B). To this end, we analyzed different peripheral organs, including spleen, lymph node, peritoneal cavity of different aged adult mice.

We observed, at all ages studied, that *H19*$^{-/-}$ mice showed an enlarged spleen size and increased spleen weight. Further investigation of cells in the spleen showed a specific increased B cell compartment, while erythrocytes and myeloid cells were not affected and T cells were modestly increased. When we subdivided B cells into different B cell subsets, such as MZ, FO, immature B cells and B1 cells, we found the increased B cells in the *H19*$^{-/-}$ was mainly caused by enlarged FO B cell subset (Fig 17C), while immature B cells showed no difference, and MZ and B1 cells showed a modest increase. Similar increased B cells was also observed in the peritoneal cavity (Fig 17D), where B1 cells mainly reside. The peritoneal cavity B cell compartment was further subdivided into three subsets according to the expression of the cell surface markers B220, CD19, IgM, CD5, and CD23 that discriminate the three main B cell populations B1a ($B220^{-/lo}CD19^{+}IgM^{+}CD5^{+}CD23^{-}$), B1b ($B220^{+}CD19^{+}IgM^{+}CD5^{-}CD23^{-}$) and B2 cells ($B220^{+}CD19^{+}IgM^{+}CD5^{-}CD23^{+}$). All these three subsets in the peritoneal cavity were increased in the *H19* mutant mice. In conclusion, loss of *H19* resulted in a specifically net increase of B cells in the adult periphery.

Of note, all B cells in both spleen and peritoneal cavity showed an upregulated B220 expression on the cell surface regardless of their respective cell subset (Fig 17A). *H19*$^{-/-}$ B cells showed an almost 2-fold increase in the mean fluorescence intensity of B220 expression on the cell surface (Fig 17B). In particular, B1a cells, which normally express very low levels of B220, exhibited a larger amount of B220 expressed on the *H19*$^{-/-}$ B1a cells. Similar upregulation of B220 expression on the surface of B cells was also observed in the *H19* maternal mutant *H19*$^{mat-/+}$, but not paternal mutant *H19*$^{+/pat-}$ (data not shown). B220 is one of the isotypes of CD45, a member of protein tyrosine phosphatase (PTP) family, which has been shown to regulate BCR signaling (Huntington and Tarlinton, 2004c; Zikherman et al., 2012), as well as GC reaction persistence (Huntington et al., 2006). Therefore, we further investigated the BCR signaling and GC formation in adult *H19* deficient mice.

Because *H19* is not expressed in the adult mature B cells we concluded that the higher levels of B220 expression on the surface of peripheral B cell of *H19*$^{-/-}$ mice was controlled by epigenetic modifications induced by *H19* expression during embryonic development.

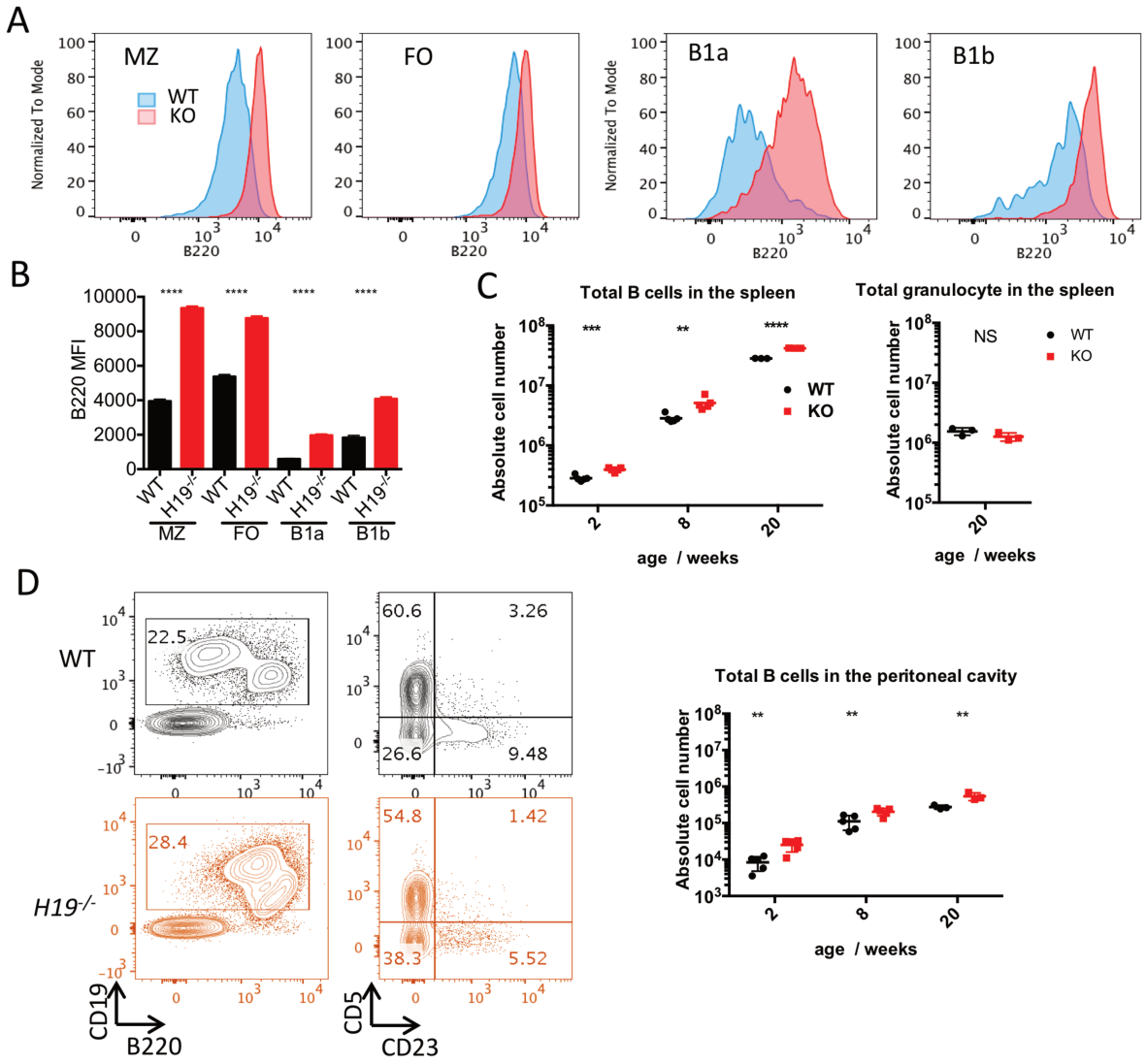

Figure 17 Increased peripheral B cell compartment and altered B cell surface phenotype in absence of *H19*

(A) Histogram of B220 expression and (B) mean fluorescence intensity(MFI) of B220 on MZ, FO, B1a and B1b cells from the spleen of adult wt and *H19*$^{-/-}$ mice; (C) absolute numbers of the total B cells in the spleen of 2-, 8- and 20-week-old mice, and granulocytes in 20-week-old mice of wt and *H19*$^{-/-}$; (D) immunostaining profile of peritoneal cavity B cells from wt and *H19*$^{-/-}$, and absolute numbers of the total B cells in the peritoneal cavity of 2-, 8-and 20-week-old mice of wt and *H19*$^{-/-}$;. Data of is representative of 3 independent experiments. *p<0.05; **p<0.01; ***p< 0.001, ****p< 0.0001 unpaired *t test.*

Loss of *H19* results in increasing newly generated B cells in BM and accelerated B cell egression to the periphery

In order to understand the mechanisms leading to increased B cell compartment, we performed EdU incorporation *in vivo* to assess the rate of B cell production in the BM.

We observed a higher frequency of proB, preB cells and newly generated B cells (defined as $CD19^{+}IgM^{+}$) labeled (45±3.7%, 59±4.7% and 13.2±0.5%) by the EdU in $H19^{-/-}$, in comparison to that of wt (33.8±1.5%, 44.8±1.6%, 7.3±0,3%) in the BM (Fig 18A and C) whereas non-B cells were identically labeled. This observation raises two possibilities, either BM of *H19* mutant was more efficient in producing B cell or more newly generated B cells were retained in the BM. To address this question, we analyzed the EdU labeling in the spleen of the same mice. *H19* mutant spleen showed increasing EdU labeled B cells (Fig 18B and C), suggesting a higher production of pro-B cells in the BM and a consequent higher frequency of EdU labeled splenic B cells.

In conclusion, loss of *H19* during embryonic development leads to increasing B cell production in the BM, contributing to larger peripheral B cell compartment in $H19^{-/-}$ mice.

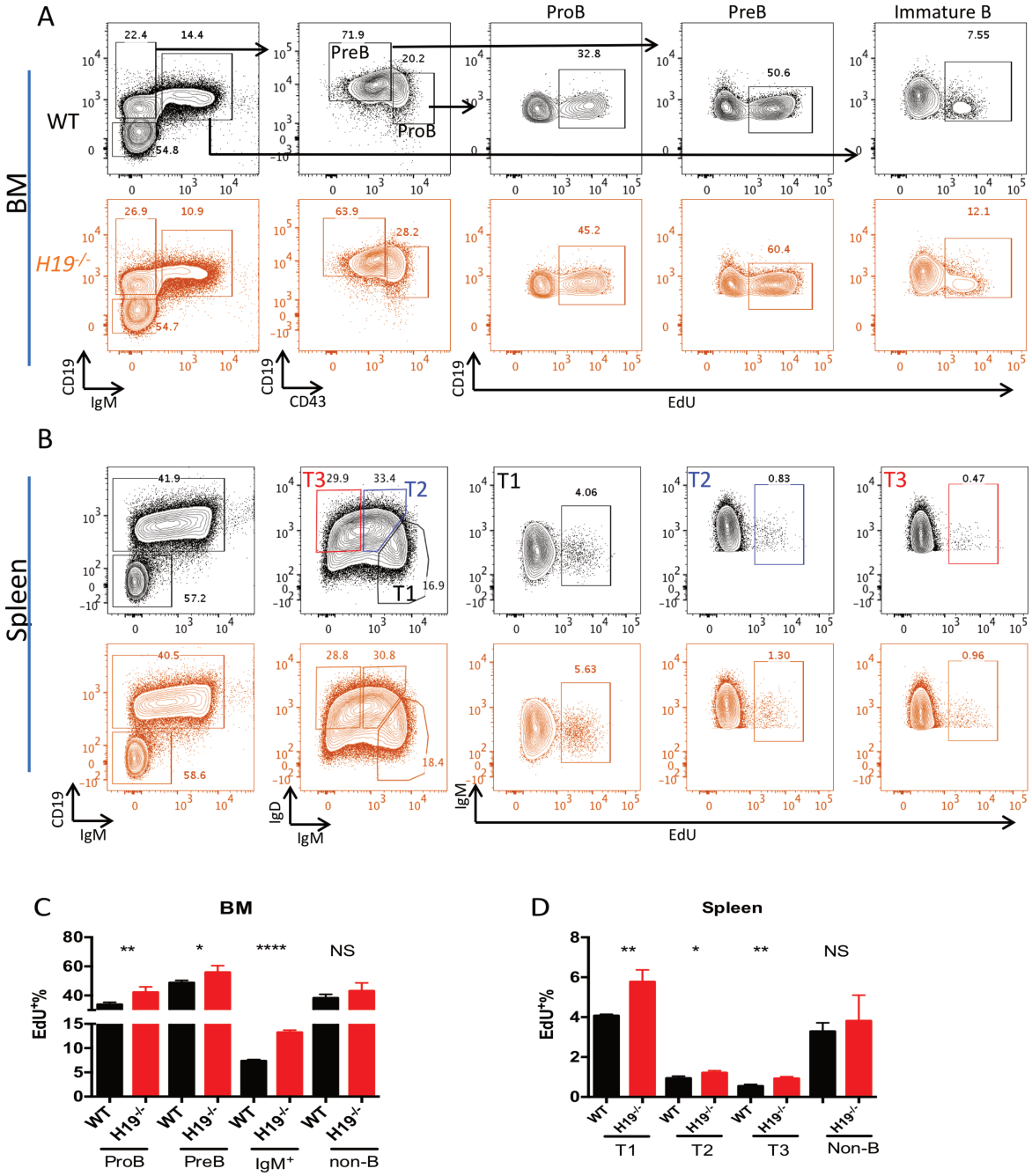

Figure 18 Loss of *H19* results in increased newly generated B cells in BM and spleen

Immunostaining plot of EdU uptake in the BM after 2 doses (separated by 12h) of EdU injection. BM and spleen from wt and $H19^{-/-}$ mice were analyzed 2 hours after the last injection. FACS plot of EdU staining in BM and spleen cells are displayed in (A) and (B), respectively. Histogram presents the frequency of EdU labeled cells in proB, preB, immature IgM^+ B and non-B cells in BM (C), and $IgM^+IgD^{lo/-}$ (T1), $IgM^{lo}IgD^+$ (T2), IgM^-IgD^+ (T3) and non-B cells in the spleen (D). Data of is representative of 2 independent experiments, 4 biological replicates per experiment. *p<0.05; **p<0.01; ***p< 0.001, ****p< 0.0001 unpaired *t test.*

Reduced germinal center reaction in *H19*$^{-/-}$

Because B220 plays an essential role in regulating BCR signaling, we next wondered whether the altered B cell surface phenotype impacts B cell function. The most straight forward way to assess B cell function is through B cell immunization, therefore we performed immunization by injecting several T cell dependent antigens. Sheep red blood cells (SRBC), ovalbumin (OVA) and NP_{25}-CGG were used to immunize *H19* mutant and wild type mice following the protocol described in Fig 19A. In brief, mice received two immunizations at D0 and D21, respectively, and on D7, D14 and D28 serum and splenic cells were collected for analysis.

After immunization, *H19* mutant mice showed smaller spleen size (Fig 19B) and decreased spleen weight (Fig 19C). Compared to non-immunized control, spleen from the wt immunization group almost doubled the spleen weight while the spleens from the *H19*$^{-/-}$ immunization group stayed similar in weight to non-immunized control mice (Fig 19C). B cell response that takes place in the peripheral organs, such as spleen and lymph nodes, occurs in specialized structures call germinal centers. The different sizes between spleen and lymph nodes in wt and H19 mutant immunized groups suggested differences in the immune response and led us to further investigate and quantify the magnitude of the GC reaction inside spleen and lymph nodes.

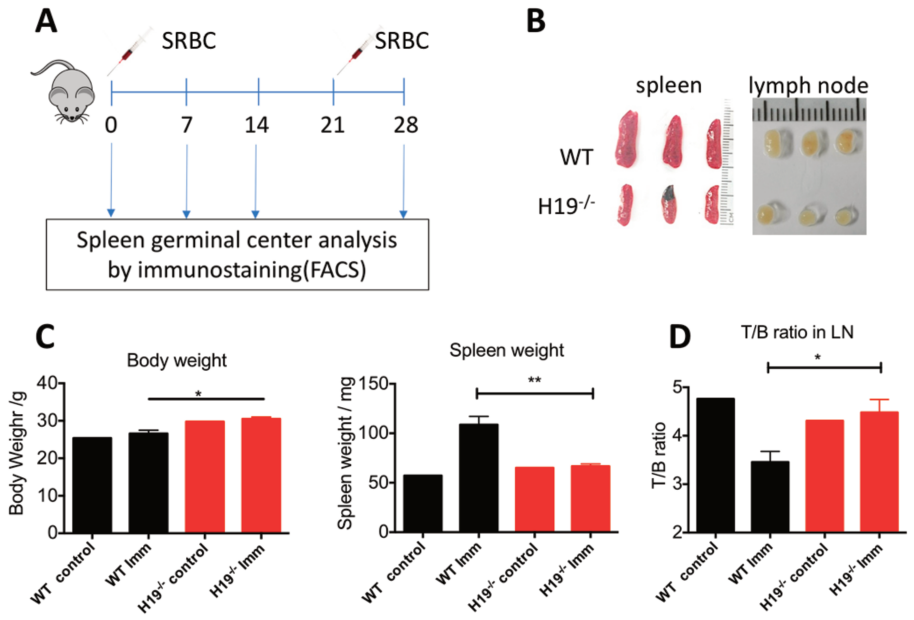

Figure 19 *H19* deficient mice display a differentially immune response

T cell dependent antigen SRBC immunization was performed following the procedure described in (A). The image shows the size of spleen and lymph nodes at 14 days after immunization(B). (C) Histogram shows the body and spleen weight of non-immunized control and immunized wt and *H19*$^{-/-}$ mice. (D) The T/B cell ratio in

the lymph nodes. Data is representative of 3 independent experiments. *p<0.05; **p<0.01; ***p< 0.001, ****p< 0.0001 unpaired *t test.*

To quantify the immune response in the spleen we analyzed the GC reaction where the immune response takes place. We used the following antibody panel comprising anti-CD19, anti-IgD, anti-CD38, anti-CD95, anti-CD86 and anti-CXCR4 that allows identifying dark and LZ cells within the GC. GC cells are defined as $CD19^{+}IgD^{+}CD38^{-}CD95^{+}$ and CD86 and CXCR4 expression further distinguish LZ ($CD86^{+}$ $CXCR4^{-}$) and DZ cells ($CD86^{-}$ $CXCR4^{+}$). After immunization, spleens from *H19*$^{-/-}$ mice exhibited approximately 2-fold decrease in the numbers of $CD19^{+}$ B cells. Although both wt and *H19* deficient mice showed increasing GC reaction compared to non-immunized control mice, spleens from *H19*$^{-/-}$ exhibited a lower magnitude of GC response in both frequency (Fig 20A and B) and absolute numbers (Fig 20C) at all time points analyzed after immunization. The frequencies of GC in the spleen of wt and *H19*$^{-/-}$ were 15.4±1.0% vs 11.6±1.7% on D7, 27±1.9% vs 19.4±1.5% on D14, 36.5±1.6% vs 25.5±1.8% on D28, respectively (Fig 20B). The absolute number of GC in *H19*$^{-/-}$ spleen showed a 2.1, 2.8 and 2.0 -fold decrease at D7, D14 and D28 after immunization (Fig 20C), respectively. The higher number of splenic B cells in the non-immunized mice of *H19*$^{-/-}$ (Fig 20C) were reversed such that after immunization the total B and GC cell numbers were now lower than those in wild type mice indicating an impaired B cell response in *H19*$^{-/-}$ mice. Similar reduced GC response pattern in *H19*$^{-/-}$ mice was also observed after OVA (in alum) immunization and spleens of *H19*$^{-/-}$ mice exhibited 6.1-fold decrease of GC cells at D15 after immunization (data not shown).

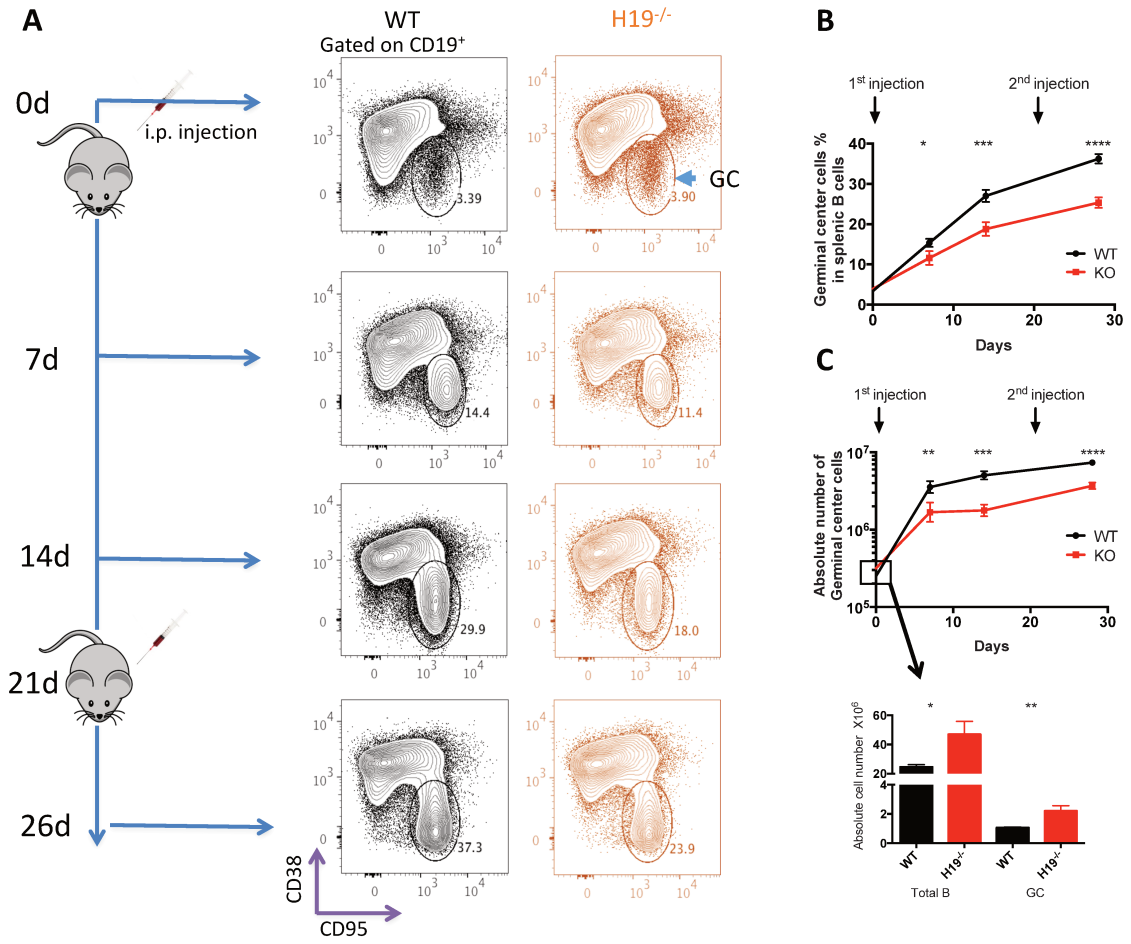

Figure 20 *H19* deficient mice display a reduced germinal center response in the spleen

(A) Immunostaining plots of GC cells at different time point of SRBC immunization procedure. GC cells ($CD19^+$ $CD38^-CD95^+$) were circled and the frequencies of GC in total B cells were indicated. Kinetic curves of the frequency (B) and absolute number (C) of GC cells in immunized wt. and $H19^{-/-}$.

Data of is representative of 3 independent experiments for each time point with at least three biological replicates. *p<0.05; **p<0.01; ***p< 0.001, ****p< 0.0001 unpaired *t test.*

The most affected cells after immunization were FO B cells whereas MZ and immature B cells were not, or less affected by the immunization (Fig 21A). Additionally, analysis of the peritoneal cavity showed B2 cells decreasing in number in $H19^{-/-}$ mice, while B1a and B1b cells were not affected. Of note, *H19* mutant mice still showed more B1a cells in the peritoneal cavity than wild type mice indicating that B1 compartment is not affected by immunization in the adult mice (Fig 21B).

Furthermore, in the lymph nodes, the ratio of T/B cells was decreased in wt compared to non-immunized control, while in $H19^{-/-}$ mice and control group the T/B cell ratios did not change

after immunization (Fig 20D), indicating limited expansion of B cell in *H19* mutant lymph nodes. The T cells in all three peripheral organs show no difference between WT and *H19*$^{-/-}$ mice after immunization (Fig 21A) and the numbers of B cell progenitors in the BM are not affected.

All together, these results indicate that upon T cell dependent antigen stimulation, *H19*$^{-/-}$ mice exhibited reduced response compared to wild type mice that is characterized by the inadequate activation of FO/B2 cells rather than B1 and MZ cells leading to reduced GC reaction.

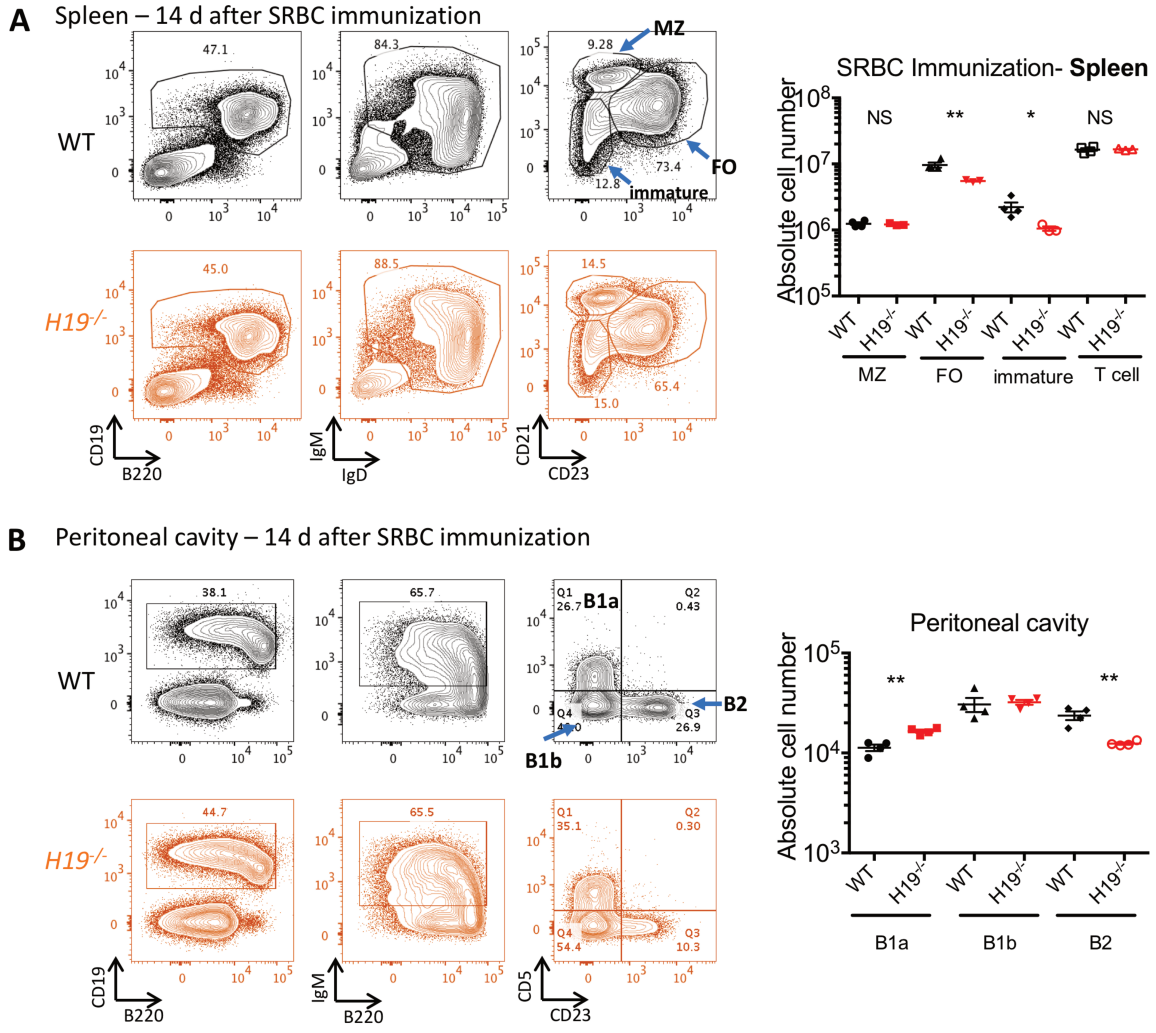

Figure 21. Peripheral B2 cells, but not B1 cells are reduced after immunization in *H19*$^{-/-}$ mice

(A) immunostaining plots display the MZ (marginal zone), FO (follicular), and immature B cell in the SRBC immunized spleen of wt and *H19*$^{-/-}$, different B cell subsets are indicated in the plot and the absolute number is shown in the histogram (right panel). (B) immunostaining plots display the B1a (marginal zone), B1b (follicular), and B2 cells in the SRBC immunized peritoneal cavity of wt and *H19*$^{-/-}$, different B cell subsets are indicated in

the plot and the absolute number is shown in the histogram (right panel). Data is representative of 2 independent experiments with 3 replicates each experiment. *p<0.05; **p<0.01; ***p< 0.001, ****p< 0.0001 unpaired *t test.*

DZ/LZ transition in GC was affected in absence of *H19*

GC can be polarized into two distinct microenvironments known as the DZ and the LZ (MacLennan, 1994). The DZ consists of highly proliferative centroblasts acting as a source of B cells with mutated BCRs which later undergo selection in the LZ. Selected B cells can be recycled to the DZ for an additional round of proliferation and mutation, termed as "feed-forward loop" or differentiate into plasma or memory B cells (Meyer-Hermann et al., 2001; Oprea and Perelson, 1997). The absolute numbers of both DZ and LZ GC cells were decreased in immunized *H19*$^{-/-}$ mice as described in Fig 20. Additionally, higher DZ/LZ ratio was observed in the GC at both D14 and D28 after immunization in H19$^{-/-}$ compared to wt mice (Fig 22A and C), indicating that GC B cells were enriched in cells with DZ phenotype and *H19* deficiency negatively regulate GC reaction and/ or DZ to LZ transition inside the GC.

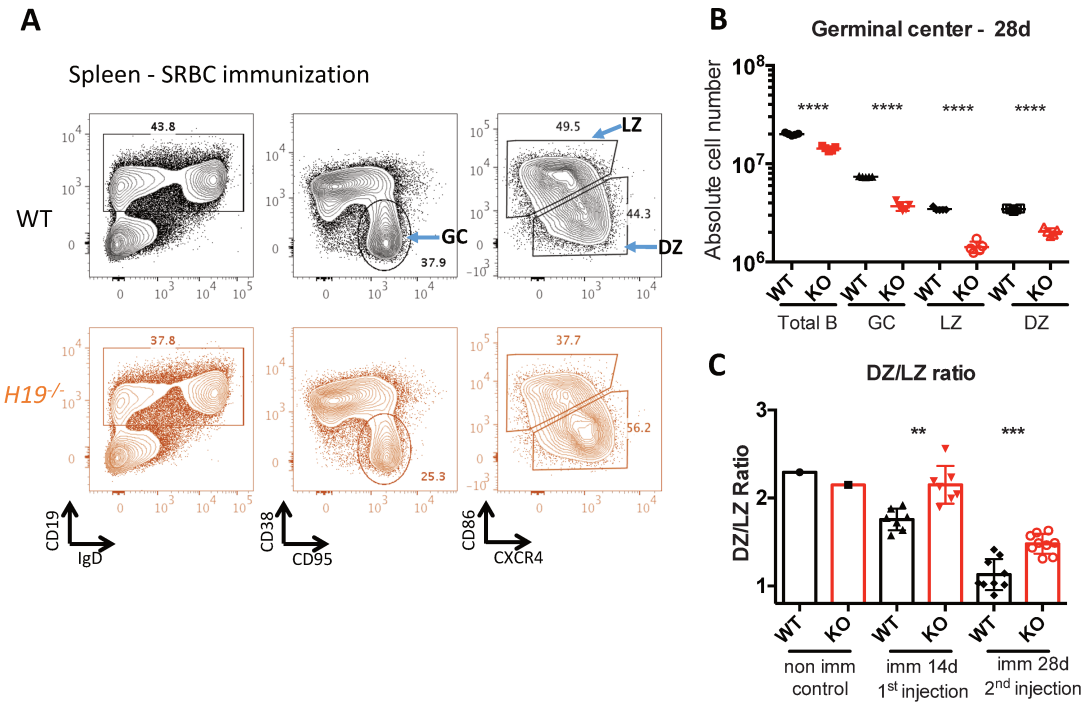

Figure 22 DZ/LZ transition in GC was reduced in absence of *H19*

(A) Representative plots showing GC cells in DZ and LZ at 28d after immunization; (B) absolute number of total B, GC, DZ, and LZ cells and (C) DZ/LZ ratio at 28d after immunization. Data is representative of 2 independent experiments with at least three biological replicates per experiment. *p<0.05; **p<0.01; ***p< 0.001, ****p< 0.0001 unpaired *t test.*

Impaired antibody specific IgM and IgG response in *H19*$^{-/-}$

An impaired GC reaction could result in a number of possible defects in the immune response. One is the amount of immunoglobulin produced, another includes the extent of class switch recombination and somatic hyper-mutation or selection of high affinity antibodies.

We therefore sought first to determine whether the antibody response was affected. To address this question, we analyzed total IgG and IgM titer before and after immunization, and antigen specific antibody, after immunization. Total serum IgG and IgM was measured by ELISA, showing both wt and *H19*$^{-/-}$ mice had comparable total IgM antibody titers in the serum before immunization (Fig 23B first panel from the top). The total IgG (all classes) however showed a two-fold decrease in mutant mice. To evaluate the titer of antigen specific antibody after immunization with SRBC we adopted the method reported by Ellen J et al. (McAllister et al., 2017)(Fig 23A). Briefly, serial dilutions of the serum were incubated with fixed number of SRBCs that were in a second step incubated with fluorescence labelled secondary anti-mouse IgG or IgM or other Ig isotypes (Fig 23A). The mean fluorescence intensity (MFI) of the complex was measured by flow cytometry and a titration curved was obtained by plotting MFI against serum dilution factor. The results showed that antigen specific IgG and IgM response were similar in WT and mutant mice at D7 after immunization, indicating the initiation of antigen specific IgG and IgM response in the *H19*$^{-/-}$ mice was normal (Fig 23B second panel from the top). However, at D14, antigen specific IgM response in *H19*$^{-/-}$ showed a 4-fold decrease (Fig 23B third panel from the top), while antigen specific IgG response was also decreased although to a lower extent than that observed in IgM. We investigated the antigen specific response of the different Ig isotypes, such as IgG1, IgG2a, IgG2b, as well as IgE. Only IgG1 that accounts for more than 80% of the IgG immune response showed a 1.5-fold decrease in *H19*$^{-/-}$ compared to WT mice (data not shown). The most striking difference lied in the antigen specific IgM response after the second immunization because *H19*$^{-/-}$ mice showed a virtually undetectable antigen specific IgM in the serum corresponding to close to 100-fold decrease compared to wt mice that exhibited a continuous increase of IgM response (Fig 23B first panel from the bottom). Further investigation of the affinity of OVA-specific IgM by ammonium thiocyanate elution method (Ferreira and Katzin, 1995) and of NP-specific IgM in NP-CGG immunization by the ELISA (Barinov et al., 2017) showed both the affinity of OVA and NP-specific IgM were lower in the *H19*$^{-/-}$ mice, compared with wt (Fig. 23C), while NP-specific IgM affinity in NP-Ficoll

immunized mice of bot genotype showed no difference. Therefore, *H19* have a role for selection of high-affinity IgM^{+} GC cells in TD response, affinity maturation is impaired and the humoral immune response is suboptimal in absence of *H19*. All of these results point to the conclusion that loss of *H19* lead to reduced GC reaction, in particularly defected IgM response.

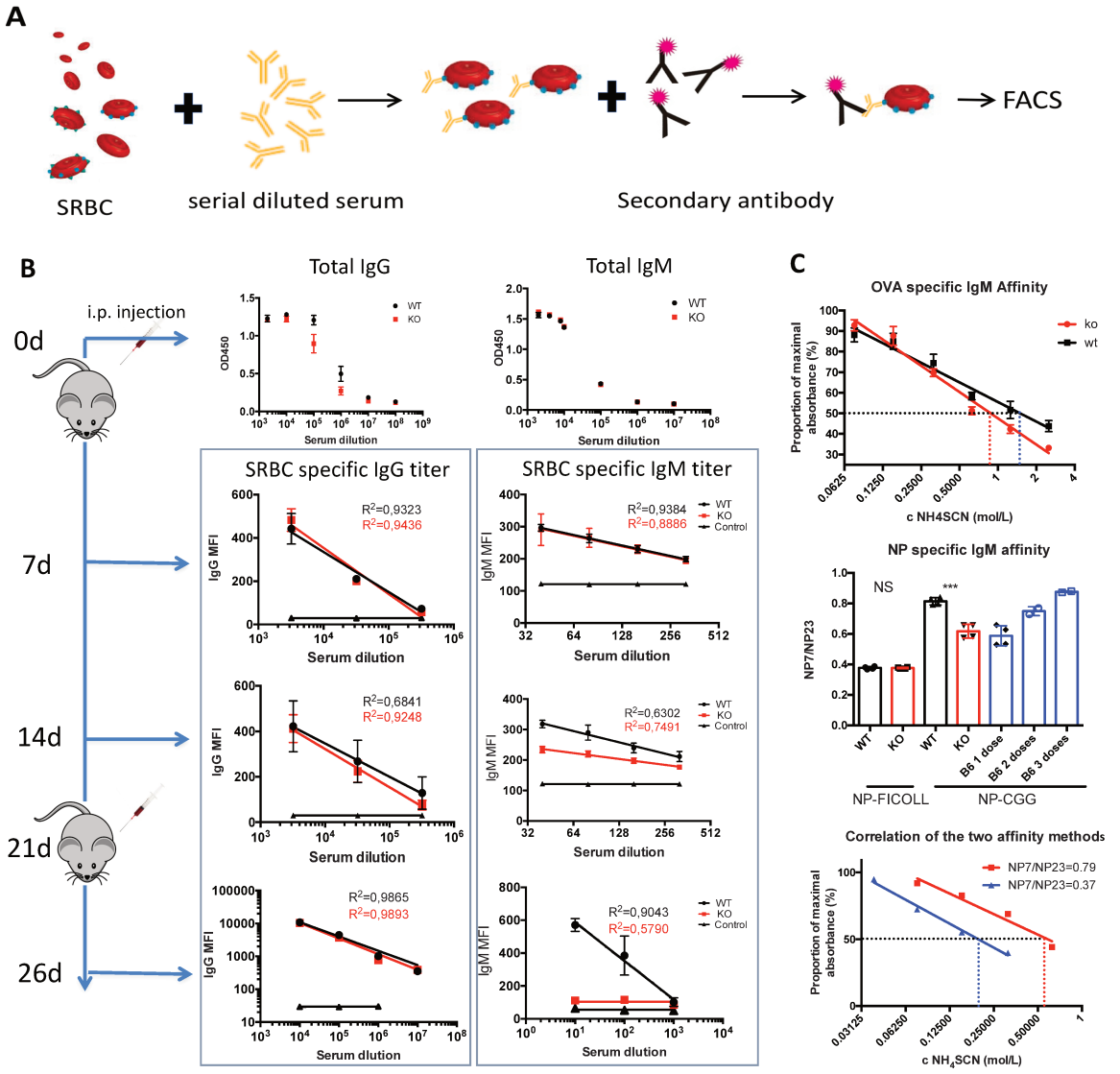

Figure 23 Impaired antigen specific IgM response and affinity maturation in T cell dependent antigen immunized *H19*$^{-/-}$ mice

(A)the methodology scheme of measuring SRBC specific antibody. (B) titration curves of total serum IgG, IgM (the first panel from the top) measured by ELISA, and titration curves SRBC specific IgG (the left square) and IgM IgG (the right square) at D7, D14 and D28 analyzed by the method described in (A), the R^2 value was indicate in the plots. The control titration curve was obtained by using serum from non-immunized mice; (C) Affinity of OVA was measured by ammonium thiocyanate elution method, relative affinity of antibody was indicated as molarity of chaotropic reagent (NH_4SCN) where the initial absorbance decreased by 50%. The affinity of NP-specific IgM was indicated as absorbance ratio of NP7/NP23 by ELISA. Data is representative of

2 independent experiments with at least three biological replicates per experiment. *p<0.05; **p<0.01; ***p< 0.001, ****p< 0.0001 unpaired *t test*.

The impaired antigen specific IgM response led us to investigate the Ig class switch recombination, plasma cell generation, as well as apoptosis of the GC cells after immunization.

To assess Ig class switch recombination process we analyzed splenic GC 14 days after the immunization with SRBC from both WT and *H19*$^{-/-}$ by flow cytometry. The GC cells ($CD19^+IgD^+CD38^-CD95^+$) were sub-divided by using anti-IgG1 and anti-IgM. We observed that GC cells from H19 mutant mice showed a ~2-fold increased frequency of $IgG1^+$ cells, which accounted for 56.3 ± 0.5% of total GC cells, while the WT was 26 ± 11,3%. On the contrary, the frequency of IgM^+ cells showed a mild decrease, 19.0 ± 1.1% in *H19*$^{-/-}$ versus 27.4 ±0,1% in WT (Fig 24A and B). Although the frequency of $IgG1^+$ cells increased and that of IgM decreased the profound reduction in the numbers of GC cells in mutant mice results in a close to 10-fold decreased number of IgM^+ GC cells whereas the numbers of $IgG1^+$ GC cells were comparable between WT and *H19* mutant mice. These results showed that after entering GC, the initial IgM^+ B cells switched to a similar number $IgG1^+$ cells in WT and mutant mice although the IgG1 antibody titers were slightly decreased, whereas left a far lower number of IgM^+ GC cells in $H19^{-/-}$, indicating a virtual normal class switch recombination but a decreased IgM^+ pool. As previously described, the Ig class switch is mediated by the activation induced cytidine deaminase (AID, encoded by *Aicda*). We next sorted the GC cells 7 days after the immunization and studied the expression of *Aicda* by qPCR, *H19*$^{-/-}$ GC cells showed a mild increase *Aicda* expression (see below in Fig 29C), reflecting the higher frequency of $IgG1^+$ cells (Fig 24A and B). This result is therefore consistent with the previous observation that GC in *H19* mutant mice showed a higher DZ/LZ ratio (Fig 22A and C), because AID is mainly expressed and exert its function of Ig class switch in highly proliferative DZ cells.

To investigate the plasma cells generated after immunization, we performed the enzyme-linked immunospot (ELISPOT) to quantify total Ig and IgM secreting cells in both BM and spleen of SRBC immunized mice. Interestingly, the number of total IgM secreting cells in both spleen and BM showed a 2-fold decrease in *H19*$^{-/-}$ mice while total antibody secreting cells revealed by an anti-kappa light chain antibody was comparable in both spleen and BM of SRBC immunized wt and *H19*$^{-/-}$ mice (Fig 24C), indicating the specific reduction of IgM

plasma cells in SRBC immunized *H19*$^{-/-}$ mice contribute to the defected antigen specific IgM response.

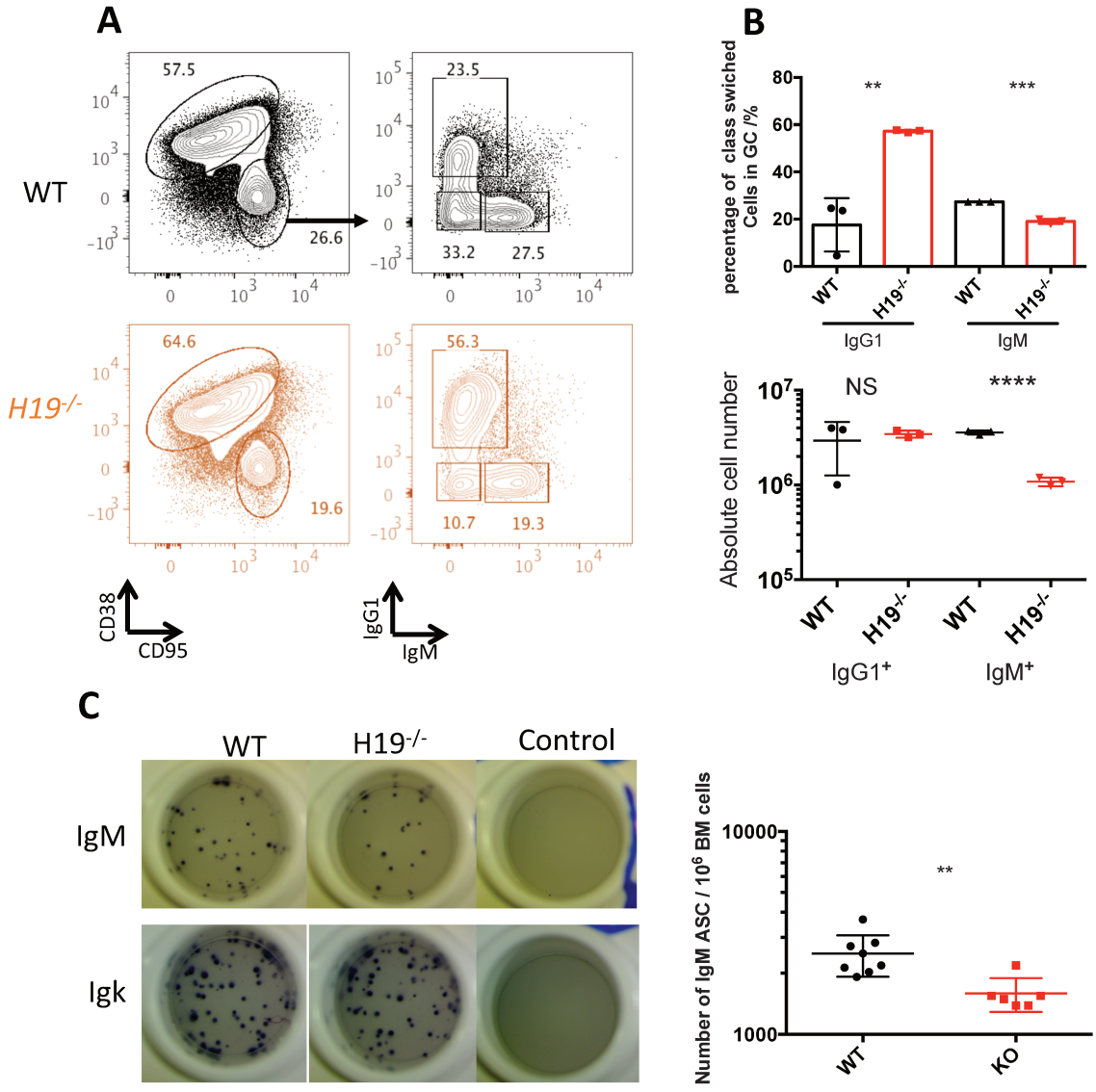

Figure 24 *H19* deficient mice display an accelerated Ig class switch to IgG1, leading to reduced IgM$^+$ GC in Spleen and IgM secreting plasma cell in the BM

(A) Representative FACS plots showing the IgG1 class switch in GC, GC cells were subdivided into IgG1$^+$ and IgM$^+$ population; the frequency (B, upper histogram) and absolute number (B, bottom plot) of IgM$^+$ and IgG$^+$ GC cells. Spleens analyzed were from SRBC immunized mice, 14 days after immunization. (C) IgM and IgG antibody secreting cells measured by ELISPOT, left panel shows representative well images of IgM and Igk secreting cells, each dot was counted as one antibody secreting cell. The statistical analysis of the absolute number of IgM secreting cells was shown in the right panel. Data is representative of 2 independent experiments

with at least three biological replicates per experiment. *p<0.05; **p<0.01; ***p< 0.001, ****p< 0.0001 unpaired *t test.*

We next evaluated the capability of the WT and *H19*$^{-/-}$ splenic B cells to generate CD138^{+} plasma cells after *in vitro* stimulation. After stimulation of splenic B cells from both genotypes with anti-CD40 and IL4 we observed a decreased number of both total B cells and plasma cells (Fig 25) indicating that mutant cells are defective in their response to thymus dependent stimuli.

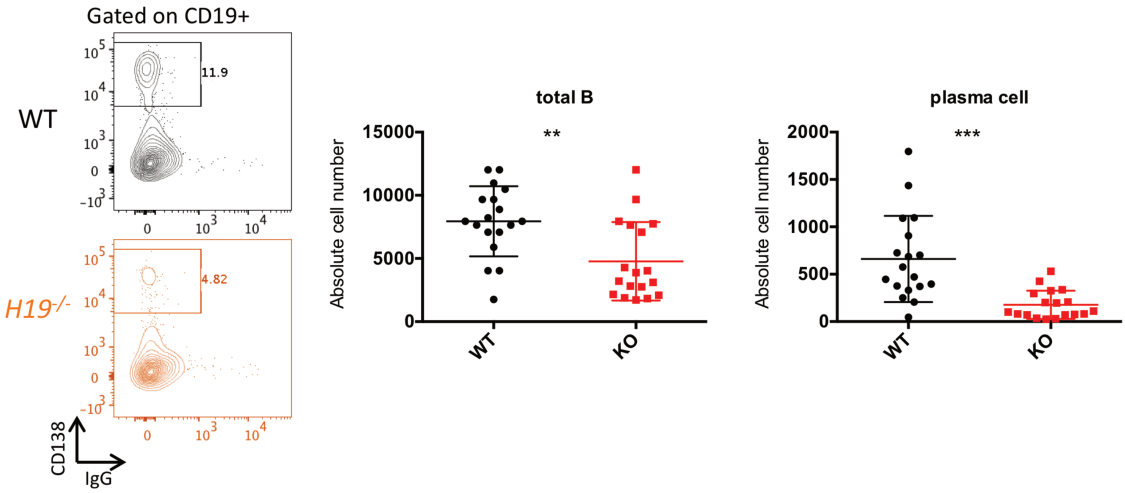

Figure 25 *H19*$^{-/-}$ splenic B cells are less efficient at differentiating to plasma cells under the stimulation of anti-CD40 and IL4 in vitro

(A) Representative FACS plots showing the percentage of plasma cells generated by the splenic B cells under the stimulation of anti-CD40 and IL4 in vitro. (B) absolute number of total B cells and plasma cells after 6 days of in vitro culture. Data is representative of 2 independent experiments with 18 replicates per experiment. *p<0.05; **p<0.01; ***p< 0.001, ****p< 0.0001 unpaired *t test.*

Reduced expression of B cell activation markers on the surface of *H19*$^{-/-}$ B cells after immunization

Because H19 mutant B cells showed a defective response to anti-CD40, we investigated the expression of the accessory molecules displayed cell surface responsible for B cell activation. Splenic B cells from SRBC immunized mice from both genotypes upregulated the B cell activation markers, MHCII, CD40 and CD86. However, *H19*$^{-/-}$ B cells showed a lower expression of MHCII, and more strikingly, of CD40 and of CD86 (Fig 26). As described previously, MHCII presents the antigenic peptides to the TCR and get the feedback signal from TFH cells for B cell activation and selection (Yang Zhang, 2018). While CD40 and CD86 paired with CD40L and CD28 expressed on TFH cells to provide co-stimulatory signal for the B cell activation and selection. The lower expression of CD40, CD86 and MHCII indicates that *H19*$^{-/-}$ B cells received weaker signals from cognate TFH cells such that activation of *H19*$^{-/-}$ B cells was less efficient. In particular, blocked CD40-CD40L costimulatory signaling after SRBC immunization has been reported to reduce the plasma cell differentiation (Foy et al., 1996) (Yang Zhang et al. 2018). This is in line with our observation that *H19*$^{-/-}$ B cells give rise to a reduced number of plasma cells in response to both *in vivo* (Fig 24C) and *in vitro* (Fig 25) stimulation. This conclusion was further reinforced by *in vitro* culture, which showed that *H19*$^{-/-}$ B cells failed to upregulate MHCII and CD86 to levels comparable to those in WT B cells after stimulation with anti-CD40 and/or anti-IgM *in vitro* for 24h (Fig 26B). Collectively, these results demonstrate that T-B cell interaction, caused by the lower costimulatory signaling (such as CD40-CD40L, CD86-CD28), is less efficient in H19 mutants compared to WT mice, resulting in defective B cell response and plasma cell differentiation, reflected by an impaired GC reaction and antigen specific IgM response.

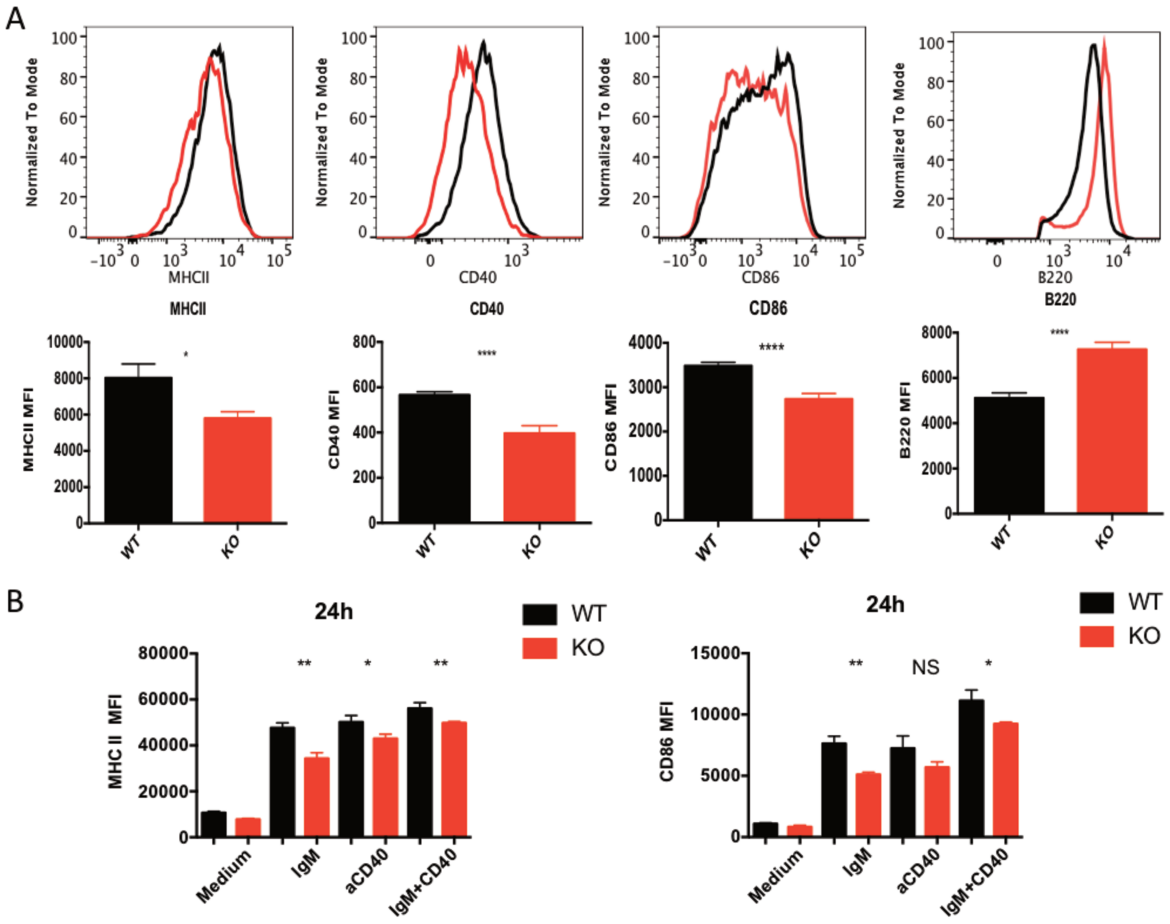

Figure 26 Reduced expression of B cell activation markers on the surface of *H19*$^{-/-}$ B cells

(A) Histogram of expression of some B cell activation molecules, such as MHCII, CD40, CD86, at 14 days after immunization, and the B220 expression on the B cells of immunized mice. (B)MHCII and CD86 expression on the surface of splenic B cells from wt and *H19*$^{-/-}$ mice after 24h *in vitro* stimulation with medium, anti-CD40 and/or anti-IgM. The level of expression was reflected by mean fluorescence intensity(MFI) measured by flow cytometry; Data is representative of 3 independent experiments with 3 replicates each experiment in (A), and 2 independent experiments with at least 5 replicates each experiment in (B) *p<0.05; **p<0.01; ***p< 0.001, ****p< 0.0001 unpaired *t test.*

We investigated the cytokine secretion as well as apoptosis profiles of the GC cells after immunization. 3 days and 7 days after immunization, we analyzed the intracellular production of a range of cytokines, including IL4, IL6, IL10, TNFa and IFRγ, none of them showed difference between WT and *H19*$^{-/-}$ B, T and non B/T cells (data not shown) and both naïve B and GC cells from both genotypes showed the same level of caspase 3/caspase 7 staining

profile (data not shown), indicating that the altered GC response in *H19*$^{-/-}$ was not caused by increased apoptosis.

H19 functions in a B cell autonomous manner to regulate B cell response

The results above indicated that *H19* expression during embryonic development affects the adult immune response. Although most effects were observed at the level of B lymphocytes and plasma cells, we considered the possibility that *H19* expression impacted other cells involved in the immune response and that the defective immunoglobulin secretion and GC reaction after immunization were an indirect consequence of the *H19* mutation. To determine whether the defective B cell response in *H19*$^{-/-}$ mice is or not a B cell autonomous phenomenon we performed reconstitution chimeras. We used E15 FL cells from WT and *H19* mutant embryos at a 1:1 ration to reconstitute Rag$^{-/-}$γc$^{-/-}$ CD45.1 recipient mice which have no B, T and NK cells. 8 weeks later a fraction of chimeric mice were immunized with SRBC and analyzed 10 days later (Fig 27A). Splenic B, T, and granulocytes from donor origin (CD45.2) were purified and submitted to quantitative genomic *H19* PCR to distinguish WT cells from *H19*$^{-/-}$ cells. Compared with the non-immunized control, the spleen in the immunized group showed a decrease in both spleen size and weight (Fig 27B), exhibiting a similar phenotype as that observed in the immunized *H19*$^{-/-}$ mice. We generated a standard curve by doing genomic PCR for *H19* in DNA obtained from freshly isolated B cells from WT and mutant mice mixed at different ratios. The PCR results of B, T, and granulocytes from both non-immunized and immunized recipients were fitted to the standard curve and frequency and number of the WT and *H19*$^{-/-}$ cells were calculated. Granulocytes and T cells from mutant mice were present at a similar frequency in both immunized and non-immunized chimeras. By contrast, mutant B cells that were present at a frequency of 54.6±4,3% before immunization decreased to 24.1±6,8% after immunization (Fig 27C and D)

When we calculated the absolute cell numbers, WT cells showed a mild increase in the immunized group, and in contrast, the *H19*$^{-/-}$ B cells exhibited a more than 4-fold decrease (Fig 27D). This result indicates that the B cell defective response in *H19*$^{-/-}$ mice is a B cell intrinsic phenomenon.

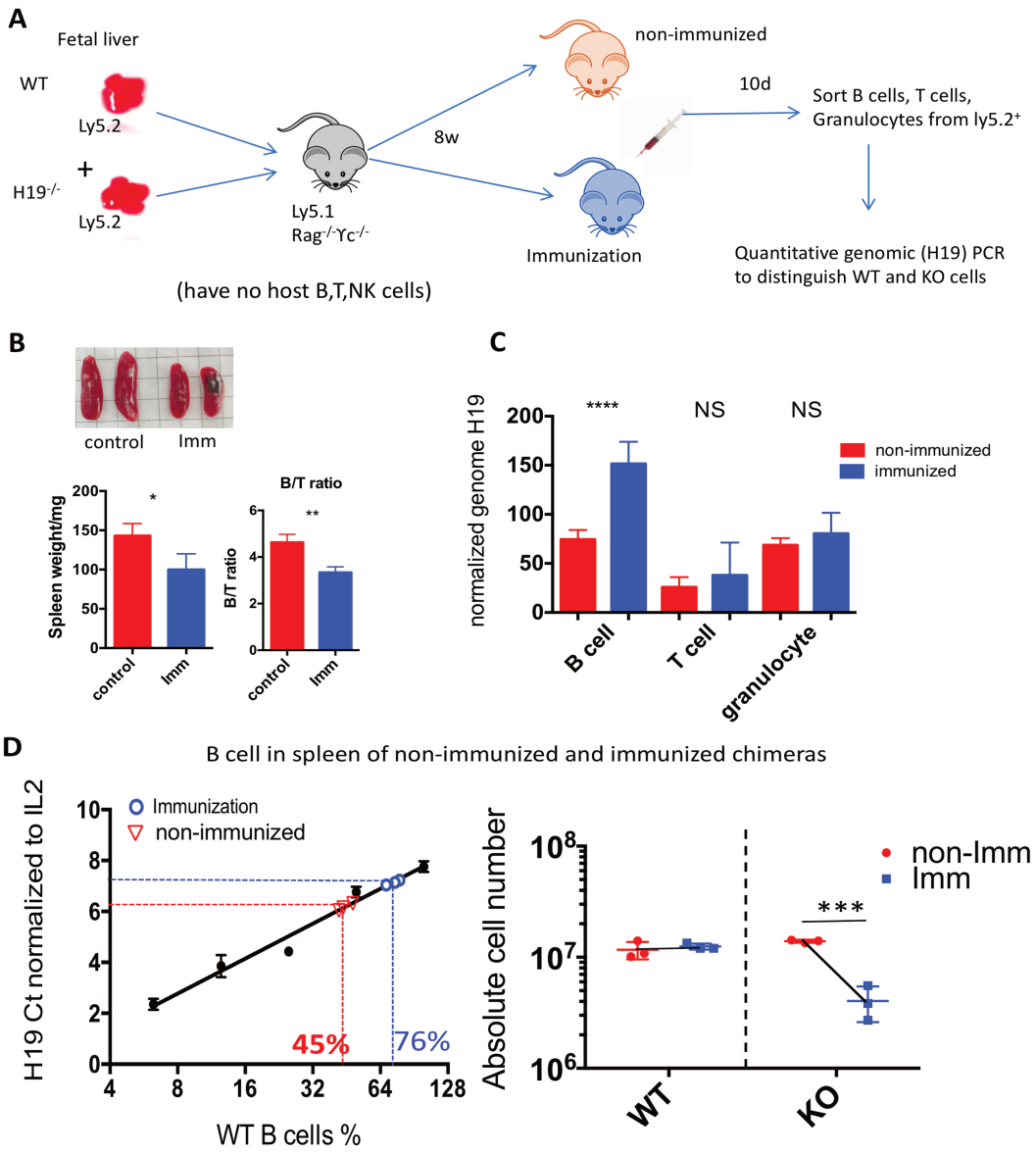

Figure 27 *H19* functions in a B cell autonomous manner to regulate B cell response

(A) Experimental scheme of the chimeras' reconstitution: Sub-lethally irradiated (400 rads) recipient mice (Ly5.1 rag$^{-/-}$rc$^{-/-}$) were transplanted with unfractionated E15 FL cells (Ly 5.2) from both wt and *H19*$^{-/-}$, at 1:1 ratio, after 8 weeks, mice were separated into two groups, one was immunized with SRBCs, the other served as non-immunized control. 10 days after immunization, the splenic B, T, and granulocytes were sorted from Ly5.2 compartment and submitted to quantitative genomic *H19* PCR to distinguish WT cells from *H19*$^{-/-}$ cells. (B) the images showed the size of spleens from both group, and the left histogram showed weight. The B/T cell ratio in both groups was indicated in the right histogram. (C) Quantitative *H19* genome PCR result of T cells, B cells and granulocytes sorted from the spleen of both immunized and non-immunized mice, the value of genome *H19* was normalized to genome IL2. (D) the left panel showed the percentage of WT B cells in all sorted B cells from both group. The setting of the titration curve is the following: 1.100% WT B cell; 2. 50% WT B cells plus 50% *H19*$^{-/-}$ B cells; 3. 25% WT B cells plus 75% *H19*$^{-/-}$ B cells; 4. 12.5% WT B cells plus 87.5% *H19*$^{-/-}$ B cells; 5.

6.25% WT B cells plus 93.75% *H19*$^{-/-}$ B cells, and titration curve is generated by plotting the normalized Ct value of *H19* against the percentage of WT B cells. (D, right panel) the absolute number of WT and *H19*$^{-/-}$ B cells calculated separately in both group. Data is representative of 1 independent experiments with 3 replicates in the control group and 5 in the immunized group. *p<0.05; **p<0.01; ***p< 0.001, ****p< 0.0001 unpaired *t test.*

B Cell Receptor-Mediated Calcium Signaling Is Impaired in *H19*$^{-/-}$ B Lymphocytes

As discussed before, the main signal for B cell activation is done through the BCR complex, and B220 can regulate BCR signaling through different mechanisms (Byth et al., 1996). Previous results indicated that the defect of *H19*$^{-/-}$ B cell response is cell autonomous phenomenon therefore we next determined whether the differential B220 expression impacts on BCR signaling by analyzing the calcium influx. In response to polyclonal IgM stimulation, splenic *H19*$^{-/-}$ B cells had dampened both basal and anti-IgM inducible calcium influx levels (Fig 28A), indicating increased threshold of BCR ligation triggered signaling, while a lower basal calcium flux levels, reminiscent of a less anergic B cells phenotype characterized in various model BCR transgenic systems (Cooke et al., 1994; Yarkoni et al., 2010). Furthermore, the similar dampened calcium flux profile was observed in the *H19*$^{-/-}$ splenic B cells after *in vivo* immunization (Fig 28B). We analyzed the B cell compartment according to the levels of B220 expression on the B cell surface, namely B220^{hi}, B220^{int} and B220^{lo}, respectively. Calcium flux was inversely correlated to the expression of B220 in both WT and *H19*$^{-/-}$ splenic B cells, suggesting the upregulated B220 expression on *H19*$^{-/-}$ B cells results in elevated threshold of BCR signaling or reduced responsiveness on BCR stimulation. Loss of *H19* tunes functional BCR responsiveness through regulating B220 expression, in an unknown manner.

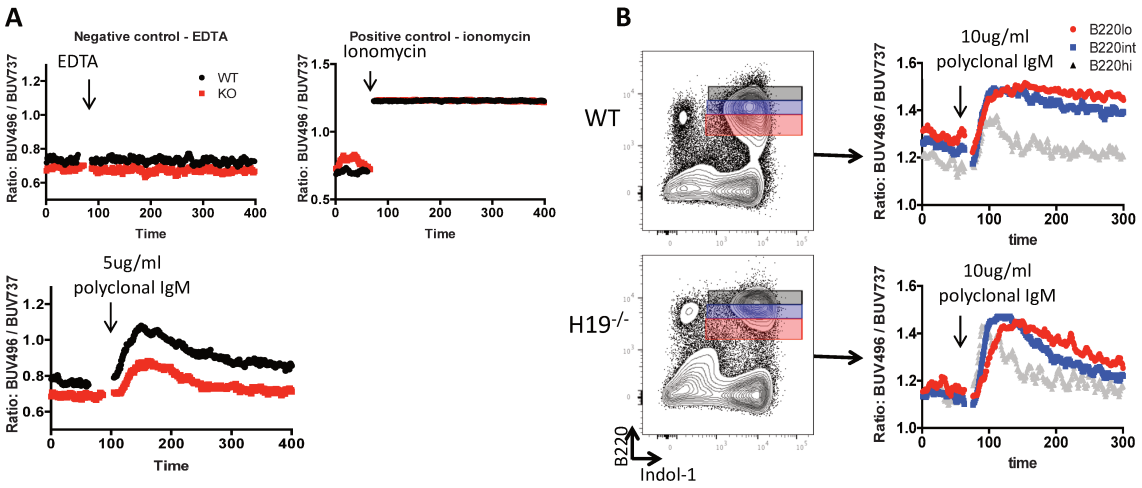

Figure 28 Reduced calcium influx in *H19*$^{-/-}$ splenic B cells were inverse correlated to the expression of B220

(A) Calcium influx profiles of normal splenic B cells of wt and *H19*$^{-/-}$ in response to the stimulation of EDTA (negative control), Ionomycin (positive control), and 5 ug/ml polyclonal IgM. (B) 14 days after SRBC immunization, the B cells in the spleen were sliced into B220^{hi}, B220^{int}, B220^{lo} three compartments, and calcium influx in response to 10ug/ml polyclonal IgM of the three sub-population was overlapped and displayed in the right panel. Data is representative of 2 independent experiments with 3 replicates each experiment.

Reduced BCR signaling related genes in *H19*$^{-/-}$ B cells are reflected in GC transcriptional profile

To further explore the nature of the reduced GC response and have a deeper understanding of the molecular mechanism underlying the impaired GC reaction and antigen specific IgM response, we performed genome wide transcriptional analysis (RNA sequencing) on the GC cells from both WT and *H19*$^{-/-}$ mice. The different sets of genes upregulated and downregulated in the GC cell from *H19*$^{-/-}$ are shown in the heat map generated from the RNA sequencing data (Fig 29A). Genes belonging to the histone gene cluster 1 and 2 (*HIST1, 2*) and cyclin-dependent kinases (CDK) are among the most upregulated genes in mutant GC B cells (Fig 29B). Histones are the major protein constituents of chromatin and H1, H2A are replication dependent histones. Thus, transcription of histone genes allowing the assembly of newly replicated DNA is tightly associated to cell cycle. Being CDKs also regulators of cell division the upregulation of HIST and CDK family genes indicated *H19*$^{-/-}$ GC cells were more

active in cell cycle. This is consistent with the higher DZ/LZ ratio observed in the GC of immunized *H19*$^{-/-}$ mice, since the DZ cells are highly proliferative in compare to LZ cells, and larger frequency of the DZ might be responsible for the upregulated genes associated to cell division. Transcripts such as *Aicda, Sh2b2*, *smarcc1* and *Usp12* show the largest fold-change genes within the upregulated gene set in GC cells of *H19*$^{-/-}$ (Fig 29 A and C), whereas among those downregulated genes in the mutant GC cells, some are related to BCR signaling and B cell activation, in particular, *CD40*, *CD69*, *CD2*, *CD48*, *Ptk2*, *Akt3* and *Rel*, were downregulated in mutant GC cells. The latter downregulated transcripts are associated with the reduced B cell response in the GC. Except the transcripts involved in BCR signaling, a number of other genes were significantly downregulated in *H19*$^{-/-}$ GC cells, such as *Xkr6*, *Bcl9*, *Bcl2*, *Uba7*, *Stag3*, *Elolv6*, etc (Fig 29A and C).

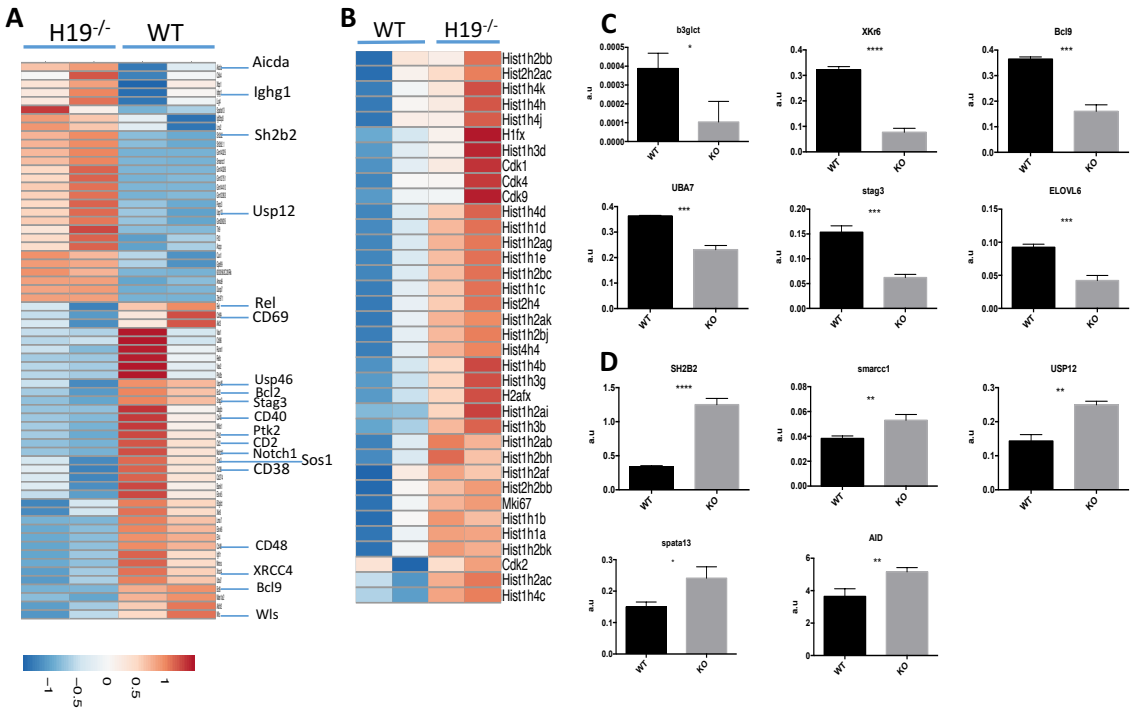

Figure 29 Reduced BCR signaling related genes in *H19*$^{-/-}$ B cells are reflected in GC transcriptional profile

(A) Heat map of a selected set of genes with different expression in *H19*$^{-/-}$ versus WT GC cells. RNAseq was done in the GC cells from 7 days post SRBC immunization. (B) Heat map of histone genes and genes related to the cell cycling; Validation of the top differentially expressed genes (downregulated genes (C) and upregulated genes(D) in GC of *H19*$^{-/-}$) from RNA sequencing by quantitative RT-PCR. Results are presented in arbitrary units (AU) normalized to expression of housekeeping gene *Hprt*. Data is representative of 1 independent experiments with 3 biologic replicates. *p<0.05; **p<0.01; ***p< 0.001, ****p< 0.0001 unpaired *t test.*

We validated a number of the differentially expressed genes by qPCR, among 22 top differentially expressed genes were tested and we found *SH2B2* is most upregulated genes in GC cells from *H19*$^{-/-}$. *SH2B2*, also named *APS*, encodes a protein that belongs to SH2B adaptor family and contains pleckstrin homology (PH) and src homology 2 (SH2) domains, which was tyrosine phosphorylated in response to B cell receptor stimulation, as well as by kinase-2 (JAK2)-STAT5 (Wakioka et al., 1999). Iseki M et al. reported that APS co-localized with BCR complexes in activated APS-Tg B cells and appeared to negative regulate BCR signaling (Iseki et al., 2005).

In addition, the *Aicda*, encoding AID, a crucial enzyme that mediates Ig class switch and somatic hyper-mutation in GC, showed also a modest increase in GC cells from *H19*$^{-/-}$ according to the qPCR (Fig 29C). This is consistent with previous observed accumulated IgG1 class switch and reduced IgM^{+} GC cells in *H19*$^{-/-}$.

We also validated that *Bcl9*, *stag3* and *Xkr6* were the most downregulated genes in *H19*$^{-/-}$ GC cells. *Bcl9* have been extensively studied to have a regulatory role for the transcription of Wnt target genes (Mosimann et al., 2009), associated with B-cell malignancies through inhibition of apoptosis and might contribute to the maintenance of the GC reaction and expansion in the immunized WT mice. Although we did not find differences in caspase 3/7 expression between WT and mutant GC cells it could be that differences in apoptotic cells that went undetected by antibody staining were revealed by transcriptional analysis.

The transcriptional landscape of GC cells revealed the links between the molecular events and the immune-phenotype of *H19*$^{-/-}$ impaired in mutant B cells. First, reduced BCR responsiveness reversely correlated to the expression of B220 is also reflected by the upregulated *Sh2b2* that has a role in negative regulation of BCR signaling. Second, lower expression of costimulatory molecule CD40, CD2 and CD69 also results in reduced B cell activation signal from T helper cells. Dampened BCR signaling and T cell help in GC cells of *H19*$^{-/-}$mice leads to decreased expression of *Rel*, one of the NF-kB subunits, which consequently slows down the GC reaction. Third, upregulated *Aicda* expression in GC cells of *H19*$^{-/-}$ reflects the accumulation of Ig class switch to IgG1. Fourth, upregulated histone genes is also consistent with the increased DZ/LZ ratio, suggesting higher frequency of DZ cells undergoing Ig class switch and somatic hyper mutation.

Taken all the observations above we concluded that loss of *H19* linked to the altered B cell development in the FL, resulting in a larger peripheral B cell compartment, which showed a reduced GC reaction and defected antigen specific IgM response after TD antigen stimulation. In this TD antigen response process, competitive reconstitution showed that *H19* functioned in a B cell autonomous manner, also reflected by the dampened BCR signaling and impaired costimulatory signal from T helper cells in GC of *H19*$^{-/-}$mice. Additional molecular evidence was added by lower expression of BCR signaling associated genes, genes related to B cell activation in response to TD antigens and higher expression of *Aicda* and cell cycle related genes, as well as *Sh2b2, a* negative regulator of BCR signaling.

Discussion

Long non-coding RNA *H19* is highly expressed in the fetal life and decreases its expression after birth. In particularly, in the FL, highly expressed *H19* has been linked to hepatocyte proliferation and differentiation, liver maturation (Pope et al., 2017) through the regulation metabolic propertied of developing hepatocytes. In the adult, expression of *H19* has been reported in the skeleton muscle satellite cell (Dey et al., 2014b) and, although at very low levels, on hematopoietic stem cell in the BM (Venkatraman et al., 2013) where loss of *H19* leads to premature exit from quiescence and drives stem cells to enter differentiation through enhanced Igf2-Igf1r signaling. Our observations that H19 is the most differentially expressed transcript in both B and T cell progenitors between embryonic and adult lymphoid cells suggested a role of these cells in the development of the immune system.

We first characterized early B cell development by analyzing different developmental stages, in both FL and adult BM. Then we assessed the B cell migration from the BM to the peripheral secondary lymphoid organs, such as spleen and lymph nodes, where B cell maturation takes place. Finally, we assessed the functional property of WT and *H19*$^{-/-}$ B cells through a characterization of the immune reaction and we assessed the molecular mechanisms underlying the differences found in the immune reaction.

Altered B cell development in FL of *H19*$^{-/-}$

Following the developmental scheme described by Hardy based on B cell surface markers we observed that *H19*$^{-/-}$ FL generated far more BP1^{+} proB cells, a compartment that is composed of fraction C (cells undergoing immunoglobulin heavy chain rearrangement) and C' (cells with a productive rearrangement). Although the Hardy scheme of B cell development was initially designed to analyze BM B lineage cells we found that the same applies to FL development and three fractions in the proB compartment could clearly be distinguished after E17.5. However, in contrast to BM cells, a discrete fraction of intracellular Igμ^{+} lymphocytes could be found in fraction B in both wt and *H19*$^{-/-}$(Fig 15B).

As the B cells developed to the fraction C' stage, the frequency of intracellular Igμ^{+} cells reached to 80% in both wt and *H19*$^{-/-}$. This result shows increased numbers of cells that completed a productive heavy chain rearrangement in mutant FL cells although the

frequencies of cells that initiate and completed rearrangement is lower in mutant than WT cells.

Transcriptional analysis of fraction C indicates elevated *Igf2* expression but also of Igf1r that binds Igf2. *Igf2* promotes cell growth and proliferation in hematopoietic cells (Martinet et al., 2016; Venkatraman et al., 2013) and upregulated *Igf2* expression by loss of imprinting is a common feature in tumors seen in Beckwith-Wiedemann syndrome (Cohen, 1994) and Wilms' tumor (Frevel et al., 1999). However, cell cycle analysis showed that mutant cells are less cycling than their WT counterparts. Because the size of fraction B is identical in both strains the increased B cell production can only be explained by a faster B into C transition in mutant B lineage cells. Therefore, we found no evidence that Igf2 increase has a role in the increased B cell compartment of $H19^{-/-}$ FL.

B cells egression from BM to the periphery

The increased peripheral adult B cell compartment suggested increased B cell production also in the BM. After two pulses of EDU within 14 hours a marked increase in IgM^{+} cells labelled cells was observed in mutant compared to WT cells. This result indicates that in adult BM B cell production is increased which could reflect higher cell division rate or a faster transit through development. Similar frequencies of cells in G1, S/G2/M stage indicated that the increased B cell production in mutant cells only be explained by a faster transition of progenitors through the successive developmental stages. Consistent with this interpretation, molecules involved in the adhesion of progenitors to different BM microenvironments that regulate the expansion of progenitors at different developmental stages were expressed at similar frequencies in WT and mutant cells.

The adhesion of the immature B cells to stromal cells is mediated by integrin α4β1, VCAM-1 and fibronectin (Beck et al., 2014). Integrin α4β1 expression is tightly regulated by the chemokine receptor CXCR4 signaling (Glodek et al., 2003). The strength of integrin α4β1 bind to VCAM-1 is enhanced by CXCL12-CXCR4 signaling. Extensive studies showed that focal adhesion kinase (FAK) also played a role in this process (Glodek et al., 2003). FAK is a cytoplasmic protein tyrosine kinase that enriched within the cell at the adhesion sites. Integrin signaling can lead to the phosphorylation and activation of FAK, which can be positively regulated by the CXCR4 signaling (Schaller, 2001). FAK deficiency (Park et al., 2013) and integrin β1 deficient mice (Pereira et al., 2009) lead to a mild reduction of developing B cells

in the BM. In the immature B cell stage, fraction E in Hardy's scheme, the newly generated IgM^+ B cells downregulate CXCR4 expression and egress from BM (Beck et al., 2014).
We measured mean fluorescence intensity (MFI) of both CXCR4 and CD49d (Integrin α4) on the B cell surface and the *Btk2* gene (encoding FAK) expression of both wt and $H19^{-/-}$ in the BM B cell development. However, no differences were observed (data not shown), indicating the CXCR4-FAK-Integrin α4 dependent cell egression from the BM to the periphery is not affected by deletion of *H19*. All the evidence indicates it is the B cell production, rather than B cell egression, that is responsible for the increased B cells in the periphery of $H19^{-/-}$.

B cell response –the role of CD45 in the immunological synapse

The B cell-T cell interaction leads to formation of a dynamic structure called the "immunological synapse" (van der Merwe, 2000), which was initially proposed by Paul and Seder (Paul and Seder, 1994) to describe the interface between T cells and B cells.

During B cell activation and response, the synapse between T and B cells forms through TCR and peptide-MHCII complex, while binding of T cell costimulatory receptors (e.g. CD40L, CD28) to their ligands (CD40, B7) expressed on the B cell surface, contribute to the stability and maturation of the immunological synapse (Victora and Nussenzweig, 2012a). The immunological synapse comprises a "bull's eye" structure with an outer ring and a central synapse (van Der Merwe and Davis, 2002). The outer ring contains adhesion molecules (such as the integrin LFA-1 and its ligand), and the central synapse, where the T cell and B cell membranes are close to each other, is composed of peptide-MHCII complex-TCR and paired costimulatory molecule (CD40-CD40L, B7-CD28, etc.). In this process, CD45 has been reported to have a pivotal role. Upon antigen engagement, CD45, protein tyrosine phosphatase receptor type C (PTPRC), co-localizes with integrin thereby inhibiting synapse formation (Johnson et al., 2000; Depoil et al., 2008).
In H19 mutant B cells B220, one of the CD45 isoforms, is highly expressed compared to that of wt. B220 has a heavier glycosylation than other CD45 isoforms in its extracellular domain and consequently it is more difficult to be excluded from the central synapse, so the higher density B220 expression on the surface of $H19^{-/-}$ B cells may impede the formation of a tight and stable synapse. We reasoned that insufficient exclusion of B220 from the central synapse might reduce the efficiency and/or the duration of B-T helper cell engagement. This is based

on the observation that after immunization, *H19* mutant B cells exhibited lower activation status which is reflected by decreased expression of costimulatory molecule MHCII, CD86 and CD40 compared to that of wt B cells, and all these molecules are the core players of B-T cell synapse.

Epigenetic mechanisms modulate gene expression by *lncRNA H19*

ProB cells from H19 mutant isolated from FL but also from BM showed upregulated B220 and downregulated CD43 expressions. Extensive studies showed that H19 plays a role in affecting transcription through chromatin remodeling. In embryonic development, H19 recruits epigenetic modifiers, acting as a guide to activate or repress gene expression. It has been shown that H19 regulates the imprinting gene network by affecting at least nine imprinted genes: *Igf2, Igf1r*, *Dlk1*, *Meg3*, *Slc38a4*, *Peg1*, *Dcn*, *Cdkn1c* and *Gnas* (Monnier et al., 2013). Some of these genes are regulated by H19 through recruitment of methyl-CpG-binding domain protein 1 (MBD1), which can bind methylated DNA and recruit histone lysine methyltransferases (KMTs) to permanently suppress expression by chromatin compaction (Monnier et al., 2013). In some cases of bladder cancer, *H19* recruits histone methyltransferase EZH2 at the E-cadherin promoter, leading to an increase in H3K27me3 repressive marks and to silence the expression of E-cadherin gene (Luo et al., 2013). In our work on B cell development in FL, fraction C cells from $H19^{-/-}$ showed increased expression of *Igf2*, *Igf1r*, and *Cdkn1c*. This can be achieved by the reduced recruitment of repressive epigenetic modifiers to the regulatory element of these genes in $H19^{-/-}$ fraction C cells and similar differential expression is also found in BM. The upregulated B220 expression in the FL B cell development of $H19^{-/-}$ and $H19^{mat-/+}$, might also be one of the consequences of loss of maternally expressed H19 mediated epigenetic repression, thus establishing an epigenetic memory on the locus of CD45.

H19 can also promote gene expression through epigenetic modification. Binding of H19 to histone acetyltransferase hnRNP U results in the upregulation of genes within the miR-200 family through histone H3 acetylation, which highlight the active role of H19 in gene expression by epigenetic mechanisms (Zhang et al., 2013). Since $H19^{-/-}$ B cells showed defects in the immune response to TD antigens and lower expression of B cell activation markers, such as CD40, CD86 and MHCII, we hypothesize that loss of H19 might also mark

epigenetic memories on these loci. Another possibility would be that H19 regulates the expression of key molecules that regulates all of the above.

Affinity maturation in *H19*$^{-/-}$ GC cells

Ig heavy chain class switch recombination (CSR) occurs rapidly after activation of mature naïve B cells. CSR is an AID-induced process taking place in the DZ of GC and the main function of this process is to switch the Ig isotype from expressing IgM to another Ig isotype such as IgG, IgE, or IgA. CSR only exchanges the Ig heavy chain constant region from the initial Cμ to an alternative set of downstream constant region exons, such as Cγ, Cε, or Cα whereas the antigen specificity determined by the variable region is not affected (Honjo et al., 2002; Stavnezer et al., 2008).

H19$^{-/-}$ mice, after SRBC immunization, generate a smaller GC compartment, and the increased DZ/LZ ratio compared to that of wt. Since the AID expression and the AID mediated CSR mainly takes place in the DZ of GC, the increased frequency of DZ cells in immunized *H19*$^{-/-}$ mice indicates larger proportion of GC cells have the chance to undergo CSR, resulting in a comparable number of IgG1 switched cells as in the immunized wt mice. This indicates the class switch in the *H19*$^{-/-}$ is normal. This is also confirmed by the EdU incorporation in GC cells, which showed an increased frequency EdU labeled IgG1^{+} GC cell, but the number remains at a similar level as that of wt. In addition, *in vitro* stimulation for CSR with LPS and IL4 also showed no differences of wt and *H19*$^{-/-}$ B cells in generating IgG1^{+} cells in absolute cell numbers (data not shown), indicating the TLR4 and IL4 signaling pathways are intact in *H19*$^{-/-}$ B cells. This added more evidence of the normal CSR in activated *H19*$^{-/-}$ B cells.

However, the dramatically decrease in IgM positive GC cells rises several possibilities: fewer naïve cells are activated and enter the GC, or there is a decreased proliferation or increased apoptosis of IgM^{+} GC cells, or an accelerated differentiation into IgM secreting plasma cells or memory cells. We excluded the possibility of an accelerated differentiation by finding decreased plasma cells, as well the impaired primary and recall IgM antibody response, which indicates a defected PC and MBC generation. Secondly, cell cycle analysis and caspase3/7 staining showed no major difference between the GC cells of *H19*$^{-/-}$ and wt, *H19*$^{-/-}$ GC cells even showed an increased expression of histone genes, indicating a higher proliferation and normal apoptosis phenotype. Altogether, the most possible cause of decreased IgM^{+} GC cells

is the fewer naïve B cells activated in the T-B border of spleen, leading to a shortage source of activated B cells entering the GC. This is also demonstrated in our *in vitro* stimulation, where *H19*$^{-/-}$ B cells generated less activated B cells, as well fewer plasma cells under the simulation of anti-CD40 and IL4. This result is consistent with the in vivo observation of impaired GC formation and the shortage outcome of the plasma cells.

Further investigation found that *Aicda* (encoding AID) expression in GC cells from *H19*$^{-/-}$ mice was increased compared to that of wt GC cells. The possible explanation is that GC cells of *H19*$^{-/-}$ mice exhibit a larger frequency cells of DZ cells where AID highly expressed, leading to higher percentage GC cells undergoing CSR from the initial IgM to a switched IgG1 isotype. This is also reflected by the reduced antigen specific IgM response.

SHM is a process that introduces random point mutations in the variable-region gene segments of the BCR, which can result in unchanged, increased or decreased BCR affinity and to self-reactive BCR. This process is mainly taking place in the DZ of GC. Some of the B cells from DZ can exit cell cycle and relocated to the LZ, where affinity selection takes place. Signals from FDCs and TFH cells, as well as cytokine signaling plays important role in affinity maturation. B cells can sense the antigens captured by FDCs to allow for antigen-driven selection of high affinity BCR. Defective BCR responsiveness of *H19*$^{-/-}$ B cells reflected by decreased Ca^{2+} influx after anti-IgM stimulation can partially contribute to the inefficiency of BCR affinity selection, leading to the reduced IgM affinity. In addition, TFH cells in the LZ is essential for affinity maturation in a TD response. BCR binding to antigen presented by FDCs triggers the internalization of the BCR-antigen, then antigenic peptides are processed and displayed on major histocompatibility complex II (MHCII), which can in pair with TCR on the surface on TFH cells to form the immunological synapses described above(Reinherz et al., 1999; Lanzavecchia, 1985). The intensity of MHCII, as well the costimulatory molecules CD40 and CD86 on the LZ B cell surface determines the strength of the signals received from TFH cells and the efficiency of affinity selection. *H19*$^{-/-}$ GC B cells display lower expression of these three molecules compared to that of wt in TD antigen response, suggesting weakened signals received from TFH cells. This also contributes to the impaired affinity selection in the LZ, leading to reduced antigen specific IgM affinity in TD antigen immunized mutant. B cells bear low affinity or self-reactive BCR are not selected and undergo apoptosis or phagocytosis by macrophages (Smith et al., 1998). This is a possible explanation for the higher DZ/LZ ratio in the GC of *H19*$^{-/-}$ mice.

Conclusions and perspectives

In this work, we investigated the B cell development and function in absence of *H19*. We have shown that H19 expression in B lineage cells decreases after E15 and that by P15 it is undetectable. However, our observations show that in the absence of *H19* B cell development is affected in FL but also in adult BM and that more importantly the thymus-dependent B cell response is impaired in the adult lymphoid organs.

B cell development in the FL of *H19* (starting at E17.5) mutant FL generate far more $BP1^+$proB cells. Although these pro-B cells show impaired Ig heavy chain VDJ rearrangement mainly caused by failure in the initiation of D-J, and/or V-DJ rearrangement, H19 mutant show a net increase in absolute cell number of intracellular IgM^+ B lineage lymphocytes and consequently of B cell production. The larger peripheral B cell compartment in $H19^{-/-}$ mice is due to enhanced B cell production not only in the embryo but also throughout life. Venkatraman and colleagues (Venkatraman et al., 2013) also observed increased B cell compartment in adult mutant mouse of the maternal *H19* DMR.

Because H19 is no longer expressed in adult lymphocytes the results above can only be explained by an epigenetic alteration induced during H19 expression. Consistent with this, loss of *H19* leads to a permanent alteration of the B cell surface phenotype, with a more than two-fold increase in B220 expression on the surface of all B cell subsets. These observations led us to analyze B cell responses in adult mice. We show that splenic B cell from $H19^{-/-}$ exhibited reduced GC reaction and antigen specific IgM response, leading to an impaired affinity maturation. Therefore, in the absence of *H19* there is a suboptimal humoral immune response. This impaired B cell response in $H19^{-/-}$ cells is B cell autonomous phenomenon as demonstrated by the decrease in mutant but not WT B cells in competitive BM chimeras.

Defective B cell responsiveness can be partially explained by decreased Ca^{2+} influx after anti-IgM stimulation but also by the partial failure to upregulate costimulatory molecules CD40, MHCII and CD86 after anti-IgM treatment of B cells *in vitro* or after in vivo immunization with SRBC.

RNA sequencing data from WT and mutant GC cells reinforced these conclusions. First, reduced BCR responsiveness, inversely correlated with the expression of B220, is reflected by the upregulation of *Sh2b2* a negative regulator of BCR signaling in mutant GC cells. Second, lower expression of CD2, CD69 and CD40 can also result in reduced B cell activation signals from T helper cells. Dampened BCR signaling and T cell help in GC cells of $H19^{-/-}$ mice, also reflected by the decreased expression of *Rel*, one of the NF-kB subunits, which consequently slow down the GC reaction. Third, upregulated *Aicda* expression indicates a decrease in the

frequency of IgM^+ in GC cells of *H19*$^{-/-}$, leading to the defected antigen specific IgM response. This result is also consistent with the increased dark zone/like zone ration in mutant GC reaction with higher frequency of Ig class switch but lower affinity selection.

We concluded that loss of *H19* linked to the altered B cell development in the FL and BM results in a larger adult peripheral B cell compartment, which showed a reduced GC reaction and defected antigen specific IgM response after TD antigen stimulation. TD antigen response defect is B cell autonomous and is accompanied by a dampened BCR signaling and impaired costimulatory signal from T helper cells in GC of *H19*$^{-/-}$mice.

Further studies on loci accessibility in H19 mutant and WT B cells are needed to understand the contribution for epigenetic regulation of this long-non-coding RNA to the function of the immune system.

Material and method

Mice

C57BL/6 and 129SV mice were purchased from Janvier Labs, *H19*$^{-/-}$ mice (provided by Luisa Dondolo) (Ripoche et al., 1997; Gabory et al., 2009), Rag$^{-/-}$γc$^{-/-}$ mice and were bred in the Pasteur Institute mouse facility under specific pathogen-free conditions. The *H19*$^{-/-}$ strain is maintained on the 129SV/Pas background. *H19*$^{\text{maternal-/paternal+}}$ and *H19* $^{\text{maternal+/ paternal-}}$ were obtained after two round crossing, the first round is crossing 129SV WT male with *H19*$^{-/-}$ female, and the F1 female cross back to 129SV male to get *H19*$^{\text{maternal-/paternal+}}$, while the F1 male cross with 129SV female to get *H19*$^{\text{maternal+/paternal-}}$. All the breeding and crossing were done in the animal house at Pasteur Institute. To obtain the FL of different embryonic date, mattings were done overnight; on the following day, mice showing a vaginal plug were isolated and were considered to be at embryonic day 0 (E0). All experiments were done in accordance to Pasteur Institute ethic guideline, approved by French Agriculture ministry and the EU guidelines.

The genotype of both 129Sv WT and *H19*$^{-/-}$ was performed by PCR using the Fire Animal Tissue Direct PCR Kit (Thermo Scientific) with the following primers:

H19 F: 5′-ccgctcaaccacctaattgt-3′; and *H19* R: 5′-cagacatgagctgggtagca-3′ for *H19* detection.

While *H19* promoter F: 5′-cggggctatatgttctcgac-3′; and Neo F(R): 5′-tgaatgaactgcaggacgag-3′ for neomycin (introduced to the *H19*$^{-/-}$ genome when the mouse model was constructed) detection. The PCR program is the following:

cycle: 94C 5min

94C 30sec 58C 30sec 72C 1min 35 cycles

72C 7min

Cell suspension.

E13 to E19 embryos were dissected under microscope to harvest FLs. Fetal organs were recovered in DPBS (Gibco) supplemented with 1% fetal calf serum (FCS) and passed through the needle of a 1-ml syringe to obtain single cell suspensions. Before staining, cell suspensions were filtered with a nylon mesh.

To recover BM cells, first dissect and harvest the femur, or tibia of the hind legs. Then perfuse the bone cavity with DPBS (Gibco) supplemented with 1% FCS by using a syringe, after collecting the BM fluid, cell suspensions were filtered with a nylon mesh.

Spleen and lymph nodes cell suspensions were obtained by smashing the spleen or lymph node inside a nylon mesh to release the cells to 3ml DPBS (Gibco) supplemented with 1% FCS.

Flow cytometry and cell sorting

Cells suspensions were stained with antibodies listed in Annex table1. Stained cells were analyzed on a FACSC LSR II and were sorted with a FACSAria III (BD Biosciences). Data were analyzed with FlowJo software.

Cell culture

First 96-well plates were coated with monolayer OP9 or OP9DL4 stromal cells (2000 cells per well), and cultured at 37 °C and 5% CO_2 and in complete medium (OptiMEM supplemented with 10% FCS, penicillin (50 units/ml), streptomycin (50 μg/ml) and β-mercaptoethanol (50 μM) from Gibco Life Technologies). Then single cells are sorted into 96-well plates with stromal cells, together with different cytokine combination. When comes to bulk cell culture, cells were sorted to DPBS plus 1%FCS, then the cells were submitted to centrifugation, and resuspended with complete medium, then distributed 100 cells to each well.

Frequency assay.

Single cells were sorted into 96-well plates containing pre-coated OP9 stromal cells (for B - NK – myeloid cell potential) and OP9DL4 stromal cells (for T-NK cell potential) in complete medium supplemented with saturating amounts of IL-7, Flt3L, KitL, IL2, GM-csf, M-csf.

Cultures were supplemented with fresh cytokines every 7 d. After 10–12 d of culture, wells showing colonies were stained for CD19, NK1.1, CD3ε, CD11b and Gr1c and were analyzed with a LSR Fortessa (from BD Biosciences). Frequency scores were assigned based on the frequency of wells positive for B cells ($CD19^+$), NK cells ($NK1.1^+$), T cells ($CD3\varepsilon^+$) or myeloid($CD11b^+Gr1^+$) relative to the total number of plated cells.

Quantitative RT-PCR.

mRNA of sorted cells was extracted using the RNeasy Micro Kit (Qiagen), and cDNA was obtained using the PrimeScript RT Kit (Takara). Briefly, cells were sorted to 350ul lysis buffer (buffer RLT), add 1 volume of 70% ethanol to the homogenized lysate, and mixed well by pipetting, followed by applying the sample to the RNeasy Spin column with 2ml collection tube, centrifuge for 15s at 10 000rpm discard the flow through and wash the column with 350ul buffer RW1 and centrifuge 15s at 10 000rpm, then wash again with 500ul RPE buffer, centrifuge 15s at 10 000rpm. The next step is washing with 500ul 80% ethanol, centrifuge 2min at 10 000rpm, transfer the spin column to a new 2ml tube, and centrifuge 5min at 10 000rpm. Finally, elute the column with 12ul RNase free water, centrifuge 1min at 10 000rpm. cDNAs are prepared by using PrimeScript RT Kit (Takara) following the standard protocol and qPCR was performed using TaqMan primers and TaqMan Universal Master Mix (Applied Biosystems) for the following genes: *Rag1, Rag2, IL7Ra, FOXO1, Bcl2, Bcl6, H19, Igf2, Igf1r, Cdkn1c, Lin28b, c-Myc, Aicda*. While genes involved in the imprinting gene network, such as *Dlk1, snurf, Igf2, Cdkn1c, MSTl1, H13, CD81, Ndn, Mstl,* expression were assessed using SYBR Green Master Mix (Applied Biosystems). qPCR reactions were performed on a ABI 7300 thermocycler (Applied Biosystems), gene expression was normalized to that of *Hprt* and relative expression was calculated using the $2^{-\Delta Ct}$ method.

Chimeras reconstitution and Quantitative genome PCR.

FL cells($5x10^5$) form both 129SV and *H19*$^{-/-}$ embryos, in a 1:1 ratio, were injected to Ly5.1 Rag$^{-/-}$rc$^{-/-}$ mice by i.v. After 8 weeks reconstitution, B cells, T cells and granulocytes ($5x10^5$ cells per cell type) from the spleen of the chimeras were sorted. Genome DNA of sorted cells was extracted using the DNeasy blood & tissue Kit (Qiagen). DNAs were submitted to quantitative PCR using *H19* and IL2 primer and SYBR Green Master Mix, qPCR reactions were performed on a ABI 7300 thermocycler (Applied Biosystems), genome *H19* was normalized to that of *IL2* using the $2^{-\Delta Ct}$ method. Relative percentage of *H19*$^{+}$ cells were calculated using the titration curve drew by serial percentages of 129SV WT B cells. The setting of the titration curve is the following: 1.100% WT B cell; 2. 50% WT B cells plus 50% *H19*$^{-/-}$ B cells; 3. 25% WT B cells plus 75% *H19*$^{-/-}$ B cells; 4. 12.5% WT B cells plus 87.5% *H19*$^{-/-}$ B cells; 5. 6.25% WT B cells plus 93.75% *H19*$^{-/-}$ B cells;

Immunization and GC analysis in the spleen

6-8 weeks old mice of both 129SV and *H19*$^{-/-}$ were immunized with sheep red blood cells, LPS, Ovalbumin, NP(31)CGG or alum only. At different time point after immunization, the spleens were harvest and GC cells were analysed using immunostaining and flow cytometry. Briefly, spleen cell suspensions were stained with antibody purchased from BD Biosciences, Biolegend, eBiosciences, and Mitlenyi Biotec. Cells were incubated with biotinylated anti-CXCR4 for 15-30min at 4 degrees in the dark, then after washing and centrifugation, cells were stained by a secondary antibody mixture, including CD19-APCCy7, IgD-BV421, CD38-AF700, CD95-PECy7, CD86-PE and APC-coupled streptavidin. After washing, the dead cells were excluded by propidium iodide. Stained cells were acquired and recorded with a LSR Fortessa and analysed by using FlowJo software.

Intracellular staining

Using flow cytometry to analyse the expression of transcriptional factor, intracellular protein, such as Ig heavy chain and cytokine, or the EdU incorporated to the genome DNA, phosphorylated proteins, or even cell cycle analysis. Cells suspensions were first followed the normal staining, then washed once in PBS without serum. Cells were fixed by using the fixation buffer, for example fixation buffer from eBioscience intracellular staining kit for transcriptional factor staining. Cells were incubated for 30 min at 4°C in the dark. Cells were washed once in PBS and twice in permeabilization buffer, then incubate 30min with another fluorescent labelled antibody against different transcriptional factors or other intracellular protein. Cells were washed twice in permeabilization buffer and resuspended in FACS medium without propidium iodide. LSRII from BD Biosciences were used for flow cytometry analysis. Data were analyzed with FlowJo10.2 software from Tree Star.

Cell cycle analysis

Cells suspensions were first followed the normal staining, then washed once in PBS without serum followed by fixation and permeabilization described in “Intracellular staining” part. Then incubate with anti-Ki67-FITC antibody for 45min. Cells were washed twice in permeabilization buffer and incubate with DAPI for another 10min in dark in room temperature, add FACS medium without propidium iodide. When the samples are acquired

and recorded, set pacific blue channel in linear scale. Data were analyzed with FlowJo10.2 software.

EdU incorporation and staining

Mice from both 129SV WT and *H19*$^{-/-}$ were immunized three or five times in a 12h interval with 100 μg of EdU dissolved in DMSO by intraperitoneal injection(i.p.). 2 hours after the last injection, the mice were sacrificed and the bone marrow, spleen were collected, cell suspensions were prepared and submitted to the normal cell surface marker staining for 15-30min (avoid using PE or PE tandem fluorescence). Samples were submitted to the EdU staining by using "Click-iT EdU pacific blue flow cytometry assay kit". Briefly, Samples washed 3 times with DPBS^{+}1%FCS, then added 100ul of Click-iT fixative buffer and incubate for 15min at room temperature, protected from light, followed by washing 3 times with DPBS^{+}1%FCS before permeabilization. Then incubate the samples with 100ul 1X Click-iT saponin-based permeabilization and washing reagent for 15min. then the Click-iT reaction cocktail was prepared according to the instruction. Add 200ul of the Click-iT reaction cocktail to each sample and incubate the cells for 30min at room temperature, protected from light. Wash cells once with 1X permeabilization buffer. Add 500ul 1X permeabilization buffer and analyse on flow cytometer.

Affinity Maturation, Serum Antibody Analysis, and Enzyme-Linked ImmunoSpot Assay.

C57BL/6,129SV WT, *H19*$^{-/-}$ were immunized with 100 μg of NP(31)CGG (Biosearch Technologies) in alum at day 0 and boosted with soluble 10 μg NP(31)CGG per mouse; at day 28 and day 42. Peripheral blood serum was collected at days 0, 7, 15, 21, 28, 42, and 49. High-affinity (anti-NP_7) and low affinity (anti-NP_{23}) IgM and IgG antibody titers were determined by ELISA using standard procedures. Briefly, plates were coated with NP_7-BSA and NP_{23}-BSA (Biosearch Technologies) at 4 °C overnight and were blocked with PBS containing 2% BSA. Diluted serum samples were incubated at 37 °C for 1 h, followed by 1-h incubation with HRP linked anti-mouse IgM and IgG antibody. Then 3,3′,5,5′-tetramethylbenzidine (TMB) was used as liquid substrate, and absorbance was read at 450 nm. Hyperimmune serum was used as standard. For the enzyme-linked immunospot (ELISPOT) assay, serial dilutions of BM and SP cells were added to a 96-well PVDF membrane plate (MSIPN4W; Millipore) coated with 10 μg/mL purified rat anti-mouse Ig kappa light chain

and rat anti mouse IgM antibody and incubated for at least 20 h at 37 °C and 5% CO_2. Antibody-secreting cells were detected with biotinylated Ig kappa antibody and streptavidin conjugated to AP (Roche) and were visualized with 5-bromo-4-chloro-3'-indolyphosphate *p*-toluidine salt (BCIP)/nitro-blue tetrazolium chloride (NBT) substrate (Sigma-Aldrich). Images of membranes were captured using an Olympus SZ61 dissection microscope equipped with a USB camera and OPTIKA Vision lite software (OPTIKA SRL). Spots were counted manually.

Calcium influx by FACS

Spleen cell suspensions were prepared as described above, then washed once in PBS without serum, cells were resuspended at 10^7 cells/mL in PBS with the calcium dye (Indol-1 AM, Invitrogen, final concentration 1mM), incubate 40min at 37°C. After washing once in complete medium, resuspended the cells at $2x10^6$ cells/mL in complete medium. Keep the cells in 50mL falcon tube in the water bath at 37°C near the flow cytometry during the experiment. Transfer the cells in FACS tube just before the acquisition.

Keep the cells in 50mL falcon tube in the water bath at 37°C during the experiment. Transfer the cells in Facs tube just before the acquisition, adjust the acquisition speed at 800-1000 events/sec, and set all the parameters as Linear. Create a ratio, set Indo-1 violet (BUV496) in Numerator and Indo-1 blue (BUV 737) in Denominator. Samples were acquired 60s to obtain the baseline, then added polyclonal anti-mouse IgM antibody to a final 10, 5, 205, 1,25ug/ml concentration, continue acquire the same sample for another 300s. For the negative and positive control, EDTA (final concentration)10ug/ml and 1ug/ml(final concentration) Ionomycin were added instead of anti-IgM antibody, respectively. Data were analyzed with FlowJo10.2 software.

Apoptosis analysis

Annexin V method: Spleen, lymph nodes, BM cell suspensions were prepared as described above, cells were stained for their surface marker, then washed once in cold PBS without serum, resuspend the cells were incubated with 100ul Annexin binding buffer (10mM Hepes, pH7,4; 0.14M NaCl; 2.5mM $CaCl_2$) 15min in room temperature. Add more 400ul binding buffer with PI. LSRII from BD Biosciences were used for flow cytometry analysis. Data were analyzed with FlowJo10.2 software.

Caspase 3/7 method: after the cell surface marker staining, Adjust the cell concentration of the sample(s) between $1x10^5$ cells/ml and $1x10^7$ cells/ml using the complete medium. Add 1 µL of CellEvent™ Caspase-3/7 Green Detection Reagent to 1 mL of sample and mix gently. Incubate the samples for 30 minutes at 37°C or 45–60 minutes at room temperature, protected from light. The final concentration of the reagent is 500 nM. During the final 5 minutes of staining, add 1 µL of the 1 mM SYTOX™ AADvanced™ dead cell stain solution in DMSO to the appropriate samples and mix gently. The final labeling concentration of stain is 1 µM. Analyze the samples without washing or fixing, using 488‑nm excitation and collecting fluorescence emission using a 530/30 bandpass filter or equivalent for CellEvent™ Caspase-3/7 Green Detection Reagent and a 690/50 BP filter or equivalent for SYTOX™ AADvanced™ dead cell stain.

VDJ PCR and sequencing

Genome DNA was extracted from sorted $BP1^+$ proB cells from both 129SV and *H19*$^{-/-}$ FL using blood and tissue Dneasy kit (Qiagen). PCR reactions were set up for each sample. Briefly, A 50 µL PCR reaction containing 10X PCR buffer, 2 mM MgCl2, 250 µM dNTPs (AB gene, Epsom, UK), 1.5 U of Taq Polymerase (AB gene), forward primers VHJ558, VHQ52, and reverse primer JH4e (for VDJ rearrangement amplification); while and reverse primer DQ52, DSP27 together with the same reverse primer JH4e were used for the DJ rearrangement. As well as genomic DNA. PCR reactions were performed using a Geneamp 9700 thermal cycler (Applied Biosystems, USA). The PCR conditions included preactivation of the enzyme for 10 min at 94℃ followed by 35 cycles at 94℃ for 60 sec, 60℃ for 30 sec and 72℃ for 1.5 min and a final extension of 10 min at 72℃. The amplified products were visualized by electrophoresing on a 2% agarose gel. The sequences of PCR primers were described previously (Possot et al., 2011).

For PCR amplification of VDJ, VDJ_H4 band was cut and recovered by using Qiaquick gel extraction kit (Qiagen), the purified VDJ_H4 fragment was connected to pCR4-TOPO vector using the TOPO TA cloning kit for sequencing (Invitrogen). Briefly, first perform the TOPO cloning reaction using the reagent in table 1. Add the TOPO cloning reaction into a vial of One Shot chemically component *E. coli* and mix gently and incubate on ice for 30min. Heat-shock the cells for 40 seconds at 42℃ without shaking and immediately transfer the tube to ice. S.O.C. medium was added to the tube, and shake the tube horizontally (200 rpm) at 37℃

for 1 hour. Then spread the transformation mixture on a pre-warmed kanamycin selective LB plate and incubated at 37℃ overnight. The clones were picked out to the tube and LB medium was add for the expansion of the clone in a horizontal shaker at 37℃ overnight. The bacteria were collected and plasmid was extracted by using Qiaprep Spin Miniprep kit (Qiagen), and the plasmids from different clones were sequenced by using T3 primer. VDJ sequences were analyzed by using DNADynamo software and productive VDJ rearrangements rate was calculated.

References

Adriaenssens, E., Dumont, L., Lottin, S., Bolle, D., Leprêtre, A., Delobelle, A., Bouali, F., Dugimont, T., Coll, J., and Curgy, J. J. (1998). H19 overexpression in breast adenocarcinoma stromal cells is associated with tumor values and steroid receptor status but independent of p53 and Ki-67 expression. Am J Pathol *153(5)*, 1597-1607.

Aguzzi, A., Kranich, J., and Krautler, N. J. (2014). Follicular dendritic cells: origin, phenotype, and function in health and disease. Trends Immunol *35(3)*, 105-113.

Allman, D., Li, J., and Hardy, R. R. (1999). Commitment to the B lymphoid lineage occurs before DH-JH recombination. J Exp Med *189(4)*, 735-740.

Allman, D., Lindsley, R. C., DeMuth, W., Rudd, K., Shinton, S. A., and Hardy, R. R. (2001). Resolution of three nonproliferative immature splenic B cell subsets reveals multiple selection points during peripheral B cell maturation. J Immunol *167(12)*, 6834-6840.

Allman, D., Sambandam, A., Kim, S., Miller, J. P., Pagan, A., Well, D., Meraz, A., and Bhandoola, A. (2003). Thymopoiesis independent of common lymphoid progenitors. Nat Immunol *4(2)*, 168-174.

Alt, F. W., Zhang, Y., Meng, F. L., Guo, C., and Schwer, B. (2013). Mechanisms of programmed DNA lesions and genomic instability in the immune system. Cell *152(3)*, 417-429.

Alugupalli, K. R., Leong, J. M., Woodland, R. T., Muramatsu, M., Honjo, T., and Gerstein, R. M. (2004). B1b lymphocytes confer T cell-independent long-lasting immunity. Immunity *21(3)*, 379-390.

Angrand, P. O., Vennin, C., Le Bourhis, X., and Adriaenssens, E. (2015). The role of long non-coding RNAs in genome formatting and expression. Front Genet *6*, 165.

Baba, Y., and Kurosaki, T. (2009). Physiological function and molecular basis of STIM1-mediated calcium entry in immune cells. Immunol Rev *231(1)*, 174-188.

Bain, G., Maandag, E. C., Izon, D. J., Amsen, D., Kruisbeek, A. M., Weintraub, B. C., Krop, I., Schlissel, M. S., Feeney, A. J., and van Roon, M. (1994). E2A proteins are required for proper B cell development and initiation of immunoglobulin gene rearrangements. Cell *79(5)*, 885-892.

Bain, G., Robanus Maandag, E. C., te Riele, H. P., Feeney, A. J., Sheehy, A., Schlissel, M., Shinton, S. A., Hardy, R. R., and Murre, C. (1997). Both E12 and E47 allow commitment to the B cell lineage. Immunity *6(2)*, 145-154.

Barinov, A., Luo, L., Gasse, P., Meas-Yedid, V., Donnadieu, E., Arenzana-Seisdedos, F., and Vieira, P. (2017). Essential role of immobilized chemokine CXCL12 in the regulation of the humoral immune response. Proc Natl Acad Sci U S A *114(9)*, 2319-2324.

Bartolomei, M. S., Zemel, S., and Tilghman, S. M. (1991). Parental imprinting of the mouse H19 gene. Nature *351(6322)*, 153-155.

Baumgarth, N. (2011). The double life of a B-1 cell: self-reactivity selects for protective effector functions. Nat Rev Immunol *11(1)*, 34-46.

Beck, T. C., Gomes, A. C., Cyster, J. G., and Pereira, J. P. (2014). CXCR4 and a cell-extrinsic mechanism control immature B lymphocyte egress from bone marrow. J Exp Med *211(13)*, 2567-2581.

Béguelin, W., Popovic, R., Teater, M., Jiang, Y., Bunting, K. L., Rosen, M., Shen, H., Yang, S. N., Wang, L., Ezponda, T., Martinez-Garcia, E., Zhang, H., Zheng, Y., Verma, S. K., McCabe, M. T., Ott, H. M., Van Aller, G. S., Kruger, R. G., Liu, Y., McHugh, C. F., Scott, D. W., Chung, Y. R., Kelleher, N., Shaknovich, R., Creasy, C. L., Gascoyne, R. D., Wong, K. K., Cerchietti, L., Levine, R. L., Abdel-Wahab, O., Licht, J. D., Elemento, O., and Melnick, A. M. (2013). EZH2 is required for germinal center formation and somatic EZH2 mutations promote lymphoid transformation. Cancer Cell *23(5)*, 677-692.

Berg, J. S., Lin, K. K., Sonnet, C., Boles, N. C., Weksberg, D. C., Nguyen, H., Holt, L. J., Rickwood, D., Daly, R. J., and Goodell, M. A. (2011). Imprinted genes that regulate early mammalian growth are coexpressed in somatic stem cells. PLoS One *6(10)*, e26410.

Berland, R., and Wortis, H. H. (2002). Origins and functions of B-1 cells with notes on the role of CD5. Annu Rev Immunol *20*, 253-300.

Berteaux, N., Aptel, N., Cathala, G., Genton, C., Coll, J., Daccache, A., Spruyt, N., Hondermarck, H., Dugimont, T., Curgy, J. J., Forné, T., and Adriaenssens, E. (2008). A novel H19 antisense RNA overexpressed in breast cancer contributes to paternal IGF2 expression. Mol Cell Biol *28(22)*, 6731-6745.

Betancur, P., Bronner-Fraser, M., and Sauka-Spengler, T. (2010). Assembling neural crest regulatory circuits into a gene regulatory network. Annu Rev Cell Dev Biol *26*, 581-603.

Bevan, M. J. (2011). Understand memory, design better vaccines. Nat Immunol *12(6)*, 463-465.

Bolland, S., and Ravetch, J. V. (2000). Spontaneous autoimmune disease in Fc(gamma)RIIB-deficient mice results from strain-specific epistasis. Immunity *13(2)*, 277-285.

Borghesi, L., Aites, J., Nelson, S., Lefterov, P., James, P., and Gerstein, R. (2005). E47 is required for V(D)J recombinase activity in common lymphoid progenitors. J Exp Med *202(12)*, 1669-1677.

Bradl, H., Wittmann, J., Milius, D., Vettermann, C., and Jäck, H. M. (2003). Interaction of murine precursor B cell receptor with stroma cells is controlled by the unique tail of lambda 5 and stroma cell-associated heparan sulfate. J Immunol *171(5)*, 2338-2348.

Braun, J., Sha'afi, R. I., and Unanue, E. R. (1979). Crosslinking by ligands to surface immunoglobulin triggers mobilization of intracellular 45Ca2+ in B lymphocytes. J Cell Biol *82(3)*, 755-766.

Busslinger, M. (2004). Transcriptional control of early B cell development. Annu Rev Immunol *22*, 55-79.

Byth, K. F., Conroy, L. A., Howlett, S., Smith, A. J., May, J., Alexander, D. R., and Holmes, N. (1996). CD45-null transgenic mice reveal a positive regulatory role for CD45 in early thymocyte development, in the selection of CD4+CD8+ thymocytes, and B cell maturation. J Exp Med *183(4)*, 1707-1718.

Caganova, M., Carrisi, C., Varano, G., Mainoldi, F., Zanardi, F., Germain, P. L., George, L., Alberghini, F., Ferrarini, L., Talukder, A. K., Ponzoni, M., Testa, G., Nojima, T., Doglioni, C., Kitamura, D., Toellner, K. M., Su, I. H., and Casola, S. (2013a). Germinal center dysregulation by histone methyltransferase EZH2 promotes lymphomagenesis. J Clin Invest *123(12)*, 5009-5022.

Caganova, M., Carrisi, C., Varano, G., Mainoldi, F., Zanardi, F., Germain, P. L., George, L., Alberghini, F., Ferrarini, L., Talukder, A. K., Ponzoni, M., Testa, G., Nojima, T., Doglioni, C., Kitamura, D., Toellner, K. M., Su, I. H., and Casola, S. (2013b). Germinal center dysregulation by histone methyltransferase EZH2 promotes lymphomagenesis. J Clin Invest *123(12)*, 5009-5022.

Cai, X., and Cullen, B. R. (2007). The imprinted H19 noncoding RNA is a primary microRNA precursor. RNA *13(3)*, 313-316.

Calame, K. L., Lin, K. I., and Tunyaplin, C. (2003). Regulatory mechanisms that determine the development and function of plasma cells. Annu Rev Immunol *21*, 205-230.

Castigli, E., Wilson, S. A., Scott, S., Dedeoglu, F., Xu, S., Lam, K. P., Bram, R. J., Jabara, H., and Geha, R. S. (2005). TACI and BAFF-R mediate isotype switching in B cells. J Exp Med *201(1)*, 35-39.

Cedar, H., and Bergman, Y. (2008). Choreography of Ig allelic exclusion. Curr Opin Immunol *20(3)*, 308-317.

Cerutti, A., Puga, I., and Cols, M. (2012). New helping friends for B cells. Eur J Immunol *42(8)*, 1956-1968.

Cheng, P. C., Dykstra, M. L., Mitchell, R. N., and Pierce, S. K. (1999). A role for lipid rafts in B cell antigen receptor signaling and antigen targeting. J Exp Med *190(11)*, 1549-1560.

Cohen, M. M. (1994). Wiedemann-Beckwith syndrome, imprinting, IGF2, and H19: implications for hemihyperplasia, associated neoplasms, and overgrowth. Am J Med Genet *52(2)*, 233-234.

Cooke, M. P., Heath, A. W., Shokat, K. M., Zeng, Y., Finkelman, F. D., Linsley, P. S., Howard, M., and Goodnow, C. C. (1994). Immunoglobulin signal transduction guides the specificity of B cell-T cell interactions and is blocked in tolerant self-reactive B cells. J Exp Med *179(2)*, 425-438.

Cooper, M. J., Fischer, M., Komitowski, D., Shevelev, A., Schulze, E., Ariel, I., Tykocinski, M. L., Miron, S., Ilan, J., de Groot, N., and Hochberg, A. (1996). Developmentally imprinted genes as markers for bladder tumor progression. J Urol *155(6)*, 2120-2127.

Court, F., Baniol, M., Hagege, H., Petit, J. S., Lelay-Taha, M. N., Carbonell, F., Weber, M., Cathala, G., and Forne, T. (2011). Long-range chromatin interactions at the mouse Igf2/H19 locus reveal a novel paternally expressed long non-coding RNA. Nucleic Acids Res *39(14)*, 5893-5906.

Craxton, A., Somers, J., Munnur, D., Jukes-Jones, R., Cain, K., and Malewicz, M. (2015). XLS (c9orf142) is a new component of mammalian DNA double-stranded break repair. Cell Death Differ *22(6)*, 890-897.

Cyster, J. G., Healy, J. I., Kishihara, K., Mak, T. W., Thomas, M. L., and Goodnow, C. C. (1996). Regulation of B-lymphocyte negative and positive selection by tyrosine phosphatase CD45. Nature *381(6580)*, 325-328.

Dao, D., Walsh, C. P., Yuan, L., Gorelov, D., Feng, L., Hensle, T., Nisen, P., Yamashiro, D. J., Bestor, T. H., and Tycko, B. (1999). Multipoint analysis of human chromosome 11p15/mouse distal chromosome 7: inclusion of H19/IGF2 in the minimal WT2 region, gene specificity of H19 silencing in Wilms' tumorigenesis and methylation hyper-dependence of H19 imprinting. Hum Mol Genet *8(7)*, 1337-1352.

Davis, R. L., Weintraub, H., and Lassar, A. B. (1987). Expression of a single transfected cDNA converts fibroblasts to myoblasts. Cell *51(6)*, 987-1000.

De Silva, N. S., and Klein, U. (2015). Dynamics of B cells in germinal centres. Nat Rev Immunol *15(3)*, 137-148.

de Vinuesa, C. G., Cook, M. C., Ball, J., Drew, M., Sunners, Y., Cascalho, M., Wabl, M., Klaus, G. G., and MacLennan, I. C. (2000). Germinal centers without T cells. J Exp Med *191(3)*, 485-494.

DeFranco, A. L., Chan, V. W., and Lowell, C. A. (1998). Positive and negative roles of the tyrosine kinase Lyn in B cell function. Semin Immunol *10(4)*, 299-307.

DeKoter, R. P., Lee, H. J., and Singh, H. (2002). PU.1 regulates expression of the interleukin-7 receptor in lymphoid progenitors. Immunity *16(2)*, 297-309.

Depoil, D., Fleire, S., Treanor, B. L., Weber, M., Harwood, N. E., Marchbank, K. L., Tybulewicz, V. L., and Batista, F. D. (2008). CD19 is essential for B cell activation by promoting B cell receptor-antigen microcluster formation in response to membrane-bound ligand. Nat Immunol *9(1)*, 63-72.

Dey, B. K., Pfeifer, K., and Dutta, A. (2014a). The H19 long noncoding RNA gives rise to microRNAs miR-675-3p and miR-675-5p to promote skeletal muscle differentiation and regeneration. Genes Dev *28(5)*, 491-501.

Dey, B. K., Pfeifer, K., and Dutta, A. (2014b). The H19 long noncoding RNA gives rise to microRNAs miR-675-3p and miR-675-5p to promote skeletal muscle differentiation and regeneration. Genes Dev *28(5)*, 491-501.

Dias, S., Silva, H., Cumano, A., and Vieira, P. (2005). Interleukin-7 is necessary to maintain the B cell potential in common lymphoid progenitors. J Exp Med *201(6)*, 971-979.

Dorshkind, K., and Montecino-Rodriguez, E. (2007). Fetal B-cell lymphopoiesis and the emergence of B-1-cell potential. Nat Rev Immunol *7(3)*, 213-219.

Douagi, I., Vieira, P., and Cumano, A. (2002). Lymphocyte commitment during embryonic development, in the mouse. Semin Immunol *14(6)*, 361-369.

Düber, S., Hafner, M., Krey, M., Lienenklaus, S., Roy, B., Hobeika, E., Reth, M., Buch, T., Waisman, A., Kretschmer, K., and Weiss, S. (2009). Induction of B-cell development in adult mice reveals the ability of bone marrow to produce B-1a cells. Blood *114(24)*, 4960-4967.

Ferreira, M. U., and Katzin, A. M. (1995). The assessment of antibody affinity distribution by thiocyanate elution: a simple dose-response approach. J Immunol Methods *187(2)*, 297-305.

Frevel, M. A., Sowerby, S. J., Petersen, G. B., and Reeve, A. E. (1999). Methylation sequencing analysis refines the region of H19 epimutation in Wilms tumor. J Biol Chem *274(41)*, 29331-29340.

Fujita, N., Jaye, D. L., Geigerman, C., Akyildiz, A., Mooney, M. R., Boss, J. M., and Wade, P. A. (2004). MTA3 and the Mi-2/NuRD complex regulate cell fate during B lymphocyte differentiation. Cell *119(1)*, 75-86.

Fujita, N., Jaye, D. L., Kajita, M., Geigerman, C., Moreno, C. S., and Wade, P. A. (2003). MTA3, a Mi-2/NuRD complex subunit, regulates an invasive growth pathway in breast cancer. Cell *113(2)*, 207-219.

Fuxa, M., and Busslinger, M. (2007). Reporter gene insertions reveal a strictly B lymphoid-specific expression pattern of Pax5 in support of its B cell identity function. J Immunol *178(12)*, 8222-8228.

Gabory, A., Ripoche, M. A., Le Digarcher, A., Watrin, F., Ziyyat, A., Forné, T., Jammes, H., Ainscough, J. F., Surani, M. A., Journot, L., and Dandolo, L. (2009). H19 acts as a trans regulator of the imprinted gene network controlling growth in mice. Development *136(20)*, 3413-3421.

Gao, W. L., Liu, M., Yang, Y., Yang, H., Liao, Q., Bai, Y., Li, Y. X., Li, D., Peng, C., and Wang, Y. L. (2012a). The imprinted H19 gene regulates human placental trophoblast cell proliferation via encoding miR-675 that targets Nodal Modulator 1 (NOMO1). RNA Biol *9(7)*, 1002-1010.

Gao, W. L., Liu, M., Yang, Y., Yang, H., Liao, Q., Bai, Y., Li, Y. X., Li, D., Peng, C., and Wang, Y. L. (2012b). The imprinted H19 gene regulates human placental trophoblast cell proliferation via encoding miR-675 that targets Nodal Modulator 1 (NOMO1). RNA Biol *9(7)*, 1002-1010.

Gatto, D., Pfister, T., Jegerlehner, A., Martin, S. W., Kopf, M., and Bachmann, M. F. (2005). Complement receptors regulate differentiation of bone marrow plasma cell precursors expressing transcription factors Blimp-1 and XBP-1. J Exp Med *201(6)*, 993-1005.

Gauthier, L., Rossi, B., Roux, F., Termine, E., and Schiff, C. (2002). Galectin-1 is a stromal cell ligand of the pre-B cell receptor (BCR) implicated in synapse formation between pre-B and stromal cells and in pre-BCR triggering. Proc Natl Acad Sci U S A *99(20)*, 13014-13019.

Georgopoulos, K., Bigby, M., Wang, J. H., Molnar, A., Wu, P., Winandy, S., and Sharpe, A. (1994). The Ikaros gene is required for the development of all lymphoid lineages. Cell *79(1)*, 143-156.

Georgopoulos, K., Moore, D. D., and Derfler, B. (1992). Ikaros, an early lymphoid-specific transcription factor and a putative mediator for T cell commitment. Science *258(5083)*, 808-812.

Glodek, A. M., Honczarenko, M., Le, Y., Campbell, J. J., and Silberstein, L. E. (2003). Sustained activation of cell adhesion is a differentially regulated process in B lymphopoiesis. J Exp Med *197(4)*, 461-473.

Gong, S., and Nussenzweig, M. C. (1996). Regulation of an early developmental checkpoint in the B cell pathway by Ig beta. Science *272(5260)*, 411-414.

Good-Jacobson, K. L. (2014). Regulation of germinal center, B-cell memory, and plasma cell formation by histone modifiers. Front Immunol *5*, 596.

Good-Jacobson, K. L., Chen, Y., Voss, A. K., Smyth, G. K., Thomas, T., and Tarlinton, D. (2014). Regulation of germinal center responses and B-cell memory by the chromatin modifier MOZ. Proc Natl Acad Sci U S A *111(26)*, 9585-9590.

Good-Jacobson, K. L., and Shlomchik, M. J. (2010). Plasticity and heterogeneity in the generation of memory B cells and long-lived plasma cells: the influence of germinal center interactions and dynamics. J Immunol *185(6)*, 3117-3125.

Good-Jacobson, K. L., Song, E., Anderson, S., Sharpe, A. H., and Shlomchik, M. J. (2012). CD80 expression on B cells regulates murine T follicular helper development, germinal center B cell survival, and plasma cell generation. J Immunol *188(9)*, 4217-4225.

Good-Jacobson, K. L., Szumilas, C. G., Chen, L., Sharpe, A. H., Tomayko, M. M., and Shlomchik, M. J. (2010). PD-1 regulates germinal center B cell survival and the formation and affinity of long-lived plasma cells. Nat Immunol *11(6)*, 535-542.

Grawunder, U., Leu, T. M., Schatz, D. G., Werner, A., Rolink, A. G., Melchers, F., and Winkler, T. H. (1995). Down-regulation of RAG1 and RAG2 gene expression in preB cells after functional immunoglobulin heavy chain rearrangement. Immunity *3(5)*, 601-608.

Gupta, N., and DeFranco, A. L. (2003). Visualizing lipid raft dynamics and early signaling events during antigen receptor-mediated B-lymphocyte activation. Mol Biol Cell *14(2)*, 432-444.

Gururajan, P., Gurumurthy, P., Victor, D., Srinivasa Nageswara Rao, G., Sai Babu, R., Sarasa Bharati, A., and Cherian, K. M. (2011). Plasma total nitric oxide and endothelial constitutive nitric oxide synthase (ecNOS) gene polymorphism: a study in a South Indian population. Biochem Genet *49(1-2)*, 96-103.

Györy, I., Boller, S., Nechanitzky, R., Mandel, E., Pott, S., Liu, E., and Grosschedl, R. (2012). Transcription factor Ebf1 regulates differentiation stage-specific signaling, proliferation, and survival of B cells. Genes Dev *26(7)*, 668-682.

Hagman, J., Belanger, C., Travis, A., Turck, C. W., and Grosschedl, R. (1993). Cloning and functional characterization of early B-cell factor, a regulator of lymphocyte-specific gene expression. Genes Dev *7(5)*, 760-773.

Hagman, J., Travis, A., and Grosschedl, R. (1991). A novel lineage-specific nuclear factor regulates mb-1 gene transcription at the early stages of B cell differentiation. EMBO J *10(11)*, 3409-3417.

Halverson, R., Torres, R. M., and Pelanda, R. (2004). Receptor editing is the main mechanism of B cell tolerance toward membrane antigens. Nat Immunol *5(6)*, 645-650.

Hao, Y., Crenshaw, T., Moulton, T., Newcomb, E., and Tycko, B. (1993). Tumour-suppressor activity of H19 RNA. Nature *365(6448)*, 764-767.

Hardy, R. R., Carmack, C. E., Shinton, S. A., Kemp, J. D., and Hayakawa, K. (1991). Resolution and characterization of pro-B and pre-pro-B cell stages in normal mouse bone marrow. J Exp Med *173(5)*, 1213-1225.

Hardy, R. R., and Hayakawa, K. (1991). A developmental switch in B lymphopoiesis. Proc Natl Acad Sci U S A *88(24)*, 11550-11554.

Hardy, R. R., and Hayakawa, K. (2001). B cell development pathways. Annu Rev Immunol *19*, 595-621.

Hayakawa, K., Hardy, R. R., Herzenberg, L. A., and Herzenberg, L. A. (1985a). Progenitors for Ly-1 B cells are distinct from progenitors for other B cells. J Exp Med *161(6)*, 1554-1568.

Hayakawa, K., Hardy, R. R., Herzenberg, L. A., and Herzenberg, L. A. (1985b). Progenitors for Ly-1 B cells are distinct from progenitors for other B cells. J Exp Med *161(6)*, 1554-1568.

Herzenberg, L. A. (2000). B-1 cells: the lineage question revisited. Immunol Rev *175*, 9-22.

Herzog, S., Reth, M., and Jumaa, H. (2009). Regulation of B-cell proliferation and differentiation by pre-B-cell receptor signalling. Nat Rev Immunol *9(3)*, 195-205.

Ho, F., Lortan, J. E., MacLennan, I. C., and Khan, M. (1986). Distinct short-lived and long-lived antibody-producing cell populations. Eur J Immunol *16(10)*, 1297-1301.

Honjo, T., Kinoshita, K., and Muramatsu, M. (2002). Molecular mechanism of class switch recombination: linkage with somatic hypermutation. Annu Rev Immunol *20*, 165-196.

Hopp, N., Hagen, J., Aggeler, B., and Kalyuzhny, A. E. (2017). Express γ-H2AX Immunocytochemical Detection of DNA Damage. Methods Mol Biol *1644*, 123-128.

Huntington, N. D., and Tarlinton, D. M. (2004a). CD45: direct and indirect government of immune regulation. Immunol Lett *94(3)*, 167-174.

Huntington, N. D., and Tarlinton, D. M. (2004b). CD45: direct and indirect government of immune regulation. Immunol Lett *94(3)*, 167-174.

Huntington, N. D., and Tarlinton, D. M. (2004c). CD45: direct and indirect government of immune regulation. Immunol Lett *94(3)*, 167-174.

Huntington, N. D., Xu, Y., Puthalakath, H., Light, A., Willis, S. N., Strasser, A., and Tarlinton, D. M. (2006). CD45 links the B cell receptor with cell survival and is required for the persistence of germinal centers. Nat Immunol *7(2)*, 190-198.

IIott, N. E., Heward, J. A., Roux, B., Tsitsiou, E., Fenwick, P. S., Lenzi, L., Goodhead, I., Hertz-Fowler, C., Heger, A., Hall, N., Donnelly, L. E., Sims, D., and Lindsay, M. A. (2014). Long non-coding RNAs and enhancer RNAs regulate the lipopolysaccharide-induced inflammatory response in human monocytes. Nat Commun *5*, 3979.

Ikawa, T., Kawamoto, H., Wright, L. Y., and Murre, C. (2004). Long-term cultured E2A-deficient hematopoietic progenitor cells are pluripotent. Immunity *20(3)*, 349-360.

Imig, J., Brunschweiger, A., Brümmer, A., Guennewig, B., Mittal, N., Kishore, S., Tsikrika, P., Gerber, A. P., Zavolan, M., and Hall, J. (2015). miR-CLIP capture of a miRNA targetome uncovers a lincRNA H19-miR-106a interaction. Nat Chem Biol *11(2)*, 107-114.

Inlay, M., Alt, F. W., Baltimore, D., and Xu, Y. (2002). Essential roles of the kappa light chain intronic enhancer and 3' enhancer in kappa rearrangement and demethylation. Nat Immunol *3(5)*, 463-468.

Inlay, M. A., Bhattacharya, D., Sahoo, D., Serwold, T., Seita, J., Karsunky, H., Plevritis, S. K., Dill, D. L., and Weissman, I. L. (2009). Ly6d marks the earliest stage of B-cell specification and identifies the branchpoint between B-cell and T-cell development. Genes Dev *23(20)*, 2376-2381.

Iseki, M., Kubo-Akashi, C., Kwon, S. M., Yamaguchi, A., Takatsu, K., and Takaki, S. (2005). APS, an adaptor molecule containing PH and SH2 domains, has a negative regulatory role in B cell proliferation. Biochem Biophys Res Commun *330(3)*, 1005-1013.

Janeway, C. A. (2002). A trip through my life with an immunological theme. Annu Rev Immunol *20*, 1-28.

Ji, Y., Resch, W., Corbett, E., Yamane, A., Casellas, R., and Schatz, D. G. (2010a). The in vivo pattern of binding of RAG1 and RAG2 to antigen receptor loci. Cell *141(3)*, 419-431.

Ji, Y., Resch, W., Corbett, E., Yamane, A., Casellas, R., and Schatz, D. G. (2010b). The in vivo pattern of binding of RAG1 and RAG2 to antigen receptor loci. Cell *141(3)*, 419-431.

Jiang, X. X., Nguyen, Q., Chou, Y., Wang, T., Nandakumar, V., Yates, P., Jones, L., Wang, L., Won, H., Lee, H. R., Jung, J. U., Müschen, M., Huang, X. F., and Chen, S. Y. (2011). Control of B cell development by the histone H2A deubiquitinase MYSM1. Immunity *35(6)*, 883-896.

Johnson, K., Pflugh, D. L., Yu, D., Hesslein, D. G., Lin, K. I., Bothwell, A. L., Thomas-Tikhonenko, A., Schatz, D. G., and Calame, K. (2004). B cell-specific loss of histone 3 lysine 9 methylation in the V(H) locus depends on Pax5. Nat Immunol *5(8)*, 853-861.

Johnson, K. G., Bromley, S. K., Dustin, M. L., and Thomas, M. L. (2000). A supramolecular basis for CD45 tyrosine phosphatase regulation in sustained T cell activation. Proc Natl Acad Sci U S A *97(18)*, 10138-10143.

Juan, V., Crain, C., and Wilson, C. (2000). Evidence for evolutionarily conserved secondary structure in the H19 tumor suppressor RNA. Nucleic Acids Res *28(5)*, 1221-1227.

Jung, D., Giallourakis, C., Mostoslavsky, R., and Alt, F. W. (2006). Mechanism and control of V(D)J recombination at the immunoglobulin heavy chain locus. Annu Rev Immunol *24*, 541-570.

Kaji, T., Ishige, A., Hikida, M., Taka, J., Hijikata, A., Kubo, M., Nagashima, T., Takahashi, Y., Kurosaki, T., Okada, M., Ohara, O., Rajewsky, K., and Takemori, T. (2012). Distinct cellular pathways select germline-encoded and somatically mutated antibodies into immunological memory. J Exp Med *209(11)*, 2079-2097.

Kallen, A. N., Zhou, X. B., Xu, J., Qiao, C., Ma, J., Yan, L., Lu, L., Liu, C., Yi, J. S., Zhang, H., Min, W., Bennett, A. M., Gregory, R. I., Ding, Y., and Huang, Y. (2013). The imprinted H19 lncRNA antagonizes let-7 microRNAs. Mol Cell *52(1)*, 101-112.

Kaminski, D. A., and Stavnezer, J. (2004). Antibody class switching: uncoupling S region accessibility from transcription. Trends Genet *20(8)*, 337-340.

Kearney, J. F. (2005). Innate-like B cells. Springer Semin Immunopathol *26(4)*, 377-383.

Keniry, A., Oxley, D., Monnier, P., Kyba, M., Dandolo, L., Smits, G., and Reik, W. (2012). The H19 lincRNA is a developmental reservoir of miR-675 that suppresses growth and Igf1r. Nat Cell Biol *14(7)*, 659-665.

Kikuchi, K., Lai, A. Y., Hsu, C. L., and Kondo, M. (2005). IL-7 receptor signaling is necessary for stage transition in adult B cell development through up-regulation of EBF. J Exp Med *201(8)*, 1197-1203.

Kim, H. G., de Guzman, C. G., Swindle, C. S., Cotta, C. V., Gartland, L., Scott, E. W., and Klug, C. A. (2004). The ETS family transcription factor PU.1 is necessary for the maintenance of fetal liver hematopoietic stem cells. Blood *104(13)*, 3894-3900.

King, L. B., and Freedman, B. D. (2009). B-lymphocyte calcium influx. Immunol Rev *231(1)*, 265-277.

Kirstetter, P., Thomas, M., Dierich, A., Kastner, P., and Chan, S. (2002). Ikaros is critical for B cell differentiation and function. Eur J Immunol *32(3)*, 720-730.

Kishihara, K., Penninger, J., Wallace, V. A., Kündig, T. M., Kawai, K., Wakeham, A., Timms, E., Pfeffer, K., Ohashi, P. S., and Thomas, M. L. (1993). Normal B lymphocyte development but impaired T cell maturation in CD45-exon6 protein tyrosine phosphatase-deficient mice. Cell *74(1)*, 143-156.

Kitamura, D., Kudo, A., Schaal, S., Müller, W., Melchers, F., and Rajewsky, K. (1992). A critical role of lambda 5 protein in B cell development. Cell *69(5)*, 823-831.

Kitamura, D., Roes, J., Kühn, R., and Rajewsky, K. (1991). A B cell-deficient mouse by targeted disruption of the membrane exon of the immunoglobulin mu chain gene. Nature *350(6317)*, 423-426.

Köhler, F., Hug, E., Eschbach, C., Meixlsperger, S., Hobeika, E., Kofer, J., Wardemann, H., and Jumaa, H. (2008). Autoreactive B cell receptors mimic autonomous pre-B cell receptor signaling and induce proliferation of early B cells. Immunity *29(6)*, 912-921.

Kondo, M., Suzuki, H., Ueda, R., Osada, H., Takagi, K., Takahashi, T., and Takahashi, T. (1995). Frequent loss of imprinting of the H19 gene is often associated with its overexpression in human lung cancers. Oncogene *10(6)*, 1193-1198.

Kondo, M., Weissman, I. L., and Akashi, K. (1997). Identification of clonogenic common lymphoid progenitors in mouse bone marrow. Cell *91(5)*, 661-672.

Koralov, S. B., Muljo, S. A., Galler, G. R., Krek, A., Chakraborty, T., Kanellopoulou, C., Jensen, K., Cobb, B. S., Merkenschlager, M., Rajewsky, N., and Rajewsky, K. (2008). Dicer ablation affects antibody diversity and cell survival in the B lymphocyte lineage. Cell *132(5)*, 860-874.

Kräutler, N. J., Suan, D., Butt, D., Bourne, K., Hermes, J. R., Chan, T. D., Sundling, C., Kaplan, W., Schofield, P., Jackson, J., Basten, A., Christ, D., and Brink, R. (2017). Differentiation of germinal center B cells into plasma cells is initiated by high-affinity antigen and completed by Tfh cells. J Exp Med *214(5)*, 1259-1267.

Kristiansen, T. A., Jaensson Gyllenbäck, E., Zriwil, A., Björklund, T., Daniel, J. A., Sitnicka, E., Soneji, S., Bryder, D., and Yuan, J. (2016). Cellular Barcoding Links B-1a B Cell Potential to a Fetal Hematopoietic Stem Cell State at the Single-Cell Level. Immunity *45(2)*, 346-357.

Kuchen, S., Resch, W., Yamane, A., Kuo, N., Li, Z., Chakraborty, T., Wei, L., Laurence, A., Yasuda, T., Peng, S., Hu-Li, J., Lu, K., Dubois, W., Kitamura, Y., Charles, N., Sun, H. W., Muljo, S., Schwartzberg, P. L., Paul, W. E., O'Shea, J., Rajewsky, K., and Casellas, R. (2010). Regulation of microRNA expression and abundance during lymphopoiesis. Immunity *32(6)*, 828-839.

Kurosaki, T., and Baba, Y. (2010). Ca2+ signaling and STIM1. Prog Biophys Mol Biol *103(1)*, 51-58.

Kurukuti, S., Tiwari, V. K., Tavoosidana, G., Pugacheva, E., Murrell, A., Zhao, Z., Lobanenkov, V., Reik, W., and Ohlsson, R. (2006). CTCF binding at the H19 imprinting control region mediates maternally inherited higher-order chromatin conformation to restrict enhancer access to Igf2. Proc Natl Acad Sci U S A *103(28)*, 10684-10689.

Lam, K. P., and Rajewsky, K. (1999). B cell antigen receptor specificity and surface density together determine B-1 versus B-2 cell development. J Exp Med *190(4)*, 471-477.

Lanzavecchia, A. (1985). Antigen-specific interaction between T and B cells. Nature *314(6011)*, 537-539.

Leighton, P. A., Ingram, R. S., Eggenschwiler, J., Efstratiadis, A., and Tilghman, S. M. (1995). Disruption of imprinting caused by deletion of the H19 gene region in mice. Nature *375(6526)*, 34-39.

Lewis, A., and Murrell, A. (2004). Genomic imprinting: CTCF protects the boundaries. Curr Biol *14(7)*, R284-6.

Limon, J. J., and Fruman, D. A. (2012). Akt and mTOR in B Cell Activation and Differentiation. Front Immunol *3*, 228.

Lin, H., and Grosschedl, R. (1995). Failure of B-cell differentiation in mice lacking the transcription factor EBF. Nature *376(6537)*, 263-267.

Lin, W. C., and Desiderio, S. (1994). Cell cycle regulation of V(D)J recombination-activating protein RAG-2. Proc Natl Acad Sci U S A *91(7)*, 2733-2737.

Lin, Y. C., Jhunjhunwala, S., Benner, C., Heinz, S., Welinder, E., Mansson, R., Sigvardsson, M., Hagman, J., Espinoza, C. A., Dutkowski, J., Ideker, T., Glass, C. K., and Murre, C.

(2010). A global network of transcription factors, involving E2A, EBF1 and Foxo1, that orchestrates B cell fate. Nat Immunol *11(7)*, 635-643.

Linterman, M. A., Beaton, L., Yu, D., Ramiscal, R. R., Srivastava, M., Hogan, J. J., Verma, N. K., Smyth, M. J., Rigby, R. J., and Vinuesa, C. G. (2010). IL-21 acts directly on B cells to regulate Bcl-6 expression and germinal center responses. J Exp Med *207(2)*, 353-363.

Liu, K., and Nussenzweig, M. C. (2010). Origin and development of dendritic cells. Immunol Rev *234(1)*, 45-54.

Liu, L., An, X., Li, Z., Song, Y., Li, L., Zuo, S., Liu, N., Yang, G., Wang, H., Cheng, X., Zhang, Y., Yang, X., and Wang, J. (2016). The H19 long noncoding RNA is a novel negative regulator of cardiomyocyte hypertrophy. Cardiovasc Res *111(1)*, 56-65.

Lo, K., Landau, N. R., and Smale, S. T. (1991). LyF-1, a transcriptional regulator that interacts with a novel class of promoters for lymphocyte-specific genes. Mol Cell Biol *11(10)*, 5229-5243.

Lottin, S., Adriaenssens, E., Dupressoir, T., Berteaux, N., Montpellier, C., Coll, J., Dugimont, T., and Curgy, J. J. (2002). Overexpression of an ectopic H19 gene enhances the tumorigenic properties of breast cancer cells. Carcinogenesis *23(11)*, 1885-1895.

Luo, M., Li, Z., Wang, W., Zeng, Y., Liu, Z., and Qiu, J. (2013). Long non-coding RNA H19 increases bladder cancer metastasis by associating with EZH2 and inhibiting E-cadherin expression. Cancer Lett *333(2)*, 213-221.

MacLennan, I. C. (1994). Germinal centers. Annu Rev Immunol *12*, 117-139.

Maher, E. R., and Reik, W. (2000). Beckwith-Wiedemann syndrome: imprinting in clusters revisited. J Clin Invest *105(3)*, 247-252.

Malumbres, R., Sarosiek, K. A., Cubedo, E., Ruiz, J. W., Jiang, X., Gascoyne, R. D., Tibshirani, R., and Lossos, I. S. (2009a). Differentiation stage-specific expression of microRNAs in B lymphocytes and diffuse large B-cell lymphomas. Blood *113(16)*, 3754-3764.

Malumbres, R., Sarosiek, K. A., Cubedo, E., Ruiz, J. W., Jiang, X., Gascoyne, R. D., Tibshirani, R., and Lossos, I. S. (2009b). Differentiation stage-specific expression of microRNAs in B lymphocytes and diffuse large B-cell lymphomas. Blood *113(16)*, 3754-3764.

Manning, B. D., and Toker, A. (2017). AKT/PKB Signaling: Navigating the Network. Cell *169(3)*, 381-405.

Mansson, R., Zandi, S., Welinder, E., Tsapogas, P., Sakaguchi, N., Bryder, D., and Sigvardsson, M. (2010). Single-cell analysis of the common lymphoid progenitor compartment reveals functional and molecular heterogeneity. Blood *115(13)*, 2601-2609.

Manz, R. A., Thiel, A., and Radbruch, A. (1997). Lifetime of plasma cells in the bone marrow. Nature *388(6638)*, 133-134.

Mårtensson, I. L., Rolink, A., Melchers, F., Mundt, C., Licence, S., and Shimizu, T. (2002). The pre-B cell receptor and its role in proliferation and Ig heavy chain allelic exclusion. Semin Immunol *14(5)*, 335-342.

Martin, C. H., Aifantis, I., Scimone, M. L., von Andrian, U. H., Reizis, B., von Boehmer, H., and Gounari, F. (2003). Efficient thymic immigration of B220+ lymphoid-restricted bone marrow cells with T precursor potential. Nat Immunol *4(9)*, 866-873.

Martinet, C., Monnier, P., Louault, Y., Benard, M., Gabory, A., and Dandolo, L. (2016). H19 controls reactivation of the imprinted gene network during muscle regeneration. Development *143(6)*, 962-971.

Massari, M. E., and Murre, C. (2000). Helix-loop-helix proteins: regulators of transcription in eucaryotic organisms. Mol Cell Biol *20(2)*, 429-440.

Matthews, A. G., Kuo, A. J., Ramón-Maiques, S., Han, S., Champagne, K. S., Ivanov, D., Gallardo, M., Carney, D., Cheung, P., Ciccone, D. N., Walter, K. L., Utz, P. J., Shi, Y., Kutateladze, T. G., Yang, W., Gozani, O., and Oettinger, M. A. (2007). RAG2 PHD finger couples histone H3 lysine 4 trimethylation with V(D)J recombination. Nature *450(7172)*, 1106-1110.

McAllister, E. J., Apgar, J. R., Leung, C. R., Rickert, R. C., and Jellusova, J. (2017). New Methods To Analyze B Cell Immune Responses to Thymus-Dependent Antigen Sheep Red Blood Cells. J Immunol *199(8)*, 2998-3003.

McKercher, S. R., Torbett, B. E., Anderson, K. L., Henkel, G. W., Vestal, D. J., Baribault, H., Klemsz, M., Feeney, A. J., Wu, G. E., Paige, C. J., and Maki, R. A. (1996). Targeted disruption of the PU.1 gene results in multiple hematopoietic abnormalities. EMBO J *15(20)*, 5647-5658.

Meade, J., Tybulewicz, V. L., and Turner, M. (2004). The tyrosine kinase Syk is required for light chain isotype exclusion but dispensable for the negative selection of B cells. Eur J Immunol *34(4)*, 1102-1110.

Medina, K. L., Pongubala, J. M., Reddy, K. L., Lancki, D. W., Dekoter, R., Kieslinger, M., Grosschedl, R., and Singh, H. (2004). Assembling a gene regulatory network for specification of the B cell fate. Dev Cell *7(4)*, 607-617.

Mercer, E. M., Lin, Y. C., Benner, C., Jhunjhunwala, S., Dutkowski, J., Flores, M., Sigvardsson, M., Ideker, T., Glass, C. K., and Murre, C. (2011). Multilineage priming of enhancer repertoires precedes commitment to the B and myeloid cell lineages in hematopoietic progenitors. Immunity *35(3)*, 413-425.

Meyer-Hermann, M., Deutsch, A., and Or-Guil, M. (2001). Recycling probability and dynamical properties of germinal center reactions. J Theor Biol *210(3)*, 265-285.

Min, H., Montecino-Rodriguez, E., and Dorshkind, K. (2006). Effects of aging on the common lymphoid progenitor to pro-B cell transition. J Immunol *176(2)*, 1007-1012.

Monnier, P., Martinet, C., Pontis, J., Stancheva, I., Ait-Si-Ali, S., and Dandolo, L. (2013). H19 lncRNA controls gene expression of the Imprinted Gene Network by recruiting MBD1. Proc Natl Acad Sci U S A *110(51)*, 20693-20698.

Montecino-Rodriguez, E., and Dorshkind, K. (2006). Stromal cell-dependent growth of B-1 B cell progenitors in the absence of direct contact. Nat Protoc *1(3)*, 1140-1144.

Moore, T., Constancia, M., Zubair, M., Bailleul, B., Feil, R., Sasaki, H., and Reik, W. (1997). Multiple imprinted sense and antisense transcripts, differential methylation and tandem repeats in a putative imprinting control region upstream of mouse Igf2. Proc Natl Acad Sci U S A *94(23)*, 12509-12514.

Mosimann, C., Hausmann, G., and Basler, K. (2009). Beta-catenin hits chromatin: regulation of Wnt target gene activation. Nat Rev Mol Cell Biol *10(4)*, 276-286.

Moulton, T., Crenshaw, T., Hao, Y., Moosikasuwan, J., Lin, N., Dembitzer, F., Hensle, T., Weiss, L., McMorrow, L., and Loew, T. (1994). Epigenetic lesions at the H19 locus in Wilms' tumour patients. Nat Genet *7(3)*, 440-447.

Mundt, C., Licence, S., Shimizu, T., Melchers, F., and Mårtensson, I. L. (2001). Loss of precursor B cell expansion but not allelic exclusion in VpreB1/VpreB2 double-deficient mice. J Exp Med *193(4)*, 435-445.

Muramatsu, M., Sankaranand, V. S., Anant, S., Sugai, M., Kinoshita, K., Davidson, N. O., and Honjo, T. (1999). Specific expression of activation-induced cytidine deaminase (AID), a novel member of the RNA-editing deaminase family in germinal center B cells. J Biol Chem *274(26)*, 18470-18476.

Murrell, A., Heeson, S., and Reik, W. (2004). Interaction between differentially methylated regions partitions the imprinted genes Igf2 and H19 into parent-specific chromatin loops. Nat Genet *36(8)*, 889-893.

Nechanitzky, R., Akbas, D., Scherer, S., György, I., Hoyler, T., Ramamoorthy, S., Diefenbach, A., and Grosschedl, R. (2013). Transcription factor EBF1 is essential for the maintenance of B cell identity and prevention of alternative fates in committed cells. Nat Immunol *14(8)*, 867-875.

Nichogiannopoulou, A., Trevisan, M., Neben, S., Friedrich, C., and Georgopoulos, K. (1999). Defects in hemopoietic stem cell activity in Ikaros mutant mice. J Exp Med *190(9)*, 1201-1214.

Niiro, H., and Clark, E. A. (2002). Regulation of B-cell fate by antigen-receptor signals. Nat Rev Immunol *2(12)*, 945-956.

Norvell, A., Mandik, L., and Monroe, J. G. (1995). Engagement of the antigen-receptor on immature murine B lymphocytes results in death by apoptosis. J Immunol *154(9)*, 4404-4413.

Nutt, S. L., Heavey, B., Rolink, A. G., and Busslinger, M. (1999). Commitment to the B-lymphoid lineage depends on the transcription factor Pax5. Nature *401(6753)*, 556-562.

Nutt, S. L., Hodgkin, P. D., Tarlinton, D. M., and Corcoran, L. M. (2015). The generation of antibody-secreting plasma cells. Nat Rev Immunol *15(3)*, 160-171.

Nutt, S. L., and Kee, B. L. (2007a). The transcriptional regulation of B cell lineage commitment. Immunity *26(6)*, 715-725.

Nutt, S. L., and Kee, B. L. (2007b). The transcriptional regulation of B cell lineage commitment. Immunity *26(6)*, 715-725.

Nutt, S. L., Morrison, A. M., Dörfler, P., Rolink, A., and Busslinger, M. (1998). Identification of BSAP (Pax-5) target genes in early B-cell development by loss- and gain-of-function experiments. EMBO J *17(8)*, 2319-2333.

Nutt, S. L., Thévenin, C., and Busslinger, M. (1997). Essential functions of Pax-5 (BSAP) in pro-B cell development. Immunobiology *198(1-3)*, 227-235.

O'Carroll, D., Mecklenbrauker, I., Das, P. P., Santana, A., Koenig, U., Enright, A. J., Miska, E. A., and Tarakhovsky, A. (2007). A Slicer-independent role for Argonaute 2 in hematopoiesis and the microRNA pathway. Genes Dev *21(16)*, 1999-2004.

Obata, Y., Furusawa, Y., and Hase, K. (2015). Epigenetic modifications of the immune system in health and disease. Immunol Cell Biol *93(3)*, 226-232.

Obukhanych, T. V., and Nussenzweig, M. C. (2006). T-independent type II immune responses generate memory B cells. J Exp Med *203(2)*, 305-310.

Ochi, T., Blackford, A. N., Coates, J., Jhujh, S., Mehmood, S., Tamura, N., Travers, J., Wu, Q., Draviam, V. M., Robinson, C. V., Blundell, T. L., and Jackson, S. P. (2015). DNA repair. PAXX, a paralog of XRCC4 and XLF, interacts with Ku to promote DNA double-strand break repair. Science *347(6218)*, 185-188.

Oprea, M., and Perelson, A. S. (1997). Somatic mutation leads to efficient affinity maturation when centrocytes recycle back to centroblasts. J Immunol *158(11)*, 5155-5162.

Ouyang, J., Zhu, X., Chen, Y., Wei, H., Chen, Q., Chi, X., Qi, B., Zhang, L., Zhao, Y., Gao, G. F., Wang, G., and Chen, J. L. (2014). NRAV, a long noncoding RNA, modulates antiviral responses through suppression of interferon-stimulated gene transcription. Cell Host Microbe *16(5)*, 616-626.

Pachnis, V., Brannan, C. I., and Tilghman, S. M. (1988). The structure and expression of a novel gene activated in early mouse embryogenesis. EMBO J *7(3)*, 673-681.

Pape, K. A., Taylor, J. J., Maul, R. W., Gearhart, P. J., and Jenkins, M. K. (2011). Different B cell populations mediate early and late memory during an endogenous immune response. Science *331(6021)*, 1203-1207.

Parekh, A. B., and Putney, J. W. (2005). Store-operated calcium channels. Physiol Rev *85(2)*, 757-810.

Park, S. Y., Wolfram, P., Canty, K., Harley, B., Nombela-Arrieta, C., Pivarnik, G., Manis, J., Beggs, H. E., and Silberstein, L. E. (2013). Focal adhesion kinase regulates the localization and retention of pro-B cells in bone marrow microenvironments. J Immunol *190(3)*, 1094-1102.

Paul, W. E., and Seder, R. A. (1994). Lymphocyte responses and cytokines. Cell *76(2)*, 241-251.

Pelanda, R., Braun, U., Hobeika, E., Nussenzweig, M. C., and Reth, M. (2002). B cell progenitors are arrested in maturation but have intact VDJ recombination in the absence of Ig-alpha and Ig-beta. J Immunol *169(2)*, 865-872.

Pelletier, N., Casamayor-Pallejà, M., De Luca, K., Mondière, P., Saltel, F., Jurdic, P., Bella, C., Genestier, L., and Defrance, T. (2006). The endoplasmic reticulum is a key component of the plasma cell death pathway. J Immunol *176(3)*, 1340-1347.

Peñaherrera, M. S., Weindler, S., Van Allen, M. I., Yong, S. L., Metzger, D. L., McGillivray, B., Boerkoel, C., Langlois, S., and Robinson, W. P. (2010). Methylation profiling in individuals with Russell-Silver syndrome. Am J Med Genet A *152A(2)*, 347-355.

Pereira, J. P., An, J., Xu, Y., Huang, Y., and Cyster, J. G. (2009). Cannabinoid receptor 2 mediates the retention of immature B cells in bone marrow sinusoids. Nat Immunol *10(4)*, 403-411.

Poirier, F., Chan, C. T., Timmons, P. M., Robertson, E. J., Evans, M. J., and Rigby, P. W. (1991). The murine H19 gene is activated during embryonic stem cell differentiation in vitro and at the time of implantation in the developing embryo. Development *113(4)*, 1105-1114.

Pope, C., Piekos, S. C., Chen, L., Mishra, S., and Zhong, X. B. (2017). The role of H19, a long non-coding RNA, in mouse liver postnatal maturation. PLoS One *12(11)*, e0187557.

Possot, C., Schmutz, S., Chea, S., Boucontet, L., Louise, A., Cumano, A., and Golub, R. (2011). Notch signaling is necessary for adult, but not fetal, development of RORγt(+) innate lymphoid cells. Nat Immunol *12(10)*, 949-958.

Prawitt, D., Enklaar, T., Gärtner-Rupprecht, B., Spangenberg, C., Lausch, E., Reutzel, D., Fees, S., Korzon, M., Brozek, I., Limon, J., Housman, D. E., Pelletier, J., and Zabel, B. (2005a). Microdeletion and IGF2 loss of imprinting in a cascade causing Beckwith-Wiedemann syndrome with Wilms' tumor. Nat Genet *37(8)*, 785-6; author reply 786.

Prawitt, D., Enklaar, T., Gärtner-Rupprecht, B., Spangenberg, C., Oswald, M., Lausch, E., Schmidtke, P., Reutzel, D., Fees, S., Lucito, R., Korzon, M., Brozek, I., Limon, J., Housman, D. E., Pelletier, J., and Zabel, B. (2005b). Microdeletion of target sites for insulator protein CTCF in a chromosome 11p15 imprinting center in Beckwith-Wiedemann syndrome and Wilms' tumor. Proc Natl Acad Sci U S A *102(11)*, 4085-4090.

Pritchard, N. R., and Smith, K. G. (2003). B cell inhibitory receptors and autoimmunity. Immunology *108(3)*, 263-273.

Rajewsky, K. (1996). Clonal selection and learning in the antibody system. Nature *381(6585)*, 751-758.

Ramachandrareddy, H., Bouska, A., Shen, Y., Ji, M., Rizzino, A., Chan, W. C., and McKeithan, T. W. (2010). BCL6 promoter interacts with far upstream sequences with greatly enhanced activating histone modifications in germinal center B cells. Proc Natl Acad Sci U S A *107(26)*, 11930-11935.

Ramond, C., Berthault, C., Burlen-Defranoux, O., de Sousa, A. P., Guy-Grand, D., Vieira, P., Pereira, P., and Cumano, A. (2014). Two waves of distinct hematopoietic progenitor cells colonize the fetal thymus. Nat Immunol *15(1)*, 27-35.

Reik, W., Brown, K. W., Slatter, R. E., Sartori, P., Elliott, M., and Maher, E. R. (1994). Allelic methylation of H19 and IGF2 in the Beckwith-Wiedemann syndrome. Hum Mol Genet *3(8)*, 1297-1301.

Reinherz, E. L., Tan, K., Tang, L., Kern, P., Liu, J., Xiong, Y., Hussey, R. E., Smolyar, A., Hare, B., Zhang, R., Joachimiak, A., Chang, H. C., Wagner, G., and Wang, J. (1999). The crystal structure of a T cell receptor in complex with peptide and MHC class II. Science *286(5446)*, 1913-1921.

Reya, T., and Grosschedl, R. (1998). Transcriptional regulation of B-cell differentiation. Curr Opin Immunol *10(2)*, 158-165.

Reynaud, D., Demarco, I. A., Reddy, K. L., Schjerven, H., Bertolino, E., Chen, Z., Smale, S. T., Winandy, S., and Singh, H. (2008). Regulation of B cell fate commitment and immunoglobulin heavy-chain gene rearrangements by Ikaros. Nat Immunol *9(8)*, 927-936.

Ribeiro de Almeida, C., Hendriks, R. W., and Stadhouders, R. (2015). Dynamic Control of Long-Range Genomic Interactions at the Immunoglobulin κ Light-Chain Locus. Adv Immunol *128*, 183-271.

Ripoche, M. A., Kress, C., Poirier, F., and Dandolo, L. (1997). Deletion of the H19 transcription unit reveals the existence of a putative imprinting control element. Genes Dev *11(12)*, 1596-1604.

Rivkin, M., Rosen, K. M., and Villa-Komaroff, L. (1993). Identification of an antisense transcript from the IGF-II locus in mouse. Mol Reprod Dev *35(4)*, 394-397.

Roessler, S., Györy, I., Imhof, S., Spivakov, M., Williams, R. R., Busslinger, M., Fisher, A. G., and Grosschedl, R. (2007). Distinct promoters mediate the regulation of Ebf1 gene expression by interleukin-7 and Pax5. Mol Cell Biol *27(2)*, 579-594.

Rolink, A., ten Boekel, E., Melchers, F., Fearon, D. T., Krop, I., and Andersson, J. (1996). A subpopulation of B220+ cells in murine bone marrow does not express CD19 and contains natural killer cell progenitors. J Exp Med *183(1)*, 187-194.

Rolink, A. G., Nutt, S. L., Melchers, F., and Busslinger, M. (1999). Long-term in vivo reconstitution of T-cell development by Pax5-deficient B-cell progenitors. Nature *401(6753)*, 603-606.

Rossi, L., Lin, K. K., Boles, N. C., Yang, L., King, K. Y., Jeong, M., Mayle, A., and Goodell, M. A. (2012). Less is more: unveiling the functional core of hematopoietic stem cells through knockout mice. Cell Stem Cell *11(3)*, 302-317.

Rumfelt, L. L., Zhou, Y., Rowley, B. M., Shinton, S. A., and Hardy, R. R. (2006). Lineage specification and plasticity in CD19- early B cell precursors. J Exp Med *203(3)*, 675-687.

Santos, P. M., and Borghesi, L. (2011). Molecular resolution of the B cell landscape. Curr Opin Immunol *23(2)*, 163-170.

Schaller, M. D. (2001). Biochemical signals and biological responses elicited by the focal adhesion kinase. Biochim Biophys Acta *1540(1)*, 1-21.

Scharenberg, A. M., Humphries, L. A., and Rawlings, D. J. (2007). Calcium signalling and cell-fate choice in B cells. Nat Rev Immunol *7(10)*, 778-789.

Schatz, D. G., and Ji, Y. (2011). Recombination centres and the orchestration of V(D)J recombination. Nat Rev Immunol *11(4)*, 251-263.

Schatz, D. G., Oettinger, M. A., and Baltimore, D. (1989). The V(D)J recombination activating gene, RAG-1. Cell *59(6)*, 1035-1048.

Schatz, D. G., and Swanson, P. C. (2011). V(D)J recombination: mechanisms of initiation. Annu Rev Genet *45*, 167-202.

Schwickert, T. A., Tagoh, H., Gültekin, S., Dakic, A., Axelsson, E., Minnich, M., Ebert, A., Werner, B., Roth, M., Cimmino, L., Dickins, R. A., Zuber, J., Jaritz, M., and Busslinger, M. (2014). Stage-specific control of early B cell development by the transcription factor Ikaros. Nat Immunol *15(3)*, 283-293.

Scott, E. W., Fisher, R. C., Olson, M. C., Kehrli, E. W., Simon, M. C., and Singh, H. (1997). PU.1 functions in a cell-autonomous manner to control the differentiation of multipotential lymphoid-myeloid progenitors. Immunity *6(4)*, 437-447.

Scott, E. W., Simon, M. C., Anastasi, J., and Singh, H. (1994). Requirement of transcription factor PU.1 in the development of multiple hematopoietic lineages. Science *265(5178)*, 1573-1577.

Seet, C. S., Brumbaugh, R. L., and Kee, B. L. (2004). Early B cell factor promotes B lymphopoiesis with reduced interleukin 7 responsiveness in the absence of E2A. J Exp Med *199(12)*, 1689-1700.

Sehgal, L., Mathur, R., Braun, F. K., Wise, J. F., Berkova, Z., Neelapu, S., Kwak, L. W., and Samaniego, F. (2014). FAS-antisense 1 lncRNA and production of soluble versus membrane Fas in B-cell lymphoma. Leukemia *28(12)*, 2376-2387.

Shaffer, A. L., Lin, K. I., Kuo, T. C., Yu, X., Hurt, E. M., Rosenwald, A., Giltnane, J. M., Yang, L., Zhao, H., Calame, K., and Staudt, L. M. (2002). Blimp-1 orchestrates plasma cell differentiation by extinguishing the mature B cell gene expression program. Immunity *17(1)*, 51-62.

Shaknovich, R., Cerchietti, L., Tsikitas, L., Kormaksson, M., De, S., Figueroa, M. E., Ballon, G., Yang, S. N., Weinhold, N., Reimers, M., Clozel, T., Luttrop, K., Ekstrom, T. J., Frank, J., Vasanthakumar, A., Godley, L. A., Michor, F., Elemento, O., and Melnick, A. (2011). DNA methyltransferase 1 and DNA methylation patterning contribute to germinal center B-cell differentiation. Blood *118(13)*, 3559-3569.

Shapiro-Shelef, M., and Calame, K. (2005). Regulation of plasma-cell development. Nat Rev Immunol *5(3)*, 230-242.

Sharma, A., Singh, K., and Almasan, A. (2012). Histone H2AX phosphorylation: a marker for DNA damage. Methods Mol Biol *920*, 613-626.

Shimizu, T., Mundt, C., Licence, S., Melchers, F., and Mårtensson, I. L. (2002). VpreB1/VpreB2/lambda 5 triple-deficient mice show impaired B cell development but functional allelic exclusion of the IgH locus. J Immunol *168(12)*, 6286-6293.

Shlomchik, M. J., and Weisel, F. (2012). Germinal center selection and the development of memory B and plasma cells. Immunol Rev *247(1)*, 52-63.

Shrivastava, P., Katagiri, T., Ogimoto, M., Mizuno, K., and Yakura, H. (2004). Dynamic regulation of Src-family kinases by CD45 in B cells. Blood *103(4)*, 1425-1432.

Sigvardsson, M., Clark, D. R., Fitzsimmons, D., Doyle, M., Akerblad, P., Breslin, T., Bilke, S., Li, R., Yeamans, C., Zhang, G., and Hagman, J. (2002). Early B-cell factor, E2A, and Pax-5 cooperate to activate the early B cell-specific mb-1 promoter. Mol Cell Biol *22(24)*, 8539-8551.

Sitnicka, E., Brakebusch, C., Martensson, I. L., Svensson, M., Agace, W. W., Sigvardsson, M., Buza-Vidas, N., Bryder, D., Cilio, C. M., Ahlenius, H., Maraskovsky, E., Peschon, J. J., and Jacobsen, S. E. (2003). Complementary signaling through flt3 and interleukin-7 receptor alpha is indispensable for fetal and adult B cell genesis. J Exp Med *198(10)*, 1495-1506.

Smith, E. M., Gisler, R., and Sigvardsson, M. (2002). Cloning and characterization of a promoter flanking the early B cell factor (EBF) gene indicates roles for E-proteins and autoregulation in the control of EBF expression. J Immunol *169(1)*, 261-270.

Smith, J. P., Burton, G. F., Tew, J. G., and Szakal, A. K. (1998). Tingible body macrophages in regulation of germinal center reactions. Dev Immunol *6(3-4)*, 285-294.

Sparago, A., Cerrato, F., Vernucci, M., Ferrero, G. B., Silengo, M. C., and Riccio, A. (2004). Microdeletions in the human H19 DMR result in loss of IGF2 imprinting and Beckwith-Wiedemann syndrome. Nat Genet *36(9)*, 958-960.

Srinivasan, L., Sasaki, Y., Calado, D. P., Zhang, B., Paik, J. H., DePinho, R. A., Kutok, J. L., Kearney, J. F., Otipoby, K. L., and Rajewsky, K. (2009). PI3 kinase signals BCR-dependent mature B cell survival. Cell *139(3)*, 573-586.

Stavnezer, J., Guikema, J. E., and Schrader, C. E. (2008). Mechanism and regulation of class switch recombination. Annu Rev Immunol *26*, 261-292.

Su, I. H., and Tarakhovsky, A. (2005). Epigenetic control of B cell differentiation. Semin Immunol *17(2)*, 167-172.

Su, R., Wang, C., Feng, H., Lin, L., Liu, X., Wei, Y., and Yang, H. (2016). Alteration in Expression and Methylation of IGF2/H19 in Placenta and Umbilical Cord Blood Are Associated with Macrosomia Exposed to Intrauterine Hyperglycemia. PLoS One *11(2)*, e0148399.

Su, S. T., Ying, H. Y., Chiu, Y. K., Lin, F. R., Chen, M. Y., and Lin, K. I. (2009). Involvement of histone demethylase LSD1 in Blimp-1-mediated gene repression during plasma cell differentiation. Mol Cell Biol *29(6)*, 1421-1431.

Sze, D. M., Toellner, K. M., García de Vinuesa, C., Taylor, D. R., and MacLennan, I. C. (2000). Intrinsic constraint on plasmablast growth and extrinsic limits of plasma cell survival. J Exp Med *192(6)*, 813-821.

Takahashi, Y., Dutta, P. R., Cerasoli, D. M., and Kelsoe, G. (1998). In situ studies of the primary immune response to (4-hydroxy-3-nitrophenyl)acetyl. V. Affinity maturation develops in two stages of clonal selection. J Exp Med *187(6)*, 885-895.

Tano, K., and Akimitsu, N. (2012). Long non-coding RNAs in cancer progression. Front Genet *3*, 219.

Taylor, J. J., Pape, K. A., and Jenkins, M. K. (2012). A germinal center-independent pathway generates unswitched memory B cells early in the primary response. J Exp Med *209(3)*, 597-606.

Thai, T. H., Calado, D. P., Casola, S., Ansel, K. M., Xiao, C., Xue, Y., Murphy, A., Frendewey, D., Valenzuela, D., Kutok, J. L., Schmidt-Supprian, M., Rajewsky, N., Yancopoulos, G., Rao, A., and Rajewsky, K. (2007a). Regulation of the germinal center response by microRNA-155. Science *316(5824)*, 604-608.

Thai, T. H., Calado, D. P., Casola, S., Ansel, K. M., Xiao, C., Xue, Y., Murphy, A., Frendewey, D., Valenzuela, D., Kutok, J. L., Schmidt-Supprian, M., Rajewsky, N., Yancopoulos, G., Rao, A., and Rajewsky, K. (2007b). Regulation of the germinal center response by microRNA-155. Science *316(5824)*, 604-608.

Thomas, M. L. (1994). The regulation of B- and T-lymphocyte activation by the transmembrane protein tyrosine phosphatase CD45. Curr Opin Cell Biol *6(2)*, 247-252.

Thompson, E. C., Cobb, B. S., Sabbattini, P., Meixlsperger, S., Parelho, V., Liberg, D., Taylor, B., Dillon, N., Georgopoulos, K., Jumaa, H., Smale, S. T., Fisher, A. G., and Merkenschlager, M. (2007). Ikaros DNA-binding proteins as integral components of B cell developmental-stage-specific regulatory circuits. Immunity *26(3)*, 335-344.

Tonegawa, S. (1983). Somatic generation of antibody diversity. Nature *302(5909)*, 575-581.

Treiber, T., Mandel, E. M., Pott, S., Györy, I., Firner, S., Liu, E. T., and Grosschedl, R. (2010). Early B cell factor 1 regulates B cell gene networks by activation, repression, and transcription- independent poising of chromatin. Immunity *32(5)*, 714-725.

Trowbridge, I. S., and Thomas, M. L. (1994). CD45: an emerging role as a protein tyrosine phosphatase required for lymphocyte activation and development. Annu Rev Immunol *12*, 85-116.

Tsang, W. P., Ng, E. K., Ng, S. S., Jin, H., Yu, J., Sung, J. J., and Kwok, T. T. (2010). Oncofetal H19-derived miR-675 regulates tumor suppressor RB in human colorectal cancer. Carcinogenesis *31(3)*, 350-358.

Tu, W. Z., Li, B., Huang, B., Wang, Y., Liu, X. D., Guan, H., Zhang, S. M., Tang, Y., Rang, W. Q., and Zhou, P. K. (2013). γH2AX foci formation in the absence of DNA damage: mitotic H2AX phosphorylation is mediated by the DNA-PKcs/CHK2 pathway. FEBS Lett *587(21)*, 3437-3443.

Tze, L. E., Schram, B. R., Lam, K. P., Hogquist, K. A., Hippen, K. L., Liu, J., Shinton, S. A., Otipoby, K. L., Rodine, P. R., Vegoe, A. L., Kraus, M., Hardy, R. R., Schlissel, M. S., Rajewsky, K., and Behrens, T. W. (2005). Basal immunoglobulin signaling actively maintains developmental stage in immature B cells. PLoS Biol *3*, e82.

Van Bortle, K., and Corces, V. G. (2012). Nuclear organization and genome function. Annu Rev Cell Dev Biol *28*, 163-187.

van der Merwe, P. A. (2000). Modeling costimulation. Nat Immunol *1(3)*, 194-195.

van Der Merwe, P. A., and Davis, S. J. (2002). Immunology. The immunological synapse--a multitasking system. Science *295(5559)*, 1479-1480.

Varrault, A., Gueydan, C., Delalbre, A., Bellmann, A., Houssami, S., Aknin, C., Severac, D., Chotard, L., Kahli, M., Le Digarcher, A., Pavlidis, P., and Journot, L. (2006). Zac1 regulates an imprinted gene network critically involved in the control of embryonic growth. Dev Cell *11(5)*, 711-722.

Venkatraman, A., He, X. C., Thorvaldsen, J. L., Sugimura, R., Perry, J. M., Tao, F., Zhao, M., Christenson, M. K., Sanchez, R., Yu, J. Y., Peng, L., Haug, J. S., Paulson, A., Li, H., Zhong, X. B., Clemens, T. L., Bartolomei, M. S., and Li, L. (2013). Maternal imprinting at the H19-Igf2 locus maintains adult haematopoietic stem cell quiescence. Nature *500(7462)*, 345-349.

Verkoczy, L., Duong, B., Skog, P., Aït-Azzouzene, D., Puri, K., Vela, J. L., and Nemazee, D. (2007a). Basal B cell receptor-directed phosphatidylinositol 3-kinase signaling turns off RAGs and promotes B cell-positive selection. J Immunol *178(10)*, 6332-6341.

Verkoczy, L., Duong, B., Skog, P., Aït-Azzouzene, D., Puri, K., Vela, J. L., and Nemazee, D. (2007b). Basal B cell receptor-directed phosphatidylinositol 3-kinase signaling turns off RAGs and promotes B cell-positive selection. J Immunol *178(10)*, 6332-6341.

Victora, G. D., and Nussenzweig, M. C. (2012a). Germinal centers. Annu Rev Immunol *30*, 429-457.

Victora, G. D., and Nussenzweig, M. C. (2012b). Germinal centers. Annu Rev Immunol *30*, 429-457.

Wakioka, T., Sasaki, A., Mitsui, K., Yokouchi, M., Inoue, A., Komiya, S., and Yoshimura, A. (1999). APS, an adaptor protein containing Pleckstrin homology (PH) and Src homology-2 (SH2) domains inhibits the JAK-STAT pathway in collaboration with c-Cbl. Leukemia *13(5)*, 760-767.

Wang, J., Lin, Q., Wu, Q., and Cooper, M. D. (1998). The enigmatic role of glutamyl aminopeptidase (BP-1/6C3 antigen) in immune system development. Immunol Rev *161*, 71-77.

Wang, J. H., Nichogiannopoulou, A., Wu, L., Sun, L., Sharpe, A. H., Bigby, M., and Georgopoulos, K. (1996). Selective defects in the development of the fetal and adult lymphoid system in mice with an Ikaros null mutation. Immunity *5(6)*, 537-549.

Wang, P., Xue, Y., Han, Y., Lin, L., Wu, C., Xu, S., Jiang, Z., Xu, J., Liu, Q., and Cao, X. (2014). The STAT3-binding long noncoding RNA lnc-DC controls human dendritic cell differentiation. Science *344(6181)*, 310-313.

Wapinski, O., and Chang, H. Y. (2011). Long noncoding RNAs and human disease. Trends Cell Biol *21(6)*, 354-361.

Weber, M., Hagège, H., Murrell, A., Brunel, C., Reik, W., Cathala, G., and Forné, T. (2003). Genomic imprinting controls matrix attachment regions in the Igf2 gene. Mol Cell Biol *23(24)*, 8953-8959.

Weintraub, B. C., Jun, J. E., Bishop, A. C., Shokat, K. M., Thomas, M. L., and Goodnow, C. C. (2000). Entry of B cell receptor into signaling domains is inhibited in tolerant B cells. J Exp Med *191(8)*, 1443-1448.

Weisel, F. J., Zuccarino-Catania, G. V., Chikina, M., and Shlomchik, M. J. (2016). A Temporal Switch in the Germinal Center Determines Differential Output of Memory B and Plasma Cells. Immunity *44(1)*, 116-130.

Wiles, M. V. (1988). Isolation of differentially expressed human cDNA clones: similarities between mouse and human embryonal carcinoma cell differentiation. Development *104(3)*, 403-413.

Willingham, A. T., Orth, A. P., Batalov, S., Peters, E. C., Wen, B. G., Aza-Blanc, P., Hogenesch, J. B., and Schultz, P. G. (2005). A strategy for probing the function of noncoding RNAs finds a repressor of NFAT. Science *309(5740)*, 1570-1573.

Wojdacz, T. K., Dobrovic, A., and Algar, E. M. (2008). Rapid detection of methylation change at H19 in human imprinting disorders using methylation-sensitive high-resolution melting. Hum Mutat *29(10)*, 1255-1260.

Woof, J. M., and Burton, D. R. (2004). Human antibody-Fc receptor interactions illuminated by crystal structures. Nat Rev Immunol *4(2)*, 89-99.

Xing, M., Yang, M., Huo, W., Feng, F., Wei, L., Jiang, W., Ning, S., Yan, Z., Li, W., Wang, Q., Hou, M., Dong, C., Guo, R., Gao, G., Ji, J., Zha, S., Lan, L., Liang, H., and Xu, D. (2015). Interactome analysis identifies a new paralogue of XRCC4 in non-homologous end joining DNA repair pathway. Nat Commun *6*, 6233.

Xu, X., Ji, S., Li, W., Yi, B., Li, H., Zhang, H., and Ma, W. (2017). LncRNA H19 promotes the differentiation of bovine skeletal muscle satellite cells by suppressing Sirt1/FoxO1. Cell Mol Biol Lett *22*, 10.

Yang, F., Bi, J., Xue, X., Zheng, L., Zhi, K., Hua, J., and Fang, G. (2012). Up-regulated long non-coding RNA H19 contributes to proliferation of gastric cancer cells. FEBS J *279(17)*, 3159-3165.

Yarkoni, Y., Getahun, A., and Cambier, J. C. (2010). Molecular underpinning of B-cell anergy. Immunol Rev *237(1)*, 249-263.

Ye, M., Ermakova, O., and Graf, T. (2005). PU.1 is not strictly required for B cell development and its absence induces a B-2 to B-1 cell switch. J Exp Med *202(10)*, 1411-1422.

Zan, H., and Casali, P. (2015). Epigenetics of Peripheral B-Cell Differentiation and the Antibody Response. Front Immunol *6*, 631.

Zhang, J., Jima, D. D., Jacobs, C., Fischer, R., Gottwein, E., Huang, G., Lugar, P. L., Lagoo, A. S., Rizzieri, D. A., Friedman, D. R., Weinberg, J. B., Lipsky, P. E., and Dave, S. S. (2009). Patterns of microRNA expression characterize stages of human B-cell differentiation. Blood *113(19)*, 4586-4594.

Zhang, L., Yang, F., Yuan, J. H., Yuan, S. X., Zhou, W. P., Huo, X. S., Xu, D., Bi, H. S., Wang, F., and Sun, S. H. (2013). Epigenetic activation of the MiR-200 family contributes to H19-mediated metastasis suppression in hepatocellular carcinoma. Carcinogenesis *34(3)*, 577-586.

Zhang, Y., Shields, T., Crenshaw, T., Hao, Y., Moulton, T., and Tycko, B. (1993). Imprinting of human H19: allele-specific CpG methylation, loss of the active allele in Wilms tumor, and potential for somatic allele switching. Am J Hum Genet *53(1)*, 113-124.

Zhang, Y., and Tycko, B. (1992). Monoallelic expression of the human H19 gene. Nat Genet *1*, 40-44.

Zhang, Y., Zhang, M., Xu, W., Chen, J., and Zhou, X. (2017). The long non-coding RNA H19 promotes cardiomyocyte apoptosis in dilated cardiomyopathy. Oncotarget *8(17)*, 28588-28594.

Zhuang, M., Gao, W., Xu, J., Wang, P., and Shu, Y. (2014). The long non-coding RNA H19-derived miR-675 modulates human gastric cancer cell proliferation by targeting tumor suppressor RUNX1. Biochem Biophys Res Commun *448(3)*, 315-322.

Zhuang, Y., Soriano, P., and Weintraub, H. (1994). The helix-loop-helix gene E2A is required for B cell formation. Cell *79(5)*, 875-884.

Zikherman, J., Doan, K., Parameswaran, R., Raschke, W., and Weiss, A. (2012). Quantitative differences in CD45 expression unmask functions for CD45 in B-cell development, tolerance, and survival. Proc Natl Acad Sci U S A *109(1)*, E3-12.

Zotos, D., Coquet, J. M., Zhang, Y., Light, A., D'Costa, K., Kallies, A., Corcoran, L. M., Godfrey, D. I., Toellner, K. M., Smyth, M. J., Nutt, S. L., and Tarlinton, D. M. (2010). IL-21 regulates germinal center B cell differentiation and proliferation through a B cell-intrinsic mechanism. J Exp Med *207(2)*, 365-378.

Annex

Table 1. Antibody list

Mouse antibody	Clone	Supplier	Staining panel
anti-B220	RA3-6B2	BD Bioscience	B cell detection
anti-BP1	6B3/BP1	BD Bioscience	proB cell staining
anti-CCR6	29-2L17	Biolegend	Memory B cell detection
anti-CD117	2B8	Biolegend	Progenitors and proB cells staining
anti-CD11b	M1/70	Biolegend	Lineage cocktail and myeloid cell detection
anti-CD11c	N418	Biolegend	Lineage cocktail and DCs detection
anti-CD127	A7R34	Biolegend	Progenitors staining
anti-CD135	A2F10	Biolegend	Progenitors staining
anti-CD150	TC15-12F12,2	Sony	HSC staining
anti-CD16/32	2.4G2	BD Bioscience	Fc block and CMP detection
anti-CD19	6D5	Biolegend	Lineage cocktail and B cell detection
anti-CD21	7G6	BD Bioscience	Splenic marginal zone B cell staining
anti-CD23	B3B4	BD Bioscience	Splenic follicular B cell staining
anti-CD24	M1-69	Biolegend	proB staining
anti-CD25	3C7	Biolegend	preB staining
anti-CD27	LG.7F9	BD Bioscience	Memory B cell staining
anti-CD3ε	145-2C11	Biolegend	Lineage cocktail and T cell detection
anti-CD34	RAM34	eBioscience	HSC staining
anti-CD38	90	eBioscience	Germinal centre B cell staining
anti-CD4	A161A1	Biolegend	Lineage cocktail and T cell detection
anti-CD40		BD Pharmingen	B cell activation
anti-CD43	S7	BD Bioscience	proB cell staining
anti-CD44	IM7	Biolegend	B cell activation and DN1,DN2 subsets staining
anti-CD45	30-F11	BD Bioscience	Pan hematopoietic marker
anti-CD45.1	A20	Biolegend	Chimeras analysis
anti-CD45.2	104	BD Bioscience	Chimeras analysis
anti-CD48	HM48-1	eBioscience	HSC staining
anti-CD49d	R1-2	BD Bioscience	Cell adhesion
anti-CD5	53-7.3	BD Bioscience	B1a cell staining
anti-CD62L	MEL-14	BD Bioscience	B cell activation
anti-CD69	-	A becton dickinson	B cell activation
anti-CD8	53-6.7	Biolegend	Lineage cocktail and T cell detection
anti-CD80	B7-1	A becton dickinson	B cell activation
anti-CD86	GL1	BD Bioscience	B cell activation
anti-CD93	AA4.1	eBioscience	B cell progenitors

anti-CD95	J02	BD Bioscience	Germinal center staining
anti-CXCR4	2B11/CXCR4	BD Bioscience	DZ and LZ staining
anti-Gr1	RB6-8C5	Biolegend	Lineage cocktail and Myeloid cells detection
anti-H2AX	N1-431	BD Bioscience	DNA double strands staining
anti-IFNg	-	BD Pharmingen	Cytokine detection
anti-IgD	11-26C.2A	BD Pharmingen	
anti-IgE	R35-118	BD Pharmingen	Ig class switch detection
anti-IgG1	-	BD Pharmingen	Ig class switch detection
anti-IgG2a	-	Southern biotech	Ig class switch detection
anti-IgG2b	-	Southern biotech	Ig class switch detection
anti-IgI	R26-46	BD Pharmingen	Ig light chain detection
anti-Igk	187.1	BD Pharmingen	Ig light chain detection
anti-IgM	RMM-1	Biolegend	B cell development
anti-IL10	-	BD Pharmingen	Cytokine detection
anti-IL13	-	BD Pharmingen	Cytokine detection
anti-IL17	-	BD Pharmingen	Cytokine detection
anti-IL2	-	BD Pharmingen	Cytokine detection
anti-IL21	-	BD Pharmingen	Cytokine detection
anti-IL4	-	BD Pharmingen	Cytokine detection
anti-IL6	-	BD Pharmingen	Cytokine detection
anti-Ki67	-	BD Pharmingen	Cell cycle analysis
anti-MHCII	M5/114.15.2	Biolegend	B cell response
anti-NK1.1	PK136	Biolegend	Lineage cocktail and NK cell detection
anti-Ter119	TER-119	Biolegend	Lineage cocktail
anti-Sca1	D7	Biolegend	Progenitors staining
DAPI	-	Sigma	Cell cycle analysis
Propidium iodide	-	Sigma	Viability dye
Annexin V	-	Biolegend	Apoptosis staining
Caspase 3/7	-	invitrogen	Apoptosis staining

Table 2. primer list

Primer	sequence
VH J558	ARGCCTGGGRCTTCAGTGAAG
VH Q52	CTCACAGAGCCTGTCCATCAC
DQ52	CATCCACCCTTCTGATGCTTGCATT
JH4e	AGGCTCTGAGATCCCTAGACA
DSP2,7	TCACTGGTCCATGTGGAGAGCTGAG
Stag3 F	TCCTCAGGCAGTGAGTCTTCC
Stag3 R	GTTCCCTGTGAGTCTCTGTCAT
Elovl6 F	GAAAAGCAGTTCAACGAGAACG
Elovl6 R	AGATGCCGACCACCAAAGATA
Bcl9 F	AGCAGCACCTAATGGGCAAAG
Bcl9 R	GGATAAGTCGAACTCAGGAATGC
Man1a2 F	TCTGGTCGTAGGATACCACCT
Man1a2 R	GAAGGCACTAAGGATGAGGAGA
Uba7 F	CTACGAGCGACTCCATATACCT
Uba7 R	TACACACAGGGTAGGGAGCAT
Lmo7 F	TTGAAACAACGGATTTTCGAGC
Lmo7 R	GACGCCAGGTTTGAGCTTATT
Daglb F	AGCGACGACTTGGTGTTCC
Daglb R	GCTGAGCAAGACTCCACCG
Aldh2 F	GACGCCGTCAGCAGGAAAA
Aldh2 R	CGCCAATCGGTACAACAGC
Wls F	ATGGCTGGGGCAATTATAGAAAA
Wls R	GGGTGCTGGAGCGATCAAG
Usp46 F	ATGACTGTCCGAAACATCGCC
Usp46 R	TTGACCAATCCGAAGTAGTGTTC
Sh2b2 F	GTGGACTTCGCACACAAGTTC
Sh2b2 R	GGGTTCCATAGTGTCGGCT
Cux1 F	TGACCTGAGCGGTCCTTACA
Cux1 R	TGGGGCCATGCCATTTACATC
Spata13 F	GTTAGGCTTCGAGTCAATCAGG
Spata13 R	ATGACGTTGGTCCGCATCTG
Parp3 F	ATGGCTCCAAAACGAAAGGC
Parp3 R	TCCTCCTCTGTCCCTTGTCG
Usp12 F	ACAGTCTCCAAATTCGCCTCC
Usp12 R	ACTGAGTTGCAGTAGCAGGTATT
Smarcc1 F	AGCTAGATTCGGTGCGAGTCT
Smarcc1 R	CCACCAGTCCAGCTAGTGTTTT
Gpr89 F	TTTTTGGATTCGGATGGCTTTTC
Gpr89 R	TGCTGTTCAGAACTCCCAAGA
Lnx2 F	CAGCACTGGGCGAGAGAAAA
Lnx2 R	CTTGTGGCAGAACGTGTGTC
Xkr6 F	TCACCATCTCATCCCGAGTTAT
Xkr6 R	GATCCCTACCACCATGTTGAAG
B3glct F	CGCTTTCGAGTACCCAGACT
B3glct R	CTTTGCCATCCTCCCAGATA
Slc24a2 F	TGGGCCAACTTTACCGTCG
Slc24a2 R	GGCGATCTTGTGGAGAATTGAAG
Nrros F	ACTGCAGCTTCCCAAGGA
Nrros R	TGGGTACCGAAGCAAGGT

Paper:

PAXX and Xlf interplay revealed by impaired CNS development and immunodeficiency of double KO mice

Introduction

Multitude external and endogenous processes can cause DNA damage during life of all living organisms (Sancar et al., 2004). DNA double strands breaks (DSBs) represents one of the most severe forms of DNA damage. Under physiological condition, DNA DSBs can be induced by the Rag1/2 protein in developing lymphocytes, where the somatic rearrangement of immunoglobulin (Ig) and TCR genes takes place in B and T lymphocytes, respectively. This endogenous physiological process leads to the diversification of the immune system through V(D)J recombination of variable (V), diversity (D), and joining (J) gene segments via a cut-and-paste mechanisms (Bassing et al., 2002). After cleavage, the RAG proteins associate with the broken DNA ends to form a post-cleavage complex (PCC), which is thought to stabilize the broken DNA ends and facilitate end joining activities (Deriano and Roth, 2013; Schatz and Swanson, 2011). Subsequently, the DNA repair is conducted for the end joining to complete V(D)J rearrangement.

In mammalian cells, two main sets of DNA repair mechanisms are used: homologous recombination (HR) and classical non-homologous end joining (C-NHEJ). The former requires a homologous template for precise restoration of DNA sequences and normally exert its repair function in S/G2 cell cycle phase (Orthwein et al., 2015), while the latter (C-NHEJ) directly ligates DSBs without homologies, but with a loss and gain of nucleotides at the joins. NHEJ functions in DNA repair can occur during all phases of the cell cycle (Lieber, 2010; Lieber et al., 2010).

The core factors required for NHEJ include Ku70, Ku80, DNA Ligase IV, DNA-PKcs (DNA-dependent protein kinase catalytic subunit) and XRCC4 (Ciccia and Elledge, 2010). In addition, several other factors were found to participate in NHEJ, such as Artemis, XLF (Kumar et al., 2014) and PAXX (Paralog of XRCC4 and XLF) (Xing et al., 2015; Ochi et al., 2015; Craxton et al., 2015). In NHEJ of V(D)J rearrangement, Rag1/2 cleavage induces broken DNA ends and activate the ataxia telangiectasia mutated (ATM)-kinase-dependent DNA damage response (DDR) (Helmink and Sleckman, 2012), then the DSBs are recognized and protected by the Ku70/Ku80/DNA-PKcs complex. Artemis participates in processing the DNA ends and finally

the XRCC4/ DNA-Ligase IV/Xlf complex together with PAXX ultimately ligate the ends and reseals the DNA breaks.

Deficiency of these core NHEJ factors results in immunodeficiency in patients and animal models due to the impaired repair of DNA breaks, which leads to blocked lymphocyte development at the early progenitor stage (Blunt et al., 1995; Deriano and Roth, 2013; Revy et al., 2005). In addition, in peripheral lymphoid organs, class switch recombination (CSR) in antigen activated B cells in GC also requires NHEJ core factors to repair the broken DNA ends induced by AID. Thus, loss of any core NHEJ factor, leads to increased NDA DSBs and reduces CSR efficiency (Franco et al., 2006; Boboila et al., 2010).

Furthermore, NHEJ plays important role in post-mitotic neurons survival in the central nervous system (CNS). Loss of core NHEJ factors results in neuronal apoptosis which can lead to embryonic lethality in *Lig4* or *XRCC*4 -deficient mice (Frank et al., 2000; Gao et al., 1998; Buck et al., 2006).

In contrast, although *Xlf* is an important NHEJ factor, *Xlf* deficiency mice showed a mild phenotype in growth, immune system and CNS (Li et al., 2008; Ahnesorg et al., 2006). In lymphocyte development, the V(D)J recombination of $Xlf^{-/-}$ B lymphocytes is normal, suggesting that there might be other mechanisms to compensate the loss of XLF.

Recently, another NHEJ factor, *Paxx* (also known as *XLS*), has been identified independently by three laboratories (Xing et al., 2015; Ochi et al., 2015; Craxton et al., 2015). *Paxx* belongs to the XRCC4 superfamily and shows structural similarities with both XRCC4 and XLF factor. However, PAXX does not directly interact with either XLF or XRCC4 (Xing et al., 2015; Ochi et al., 2015), instead, PAXX is recruited to DNA DSBs and interact with Ku/DNA-PKcs complex through binding to Ku70 (Craxton et al., 2015). However, similar to $Xlf^{-/-}$ mice, $Paxx^{-/-}$ mice are viable, grow normally, are fertile, and do not show severely impaired lymphocyte development (Kumar et al., 2014; Lescale et al., 2016). This suggests a possible functional complementation of PAXX deficiency in certain conditions.

However, *Paxx/Xlf* double-knockout mice display embryonic lethality associated with genomic instability, neuron apoptosis in the CNS, and an almost complete block in lymphopoiesis (Balmus et al., 2016; Kumar et al., 2014; Lescale et al., 2016). Thus, combined loss of *Paxx* and *Xlf* plays crucial role in NHEJ and *Paxx* provides core NHEJ factor functions in the absence of *Xlf* and vice versa.

In this work, we analyzed the role of *Paxx* during mouse development and investigate the impact of *Paxx* and *Xlf* double deficiency on the CNS and lymphopoiesis. The results showed that mice with *Xlf* or *Paxx* loss of function are viable and present with very mild immune phenotypes, although their lymphoid cells are more sensitive to ionizing radiation compared to the wt cells, showing these two factors have a role in NHEJ. In contrast, mice defective for both *Xlf* and *Paxx* are embryonically lethal owing to a massive apoptosis of post-mitotic neurons, a phenotype similar to XRCC4 or DNA Ligase IV KO mice. The lymphopoiesis in E18.5 embryos of $Paxx^{-/-}Xlf^{-/-}$ is severely blocked at the stage of IgH and TCRβ gene rearrangements in B and T lymphocyte, respectively. This phenotype highlights the functional links between *Xlf* and *Paxx*, which is critical for the completion of NHEJ-dependent mechanisms during mouse development.

Reference

Ahnesorg, P., Smith, P., and Jackson, S. P. (2006). XLF interacts with the XRCC4-DNA ligase IV complex to promote DNA nonhomologous end-joining. Cell *124(2)*, 301-313.

Balmus, G., Barros, A. C., Wijnhoven, P. W., Lescale, C., Hasse, H. L., Boroviak, K., le Sage, C., Doe, B., Speak, A. O., Galli, A., Jacobsen, M., Deriano, L., Adams, D. J., Blackford, A. N., and Jackson, S. P. (2016). Synthetic lethality between PAXX and XLF in mammalian development. Genes Dev *30(19)*, 2152-2157.

Bassing, C. H., Swat, W., and Alt, F. W. (2002). The mechanism and regulation of chromosomal V(D)J recombination. Cell *109 Suppl*, S45-55.

Blunt, T., Finnie, N. J., Taccioli, G. E., Smith, G. C., Demengeot, J., Gottlieb, T. M., Mizuta, R., Varghese, A. J., Alt, F. W., Jeggo, P. A., and Jackson, S. P. (1995). Defective DNA-dependent protein kinase activity is linked to V(D)J recombination and DNA repair defects associated with the murine scid mutation. Cell *80(5)*, 813-823.

Boboila, C., Jankovic, M., Yan, C. T., Wang, J. H., Wesemann, D. R., Zhang, T., Fazeli, A., Feldman, L., Nussenzweig, A., Nussenzweig, M., and Alt, F. W. (2010). Alternative end-joining catalyzes robust IgH locus deletions and translocations in the combined absence of ligase 4 and Ku70. Proc Natl Acad Sci U S A *107(7)*, 3034-3039.

Buck, D., Moshous, D., de Chasseval, R., Ma, Y., le Deist, F., Cavazzana-Calvo, M., Fischer, A., Casanova, J. L., Lieber, M. R., and de Villartay, J. P. (2006). Severe combined immunodeficiency and microcephaly in siblings with hypomorphic mutations in DNA ligase IV. Eur J Immunol *36(1)*, 224-235.

Ciccia, A., and Elledge, S. J. (2010). The DNA damage response: making it safe to play with knives. Mol Cell *40(2)*, 179-204.

Craxton, A., Somers, J., Munnur, D., Jukes-Jones, R., Cain, K., and Malewicz, M. (2015). XLS (c9orf142) is a new component of mammalian DNA double-stranded break repair. Cell Death Differ *22(6)*, 890-897.

Deriano, L., and Roth, D. B. (2013). Modernizing the nonhomologous end-joining repertoire: alternative and classical NHEJ share the stage. Annu Rev Genet *47*, 433-455.

Franco, S., Gostissa, M., Zha, S., Lombard, D. B., Murphy, M. M., Zarrin, A. A., Yan, C., Tepsuporn, S., Morales, J. C., Adams, M. M., Lou, Z., Bassing, C. H., Manis, J. P., Chen, J., Carpenter, P. B., and Alt, F. W. (2006). H2AX prevents DNA breaks from progressing to chromosome breaks and translocations. Mol Cell *21(2)*, 201-214.

Frank, K. M., Sharpless, N. E., Gao, Y., Sekiguchi, J. M., Ferguson, D. O., Zhu, C., Manis, J. P., Horner, J., DePinho, R. A., and Alt, F. W. (2000). DNA ligase IV deficiency in mice leads to defective neurogenesis and embryonic lethality via the p53 pathway. Mol Cell *5(6)*, 993-1002.

Gao, Y., Chaudhuri, J., Zhu, C., Davidson, L., Weaver, D. T., and Alt, F. W. (1998). A targeted DNA-PKcs-null mutation reveals DNA-PK-independent functions for KU in V(D)J recombination. Immunity *9(3)*, 367-376.

Helmink, B. A., and Sleckman, B. P. (2012). The response to and repair of RAG-mediated DNA double-strand breaks. Annu Rev Immunol *30*, 175-202.

Kumar, V., Alt, F. W., and Oksenych, V. (2014). Functional overlaps between XLF and the ATM-dependent DNA double strand break response. DNA Repair (Amst) *16*, 11-22.

Lescale, C., Abramowski, V., Bedora-Faure, M., Murigneux, V., Vera, G., Roth, D. B., Revy, P., de Villartay, J. P., and Deriano, L. (2016). RAG2 and XLF/Cernunnos interplay reveals a novel role for the RAG complex in DNA repair. Nat Commun *7*, 10529.

Li, G., Alt, F. W., Cheng, H. L., Brush, J. W., Goff, P. H., Murphy, M. M., Franco, S., Zhang, Y., and Zha, S. (2008). Lymphocyte-specific compensation for XLF/cernunnos end-joining functions in V(D)J recombination. Mol Cell *31(5)*, 631-640.

Lieber, M. R. (2010). The mechanism of double-strand DNA break repair by the nonhomologous DNA end-joining pathway. Annu Rev Biochem *79*, 181-211.

Lieber, M. R., Gu, J., Lu, H., Shimazaki, N., and Tsai, A. G. (2010). Nonhomologous DNA end joining (NHEJ) and chromosomal translocations in humans. Subcell Biochem *50*, 279-296.

Ochi, T., Blackford, A. N., Coates, J., Jhujh, S., Mehmood, S., Tamura, N., Travers, J., Wu, Q., Draviam, V. M., Robinson, C. V., Blundell, T. L., and Jackson, S. P. (2015). DNA repair. PAXX, a paralog of XRCC4 and XLF, interacts with Ku to promote DNA double-strand break repair. Science *347(6218)*, 185-188.

Orthwein, A., Noordermeer, S. M., Wilson, M. D., Landry, S., Enchev, R. I., Sherker, A., Munro, M., Pinder, J., Salsman, J., Dellaire, G., Xia, B., Peter, M., and Durocher, D. (2015). A mechanism for the suppression of homologous recombination in G1 cells. Nature *528(7582)*, 422-426.

Revy, P., Buck, D., le Deist, F., and de Villartay, J. P. (2005). The repair of DNA damages/modifications during the maturation of the immune system: lessons from human primary immunodeficiency disorders and animal models. Adv Immunol *87*, 237-295.

Sancar, A., Lindsey-Boltz, L. A., Unsal-Kaçmaz, K., and Linn, S. (2004). Molecular mechanisms of mammalian DNA repair and the DNA damage checkpoints. Annu Rev Biochem *73*, 39-85.

Schatz, D. G., and Swanson, P. C. (2011). V(D)J recombination: mechanisms of initiation. Annu Rev Genet *45*, 167-202.

Xing, M., Yang, M., Huo, W., Feng, F., Wei, L., Jiang, W., Ning, S., Yan, Z., Li, W., Wang, Q., Hou, M., Dong, C., Guo, R., Gao, G., Ji, J., Zha, S., Lan, L., Liang, H., and Xu, D. (2015). Interactome analysis identifies a new paralogue of XRCC4 in non-homologous end joining DNA repair pathway. Nat Commun *6*, 6233.

Cell Death and Differentiation (2018) 25, 444–452
 1350-9047/18

www.nature.com/cdd

PAXX and Xlf interplay revealed by impaired CNS development and immunodeficiency of double KO mice

Vincent Abramowski[1,7], Olivier Etienne[2,7], Ramy Elsaid[3,4,5,7], Junjie Yang[3,4,5,7], Aurélie Berland[1], Laetitia Kermasson[1], Benoit Roch[1], Stefania Musilli[1], Jean-Paul Moussu[6], Karelia Lipson-Ruffert[6], Patrick Revy[1], Ana Cumano[3,4,5], François D Boussin[2] and Jean-Pierre de Villartay*[,1]

The repair of DNA double-stranded breaks (DNAdsb) through non-homologous end joining (NHEJ) is a prerequisite for the proper development of the central nervous system and the adaptive immune system. Yet, mice with Xlf or PAXX loss of function are viable and present with very mild immune phenotypes, although their lymphoid cells are sensitive to ionizing radiation attesting for the role of these factors in NHEJ. In contrast, we show here that mice defective for both Xlf and PAXX are embryonically lethal owing to a massive apoptosis of post-mitotic neurons, a situation reminiscent to XRCC4 or DNA Ligase IV KO conditions. The development of the adaptive immune system in Xlf$^{-/-}$PAXX$^{-/-}$ E18.5 embryos is severely affected with the block of B- and T-cell maturation at the stage of IgH and TCRβ gene rearrangements, respectively. This damaging phenotype highlights the functional nexus between Xlf and PAXX, which is critical for the completion of NHEJ-dependent mechanisms during mouse development.
Cell Death and Differentiation (2018) **25,** 444–452; doi:10.1038/cdd.2017.184; published online 27 October 2017

All living organisms are subjected to multitude sources of DNA damage during their lifespan, either as a result of external assault or endogenous physiological processes.[1] Among endogenous sources of physiological DNAdsb is the somatic rearrangement of immunoglobulin (Ig) and TCR genes in B and T lymphocytes, respectively, during the diversification of the adaptive immune system through V(D)J recombination.[2] DNA double-stranded breaks (DNAdsb) are considered the most toxic lesions. DNAdsbs are repaired by two main mechanisms: the homologous recombination (HR) in cycling cells, when a sister chromatid is available as DNA repair template, and the non-homologous end joining (NHEJ) during all phases of the cell cycle.

NHEJ proceeds via the simple religation of DNA ends without the need for a repair template.[3] Briefly, the NHEJ is composed of seven core factors comprising the Ku70/80/DNA-PKcs (DNA-dependent protein kinase catalytic subunit) complex, which recognizes and protects the broken DNA ends, the Artemis endo/exonuclease, which participates, when needed, in processing the DNA ends and the XRCC4/DNA-Ligase IV/Xlf complex, which ultimately reseals the DNA break. The critical function of the NHEJ apparatus in various aspects of higher eukaryote development has been extensively perceived in several animal and human pathological conditions. As emblematic examples, loss of function of either XRCC4 or DNA ligase IV results in embryonic lethality in mice[4,5] and mutations in Artemis or DNA-PKcs result in severe combined immunodeficiency conditions in both men and mice, owing to aborted V(D)J recombination.[6] In addition, defects in NHEJ results in genetic instability and the propensity to develop various types of cancers, notably leukemia and lymphomas.[7]

Recently, a new DNA repair factor, PAXX (PAralog of XRCC4 and Xlf, also known as C9orf142 or XLS), has been identified independently by three laboratories based on bioinformatics and biochemistry approaches.[8–10] PAXX belongs to the XRCC4 superfamily and shows structural similarities with both XRCC4 and Xlf. PAXX is recruited to DNAdsb and is a physical interactor of the Ku/DNAPK complex, notably through its interaction with Ku70.[11] Surprisingly, for a NHEJ factor, the deficiency of PAXX does not systematically result in an increased sensitivity to ionizing radiation (IR) and the results of the various DNA repair assays are highly controversial, depending on the experimental settings.[8–10,12–15] This suggested a possible functional complementation of PAXX deficiency in certain conditions.

To analyze the role of PAXX during mouse development *in vivo* and identify a possible redundant function with another DNA repair factor, we created CRISPR/Cas9 PAXX mutant mouse lines. Although the sole inactivation of PAXX did not result in an overwhelming phenotype, the concomitant deletion of PAXX and Xlf had severe consequences resulting in embryonic lethality and arrest of V(D)J recombination in embryos. Altogether, these results are consistent with PAXX being a *bona fide* NHEJ factor and highlight the critical functional interplay between PAXX and Xlf during mouse development.

[1]Laboratory "Genome Dynamics in the Immune System", INSERM UMR1163, Université Paris Descartes Sorbonne Paris Cité, Institut Imagine, Paris, France; [2]Laboratoire de Radiopathologie, UMR 967, DRF, CEA-INSERM-Université Paris Diderot-Université Paris Sud, Fontenay-aux-Roses, Paris, France; [3]Lymphopoiesis Unit, Department of Immunology, Institut Pasteur, Paris, France; [4]University Paris Diderot, Sorbonne Paris Cité, Cellule Pasteur, Paris, France; [5]INSERM U1223, Paris, France and [6]SEAT-TAAM CNRS Phenomin UPS44, Villejuif, France

*Corresponding author: Dr J-P de Villartay, Laboratory "Genome Dynamics in the Immune System", INSERM UMR1163, Equipe Labellisée Ligue Contre le Cancer Institut Imagine, 24 bd du Montparnasse, 75015 Paris, France. Tel: +33 1 42 75 42 93; E-mail: devillartay@gmail.com

[7]These authors contributed equally to this work

Received 03.7.17; revised 19.9.17; accepted 21.9.17; Edited by H-U Simon; published online 27.10.17

Results and discussion

Generation of PAXX KO mice. PAXX KO mice were generated using CRISPR/Cas9. Two guide RNA target sequences were selected in exon 1 (PAXX1) and exon 2 (PAXX2) of the murine *PAXX* gene (Figure 1a and Supplementary Figure S1A). The efficacy of the two gRNA was scored through the disappearance of restriction sites *Bsr*BI and *Sac*I upon transfection of MEFs with the pX330 vector expressing the gRNAs and Cas9 (Supplementary Figure S1B). To generate mutant mouse lines, zygotes were microinjected with pX330 according to the protocol of Mashiko *et al*.[16] Thirteen and five F0 mice were obtained for PAXX1 and PAXX2, respectively. Tail DNA was analyzed by PCR and restriction digest (PCR-RE) to identify four PAXX1 and two PAXX2 F0 mutant mice showing clear retention of undigested DNA above background (Supplementary Figure S1C). F0 mice were crossed onto C57Bl/6 to segregate the various CRISPR/Cas9-generated mutant alleles. Two F0-derived F1 mice, #2 for PAXX1 and #14 were selected upon direct DNA sequencing of the mutant alleles. CRISPR/Cas9 mutagenesis resulted in an 8-bp deletion and subsequent frameshift in both cases (Figure 1a). Each line was backcrossed up to six times on C57Bl/6 to segregate away any off-target event outside of chromosome 2. Homozygous mutant mice were obtained by intercross of either PAXX1$^{+/-}$ or PAXX2$^{+/-}$ heterozygous founders. Homozygous mice were viable and were produced at Mendelian frequencies ruling out a major effect of PAXX deficiency during embryogenesis. The loss of function of the CRISPR/Cas9-generated PAXX mutant allele were ascertained by western blotting using protein extracts from thymus, spleen, and MEFs from PAXX2 mouse line. As shown in Figure 1b, PAXX protein expression was undetectable in PAXX2$^{-/-}$ mice, in contrast to wild-type littermates. We conclude that CRISPR/Cas9 mutagenesis resulted in complete PAXX loss of function.

Normal development of the immune system in PAXX KO mice. Proficiency of the DNA Damage Response (DDR) machinery, in particular the NHEJ pathway, is critical for the appropriate development of B and T lymphocytes, owing to the generation of DNAdsb during the somatic DNA rearrangement of both Ig and TCR genes.[6] Nevertheless, Xlf deficiency does not have a severe impact on the V(D)J recombination process and Xlf-deficient mice present with a very mild defect in their immune system, characterized mainly by a slight reduction in lymphocyte numbers and an

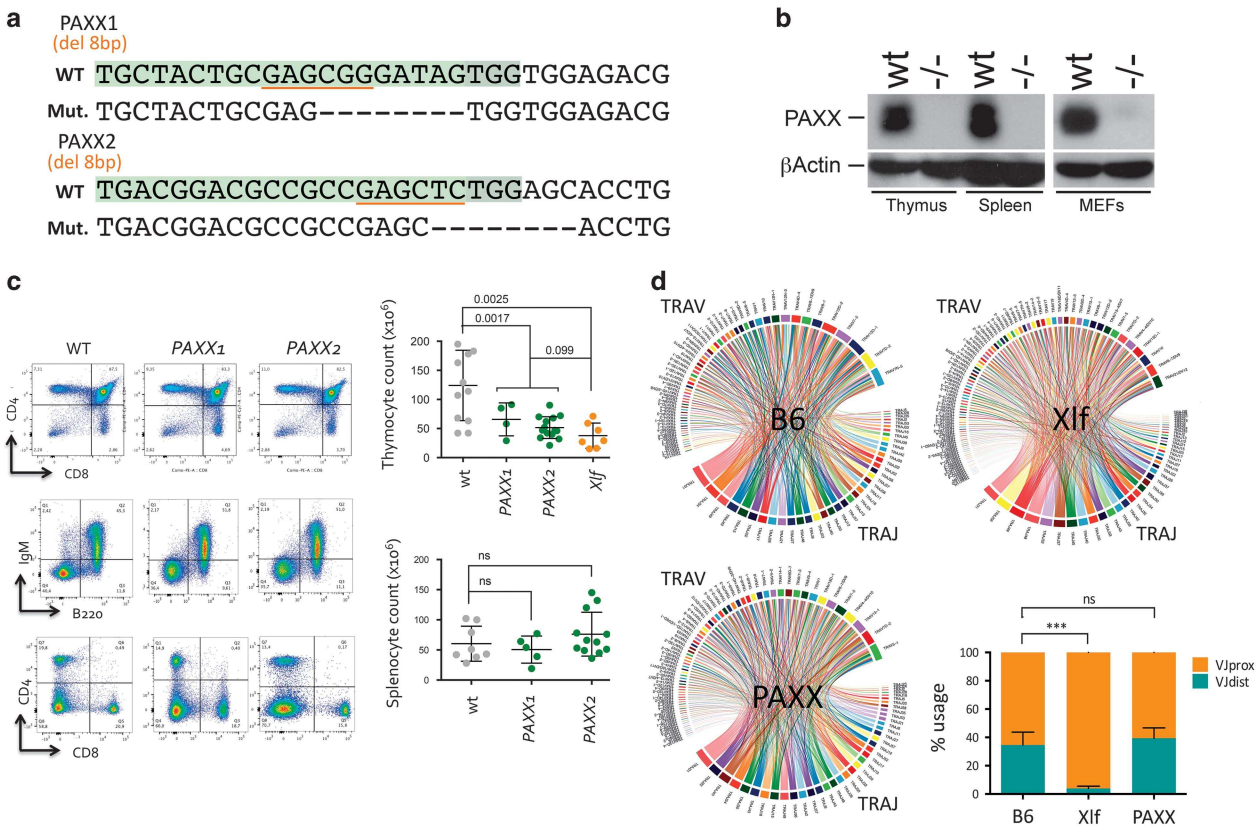

Figure 1 Design and immunophenotyping of PAXX KO mice. (**a**) Design of gRNA used to create CRISPR/Cas9 mutations in the *PAXX* gene. The *Bsr*BI and *Sac*I restriction enzyme sites used to screen for mutagenesis are underlined. The two lines PAXX1 and PAXX2 harbor an 8-bp deletion resulting in frameshift. (**b**) Western blot analysis confirming the PAXX loss of function in PAXX2 mutant mice, with the absent protein in the thymus, spleen, and MEFs. (**c**) Immunophenotyping of wt. ($N=11$), PAXX1 ($N=4$), PAXX2 ($N=12$), and Xlf ($N=7$) mice. FACS representation of thymocytes and splenocytes and representation of absolute count numbers. (**d**) Illustrative Circos-plot representations of TCRα repertoire in thymocytes from C57Bl/6, Xlf, and PAXX2 mice. Each chord line represents the association between one TRAV and one TRAJ segment as determined by TCRα transcript sequencing. Quantification of TCRα TRAV gene usage in C57Bl/6, Xlf, and PAXX2 mice. TCRα repertoire determination was repeated two times using an overall six PAXX2 KO, five C57Bl/6, and six Xlf KO mice. Statistical analyses were performed using Mann–Whitney non-parametric *t*-test using Prism v6 (***$P < 0.001$)

increased in thymocyte apoptosis.[17,18] Qualitatively, this translates into a skewing in the TCR*α* repertoire with the under-representation of distal TRAV and TRAJ gene segments.[17] Analysis of the immune system in both PAXX1 and PAXX2 KO mice revealed an overall normal development of T cells in the thymus, despite a statistically significant reduction in thymocyte numbers in the range of what observed in Xlf mice (Figure 1c). Mature B- and T-cell numbers in the spleen were comparable between PAXX mice and WT littermates. This is in general agreement with previously described PAXX mutant mice.[12,15] Analysis of the TCR*α* repertoire through 5' RACE RT-PCR and next-generation sequencing revealed a well-diversified TCR*α* repertoire in PAXX mice, comparable to WT and Xlf animals (Figure 1d). However, in contrast to the important decrease in distal V*α*J*α* usage in Xlf thymocytes as previously described,[17] thymocytes from PAXX mice did not show any skewing in the representation of these TCR*α* gene segments.

From these observations, we conclude that PAXX loss of function does not have any detrimental impact on the V(D)J recombination process and/or the overall viability of thymocytes.

DNAdsb repair defect in PAXX KO mice. Given its homology with both XRCC4 and Xlf, PAXX is thought to intervene during DNA repair through NHEJ.[8–10] T lymphocytes isolated from blood or spleen are mainly non-cycling resting cells which, as a result, utilize NHEJ to cope with DNAdsb when HR is operational only in cycling cells. We set up to analyze the role of PAXX during NHEJ through the survey of splenic T-cell sensitivity to IRs (Figure 2a). *Ex vivo* isolated resting splenic mature T cells were subjected to various doses of IR (0–4 Gy). After 4 h of recovery to allow for repair of IR-induced DNAdsb, cells were incubated with anti-CD3/anti-CD28-coated beads during 4 days, which activates and induces a strong proliferative response of T lymphocytes

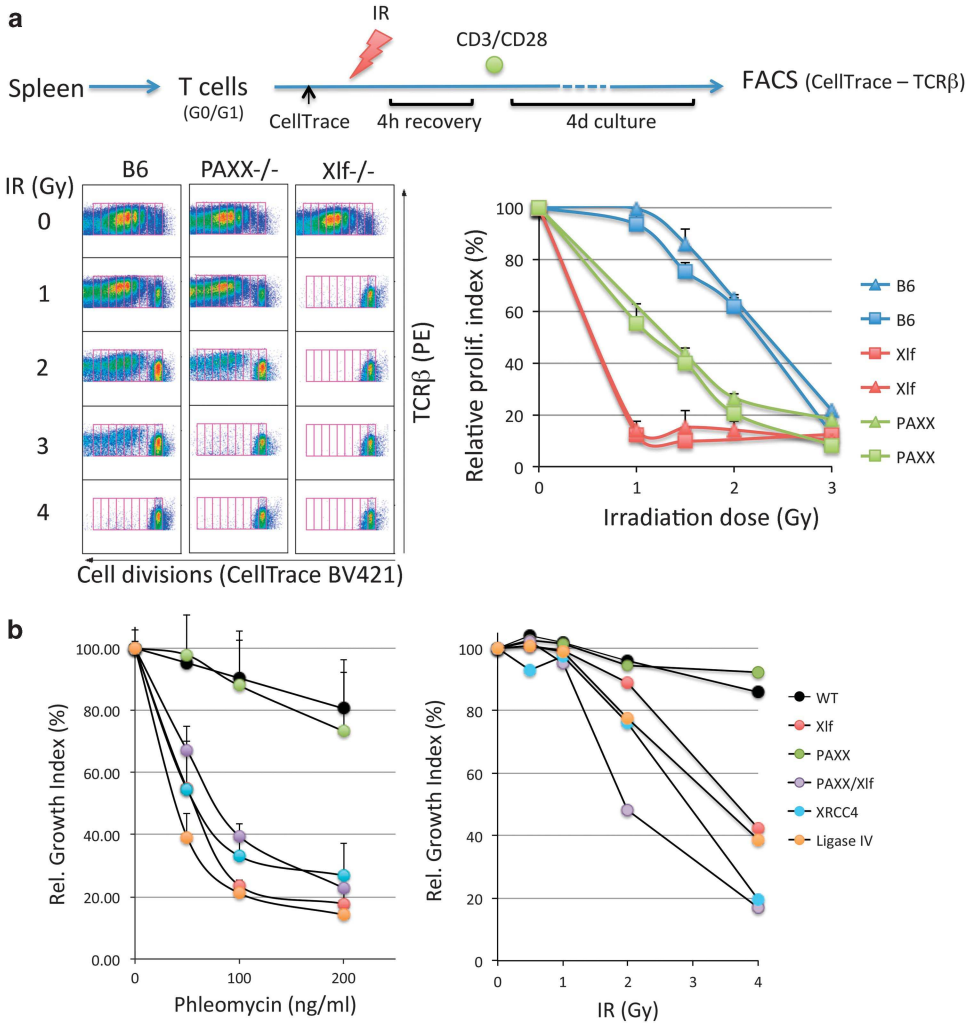

Figure 2 DNA repair defect in PAXX KO mice. (**a**) Radiosensitivity assay performed on mature splenic T lymphocytes. For FACS analysis, doubling populations were scored in gates defined by the dilution of the CellTrace signal and the proliferative index calculated according to Roederer.[26] The relative proliferative indexes were plotted for each sample according to the proliferation in the absence of IR and used to define the radiosensitivity level. The experiment was repeated twice with two mice per genotype each time. (**b**) Phleomycin and IR sensitivity on SV40-transformed MEFs. MEFs from XRCC4, DNA-Ligase IV, and Xlf KO mice were used as radiosensitive controls. The relative growth indexes were calculated by comparing the confluence of treated cells and non-treated cells during culture with real-time Incucyte monitoring (see Materials and Methods). This experiment was repeated three times

that can be readily quantified through the dilution of the CellTrace dye upon cell divisions. We used this readout as a mean to score the relative index of proliferation, and hence the cell survival, following IR. Using this protocol, T cells from Xlf mice showed an extreme sensitivity to IR as compared with WT (Figure 2a) with a fall in cell survival already at the first dose of 1 Gy, as expected for Xlf deficiency. PAXX-deficient T lymphocytes were also strikingly radiosensitive, although to a lesser extent than Xlf-defective T cells. In contrast, murine embryonic fibroblasts (MEFs) derived from PAXX mutants were resistant to either IR or the DNAdsb inducer Phleomycin with cell survival comparable to that of WT MEFs (Figure 2b), whereas MEFs defective for XRCC4, DNA-Ligase IV, or Xlf were highly sensitive as expected. This is in accord with the previously noted mild sensitivity of $PAXX^{-/-}$ MEFs to IR[15] but contrasts with the results from Balmus *et al*.[12] Ever since the identification of PAXX by three different groups, its implication in the DDR as judged by the sensitivity to genotoxic drugs or IR has been highly controversial, depending on the cell line analyzed *in vitro*, the experimental conditions, and the drugs used to inflict DNA damage.[8–10] Interestingly, asynchronous PAXX-defective CH12 B-cell lines or v-Abl-transformed Pro-B-cell lines do not demonstrate any IR sensitivity above that of their wt counterparts, as we found in MEFs, and the concomitant PAXX and Xlf deficiency does not worsen the sensitivity caused by Xlf mutation alone in these cycling cells.[13] In contrast, the synchronization of $PAXX^{-/-}/Xlf^{-/-}$ v-Abl pro-B cells into the G1 phase of the cell cycle with either STI-571 (v-Abl kinase inhibitor) or PD033991 (CDK4/6 inhibitor) results in an extreme sensitivity to IR, well beyond that of $Xlf^{-/-}$ single mutants in the same conditions arguing for a unique role of PAXX in classical NHEJ when DNA damage occurs in G1, hence in the absence of functional HR. Our observation of an IR sensitivity of small resting, *ex vivo* purified T lymphocytes from $PAXX^{-/-}$ mice concords with this conclusion of a specific role of PAXX during C-NHEJ.

PAXX-Xlf interplay during neuronal development. We next set up to evaluate the possible functional relationship between PAXX and Xlf during the DNA damage response (DDR) by generating doubly deficient mice through intercrossing either $PAXX^{-/-}Xlf^{+/-}$ or $PAXX^{+/-}Xlf^{-/-}$ animals. In no instance did we obtain $PAXX^{-/-}/Xlf^{-/-}$ mice on a total of 176 newborns (44 PAXX1 and 132 PAXX2) obtained from crosses of various genotype combinations for which about 31 (11 PAXX1 and 20 PAXX2) were expected to harbor the $PAXX^{-/-}/Xlf^{-/-}$ DKO genotype, arguing for an embryonic lethality of the concomitant inactivation of both factors (Figure 3a) as previously noted in two different studies.[12,15] The embryonic lethality was observed with both PAXX1 and PAXX2 mutant lines, excluding an off-target effect as responsible for this phenotype. Lived DKO embryos could be readily obtained in E18.5 mice downward (Figure 3b) arguing for a late embryonic lethality of DKO animals, similar to the previously described late embryonic lethality of XRCC4 and DNA Ligase IV KO mice.[4,5] Nevertheless, embryos at E18.5 usually appeared smaller than their heterozygous littermates (Figure 3b), confirming their overall abnormal development. The lethality of PAXX/Xlf DKO embryos was to us the first evidence of a functional interplay between PAXX and Xlf, the co-inactivation of which results in a major viability phenotype, when both single mutants do not present evidence for developmental defect (this study and Vera *et al*.[17]). In XRCC4 and DNA-Ligase IV KO mice, the embryonic lethality is caused by the massive apoptosis of post-mitotic neurons.[4,5] Likewise, the presence of numerous pyknotic nuclei and the cleaved-caspase 3 (CC3) immunostaining[19] revealed a severe neuronal apoptosis in the brain of $Xlf^{-/-}PAXX^{-/-}$ embryos (Figures 3c–e, Supplementary Figure S3) as previously reported.[12,15] This contrasted with the scarce apoptotic cells in the brains of $Xlf^{-/-}$ embryos and their absence in that of $PAXX^{-/-}$ embryos (Figures 3c–e, and Supplementary Figure S3A). The observation of a massive neuronal apoptosis in $PAXX^{-/-}Xlf^{-/-}$ DKO whatever the type of PAXX1 or PAXX2 mutants used in intercrosses again ruled out a CRISPR/Cas9 off-target effect as responsible for this phenotype. Although apoptosis was detected in the regions where neural progenitors proliferate (that is, the ventricular (VZ) and subventricular zones (SVZ), surrounding the lateral hemispheres), it was most prominent in the regions that contain post-mitotic neurons. Indeed, consistent with the kinetics of neuronal production in the different brain structures, apoptosis was predominantly found in the ventral telencephalon at E12.5 (Figure 3a) and in the dorsal telencephalon at E15.5 (Figures 3b and c and Supplementary Figure S3B).

PAXX-Xlf interplay during lymphoid development. The profound impact of the concomitant deletion of PAXX and Xlf on the development of the central nervous system, resulting in late embryonic lethality, is highly reminiscent of both XRCC4 and DNA Ligase IV-deficient conditions, in which NHEJ is severely affected.[4,5] As a major defect in the development of the immune system is also one typical feature of these NHEJ-deficient murine models, we aimed at analyzing this question qualitatively and quantitatively in $Xlf^{-/-}PAXX^{-/-}$ DKO embryos. TCR gene rearrangements begin around E13 and thymuses are easily recovered at E18.5, the gestation day we choose for this analysis. At E18.5, thymuses from wt mice contained 1.71×10^6 thymocytes on average (Figures 4a and b), a number that was not affected by the deletion of PAXX alone (1.84×10^6) but was significantly reduced around twofold in the context of Xlf KO (0.9×10^6, $P < 0.0001$) as previously found in thymuses from 6- to 8-week-old mutant mice.[17,18] Strikingly, $Xlf^{-/-}PAXX^{-/-}$ embryos exhibited a 10-fold decrease in thymocyte number (1.7×10^5, $P < 0.0001$). This reduction in the total numbers of thymocytes was mainly accounted for by the loss of CD4+ CD8+ double-positive (DP) thymocytes in $Xlf^{-/-}PAXX^{-/-}$ mice when compared with wt mice (7.40×10^3 *versus* 7.75×10^5, $P < 0.0001$), arguing for an abnormal maturation process. CD4 – CD8 – double-negative (DN) thymocytes, which precede the maturation to DP, can be further divided into various populations according to their differential expression of the CD44, CD25, and CD28 surface markers.[20] In particular, the CD44 – CD25+CD28+ (DN3b) fraction represents thymocytes that have undergone β-selection upon successful rearrangement of their TCR-β locus. They will subsequently progress to DN3c, DN4a, and

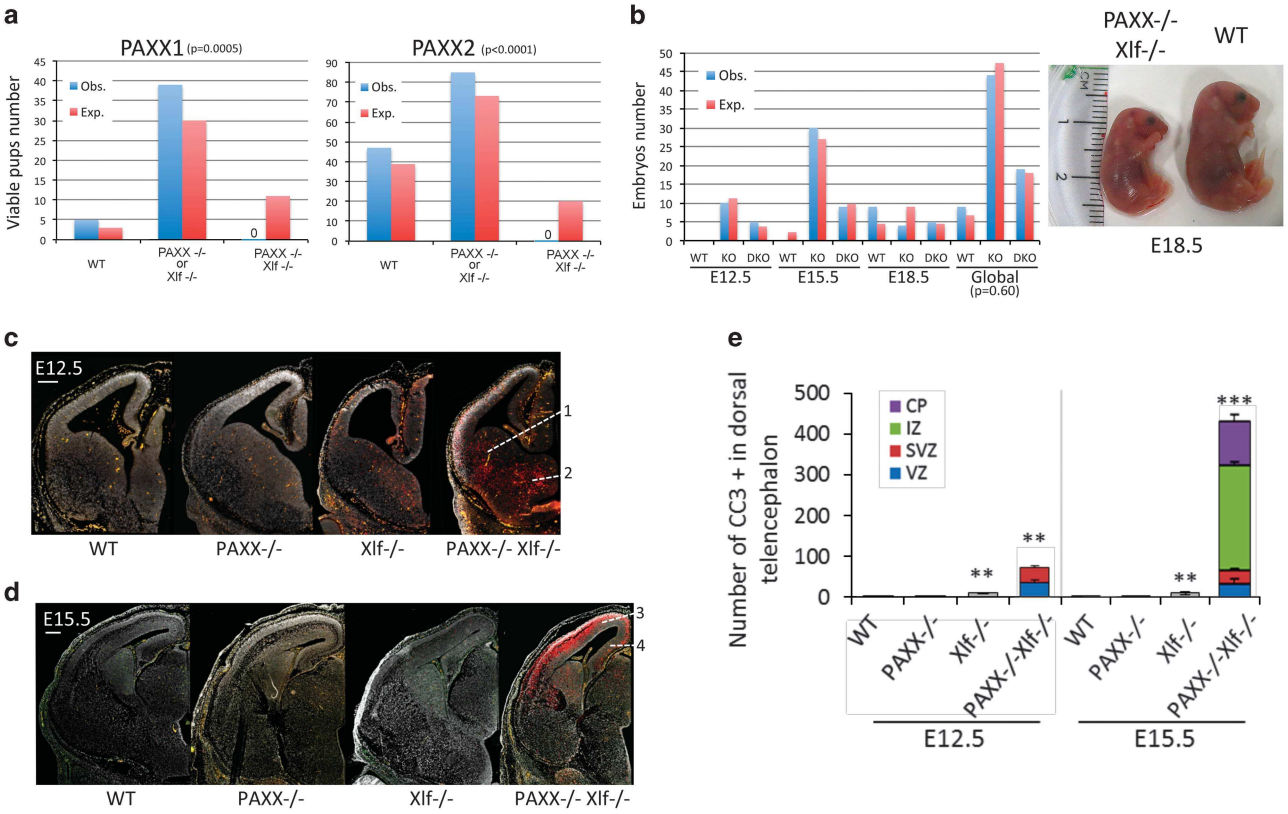

Figure 3 Embryonic lethality and massive neuronal apoptosis in PAXX$^{-/-}$Xlf$^{-/-}$ embryos. (**a**) Impaired development of PAXX$^{-/-}$Xlf$^{-/-}$ DKO mice. No DKO mice were born from various combinations of PAXX1 or PAXX2 and Xlf crosses (44 and 132 pups, respectively). Statistical significance of the differences between the observed (Obs.) and expected (Exp.) genotype distributions was assessed by χ^2-test. (**b**) Survival of PAXX$^{-/-}$Xlf$^{-/-}$ embryos up to E18.5. Photograph showing the reduced size of PAXX$^{-/-}$Xlf$^{-/-}$ E18.5 embryos. (**c** and **d**) Coronal sections of cerebral hemispheres of *wt*., PAXX$^{-/-}$, Xlf$^{-/-}$, and PAXX$^{-/-}$Xlf$^{-/-}$ embryos collected at E12.5 (**c**) and E15.5 (**d**) and stained with 4'-6-Diamidino-2-phenylindole (DAPI; gray) and CC3 (red). Blood vessels are colored in orange. Scale bars: 200 μm. (**c**) At E12.5, apoptosis in PAXX$^{-/-}$Xlf$^{-/-}$ embryos is massively detected in the intermediate zones (IZs) of the ganglionic eminences (1, 2) containing newly generated neurons for the striatum and the globus pallidus. (**d**) At E15.5, apoptosis in PAXX$^{-/-}$Xlf$^{-/-}$ embryos is predominant in the IZ and the cortical plates (CPs) of the dorsal telencephalon containing newly generated post-mitotic neurons of the neocortex (3) and the hippocampus (4). (**e**) The bar graph shows the mean numbers per cortical slice of cleaved-caspase-3-positive cells ± S.D. detected in the ventricular zone (VZ), subventricular zone (SVZ), IZ, and CP of the neocortex of *wt*., PAXX$^{-/-}$, Xlf$^{-/-}$, and PAXX$^{-/-}$Xlf$^{-/-}$ embryos at E12.5 and E15.5. Data have been obtained from at least three embryos per group. Stars indicate the statistical significance in comparison to the *wt* controls. $^{**}P \leq 0.01$, $^{***}P \leq 0.001$; Mann–Whitney test

DN4b, and ultimately to DP as depicted in Figure 4a. Analyses of these archetypical thymocyte populations in Xlf$^{-/-}$PAXX$^{-/-}$ DKO E18.5 embryos revealed a major block at the transition DN3a to DN3b (Figures 4a and b), resulting in a significant decrease in the number of thymocytes from DN3b stage onward when compared with wt mice (1.3×10^4 *versus* 8.3×10^4, $P < 0.0001$). This developmental arrest at the critical step of β-selection strongly suggested a possible impairment of V(D)J recombination at the TCR-β locus in thymocytes from Xlf$^{-/-}$PAXX$^{-/-}$ embryos. TCR-β rearrangements involving Vβ_{10} and the Dβ_2-Jβ_2 cluster were analyzed by PCR in thymocytes from mice with various genotypes as depicted in Figure 4c. Rearrangements of Dβ_2 or Vβ_{10}Dβ_2 segments to Jβ_2 elements resulted in a ladder of PCR products identified by an intronic 3'Jβ_2 probe the length of which depends on the Jβ_2 element utilized during the recombination process. No detectable PCR product corresponding to either Dβ_2Jβ or Vβ_{10}Dβ_2Jβ rearrangements could be detected in DNA from Xlf$^{-/-}$PAXX$^{-/-}$ thymocytes (Figure 4c, lanes 8, 9,16, and 20), although they were readily identified in PAXX and Xlf single KO mice, attesting for the severely impaired V(D)J recombination process in the concomitant absence of PAXX and Xlf.

B-cell maturation in fetus takes place in the fetal liver (FL) with rearrangement and expression of the Ig heavy chain locus occurring around E17.5 at which time μH chain becomes detectable intracellularly.[21] CD19+B220+ B-lineage cells were present in the FL of WT, Xlf$^{-/-}$ and PAXX$^{-/-}$Xlf$^{-/-}$ E18.5 embryos, attesting for the normal B-cell lineage commitment in all conditions (Figure 5a). However, whereas ~20% of CD43+B220+ pro-B cells expressed the intracytoplasmic μH chain (iIgM) in FL of littermates PAXX$^{+/-}$Xlf$^{+/-}$ embryos, this population represented only 5% of the CD43+B220+ population in the PAXX$^{-/-}$Xlf$^{-/-}$ DKO embryos (Figures 5a and b), attesting for a major defect in either rearrangement or expression of the IgH locus in these embryos. Interestingly, a gradient of severity of this phenotype followed the severity of the genotype involved with a statistically significant contribution of Xlf KO on its own (Figure 5b). This could also be noticed in the fetal thymus with the partial block of Xlf$^{-/-}$ thymocytes at the DN3a stage when compared with wt embryos (Figure 4a). As for TCRβ rearrangement in the thymus, we used a PCR approach to analyze the recombination of the IgH locus in

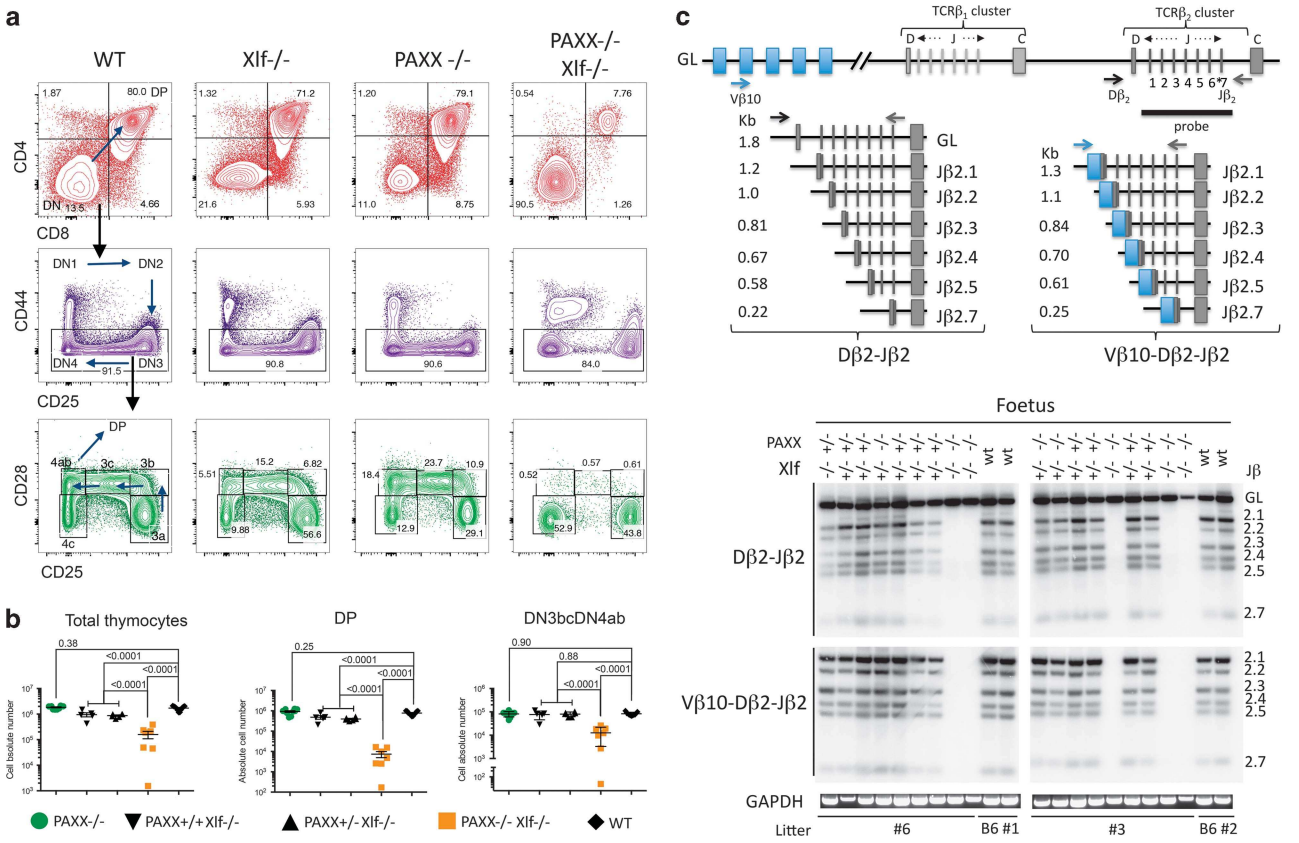

Figure 4 V(D)J recombination defect and impaired development of thymocytes in PAXX$^{-/-}$/Xlf$^{-/-}$ E18.5 embryos. (**a**) Immunostaining of thymocytes from wt, Xlf$^{-/-}$, PAXX$^{-/-}$, and PAXX$^{-/-}$Xlf$^{-/-}$ E18.5 embryos. Upper panel (red) shows the important decrease in CD4^{+}CD8^{+} DP in the thymus from PAXX$^{-/-}$Xlf$^{-/-}$ embryos. DN (CD4^{-}CD8^{-}CD3^{-}) thymocytes were subdivided into DN1–DN4 according to the expression of CD44 and CD25 (middle panel). Lower panel (green) shows the severe block at the transition DN3a (CD44^{-}CD25^{+}CD28^{-}) to DN3b (CD44^{-}CD25^{+}CD28^{+}) in PAXX$^{-/-}$Xlf$^{-/-}$ embryos. B220^{+}CD19^{+} FL cells were analyzed for the expression of CD43 that marks pro-B cells (middle panel). In the lower panel, cells were gated on the CD43^{+}B220^{+}CD19^{+} population and analyzed for iIgM expression. (**b**) Quantification of thymocyte subpopulations in the various PAXX/Xlf genotypes. Mann–Whitney test was used for statistical analysis. (**c**) PCR strategy to analyze TCRβ rearrangement according to Gartner *et al.*[29] and autoradiogram of PCR products revealed with the TCR-Jβ probe demonstrating the absence of either Dβ-Jβ or VβDJβ rearrangements in thymocytes from PAXX$^{-/-}$Xlf$^{-/-}$ embryos. GAPDH-specific PCR was used as loading control

B-commited cell within the FL. This analysis clearly demonstrated an almost complete absence of detectable VH–DJH rearrangement in FL from PAXX$^{-/-}$Xlf$^{-/-}$ embryos (Figure 5c, lanes 9, 10, and 11) in contrast to wt animals. Interestingly, all embryos carrying the Xlf$^{-/-}$ genotype already demonstrated a decrease in V(D)J recombination efficiency, as judged by the decreased signal intensity of the PCR products, in line with the fall in IgM-expressing pro-B cells in these animals.

Our observations of an impaired V(D)J recombination *in vivo* in both B- and T-cell lineages in PAXX$^{-/-}$Xlf$^{-/-}$ E18.5 embryos are in agreement with the reports of a similar malfunction in v-Abl-transformed pro-B-cell lines *in vitro* using chromosome-integrated V(D)J recombination substrates.[13–15,22] Altogether, these experiments demonstrate that, although Xlf and PAXX are largely dispensable for V(D)J recombination, their concomitant defect sharply impairs the rearrangement of the TCRβ and IgH loci in T- and B-cell lineages, respectively, resulting in the block of their maturation in the thymus and the FL. This is consistent with the single ever born PAXX$^{-/-}$Xlf$^{-/-}$ mouse that had no thymus and had a microspleen.[12] We anticipate that the conditional ablation of these two genes in the hematopoietic system to bypass the embryonic lethality should result in live animals with a severe combined immunodeficiency phenotype characterized by the absence of mature B and T lymphocytes.

We identified here a robust functional interplay *in vivo* between the two DNA repair factor paralogs Xlf and PAXX, as evidenced by the synthetic lethality of their concomitant defect owing to a massive apoptosis of post-mitotic neurons and the negative impact on V(D)J recombination in immature B and T lymphocytes. In that sense, PAXX$^{-/-}$Xlf$^{-/-}$ DKO mice share most of the phenotypic characteristics of XRCC4 and DNA-Ligase IV single-mutant mice. The survival of post-mitotic neurons and the development of the adaptive immune system both rely on efficient NHEJ as demonstrated in several animal models and human conditions.[6] The impairment of these two functions specifically in PAXX$^{-/-}$Xlf$^{-/-}$ animals, therefore, confirms the role of PAXX as a *bona fide* NHEJ factor. Others and we have previously reported that Xlf, like PAXX, is largely dispensable during V(D)J recombination.[17,18] We have recently highlighted the relationship between RAG2 and Xlf as a mean to provide a two-tier mechanism ensuring the proper repair of DNAdsb generated during V(D)J recombination and, hence to avoid genetic instability.[14] A similar functional interaction between PAXX and Xlf can be proposed to account for the unaffected V(D)J recombination in PAXX$^{-/-}$ mice as

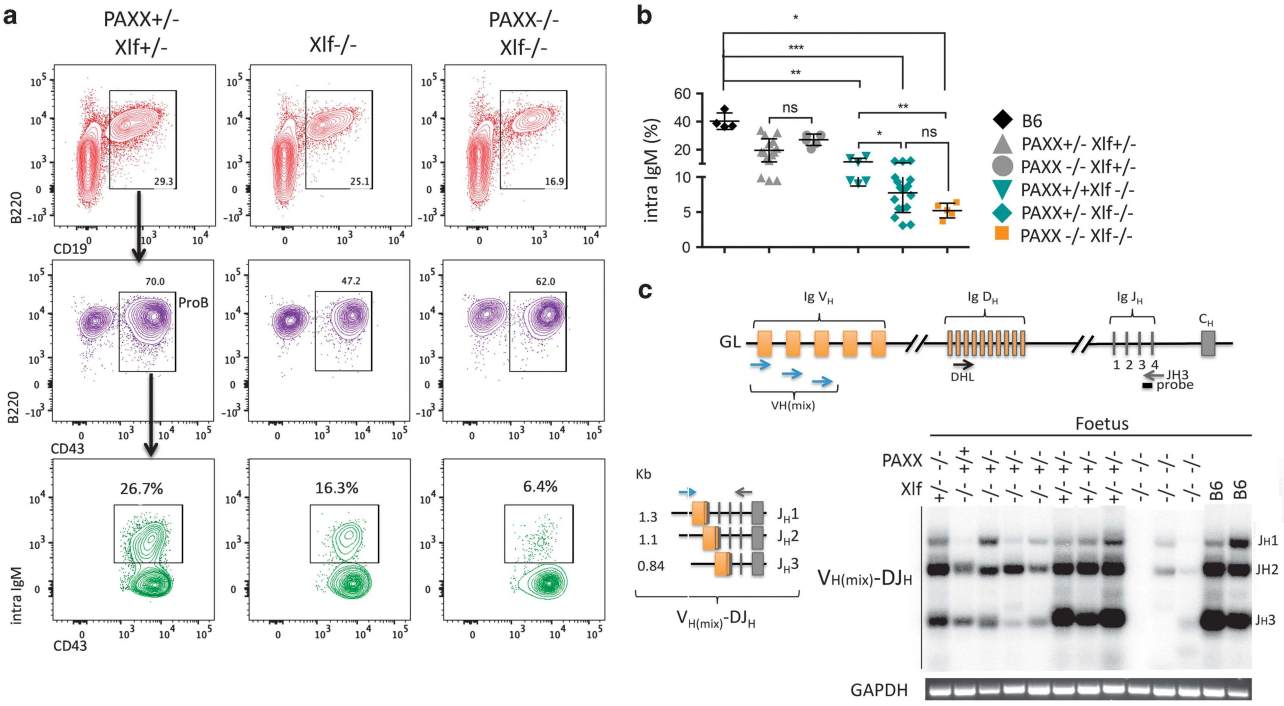

Figure 5 V(D)J recombination defect and impaired B-cell development in PAXX$^{-/-}$/Xlf$^{-/-}$ E18.5 embryos. (**a**) Immunostaining of FL cells from PAXX$^{-/-}$Xlf$^{-/-}$, Xlf$^{-/-}$, and PAXX$^{-/-}$Xlf$^{-/-}$ E18.5 embryos. In the lower panel, B-lineage cells were gated on CD43+B220+ population and analyzed for intracytoplasmic IgM (iIgM) staining. (**b**) Quantification of iIgM-positive cells among various PAXX/Xlf genotypes showing the severe deficit in PAXX$^{-/-}$Xlf$^{-/-}$ embryos. (**c**) PCR strategy to analyze IgH rearrangement according to Schlissel *et al.*[30] and autoradiogram of PCR products revealed with the JH3 probe demonstrating the profound defect of IgH rearrangement in FL cells from PAXX$^{-/-}$Xlf$^{-/-}$ embryos. GAPDH-specific PCR was used as loading control

opposed to PAXX$^{-/-}$Xlf$^{-/-}$ embryos. This would place PAXX on the same side as RAG2 in this safeguard mechanism. Accordingly, RAG2 and PAXX are epistatic, as their combined mutations do not impair V(D)J recombination in v-Abl pro-B cells *in vitro*.[14] Likewise, whereas V(D)J recombination is severely compromised in ATM$^{-/-}$Xlf$^{-/-}$ mice,[23] it is efficient in ATM$^{-/-}$RAG2^{cc} mutated v-Abl cells,[14] positioning ATM on the 'same side' as RAG2 and PAXX, opposite to Xlf. Indeed, ATM$^{-/-}$PAXX$^{-/-}$ animals do not present defect in the development of their adaptive immune system beyond that of the sole ATM deficiency as expected according to this model.[12]

Materials and Methods

gRNA design, cloning, and validation. Two guide RNA sequences were selected on exons 1 and 2 of the *MuPAXX* gene using the CRISPOR web tool (http://crispor.tefor.net/crispor.py).[24] gRNA-overlapping restriction enzyme (RE) diagnostic sites near the Cas9 cleavage site were selected to facilitate mutagenesis screening and subsequent mouse genotyping (Supplementary Figures S1A and B). Double-stranded DNA oligonucleotides corresponding to the selected guide RNA were cloned into the pX330-U6-Chimeric_BB-CBh-hSpCas9 vector (the generous gift of Feng Zhang, Addgene, Cambridge MA, USA, #42230) according to Zhang lab's recommendations.[25] For mutagenesis scoring and mouse genotyping, genomic DNA surrounding the guide RNA target sequences were PCR-amplified (MuPAXX_F1: 5′-CAACCTTGAGTACCGCCCAT-3′, MuPAXX_R1: 5′-CAACCTTGAGTACCGCCCAT-3′, 500 bp) and the resulting PCR products digested with either *Bsr*BI or *Sac*I RE to analyze PAXX1 and PAXX2 mutagenesis, respectively (Supplementary Figure S1C and D). Undigested PCR products represent mutagenized DNA molecules. To validate CRISPR/Cas9 mutagenesis, the two gRNA expressing pX330 constructs were transfected into MEFs using the NEPA21 electroporator (Nepagene, Ichikawa-City, Chiba, Japan) with the following settings: pulse1 175v/5 ms/50 ms/2 × /10%/+ -pulse2 20v/50 ms/50 ms/5 × /40%/+-. Genomic DNA was recovered 5 days later and was analyzed using PCR-RE (Supplementary Figure S1C).

Generation of mutant mice. PAXX mutant mice were generated using CRISPR/Cas9 according to the protocol developed by Masahito Ikawa's laboratory.[16] Briefly, the pX330-derived plasmid coding for Cas9 and the guide RNA were microinjected into mouse zygotes that were isolated from the ampullae of superovulated mice. For superovulation, 5 IU PMS and, 48 h later, 5 IU HCG was injected intraperitoneally into female B6/CBA F1 mice of ~6 weeks. Subsequently, they were mated with male B6/CBA F1 mice (C57Bl6NCr and CBA mice: Charles River Laboratories, Saint-Germain-Nuelles, France). The day after, embryos were isolated and placed into M2 medium (Sigma, St. Louis, CA, USA) and the plasmid was injected at a concentration of 5 ng/μl into the pronucleus using a microscope (Nikon, Tokyo, Japan) with micromanipulators (Narishige, London, UK), Vacutip holding pipettes (Eppendorf, Hamburg, Germany), and homemade injection pipettes prepared from borosilicate capillary glass (Harvard Apparatus, Holliston, MA, USA) as well as a Femtojet apparatus (Eppendorf). Pseudopregnant mice received ~20 zygotes. The procedure was approved by the local ethical committee and the French Ministry of Education and Research (#01501.03).

PAXX1 and PAXX2 mice were genotyped by PCR-RE (MuPAXX_F1, MuPAXX_R1, 500 bp) followed by *Bsr*BI or *Sac*I RE digestion, respectively (Supplementary Figures S1C and D). Xlf KO mice were genotyped as previously described.[17] PAXX1 and PAXX2 mice were backcrossed up to six times on C57Bl/6 to segregate away any putative off-target mutation. PAXX/Xlf double KO mice were generated by intercrossing PAXX$^{-/-}$/Xlf$^{+/-}$ or PAXX$^{+/-}$/Xlf$^{-/-}$ mice. All mice were sacrificed humanely.

Phleomycin and IR sensitivity assay. T lymphocytes were isolated from 6- to 10-week-old spleens and enriched for CD3+ cells using magnetic sorting (Dynabeads Untouched mouse T cells, Invitrogen). Purified T cells were stained with CellTrace BV421 fluorescent dye (Thermo-Fisher Scientific, Villebon sur Yvette, France). Overall, 3×10^5 T cells were plated in 48-well plates in triplicate in DMEN-Glutamax, FCS 10%, β-Me 0.1%, sodium pyruvate 1%, penicillin and streptomycin 1%, and NEAA 1%. Culture plates were irradiated (0–4 Gy) and let for 4 h in incubator at 37 °C to allow for DNAdsb repair. T cells were then activated by the

addition of CD3/CD28-coated dynabeads (Thermo-Fisher Scientific) and 1000 u/ml IL2. After 4 days of culture, cells were stained with anti-TCRβ – PE (Sony, Weybridge, Surrey, UK) and analyzed by FACS (LSR-Fortessa, Becton Dickinson, Rungis, France) to score the number of T-cell divisions through the dilution of the CellTrace dye (Figure 2a). The index of proliferation (EI) was calculated according to the following formula:

$$\mathrm{EI} = \sum_{0}^{i} Ni/(\sum_{0}^{i} Ni/2^{i})$$

where *N* represents the number of cells in each (0–*i*) divided cell population.[26] For each sample, the relative proliferative index after IR was calculated relative to the proliferation without IR and dose–response curves were drawn to compare samples.

MEFs were obtained and transformed with SV40 Large T antigen (MEF-SV) as previously described.[17] Phleomycin sensitivity assays were performed on MEF-SV using the IncuCyte Live Cell Analysis System (Essen BioScience, Ann Harbor, MI, USA). Briefly, MEF-SV of various genotypes were plated in triplicates at 3500 cells/well in 48-well plates and incubated with increasing doses (0, 50, 100, and 200 ng/ml) of Phleomycin. Real-time images of the wells were recorded (×4 lens) every 12 h over 7 days to monitor cell proliferation. A mask, which identifies visible objects in each image, was applied to quantify the occupied area (% confluence) of every well at each time points (Supplementary Figure S2A). The final score of cell viability/proliferation was determined by integrating the area under the % confluence curves over time by using rectangular approximation as depicted in Supplementary Figure S2B). Given *i,* the various time points used for recording (from 1 to *n*), the growth index (GI), represented by the area under the curve, is calculated by the formula:

$$GI = \sum_{i=1}^{n} (L * H1) + (L * H2)/2$$

For each experimental condition, cell viability is calculated relative to the GI in the absence of drug (set as 100% growth) and plotted according to Phleomycin concentrations.

Immunoblotting, histology, and immunohistochemistry. Expression of PAXX was analyzed by western blotting on thymic protein extracts using rabbit polyclonal anti-C9orf142 antibody (ab126353, Abcam, Paris, France). Embryonic heads were fixed overnight at 4 °C by immersion in 4% paraformaldehyde and embedded in paraffin with a Tissu-tek processor (VIP, Leica, Wetzlar, Germany). Five μm coronal sections were then obtained using a microtome (Leica RM2125RT) and mounted onto glass slides for histologic analyses. After paraffin removal and citrate treatment, the brain sections were permeabilized with 0.5% Triton X-100 in phosphate-buffered saline (PBS) for 15 min and incubated for 2 h with 7.5% fetal bovine serum and 7.5% goat serum in PBS. The sections were incubated with rabbit anti-CC3 (Cell Signaling, Leiden, The Netherlands, 9661, 1 : 200) overnight at 4 °C. After washing, the sections were incubated with goat anti-rabbit Alexa Fluor 488 or 594 conjugated secondary antibody (Thermo-Fisher Scientific, 1 : 400) for 1 h. After washing, nuclear staining was achieved by incubation with 4'-6-Diamidino-2-phenylindole to quantify apoptosis induction by the detection of pyknotic nuclei. Slides were mounted under Fluoromount (Southern Biotechnologies Associates, Birmingham, AL, USA). Tissues were examined under a fluorescence microscope (Pathfinder, Nikon) with a × 10 or × 20 objective in three channels (appearing red, green, and blue in all figures) as separate files. These images were then stacked with Photoshop software (Adobe, San Jose, CA, USA). All statistical analyses were performed on Prism (GraphPad, La Jolla, CA, USA, Version 7.00).

Immunophenotyping. Immunophenotyping of PAXX mice was performed as described.[17] T-cell populations from the thymus and spleen were identified with anti-CD8 (clone 5.3–6.7), anti-CD4 (GK1.5), and anti-CD3 (145-2C11). Splenic B cells were analyzed using anti-B220 (R6-60.2) and anti-IgM (II/41) and anti-CD19 (6D5). All antibodies were from BD Biosciences. Flow cytometry was performed on the BD LSR-Fortessa (Becton Dickinson, Rungis, France) and analyzed with FlowJo (Ashland, OR, USA). For immunophenotyping of PAXX/Xlf DKO embryos, FLs and thymuses were microdissected under a binocular magnifying lens and passed through a 26-gauge needle of 1-ml syringe and filtered. For thymocytes, cell suspensions were stained with fluorescent-labeled antibodies from BD Biosciences (Becton Dickinson, Rungis, France) Anti-CD25 (clone PC61) and Anti-CD3ε (145-2C11) and from Sony anti-CD4 (GK1.5), anti-CD8β (YTS156.7.7), anti-CD44 (IM7), anti-CD117 (2B8), and anti-CD28 (E18). For B-lineage, cell suspensions were stained with fluorescent-labeled antibodies from Biolegend (San Diego, CA, USA): anti-IgM (clone RMM-1) and anti-CD43 (S11), and from the Sony: anti-CD19-APCCy7 (6D5) and anti-B220 (RA3-6B2). For intracellular IgM staining, cell suspensions were first labeled as above, fixed with the fixation buffer from eBioscience (ThermiFischer Scientific, Villebon sur Yvette, France) intracellular staining kit, and incubated 30 min with anti- IgM from Sony (clone RMM-1).

TCR*α* repertoire study. TCRα repertoire analyses were performed by SMARTer 5' RACE cDNA amplification as previously described on thymocytes.[17] CDR3 sequences were identified using LymAnalyzer[27] and represented by circos-plot using VDJtools.[28] Each TRAV–TRAJ association was recorded in a FlowJo-based file to calculate frequencies of TRAV and TRAJ proximal and distal gene usage. Statistical analyses were performed using Mann–Whitney non-parametric *t*-test under Prism v6.

TCR*β* and IgH V(D)J rearrangement analysis. TCRβ rearrangements (D-Jβ2 and Vβ10-D-Jβ2) were analyzed by PCR on genomic DNA from E18.5 fetal thymuses of various genotypes according to Gartner *et al.*[29] Briefly, 1ng of thymic gDNA were amplified using primers TCRB-D2U-S 5′-GTA GGCACCTGTGGGGAAGAAACT-3′, TCRB-J2D-A 5′-TGAGAGCTGTCTCCTACT ATCGATT-3′, TCRB-V10-S 5′-GCGCTTCTCACCTCAGTCTTCAG-3′, blotted, and hybridized using a PCR-derived TCR-Jβ2 DNA probe (Jbeta2F-5′-GAATTCTTG GTAGCCCTTTTCTGC-3′ and Jbeta2 R-5′-GGGTGGAAGCGAGAGATGT-3′) as depicted on Figure 3b. For IgH rearrangements (VH–DJH) studies, FL CD19+ B-lineage cells were sorted on FACSAriaIII and analyzed by PCR on 1ng genomic DNA according to Schlissel *et al.*[30] Input DNA was analyzed using a GAPDH PCR.

Conflict of Interest

The authors declare no conflict of interest.

Acknowledgements. We thank Catherine Cailleau (SEAT) for exceptional care of our mouse lines, Sophie Berissi for help in immunohistochemistry and Olivier Alibeu, Aurore Pouliet, and Christine Bole-Feyssot (Genomic facility, Imagine Institute) for their assistance in NGS. This work was supported by institutional grants from INSERM, the Institut National du Cancer (PLBIO16-280), the Agence Nationale de la Recherche ('Investissement d'Avenir' program ANR-10-IAHU-01), and by grants from La Ligue Nationale contre le Cancer (Equipe Labellisée LA LIGUE), Pasteur Institute, ANR (Program REVIVE and grant Twothyme) to AC.

1. Sancar A, Lindsey-Boltz LA, Unsal-Kacmaz K, Linn S. Molecular mechanisms of mammalian DNA repair and the DNA damage checkpoints. *Annu Rev Biochem* 2004; **73**: 39–85.
2. Jung D, Giallourakis C, Mostoslavsky R, Alt FW. Mechanism and control of V(D)J recombination at the immunoglobulin heavy chain locus. *Annu Rev Immunol* 2006; **24**: 541–570.
3. Lieber MR. The mechanism of double-strand DNA break repair by the nonhomologous DNA end-joining pathway. *Annu Rev Biochem* 2010; **79**: 181–211.
4. Gao Y, Sun Y, Frank KM, Dikkes P, Fujiwara Y, Seidl KJ *et al.* A critical role for DNA end-joining proteins in both lymphogenesis and neurogenesis. *Cell* 1998; **95**: 891–902.
5. Frank KM, Sekiguchi JM, Seidl KJ, Swat W, Rathbun GA, Cheng HL *et al.* Late embryonic lethality and impaired V(D)J recombination in mice lacking DNA ligase IV. *Nature* 1998; **396**: 173–177.
6. de Villartay JP, Fischer A, Durandy A. The mechanisms of immune diversification and their disorders. *Nat Rev Immunol* 2003; **3**: 962–972.
7. Alt FW, Zhang Y, Meng FL, Guo C, Schwer B. Mechanisms of programmed DNA lesions and genomic instability in the immune system. *Cell* 2013; **152**: 417–429.
8. Xing M, Yang M, Huo W, Feng F, Wei L, Jiang W *et al.* Interactome analysis identifies a new paralogue of XRCC4 in non-homologous end joining DNA repair pathway. *Nat Commun* 2015; **6**: 6233.
9. Ochi T, Blackford AN, Coates J, Jhujh S, Mehmood S, Tamura N *et al.* DNA repair. PAXX, a paralog of XRCC4 and XLF, interacts with Ku to promote DNA double-strand break repair. *Science* 2015; **347**: 185–188.
10. Craxton A, Somers J, Munnur D, Jukes-Jones R, Cain K, Malewicz M. XLS (c9orf142) is a new component of mammalian DNA double-stranded break repair. *Cell Death Differ* 2015; **22**: 890–897.
11. Tadi SK, Tellier-Lebegue C, Nemoz C, Drevet P, Audebert S, Roy S *et al.* PAXX is an accessory c-NHEJ factor that associates with Ku70 and has overlapping functions with XLF. *Cell Rep* 2016; **17**: 541–555.
12. Balmus G, Barros AC, Wijnhoven PW, Lescale C, Hasse HL, Boroviak K *et al.* Synthetic lethality between PAXX and XLF in mammalian development. *Genes dev* 2016; **30**: 2152–2157.

13. Kumar V, Alt FW, Frock RL. PAXX and XLF DNA repair factors are functionally redundant in joining DNA breaks in a G1-arrested progenitor B-cell line. *Proc Natl Acad Sci USA* 2016; **113**: 10619–10624.
14. Lescale C, Abramowski V, Bedora-Faure M, Murigneux V, Vera G, Roth DB *et al.* RAG2 and XLF/Cernunnos interplay reveals a novel role for the RAG complex in DNA repair. *Nat Commun* 2016; **7**: 10529.
15. Liu X, Shao Z, Jiang W, Lee BJ, Zha S. PAXX promotes KU accumulation at DNA breaks and is essential for end-joining in XLF-deficient mice. *Nat Commun* 2017; **8**: 13816.
16. Mashiko D, Fujihara Y, Satouh Y, Miyata H, Isotani A, Ikawa M. Generation of mutant mice by pronuclear injection of circular plasmid expressing Cas9 and single guided RNA. *Sci Rep* 2013; **3**: 3355.
17. Vera G, Rivera-Munoz P, Abramowski V, Malivert L, Lim A, Bole-Feysot C *et al.* Cernunnos deficiency reduces thymocyte life span and alters the T cell repertoire in mice and humans. *Mol Cell Biol* 2013; **33**: 701–711.
18. Li G, Alt FW, Cheng HL, Brush JW, Goff PH, Murphy MM *et al.* Lymphocyte-specific compensation for XLF/cernunnos end-joining functions in V(D)J recombination. *Mol Cell* 2008; **31**: 631–640.
19. Roque T, Haton C, Etienne O, Chicheportiche A, Rousseau L, Martin L *et al.* Lack of a p21waf1/cip -dependent G1/S checkpoint in neural stem and progenitor cells after DNA damage *in vivo*. *Stem cells* 2012; **30**: 537–547.
20. Teague TK, Tan C, Marino JH, Davis BK, Taylor AA, Huey RW *et al.* CD2 expression redefines thymocyte development during the pre-T to DP transition. *Int Immunol* 2010; **22**: 387–397.
21. Kajikhina K, Tsuneto M, Melchers F. B-lymphopoiesis in fetal liver, guided by chemokines. *Adv Immunol* 2016; **132**: 71–89.
22. Hung PJ, Chen BR, George R, Liberman C, Morales AJ, Colon-Ortiz P *et al.* Deficiency of XLF and PAXX prevents DNA double-strand break repair by non-homologous end joining in lymphocytes. *Cell Cycle* 2017; **16**: 286–295.
23. Zha S, Guo C, Boboila C, Oksenych V, Cheng HL, Zhang Y *et al.* ATM damage response and XLF repair factor are functionally redundant in joining DNA breaks. *Nature* 2011; **469**: 250–254.
24. Haeussler M, Schonig K, Eckert H, Eschstruth A, Mianne J, Renaud JB *et al.* Evaluation of off-target and on-target scoring algorithms and integration into the guide RNA selection tool CRISPOR. *Genome Biol* 2016; **17**: 148.
25. Cong L, Ran FA, Cox D, Lin S, Barretto R, Habib N *et al.* Multiplex genome engineering using CRISPR/Cas systems. *Science* 2013; **339**: 819–823.
26. Roederer M. Interpretation of cellular proliferation data: avoid the panglossian. *Cytometry A* 2011; **79**: 95–101.
27. Yu Y, Ceredig R, Seoighe C. LymAnalyzer: a tool for comprehensive analysis of next generation sequencing data of T cell receptors and immunoglobulins. *Nucleic Acids Res* 2016; **44**: e31.
28. Shugay M, Bagaev DV, Turchaninova MA, Bolotin DA, Britanova OV, Putintseva EV *et al.* VDJtools: Unifying Post-analysis of T Cell Receptor Repertoires. *PLoS Comput Biol* 2015; **11**: e1004503.
29. Gartner F, Alt FW, Monroe R, Chu M, Sleckman BP, Davidson L *et al.* Immature thymocytes employ distinct signaling pathways for allelic exclusion versus differentiation and expansion. *Immunity* 1999; **10**: 537–546.
30. Schlissel MS, Corcoran LM, Baltimore D. Virus-transformed pre-B cells show ordered activation but not inactivation of immunoglobulin gene rearrangement and transcription. *J Exp Med* 1991; **173**: 711–720.

Supplementary Information accompanies this paper on Cell Death and Differentiation website (http://www.nature.com/cdd)

Supplementary information

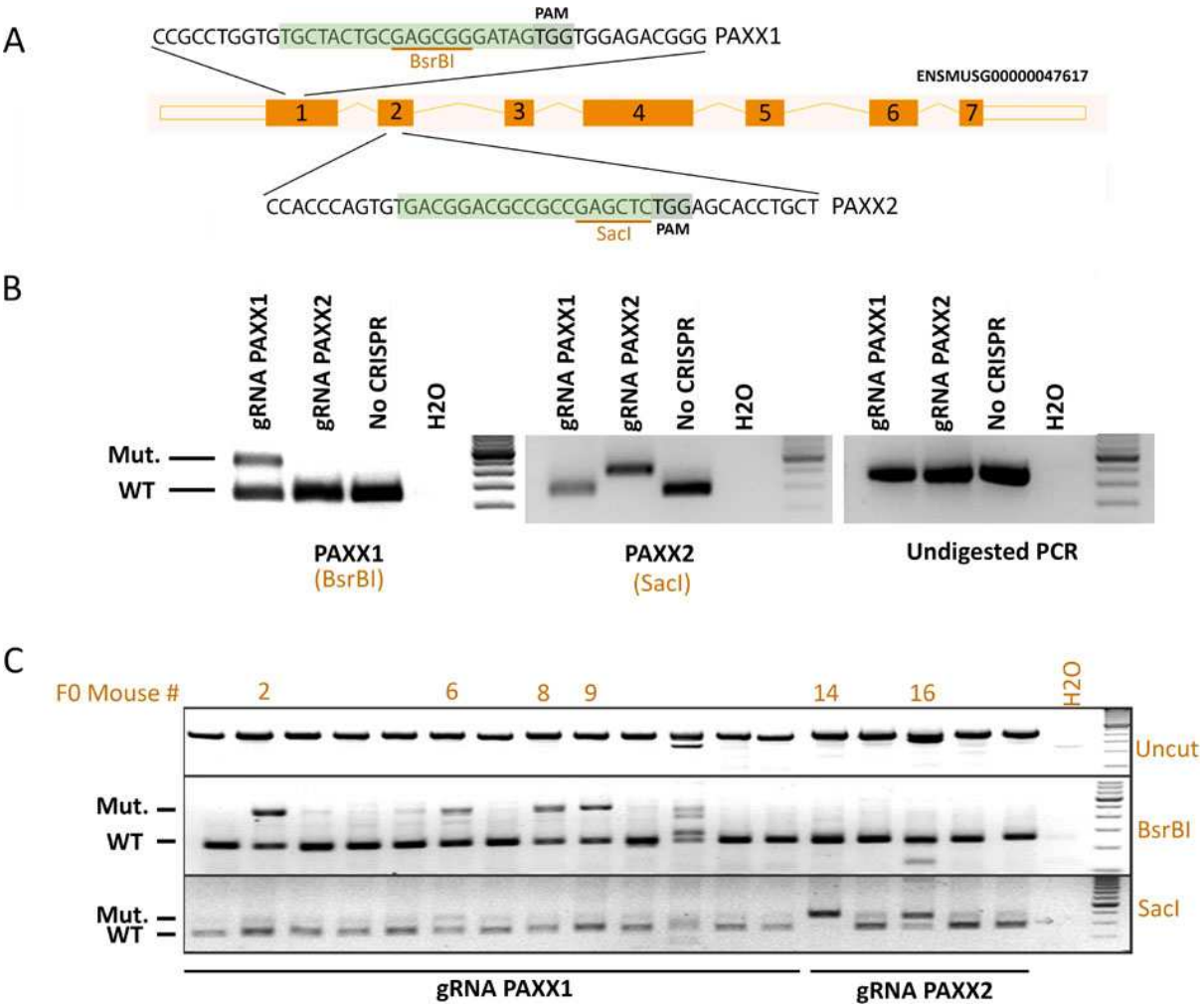

Figure S1: Strategy for CRISPR/Cas9 mutagenesis. A) Design of gRNA target sequences on the murine PAXX gene. The PAXX1 (Exon 1) and PAXX2 (Exon 2) gRNA encompass restriction enzyme sites to facilitate the subsequent analysis of mutagenesis through the loss of PCR product restriction digest (PCR-RE) using BsrB1 and SacI respectively. **B)** Validation of CRISPR/Cas9 mutagenesis upon transfection of MEFs with the two gRNA cloned into the pX330 vector. BsrBI and SacI undigested PCR products are diagnostic of mutagenesis using PAXX1 and PAXX2 gRNA respectively. **C)** Screening of F0 mice by PCR-RE showing specific retention of undigested PCR products for PAXX1 and PAXX2 in 4 and 2 animals respectively.

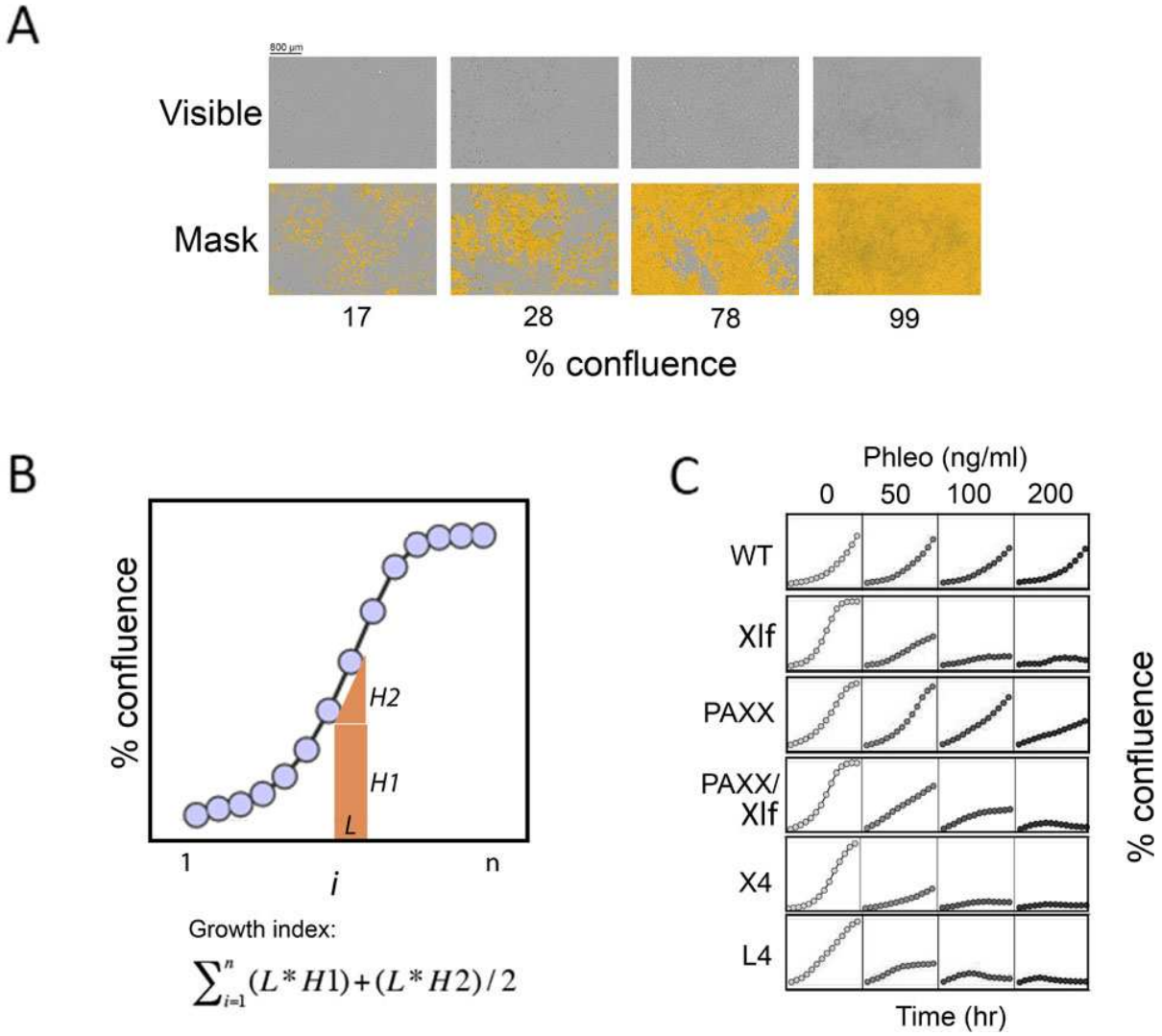

Figure S2: Schematic representation of Phleomycin sensitivity assay using the IncuCyte® Live Cell Analysis System. A) Sample images of the IncuCyte® Live Cell Analysis System showing various degrees of cell confluence and the mask (orange) applied to calculate the % of confluence. **B)** Calculation of the Growth Index by integrating the area under the confluence curve using rectangular approximation. Given *i* the various time points ranging from 1 to n, the sum of the area of the rectangle L*H1 plus half the area of the rectangle L*H2 gives the area under the curve between the time-points *i* and (*i*+1). Summing all these intermediate values gives the total area under the confluence curve, which is considered as the Growth index (GI). **C)** Schematic representation of the survival/confluence curves obtained with various MEFs incubated with increasing doses of Phleomycin (0-200 ng/ml) over time. X4 and

L4 represent XRCC4$^{-/-}$ and DNA-LigaseIV$^{-/-}$ MEFs respectively. The IncuCyte® software delivers Excel files with raw data of confluence for each time points, from which the Growth indexes are calculated as described in **B)**.

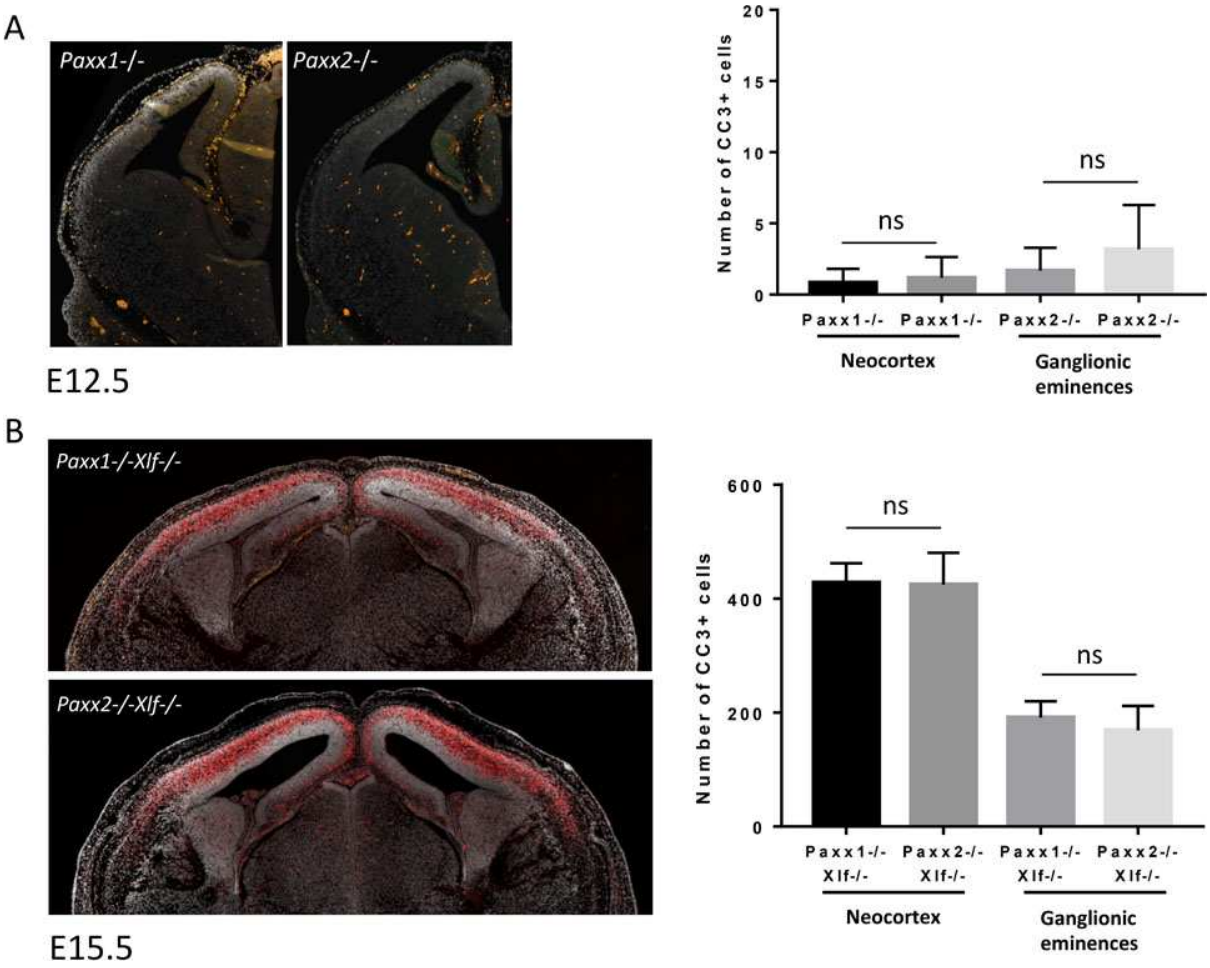

Figure S3: No difference in the level of spontaneous apoptosis in the brain of PAXX1$^{-/-}$ and PAXX2$^{-/-}$ embryos. On the left**:** Coronal sections of cerebral hemispheres of PAXX1$^{-/-}$ and PAXX2$^{-/-}$ embryos at E12.5. **A)** and of PAXX1$^{-/-}$Xlf$^{-/-}$ and PAXX2$^{-/-}$Xlf$^{-/-}$ embryos at E15.5 **B)** stained with DAPI (gray) and CC3 (red). Blood vessels are colored in orange. On the Right: quantification of the numbers of CC3+ cells in the Neocortex **A)** and the ganglionic eminences at E12.5 **B)**. Data have been obtained from 3 embryos per group.